Aldehyde dehydrogenases (ALDH) expression in cancer tissues as potential pharmacological targets for therapeutic intervention

Probing ALDH expression and function in 2D- and 3D-cultured cancer cell lines

Lina Mohammedsuhail Ibrahim ELSALEM

Submitted for the Degree of Doctor of Philosophy

Institute of Cancer Therapeutics

University of Bradford

2016

Abstract

Lina Mohammedsuhail Ibrahim Elsalem

Title: Aldehyde dehydrogenases (ALDH) expression in cancer tissues as potential pharmacological targets for therapeutic intervention

Subtitle: Probing ALDH expression and function in 2D- and 3D-cultured cancer cell lines

Keywords: ALDH, Colorectal cancer, Hypoxia, Antioxidant, anticancer drugs, ALDH inhibitors

The aldehyde dehydrogenase (ALDH) superfamily is gaining momentum in regard to stem cell and cancer research. However, their regulation and expression in the cancer microenvironment is poorly understood. The aim of this work was to understand the role of selected ALDH isoforms (1A1, 1A2, 1A3, 1B1, 2, 3A1 and 7A1) in colorectal cancer (CRC) and explore the impact of hypoxia on their expression. CRC cell lines (HT29, DLD-1, SW480 and HCT116) were grown under normoxic or hypoxic conditions (0.1% O_2) and HT29 and DLD-1 in spinner flasks to generate multicellular spheroids (MCS). Hypoxia was demonstrated to have an impact on the ALDH expression, which appeared cell-specific. Notably, ALDH7A1 was induced upon exposure to hypoxia in both HT29 and DLD-1 cells, shown to be expressed in the hypoxic region of the MCS variants and in 5/5 CRC xenografts (HT29, DLD-1, HCT116, SW620, and COLO205). ALDH7A1 siRNA knockdown studies in DLD-1 cells resulted in significant reduction of viable cells and significant increase in ROS levels, suggesting ALDH7A1 to possess antioxidant properties. These findings were further supported using isogenic H1299/RFP and H1299/ALDH7A1 lung cancer cell lines. ALDH7A1, however, was found not to be involved in inhibiting the pharmacological effect or causing resistance to different cytotoxic and molecularly targeted anticancer drugs. To unravel the functional role of ALDH7A1, 9 compounds obtained from a virtual screening of 24,000 compounds from the Maybridge collection of compounds were used to probe ALDH7A1 functional activity.

One compound, HAN00316, was found to inhibit the antioxidant properties of ALDH7A1 and thus could be a good starting point for further chemical tool development. Although this study underpins a potential important role of ALDH7A1 in hypoxic CRC, further work is required to fully validate its potential as a biomarker and/or pharmacological target.

Acknowledgements

First and foremost I thank my God for giving me the strength throughout my life. I am blessed and I thank God every day for everything that happens to me. I am grateful for the favour which God has bestowed upon me.

I would like to offer my sincerest gratitude to my supervisor, Dr. Klaus Pors, who has supported me throughout my work with his patience and knowledge whilst allowing me the room to work in my own way. He holds the credit of keeping me on the right track through his continuous guidance and stimulating discussions. I am also thankful to him for encouraging the use of correct grammar and consistent notation in my writings and for carefully reading and commenting on revisions of this thesis. One simply could not wish for a better or friendlier supervisor.

I am also thankful for Prof Laurence Patterson for his generous and unconditional support.

I'm deeply grateful to Prof. Roger Phillips for his guidance and patience throughout the period of study. I consider myself very fortunate for being able to work with a very considerate and encouraging instructor like him. I am thankful to him for his advices that helped me sort out the technical details of my work.

I would like to thank Mrs Patricia Cooper and Mr Gary Lawson for their help in cell culture lab. I extend my sincere thanks to Dr Mark Sutherland who taught me the techniques of gene analysis. I'd like also to thank Dr Charlotte Evan and Haneen Basheer who taught me how to culture spheroids. I'm also indebted to Amit, Hanady and Djev who showed me how to do histology experiments.

I would like to express my appreciation to Dr. Simon Allison for teaching me western blot, knockdown, ROS detection and cell cycle procedures and helping me with his pointers and expertise in molecular biology and cell culture lab work.

In my daily work, I have also been blessed with a friendly and cheerful group of PhD students (Sara, Rene, Manar, Rida, Dany) who supported me during lab work.

I'd like to convey my heartfelt thanks to my home university, Jordan University of Science and Technology, for their generous sponsorship and continuous support.

I'd like to also thank my flatmate, Sara, with whom I shared a living for three months. It was great time during which we were mutually supportive for each

other. Sara was my backbone when I couldn’t stand up for myself. She was like a real sister.

Finally, and most importantly, I wish to express my sincere thanks to my family. I would like to thank my husband Dr. Ahmad Jumah. His full support, encouragement, quiet patience and unwavering love were undeniably the bedrock upon which the past five years of my life have been built. His tolerance of my occasional bad moods is a testament in itself of his unyielding devotion and love. He has done all that and more while working on his own PhD!

I also would like to thank my parents (Dr MohammedSuhail Elsalem and Mrs Rasmieh Elkateeb) and my brothers (Ala’a, Omar and Anas), for their faith in me and allowing me to be as ambitious as I wanted. It was under their watchful eye that I gained so much drive and an ability to tackle challenges. I owe them everything and wish I could show them just how much I love and appreciate them. I’m also thankful to my sisters-in-law (Ayat and Sarait), and my darling candy nephew, Amr, your smiley face was my inspiration throughout my writing period.

This work is dedicated for my late father-in-law (Mr Abdelhaleem Jumah). I hope it will make him proud of me and my other half, Ahmad.

Table of Content

List of Figures

List of Tables

List of Abbreviations

AASA: alpha-aminoadipic semialdehyde
ABC: ATP binding cassette
Ago-2: Argonaute-2
AhR: aryl hydrocarbon receptor
ALDHs: Aldehyde dehydrogenases
AML: Acute myeloid leukaemia
Amps: plural for ampere, a unit of electric current
APC: Adenomatous polyposis coli
APES: aminopropyltriethoxysilane
AraC: 1-β-D-arabinofuranosylcytosine
ARNT: Aryl hydrocarbon receptor nuclear translocator
ATCC: American Type Culture Collection
ATRA: All-trans retinoic acid
AV: arteriovenous shunt
BAA: BODIPY aminoacetate
BAAA: BODIPY aminoacetaldehyde
BAAA-DA: Bodipy-aminoacetaldehyde diethyl acetal
BCAT1: Branched Chain Amino-Acid Transaminase 1
BODIPY: Boron-dipyrromethene
bps: base pairs
BSA: bovine serum albumin
˚**C**: Celsius
CAIX: carbonic anhydrase IX
cDNA: Complementary DNA
c-Kit: proto-oncogene c-Kit
cm: centimetre
CO_2: Carbon dioxide
$CoCl_2$: cobalt chloride
CPA: Cyclophosphamide
CCNG1: Cyclin-G1
CRC: colorectal carcinoma
CSCs: Cancer stem cells
CYPs: Cytochromes P450
d: Day
2D: two dimensional
3D: three dimensional
DAB: 3,3-diaminobenzidine
DAC: Decitabine
DCIS: ductal carcinoma in situ
DEAB: Diethylaminobenzaldehyde
DMEs: Drug metabolising enzymes
DMSO: Dimethyl sulfoxide
DNA: Deoxyribonucleic acid
dNTPs: Deoxynucleotide triphosphate
dsDNA: double-stranded DNA
dsRNA: double-stranded RNA
EBV: Epstein-Barr virus
ECM: extracellular matrix
EDTA: Ethylene diaminetetracetic acid
EGF: epidermal growth factor
EGFR: epidermal growth factor receptor
ELISA: enzyme-linked immunosorbent assay.
EMT: epithelial-to-mesenchymal transition
EPAS1: Endothelial PAS-domain protein 1
ERK: extracellular-signal-regulated kinases
FACS: Flurescence activated cell sorting

FBS: foetal bovine serum
FGFR: fibroblast growth factor receptor
5-FU: 5-Fluoro Uracil
g: gram
G1 phase: Gap 1 phase
G2 phase: Gap 2 phase
GFP: green fluorescent protein
h: hours
HCl: hydrochloric acid
H2AX: histone family, member X
H2DCFDA: dichlorodihydrofluorescein
H_2O_2: hydrogen peroxide
HB-EGF: heparin-binding EGF-like factor
HBV: hepatitis B virus
4-HCPA: 4–hydroperoxycyclophosphamide
H & E: Haematoxylin and Eosin
HIFs: Hypoxia inducible factors
HIF1: Hypoxia inducible factor 1
4HNE: 4-Hydroxynonenal
HPV: human papilloma virus
HR: hypoxic region
HSC: haematopoietic SC
JNK: c-Jun N-terminal kinases
KSHV: Kaposi sarcoma herpesvirus
ICT: Institute of Cancer Therapeutics
IHC: immunohistochemistry
KIT: v-kit Hardy-Zuckerman 4 feline sarcoma viral oncogene homolog
l: litre
LDH-A: lactate dehydrogenase A
LPO: lipid peroxidation
m: milli
m: meter
M: Molar
MAPK: Mitogen-activated protein kinases
MAO: monoamine oxidase
MCS: Multicellular spheroids
MDR: Multidrug resistance
MET: Met proto-oncogene
min: minutes
miRNA: microRNA
$MgCl_2$: magnesium chloride
ml: milli litre
ML: monolayer
MMP: matrix metalloproteinases
M phase: Mitosis phase
MRI: Magnetic resonance image
mRNA: Messenger Ribonucleic acid
MRS: Magnetic resonance spectroscopy
MTT: 3-(4,5-dimethylthiazol-2-yl)-2,5-diphenyltetrazolium bromide
n: nano
NaCl: sodium chloride
NAD^+: Nicotinamide adenine dinucleotide
$NADP^+$: Nicotinamide adenine dinucleotide phosphate
NaOH: Sodium hydroxide
N-BPs: nitrogen-containing bisphosphonates N-BPs
NM: nodular melanoma
NSCLC: non-small cell lung cancer
O_2: oxygen
PAX: Paclitaxel

PBS: Phosphate buffered saline
PBST: PBS Tween 20
PDE: pyridoxine-dependent epilepsy
PDGFRA: Platelet-derived growth factor receptor, alpha polypeptide
PET: Positron emission tomography
PPARG: Peroxisome proliferator-activated receptor gamma
PTEN: Phosphatase and tensin homolog
Q-RT-PCR: quantitative real time polymerase chain reaction
RA: retinoic acid
rcf: relative centrifugal force
RET: proto-oncogene encodes a receptor tyrosine kinase
RFP: red fluorescent protein
RISC: RNA-induced silencing complex
RNA: Ribonucleic acid
RNAi- RNA interference
rpm: Revolutions per minute
ROS: Reactive oxygen species
RQ: Relative quantity
s: second
SCID: Severe combined immunodeficient
SD: Standard deviation
SDS: sodium dodecyl sulfate
shRNAs: short hairpin RNAs
siRNAs: small interfering RNAs
SL: surface layer
SPECT: Single photon emission computed tomography
S phase: Synthesis phase
Src: Proto-oncogene tyrosine-protein kinase
SSM: superficial spreading melanoma
t; time
t: test
TEMED: Tetramethylethylenediamine
TICs: tumour-initiating cells
TKIs: tyrosine kinase inhibitors
TNM: tumour, node and metastasis
TP53: Tumour suppressor p53
TRBP: TAR-RNA-binding protein
TSG: Tumour suppresser gene
UK: United Kingdom
UV: Ultraviolet
v:volume
VEGFA: Vascular endothelial growth factor A
VEGFR: Vascular endothelial growth factor receptor
VHL: Von Hippel–Lindau
Volt: voltage
XREs: xenobiotic response element
ZOL: zoledronic acid
µ: micro

Chapter 1: Introduction

1.1 Cancer definition and epidemiology

Cancer is considered as the foremost cause of death in developed countries and the second cause of death in developing countries with more than 200 different types of cancer registered to date (Jemal et al., 2011). Worldwide, prostate cancer is the most common type in male and breast cancer in female. In 2008, about 12.7 million new cases and 7.6 million cancer deaths were reported with the most common cause of death being breast cancer and lung cancer in females and males, respectively (Jemal et al., 2011). Colorectal cancer (CRC) is the second leading cause of cancer deaths worldwide and is described in greater detail in Chapters 2 and 3 of this thesis.

Cancer is defined as a condition where certain cells in the body have lost the ability to control their growth and started to replicate in a limitless manner. Such cells may also have acquired the ability to invade and destroy the local healthy tissues. In addition, they can spread to another part of the body away from their primary location in a process known as metastasis.

1.2 Hallmarks of cancer

The hallmarks of cancer were early described to comprise six biological capabilities acquired during the multistep development of human tumours, which have essential roles in contributing to tumour complexity. They include sustaining proliferative signalling, evading growth suppressors, resisting cell death, enabling replicative immortality, inducing angiogenesis, and activating invasion and metastasis (Figure 1A) (Hanahan and Weinberg, 2000). In 2011 Hanahan and Weinberg described two enabling characteristics underlying

these hallmarks including genome instability and inflammation (Hanahan and Weinberg, 2011). In addition, advances in cancer research during the last decade have added two emerging hallmarks of potential generality to this list including reprogramming of energy metabolism and evading immune destruction (Hanahan and Weinberg, 2011) (Figure 1B).

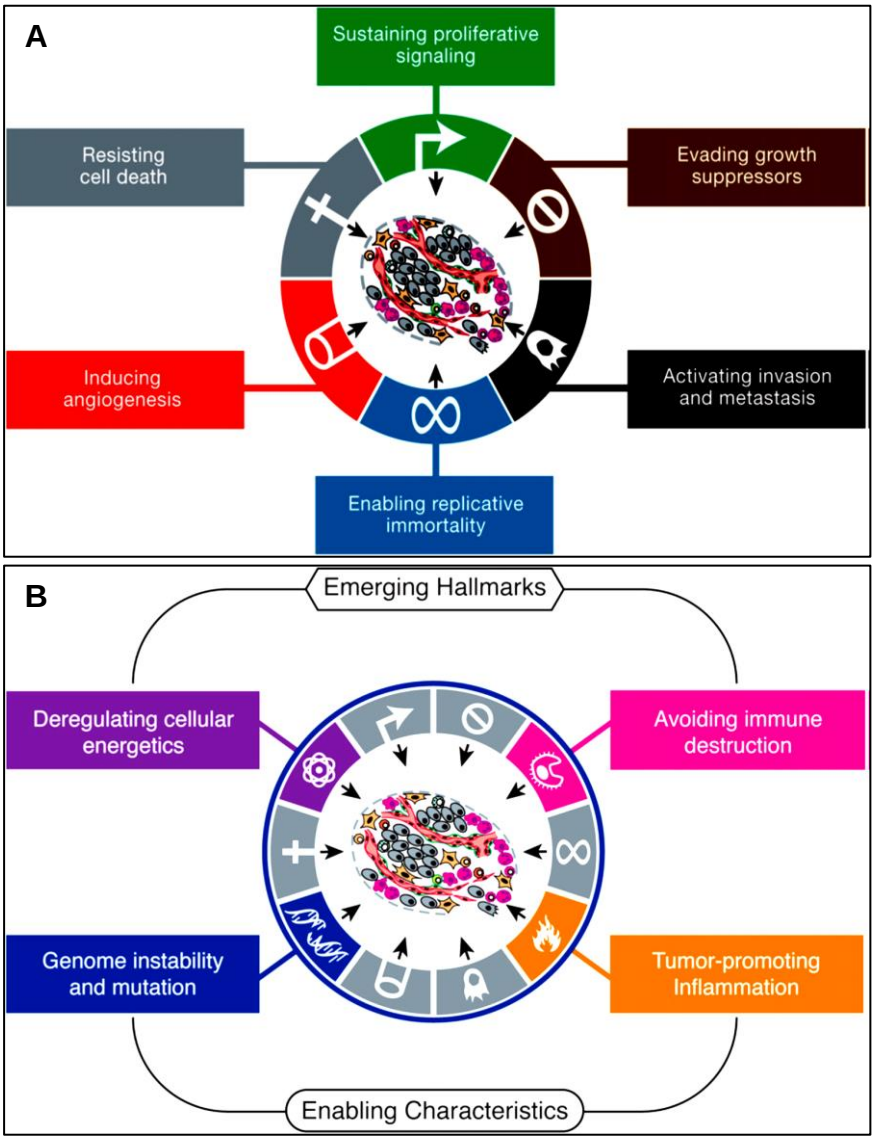

Figure 1 The Hallmarks of Cancer. The six hallmark capabilities originally proposed in Hanahan and Weinberg, 2000 review (A), Emerging Hallmarks and Enabling Characteristics described in Hanahan and Weinberg, 2011 review. Adopted from Hanahan and Weinberg, 2011 with License Number: 3833250420363.

Tumours exhibit another dimension of complexity relating to the presence of unique tumour microenvironments, which are less easily assayed but have profound effects on cancer progression (Semenza, 2016). The tumour microenvironment can be subdivided into the cellular microenvironment and the chemical microenvironments. The former includes tumour cells, stromal cells, and the extracellular matrix (ECM) produced by these cells. The chemical microenvironment encompasses pH, PO_2 and the concentration of other small molecules (e.g. NO) and metabolites (e.g. glucose, glutamine, lactate) (Semenza, 2016). Tumour hypoxia (low PO_2) contributes to the foundation of chemical tumour microenvironment, which has biological and therapeutic implications such as stimulating tumour proliferation, aggressiveness and drug resistance (Mathonnet et al., 2014). Here, the role of hypoxia in cancer progression will be discussed further.

1.3 Tumour hypoxia

Human cells require adequate oxygen supply for their proliferation, survival, metabolism and other biological functions (Dachs and Tozer, 2000, Semenza, 2012). In normal cells, both the delivery and consumption of O_2 are highly regulated processes. In contrast, these processes are altered during tumour pathogenesis and therefore most solid tumours larger than 1 mm^3 contain regions of low oxygen tension (hypoxia) due to imbalances between O_2 supply and consumption (Hockel and Vaupel, 2001, Dachs and Tozer, 2000).

1.3.1 Causes of hypoxia

The tumour hypoxia initially arises due to limitations in oxygen diffusion in the primary or metastatic tumours (Wilson and Hay, 2011). Cells that are located next to the perfused blood vessel are exposed to relatively high O_2 concentrations, which decline steeply as distance from the vessel increases (Semenza, 2010). As a consequence, cells at low oxygen level respond by generating new vessel growth from the existing vasculature structure surrounding the tumour in a process known as angiogenesis (Liao and Johnson, 2007, Semenza, 2010, Dachs and Tozer, 2000). However, the new vasculature is often structurally and functionally abnormal and therefore, does not adequately or consistently supply the whole tumour with oxygen and nutrients (Wilson and Hay, 2011). As a result of chaotic vasculature, irregular blood and oxygen flow cancer cells experience hypoxia (Semenza, 2010) (Figure 2).

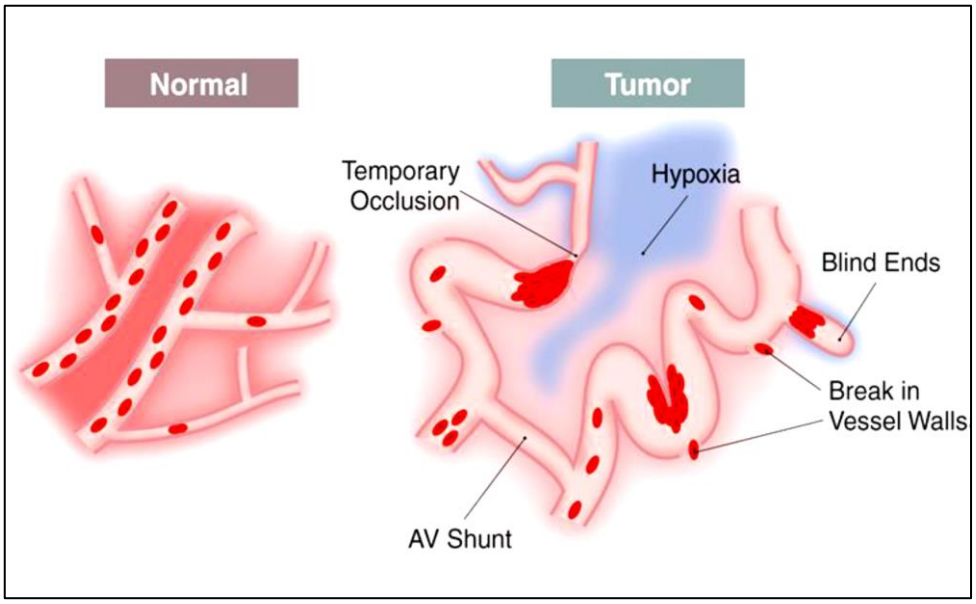

Figure 2 Diagram showing the principal differences between the vasculature of normal and malignant tissues. AV: arteriovenous shunt. Adopted from (Brown and Giaccia, 1998) with License Number: 3833250840650.

1.3.2 Measuring tumour hypoxia

Many invasive and non-invasive methods are currently available to measure the oxygen levels of tumours in both animal models and humans (Hockel and Vaupel, 2001). Hypoxia in human tumours has been measured by oxygen sensitive electrodes and by hypoxia marker techniques using various labels that can be detected by different methods such as positron emission tomography (PET), single photon emission computed tomography (SPECT), magnetic resonance spectroscopy (MRS), autoradiography, and immunohistochemistry (Sutherland, 1998, Hockel and Vaupel, 2001) (Table 1).

Methods to measure tumour hypoxia
1. Invasive microsensor techniques for direct tissue pO2 measurements
• Polarographic O_2 sensors
• Luminescence-based optical sensors
2. Electron paramagnetic resonance oximetry
3.Techniques for intravascular O_2 detection
• Cryospectrophotometry [HbO_2 saturation]
• Near-infrared spectroscopy [HbO_2 saturation]
• Phosphorescence imaging
4. Nuclear magnetic resonance spectroscopy and imaging techniques
• 1H-MRI, BOLD effect
• 19F-magnetic resonance relaxometry
5. Non-invasive detection of sensitizer adducts
• [18F]Fluoromisonidazole [PET]
• [123I]Iodoazomycin-arabinoside [SPECT]
6. Invasive immunohistochemical hypoxia marker techniques
• Misonidazole [3H-labeled]
• Pimonidazole
• Etanidazole
• Nitroimidazole-theophylline
• Carbonic anhydrase IX (CAIX)
• Glucose transporter (Glut-1)

Table 1 Invasive and non-invasive methods to measure tumour hypoxia. Adopted from (Hockel and Vaupel, 2001) with License Number: 3833260663039.

1.3.3 Hypoxia-inducible factors

The major mechanism mediating adaptive responses to reduced O_2 availability (hypoxia) is the regulation of transcription by hypoxia-inducible factors (HIFs) (Carroll and Ashcroft, 2005, Poon et al., 2009, Rohwer et al., 2013). In the process of doing so, hypoxic cancer cells acquire invasive and metastatic properties as well as resistance to certain chemotherapeutic agents and radiation therapy, which together constitute lethal cancer phenotypes that ultimately lead to patient mortality (Dachs and Tozer, 2000, Semenza, 2010).

The HIF transcriptional complex exists as heterodimers, consisting of alpha and beta subunits. There are three isoforms of the alpha subunit which are tightly regulated at the protein level by changes in cellular oxygen tension: HIF-1α, HIF-2α (also known as endothelial PAS-domain protein 1, EPAS1), and HIF-3α (Bárdos and Ashcroft, 2005). The HIF-β isoforms, also known as aryl hydrocarbon receptor nuclear translocator (ARNT), are constitutively and ubiquitously expressed across many cell types and are not sensitive to oxygen levels (Dachs and Tozer, 2000, Heddleston et al., 2010).

The majority of primary human cancers and their metastases are characterised by increased levels of HIF-1α or HIF-2α protein (or both) compared to normal tissues, with intra-tumoural hypoxia being the major cause of their upregulation (Carroll and Ashcroft, 2005, Semenza, 2010, Rohwer et al., 2013). Little is known about the third isoform, HIF-3α. Some evidence indicates HIF-3α to be involved in the negative feedback regulation of HIF-1 because its expression is transcriptionally regulated by the latter

(Bárdos and Ashcroft, 2005, Semenza, 2010). However, the primary function and regulatory mechanism of HIF-3α is still to be elucidated (Heddleston et al., 2010, Balamurugan, 2016).

In addition to intra-tumoural hypoxia, genetic and epigenetic alterations resulting in oncogene gain of function or tumour suppressor gene (TSG) loss of function (most notably, von Hippel–Lindau, VHL) also affect HIF levels either by increasing HIF-1α synthesis or by reducing HIF-1α degradation (Bárdos and Ashcroft, 2004, Bárdos and Ashcroft, 2005, Asby et al., 2014) (Figure 3). This results in HIF-1α upregulation even under normoxic conditions (Bárdos and Ashcroft, 2005). In addition, a large number of proteins encoded by transforming viruses that cause tumours in humans also induce HIF-1 activity (Nakamura et al., 2009). For example, herpes virus which causes Kaposi sarcoma, encodes three different proteins that together increase HIF-1α protein half-life, nuclear localisation, and transactivation under non-hypoxic conditions, thereby mimicking the effect of hypoxia (Semenza, 2010, Semenza, 2012).

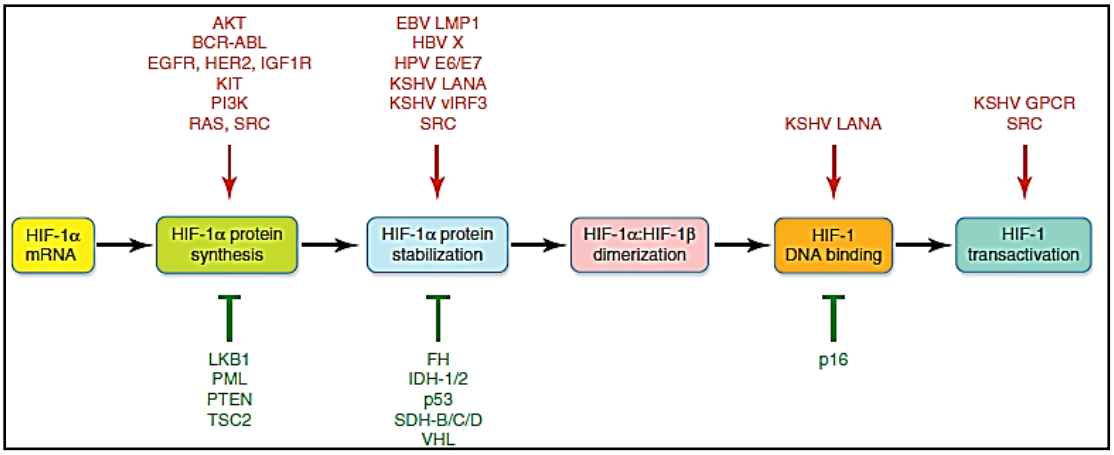

Figure 3 Regulation of HIF-1 activity by oncoproteins (red) and tumor suppressors (green). Transforming proteins encoded by Epstein-Barr virus (EBV), hepatitis B virus (HBV), human papilloma virus (HPV), and Kaposi sarcoma herpesvirus (KSHV) also activate HIF-1. Adopted from (Semenza, 2012) with License Number: 3833251190781.

1.3.4 Hypoxia-inducible factors in cancer progression

Many biologic parameters that affect the malignant potential of a neoplasm have been found to be affected by hypoxia (Hockel and Vaupel, 2001, Semenza, 2012) (Figure 4). These include the selection of genotypes that can survive hypoxia-reoxygenation injury (Verduzco et al., 2015), pro-survival changes in gene expression that suppress apoptosis (Carroll and Ashcroft, 2005) and support autophagy (Bellot et al., 2009) and the anabolic switch in energy metabolism (Weljie and Jirik, 2011, Song et al., 2009, Yang et al., 2012, Zeng et al., 2015). In addition, hypoxia enhances autocrine growth factor signalling that results in increased cell proliferation (Barr et al., 2008), tumour angiogenesis (Koukourakis et al., 2002), the epithelial-to-mesenchymal transition (EMT) (Jiang et al., 2011), stem cell maintenance (Heddleston et al., 2010, Li et al., 2013), invasiveness and metastasis (Gruber et al., 2004), as well as suppression of the immune response (Doedens et al., 2010, Ruan et al., 2009, Semenza, 2012).

Hypoxia also contributes to loss of genomic stability through the increased generation of reactive oxygen species (ROS) (Kondoh et al., 2013) and the downregulation of DNA repair pathways (Wilson and Hay, 2011, Luoto et al., 2013, Zeng et al., 2015). Furthermore, hypoxia has been found to be implicated in cancer cell resistance to radiotherapy and certain chemotherapeutic agents through multiple mechanisms (Wilson and Hay, 2011, Warfel and El-Deiry, 2014) (Table 2).

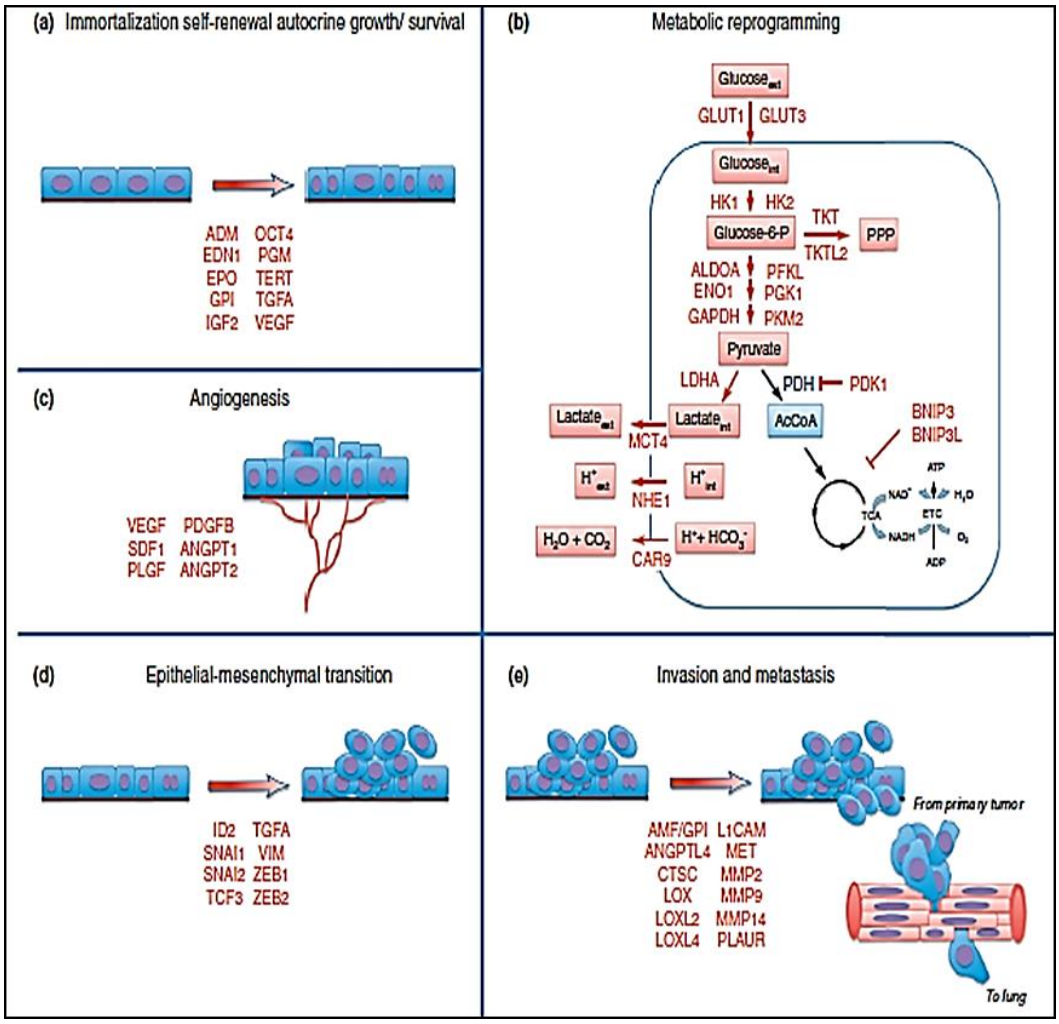

Figure 4 HIF target genes that encode proteins involved in crucial aspects of cancer progression. Adopted from (Semenza, 2012) with License Number: 3833251190781..

Effect of hypoxia	Resistance or sensitivity?	Mechanism	Agents affected	Example
Lack of oxidation of DNA free radicals by O_2	Resistance	Failure to induce DNA break	Ionising radiation	2-3 fold increase in ionising radiation dose required for equivalent cell kill
			Antibiotics that induce DNA breaks	Bleomycin
Cell cycle arrest in G1 or G2 phase	Resistance	Repair before progression to S or M phase	Cycle selective chemotherapy drugs	5-fluorouracil
Cell cycle arrest in S phase	Sensitivity	Collapse of stalled replication forks	PARP inhibitors	Veliperib (ABT-888)
Distance from vasculature (indirect)	Resistance	Compromised drug exposure	Drugs extensively bound in tumour cells	Taxanes
Extracellular acidification (indirect)	Resistance	Decreased uptake	Basic drugs	Doxorubicin
	Sensitivity	Increased uptake	Acidic drugs	Chlorambucil
Resistance to apoptosis	Resistance	Genetic selection of *TP53* mutants	Multiple	-
		Downregulation of BID and BAX	Multiple	Etoposide
Genomic instability	Resistance	Mutagenesis	Multiple	DHFR amplification and methotrexate
Suppression of DNA repair	Resistance	Downregulation of MMR	DNA methylation agents	-
	Sensitivity	Downregulation of NER	Bulky DNA monoalkylating and crosslinking agents	-
		Downregulation of HR	DNA cross linking agents	Cisplatin
HIF1 stabilisation	Resistance	Expression of ABC transporters	ABC transporter substrates	MDR1 and doxorubicin
		Downregulation of NHEJ	Agents that induce DSBs	Etoposide

Table 2 Mechanisms of resistance (and sensitivity) of hypoxic cells to cytotoxic therapy. BCL2-associated X protein (BAX), BH3 interacting domain death agonist (BID), dihydrofolate reductase (DHFR), double strand break (DSB), hypoxia-inducible factor 1 (HIF1), homologous recombination (HR), multidrug resistance protein 1 (MDR1), mismatch repair (MMR), nucleotide excision repair (NER), non-homologous end joining (NHEJ), poly(ADP-ribose) polymerase (PARP). Adopted from (Wilson and Hay, 2011) with License Number: 3833260919909.

1.4 Aldehyde dehydrogenase superfamily

Although the effect of hypoxia on drug sensitivity is well known, the impact of low oxygen tension on drug metabolising enzymes that also play a role in signalling pathways, such as aldehyde dehydrogenases (ALDH), is still to be elucidated. Accordingly, the main focus of this project is to study the impact of hypoxia on the expression of ALDH.

1.4.1 Aldehyde compounds

Aldehyde-containing agents are considered as highly reactive electrophilic molecules that originated from various internal and external sources during multiple physiological processes. Endogenous aldehydes can be generated from the metabolism of many agents including neurotransmitters, amino acids, lipids, and carbohydrates, as well as through metabolism of vitamins (retinoic acid biosynthesis) and steroids (Marchitti et al., 2008, Elizondo et al., 2000). Among the external sources of aldehydes, the metabolism of some xenobiotics and drugs including ethanol and anticancer prodrugs (e.g. cyclophosphamide (CPA) and ifosfamide) contribute to aldehyde production. In addition, many industrial applications such as resins, polyurethane and polyester plastics manufacturing use or generate aldehydes. Many aldehydes are also present in food either as naturally occurring or approved additives to enhance flavour and odour. Moreover, many aldehydes are present in the environment as a result of cigarette smoke and motor vehicle exhaust (Marchitti et al., 2008).

1.4.2 ALDH in normal physiological processes

Aldehydes have important contribution to normal physiological processes, such as embryonic development, vision and neurotransmission. However, many of them are very harmful and have been shown to elicit both cytotoxic and carcinogenic effects (Vasiliou and Nebert, 2005). Aldehydes react with cellular components including nucleic acids and amino acids, which have direct or indirect effects on cellular homeostasis, enzyme inactivation, DNA damage, and cell death (Marchitti et al., 2008).

The aldehyde dehydrogenase (ALDH) superfamily belongs to phase 1 drug metabolising enzymes (DMEs) and plays an important role in the metabolism of a wide range of aliphatic and aromatic aldehydes (Sládek, 2003). These enzymes catalyse the irreversible oxidation and conversion of aldehydes into their corresponding carboxylic acids through pyridine nucleotide-dependent reaction (Vasiliou et al., 2004). The hydrogen acceptor in this reaction is usually NAD^+, however, $NADP^+$ has also been shown to serve as a cofactor in certain cases of some of these enzymes (Sládek, 2003).

The ALDH superfamily is represented in all three taxonomic domains (Archaea, Eubacteria and Eukarya), suggesting a vital role throughout evolutionary history (Jackson et al., 2011). Mammalian ALDH activity was first detected in ox liver more than five decades ago (Farres et al., 1989), after which many types of ALDH have been identified based on their physico-chemical characteristics, enzymological properties, subcellular localisation, and tissue distribution (Yoshida et al., 1998) (Table 3).

ALDH	Tissue/Organ Distribution	Cellular Localisation
1A1	Liver, kidney, erythrocytes, skeletal muscle, lung, breast, lens, stomach mucosa, brain, pancreas, testis, prostate, ovary	Cytosol
1A2	Testis, small amounts in liver, kidney	Cytosol
1A3	Kidney, skeletal muscle, lung, breast, testis, stomach mucosa, salivary, glands	Cytosol
1B1	Liver, kidney, heart, skeletal muscle, brain, prostate, lung, testis, placenta, more	Mitochondria
1L1	Liver, kidney, skeletal muscle	Cytosol
1L2	Pancreas, heart, brain	Mitochondria
2	Liver, kidney, heart, skeletal muscle, lung, lens, brain, pancreas, prostate, spleen	Mitochondria
3A1	Stomach mucosa, cornea, breast, lung, lens, esophagus, salivary glands, skin	Cytosol
3A2	Liver, kidney, heart, skeletal muscle, lung, brain, pancreas, placenta, most tissues	Endoplasmic reticulum
3B1	Kidney, lung, pancreas, placenta	Cytosol and Endoplasmic reticulum
3B2	Parotid gland	Cytosol and Endoplasmic reticulum
4A1	Liver, kidney, heart, skeletal muscle, brain, placenta, lung, pancreas, spleen	Mitochondria
5A1	Liver, kidney, heart, skeletal muscle, brain	Mitochondria
6A1	Liver, kidney, heart, skeletal muscle	Mitochondria
7A1	Fetal liver, kidney, heart, lung, brain, ovary, eye, cochlea, spleen, adult spiral cord	Cytosol, Mitochondria and nucleus
8A1	Liver, kidney, brain, breast, testis	Cytosol
9A1	Liver, kidney, heart, skeletal muscle, brain, pancreas, adrenal gland, spinal cord	Cytosol
16A1	Neuronal cells	Cytosol
18A1	Kidney, heart, skeletal muscle, pancreas, testis, prostate, spleen, ovary, thymus	Mitochondria

Table 3 ALDH superfamily, Tissue/Organ Distribution and Cellular Localisation. Adopted from (Ma and Allan, 2011) with License Number: 3833601253515.

The standardised gene nomenclature system for the ALDH superfamily was established in 1998 based on divergent evolution and amino acid identity (Marchitti et al., 2008), in which the families within the superfamily shared more than 40% sequence identity and members of the same subfamily shared more than 60% sequence identity. To date, the human genome contains 19 known functional ALDH genes, divided into 11 families and 4 subfamilies, and three pseudogenes (Black et al., 2009, Vasiliou et al., 2004).

ALDH isoforms are characterised by a wide tissue distribution, with the highest expression most often occurring in the liver and/or kidney (Sládek, 2003). Furthermore, they are found in all cellular regions such as cytosol, endoplasmic reticulum, nucleus and mitochondria with many of them located in more than one organelle (Jackson et al., 2011). It has been shown that ALDH isoforms located in regions other than the cytosol have leader or signal sequences that allow their translocation to specific cellular locations (Braun et al., 1987). In addition, ALDH enzymes that are present in the nucleus have been suggested to have effects on gene expression and cellular proliferation (Marchitti et al., 2008, Chan et al., 2011). ALDH enzymes have also been shown to have broad substrate specificity (Yoshida et al., 1998) although the preferred substrates have been identified for most of them (Sládek, 2003).

The physiological role of several of the human ALDH isoforms is yet to be elucidated, however, the activity of certain ALDH has been shown to be critical in the detoxification of specific endogenous and exogenous aldehyde

substrates and in the prevention of their accumulation (Jackson et al., 2011). This capacity has a critical role in the protection of cellular homeostasis and organismal functions against toxic effects of the aldehydes (Jackson et al., 2011). The ALDH activity, through aldehyde metabolism, has also been found to be essential for the synthesis of vital molecules such as retinoic acid (RA), betaine and gamma-aminobutyric acid that are important for cell proliferation, differentiation and survival (Jackson et al., 2011).

Apart from their importance in aldehyde metabolism, members of ALDH superfamily also have other catalytic functions, although many of these are yet to be clearly defined, including ester hydrolysis (ALDH1A1, ALDH2, ALDH4A1), nitrate reductase activity (ALDH2) and drug bioactivation (ALDH2) (Marchitti et al., 2008, Vasiliou and Nebert, 2005). In addition, some members of ALDH superfamily have the capacity for non-catalytic functions such as, antioxidant functionalities (ALDH1A1, ALDH3A1, ALDH7A1), osmoregulation (ALDH7A1) and the absorption of ultraviolet (UV) light (ALDH1A1, ALDH3A1). In addition, some enzymes (ALDH1A1, ALDH1L1, ALDH2) have been found to act as binding proteins for many endogenous (e.g., androgen, cholesterol and thyroid hormone) and exogenous (e.g., acetaminophen) compounds (Black et al., 2009, Jackson et al., 2011).

The clinical importance of ALDH superfamily is supported by the fact that mutations and polymorphism in ALDH genes, leading to failure of aldehyde metabolism, are considered as the molecular basis of several disease conditions and metabolic anomalies (Ma and Allan, 2011) (Table 4).

ALDH	Major substrates	Pathologies associated with altered expression
1A1	Retinal, aldophosphamide, acetaldehyde, lipidperoxidation-derived aldehydes	Drug resistance, alcohol sensitivity
1A2	Retinal	Tumours
1A3	Retinal	Perinatal lethality
1B1	Acetaldehyde, lipid peroxidation-derived aldehydes	Various phenotypes
1L1	10-Formyltetrahydrofolate	Tumours
1L2	10-Formyltetrahydrofolate	-
2	Acetaldehyde, nitroglycerin	Ethanol-induced cancers, Hypertension, Alcohol sensitivity
3A1	Medium-chain aliphatic and aromatic aldehydes	Tumours
3A2	Long-chain aliphatic aldehydes	Sjögren–Larsson syndrome
3B1	Lipid peroxidation-derived aldehydes	Paranoid schizophrenia
3B2	Unknown	-
4A1	Proline metabolism	Type II hyperprolinemia
5A1	Succinic semialdehyde	Neurological disorders
6A1	Methylmalonate semialdehyde	Elevated levels in urine of β-alanine, 3-hydroxypropionicacid, 3-amino acids, and 3-hydroxyisobutyric acids
7A1	Betaine aldehyde, lipid peroxidation-derived aldehydes	Hyperosmotic stress
8A1	Retinal	-
9A1	γ-Aminobutyraldehyde, aminoaldehydes	-
16A1	Unknown	-
18A1	Glutamatic γ-semialdehyde	Hypoprolinemia, hypoornithinemia, hypocitrullinemia,hypoargininemia, hyperammonemia with cataract formation, neurodegeneration, connective tissue anomalies

Table 4 ALDH superfamily, Major substrates and Pathologies associated with altered expression. Adopted from (Ma and Allan, 2011) with License Number: 3833601253515 and (Muzio et al., 2012) with License Number: 3833601442994 .

1.4.3 ALDH in cancer

ALDH isoforms play important physiological functions as mentioned earlier, however their presence has implications in drug sensitivity and clinical prognosis while also being employed as a cancer stem cell marker (Pors and Moreb, 2014). In the following sections, the most prominent ALDH isoforms will be described.

ALDH1A2 is a cytoplasmic enzyme that is involved in retinoic acid (RA) synthesis, which is known to enhance cell differentiation, growth arrest and apoptosis (De Luca, 1991). ALDH1A2 has been found to be downregulated in prostate cancer compared to normal prostate tissues (Kim et al., 2005). In addition, suppression of colony growth has been observed after transfection-mediated re-expression of ALDH1A2 in DU145 prostate cancer cells, indicating ALDH1A2 acts as a tumour suppressor gene (TSG) in prostate cancer (Kim et al., 2005).

The expression of ALDH1L1, 10-formyltetrahydrofolate dehydrogenase, has also been found to be associated with suppression of cancer cell proliferation. This cytoplasmic enzyme was found to be downregulated in several types of cancer including liver, lung, prostate, pancreas and ovarian cancers (Krupenko and Oleinik, 2002). In addition, transient expression of ALDH1L1 in many human cancer cell lines including prostate, hepato-carcinoma, and lung cancer cell lines resulted in the suppression of cell proliferation and increased cytotoxicity (Krupenko and Oleinik, 2002) through induction of G1 cell cycle arrest and caspase dependent apoptosis (Oleinik and Krupenko, 2003). It is known that 10-formyltetrahydrofolate is required

for *de novo* purine biosynthesis and therefore, the ultimate impact of the depletion of intracellular 10-formyltetrahydrofolate by ALDH1L1 activity is diminished DNA/RNA biosynthesis. Hence, downregulation of ALDH1L1 in tumours has been proposed to be one of the cellular mechanisms that enhance cancer cell proliferation (Krupenko and Oleinik, 2002).

In contrast to ALDH1A2 and ALDHL1, several other ALDH isoforms have been suggested to be associated with malignant transformation (Ucar et al., 2009). ALDH1A1 is a cytosolic isoform that is crucial in regulating RA signalling and is expressed in tissues during vertebrate development (Yanagawa et al., 1995). Its expression in non-small cell lung cancer (NSCLC) was found to gradually increase during the transition from normal to adenocarcinoma (Patel et al., 2008). In addition, its expression in primary colon cancer samples was found to be significantly associated with shorter overall survival rates, suggesting its clinical relevance as a prognostic or predictive marker in colorectal carcinoma (CRC) (Kahlert et al., 2012).

ALDH1A3, a cytoplasmic enzyme that is also involved in RA synthesis, has been found to be downregulated in many tumour types including breast, gastric and colon cancers (Okamura et al., 1999, Yamashita et al., 2006, Rexer et al., 2001). In contrast, its expression has been found to be upregulated in mice that are resistant to induced mammary tumours suggesting that it might have tumour suppression properties (Kuperwasser et al., 2000). Conflicting information on ALDH1A3 has however been reported as more recent studies support a role for this enzyme in cancer malignancy as it correlates significantly with tumour grade, metastasis, and cancer stage

in breast cancer patients (Marcato et al., 2011b). In addition, a recent investigation revealed that ALDH1A3 is overexpressed in clinical high grade glioma tissues compared to low grade glioma or normal brain (Mao et al., 2013). ALDH1A3 was also found to be closely associated with clinical pathological behaviours, poor prognosis and decreased overall survival in patients with gallbladder cancer as it is associated with lymph node metastasis and invasion (Yang et al., 2013). Furthermore, ALDH1A3 appears to be highly expressed in cancer stem cells (CSCs) of the breast, gallbladder, glioma, melanoma and prostate and hence could be a contributing factor to cancer and malignancy (Pors and Moreb, 2014).

ALDH1B1 is a mitochondrial isoform that is catalytically active towards a wide range of aldehyde substrates, including aliphatic and aromatic aldehydes and the products of lipid peroxidation (LPO). Immunohistochemical studies have shown approximately 5-fold higher expression of ALDH1B1 compared to ALDH1A1 in some cancer tissues (breast, lung, ovarian and colon cancer). Furthermore, 98% of colon cancer samples (39/40) were stained positive for ALDH1B1 using immunohistochemistry (Chen et al., 2011).

The ALDH2 isoform is a mitochondrial enzyme and predominantly linked with acetaldehyde detoxification in alcohol metabolism (Yokoyama et al., 1998). Diminished activity of ALDH2 enzyme caused by a mutant allele has been found to dramatically increase the risk for oesophageal cancer (Yokoyama et al., 1998). However, its expression in leukaemia and lung cancer has been

associated with higher cancer cell proliferation rates and higher clonal efficiency (Moreb et al., 2012).

ALDH3A1 is a cytoplasmic enzyme and plays an important role in cellular homeostasis through protection from ROS generated under oxidative stress (Pappa et al., 2003a, Pappa et al., 2003b). Chang *et al.* reported the increased expression of ALDH3A1 in hepatocellular carcinoma tissues derived from 50% of patients, while no detectable level was observed in normal liver (Chang et al., 1998). ALDH3A1 inhibition or deficiency has also been shown to strongly inhibit hepatoma cellular growth (Muzio et al., 2003). In addition, ALDH3A1 has been shown to be among the genes that were highly upregulated in mechanically-induced colon cancer cell population and correlated with cancer cell migration and invasion in athymic nude mice (Tang et al., 2014).

In NSCLC, ALDH3A1 together with ALDH1A1 were found to be highly expressed in both cancer cell lines and primary tumour samples (Patel et al., 2008). In addition, the expression of both enzymes has been observed to gradually increase during the transition from normal to atypical pneumocyte, carcinoma *in situ* and adenocarcinoma (Patel et al., 2008). Moreover, elevation in their expression in normal pneumocytes has been shown to be induced by cigarette smoking (Patel et al., 2008). ALDH3A1 has been suggested as a potential diagnostic marker for NSCLC (Kim et al., 2007) and it might serve as a candidate biomarker in the pathogenesis of oesophageal squamous cell carcinoma (Huang et al., 2000).

ALDH3B1 is a cytosolic isoform whose enzymatic activity is directed towards various aldehyde substrates including 4-Hydroxynonenal (4HNE), one of the most reactive and cytotoxic aldehydes formed during LPO. Marchitti *et al.* reported high expression of ALDH3B1 in a high percentage of human tumours (lung > breast = ovarian > colon) where it was shown to play an important physiological role against oxidative stress (Marchitti et al., 2010).

ALDH4A1 is a mitochondrial enzyme catalysing the second step of the proline degradation pathway. Expression of ALDH4 mRNA was found to be upregulated in HCT116 colon cancer cells in response to DNA damage caused by adriamycin treatment (Yoon et al., 2004). In addition, induction of overexpression of ALDH4 in H1299, a NSCLC cell line, showed lower intracellular ROS levels than parental or control cells after treatment with hydrogen peroxide (H_2O_2) or UV. These findings suggest that it has protective role against oxidative stress (Yoon et al., 2004).

ALDH5, a mitochondrial enzyme involved in glutamate metabolism, has been found to be highly expressed in a human hepatoma (Stewart et al., 1995). In addition, it has been shown to be overexpressed in breast ductal carcinoma *in situ* (DCIS) at both the mRNA and protein levels. Treatment using disulfiram and valproic acid, which are known to inhibit ALDH5A1, resulted in significant inhibition of net proliferation of DCIS three dimensional spheroids, suggesting that ALDH5A1 may play an important role in DCIS and potentially serve as a novel molecular therapeutic target (Kaur et al., 2012).

ALDH7A1 was found to be expressed in the cytoplasm, mitochondria and nucleus (Chan et al., 2011). It is known to be involved in protection against

hyperosmotic stress presumably through the generation of betaine, an important cellular osmolyte, formed from betaine aldehyde (Brocker et al., 2010). In addition, it was found to attenuate reactive aldehyde and oxidative stress induced cytotoxicity through its antioxidant activity (Brocker et al., 2011). Abnormally high expression of ALDH7A1 has been found in ovarian cancer (Saw et al., 2012). In addition, it is upregulated in prostate cancer and matched bone metastasis samples, where it is associated with increased colony formation and cell migration (van den Hoogen et al., 2010, van den Hoogen et al., 2011), while its expression in NSCLC patients has been linked with increased incidence of cancer recurrence (Giacalone et al., 2013).

1.4.4 ALDH and drug resistance

The increased expression and activity of certain ALDH isoforms in tumour tissues has been found to be associated with drug resistance and cancer relapse (Su et al., 2010, Januchowski et al., 2013). ALDH1A1 has a regulatory and metabolic role in cancer, which can confer resistance to selected anticancer agents by metabolic inactivation (Moreb et al., 2007). In a retrospective study conducted by Sladek *et al.*, the cellular levels of ALDH1A1 have been reported to be predictors of treatment responses to cyclophosphamide (CPA) based therapy (Sladek et al., 2002). Breast cancer patients with low levels of this enzyme have been shown to respond better to CPA-based treatment compared with those patients possessing high ALDH1A1 levels (Sladek et al., 2002). In breast cancer, a direct correlation between ALDH3A1 activity and resistance to oxazaphosphorines has also been reported (Sreerama and Sladek, 1993). Drug resistance can be

reversed using the ALDH inhibitor, diethylaminobenzaldehyde (DEAB) (Sreerama and Sladek, 1997). In addition, Moreb *et al.* have shown that RNA interference (RNAi)-mediated knockdown of ALDH1A1 and ALDH3A1 resulted in increased cellular sensitivity of lung cancer cell lines to CPA and its metabolite, 4–hydroperoxycyclophosphamide (4-HCPA) (Moreb et al., 2007) (Figure 5). Accordingly, the expression level of these isoforms has been suggested to serve as predictors of therapeutic responses to oxazaphosphorines (Moreb et al., 2007). More recently, selective inhibition of ALDH3A1 in ALDH3A1-expressing lung adenocarcinoma and glioblastoma cell lines (A549 and SF767, respectively) caused re-sensitisation of these cells toward mafosfamide (Parajuli et al., 2014).

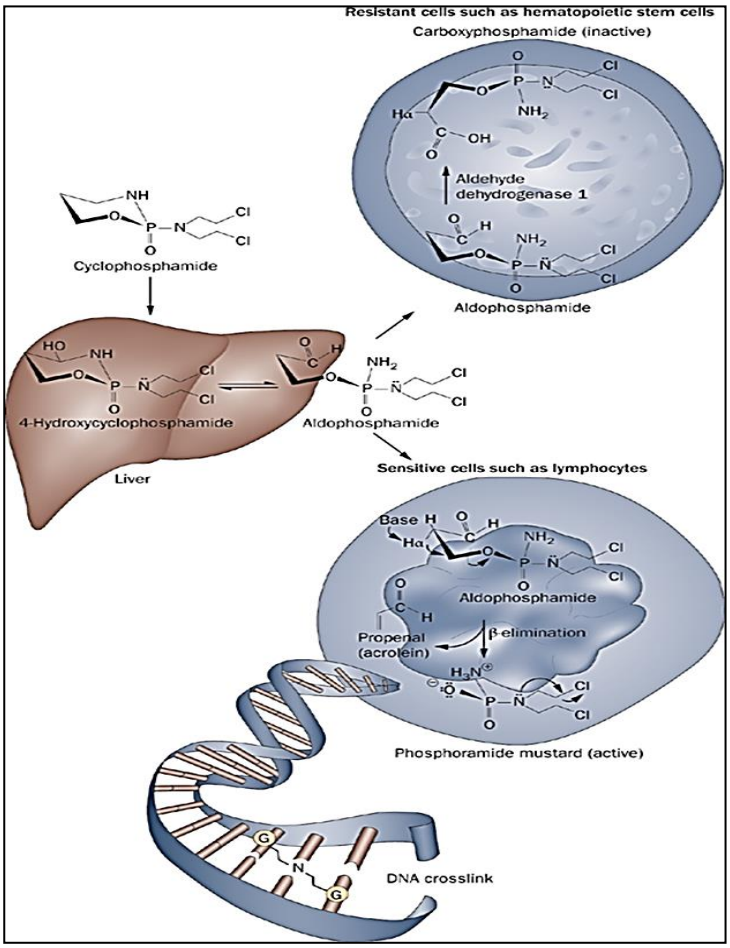

Figure 5 Mechanism of cyclophosphamide drug resistance by the activity of ALDH. Adopted from (Emadi et al., 2009) with License Number: 3833251467327.

Apart from the reported role of ALDH1A1 and ALDH3A1 in the metabolic inactivation of aldehyde drugs (e.g. CPA and 4-HCPA), recent studies described the involvement of ALDH in resistance to conventional cytotoxic drugs that do not contain aldehydes. Sun *et al.* demonstrated using proteomic analysis that ALDH1 was among the proteins that were upregulated in paclitaxel resistant human lung adenocarcinoma (A549) compared to sensitive cells (Sun et al., 2011). In addition, when analysing cisplatin resistant ovarian tumours and NSCLC cell lines, ALDH1 was found to be upregulated compared to their parental cells (Le Moguen et al., 2007, Barr et al., 2013). Recent investigations by Croker and Allan have also shown that breast cancer cell lines that overexpressed ALDH1 demonstrated significant resistance to doxorubicin, paclitaxel and radiotherapy compared to cells with low ALDH1 expression (Croker and Allan, 2012). Furthermore, inhibiting ALDH activity through RA or DEAB re-sensitised resistant cells (Croker and Allan, 2012). The ALDH1 isoform, however, was not specified in the aforementioned studies. ALDH1A2 was found to be associated with acquired resistance of leukaemic cells exposed to 1-β-D-arabinofuranosylcytosine (AraC) while ALDH1A2 knockdown induced sensitivity to AraC treatment (Kawasoe et al., 2013).

Recent studies have shown that ALDH2 expression is also associated with increased drug resistance to CPA and doxorubicin in leukaemia and lung cancer cell lines (Moreb et al., 2012). Moreover, Touil *et al.* reported the upregulation of ALDH1A3 in 5-Fluorouracil (5-FU) resistant cells compared to the parental HT29 cells, perhaps indicating that colon cancer cells escape 5-

FU chemotherapy-induced cell death by entering stemness state (Touil et al., 2014).

Recently, ALDH has also been shown to be involved in drug resistance to molecularly-targeted therapeutics. Raha *et al.* showed that ALDH1 is highly expressed in gastric carcinoma cell lines that are resistant to the MET kinase inhibitor, crizotinib (Raha et al., 2014). A more recent study using proteomics analysis revealed high expression of ALDH7A1 in DU145, a prostate cancer cell line resistant to zoledronic acid (ZOL), a nitrogen-containing bisphosphonates (N-BPs) (Milone et al., 2015).

These novel findings suggest a much broader role for ALDH in treatment response than previously reported (Croker and Allan, 2012). Therefore, it has been suggested that a patient's ALDH genotype should be taken into consideration in order to design the most efficacious treatment strategy (Croker and Allan, 2012).

1.4.5 ALDH in cancer stem cells (CSCs)

Growing evidence suggests that the cells responsible for initiating, maintaining and the spread of cancer are "cancer stem cells" (CSCs) or tumour-initiating cells (TICs) (Ma and Allan, 2011). These cells are characterised by limitless proliferation potential, ability to self-renew, and capacity to produce a progeny of differentiated cells that form the major tumour population (Clevers, 2011). CSCs can divide asymmetrically, generating an identical daughter cell and a more differentiated cell, which during subsequent divisions produces most of the tumour bulk (Clevers, 2005).

CSCs were first identified in acute myeloid leukaemia (AML) by Dr. John Dick's group in 1994 (Lapidot et al., 1994). They observed that $CD34^+/CD38^-$ leukaemia-initiating cells were able to engraft into severe combined immune-deficient (SCID) mice and recapitulate the original tumour population as seen in AML patients (Lapidot et al., 1994).

Characteristically, CSCs are resistant to radiotherapy and chemotherapy. In comparison to differentiated tumour cells, CSCs are relatively quiescent and have a slow cycling rate. These features protect them against conventional chemotherapeutic agents that target rapidly proliferating cells (Zhou et al., 2009). Their resistance to radiotherapy and chemotherapy results also from the presence of an arsenal of defence mechanisms such as the expression of ABC transporters (Hirschmann-Jax et al., 2004) and strong responses to DNA damage compared with their progeny (Viale et al., 2009).

The evolution of a CSC theory has provided a paradigm shift in our understanding of carcinogenesis, metastasis, and tumour biology (van den Hoogen et al., 2010). As a consequence, the identification of normal SCs and CSCs has important implications in the way cancer treatment should be conceived and future therapeutic approaches will be designed (van den Hoogen et al., 2010).

CSCs are most commonly identified by expression of cell surface markers (Table 5). However, not all tumour cells that are isolated by certain markers are necessarily CSCs. In addition, as solid cancers are characterised by their heterogeneity, the prospective isolation of CSCs depending on the expression of certain cell surface markers such as $CD44^+$, integrin α2β1, and

$CD133^+$ alone remains controversial and an unfeasible way to identify all putative stem or progenitor cell types (van den Hoogen et al., 2010). Accordingly, there is a real need to identify novel markers that can be utilised to refine the CSC population (Marcato et al., 2011a).

Cancer type	Cell Surface Markers	References
Leukaemia	$CD34^+$, $CD38^-$, $CD19^+$	(Kong et al., 2008)
Breast	$CD44^+$, $CD24^-$, Lin^-, $ALDH1^+$	(Ginestier et al., 2007, Al-Hajj et al., 2003)
Brain	$CD133^+$	(Hemmati et al., 2003)
Melanoma	$CD20^+$, $ABCB5^+$	(Fang et al., 2005, Schatton et al., 2008)
Colorectal	$CD133^+$, $EpCAM^+$, $CD44^+$, $CD166^+$, $ALDH1^+$	(O/'Brien et al., 2007, Ricci-Vitiani et al., 2007, Dalerba et al., 2007, Huang et al., 2009)
Lung	$CD24^+$, $CD44^+$, $CD133^+$	(Ho et al., 2007, Eramo et al., 2007)
Sarcomas	$CD105^+$, $CD44^+$, $Stro1^+$	(Parker Gibbs, 2005)
Head and Neck Squamous Cell Carcinoma	$CD44^+$	(Prince et al., 2007)
Liver	$CD133^+$, $CD90^+$, $CD44^+$	(Ma et al., 2007, Yang et al., 2008)
Pancreatic	$CD44^+$, $CD24^+$, ESA^+, $CD133^+$	(Li et al., 2007, Hermann et al., 2007)

Table 5 Cancers with identified stem cells and cells surface markers expressed. Adopted from (Ebben et al., 2010) and perrmission is not required for reuse in thesis.

Currently, the increased activity of certain ALDHs has been considered as a hallmark of CSCs and appears as a novel marker for stem cell isolation (Marcato et al., 2011a). In fact, the role of certain isoforms of ALDHs (ALDH1A1, ALDH1A2, ALDH1A3 and ALDH8A1) in RA cell signalling has been suggested to contribute to “stemness” characteristics of CSCs (Marcato et al., 2011a). In addition, as ALDH enzymes are frequently involved in the detoxification of endogenous or exogenous compounds, this provides a mechanism for SC protection and maintenance of cellular integrity (van den Hoogen et al., 2010). Furthermore, the role of ALDH enzymes in the metabolism and inactivation of certain anticancer drugs as discussed before has been considered as one of the suggested mechanisms for the apparent resistance of CSCs to current anti-cancer therapies (Marcato et al., 2011a, Dylla et al., 2008). Tanei *et al.* showed that ALDH1 positive breast CSCs are valuable predictors of resistance to chemotherapeutic drugs such as taxanes (Tanei et al., 2009).

The isolation of CSCs based on increased ALDH activity was first reported in haematopoietic cancers (acute myeloid leukaemia) in a study conducted by Cheung *et al*. (Cheung et al., 2007) The team showed that the $ALDH^+$ AML cells were associated with adverse prognosis and engrafted significantly better than $ALDH^-$ AML cells in immunocompromised mice (Cheung et al., 2007). The same year, the pioneering work of Ginestier and co-workers showed the potential applicability of using ALDH activity to isolate CSCs in solid tumours (Ginestier et al., 2007). ALDH1 has been shown to act as a

marker of breast CSCs and has been linked with poor clinical outcome (Ginestier et al., 2007).

ALDH activity has also been used successfully to isolate CSCs in many solid cancers including lung (Ucar et al., 2009), liver (Ma et al., 2007), colon (Huang et al., 2009), pancreatic (Hermann et al., 2007), prostate (van den Hoogen et al., 2010), head and neck (Prince et al., 2007), bladder (Su et al., 2010), thyroid (Todaro et al., 2010), brain (Corti et al., 2006, Mao et al., 2013), melanoma (Boonyaratanakornkit et al., 2010), ovarian (Silva et al., 2011) and renal (Wang et al., 2015) carcinomas. These studies provide evidence regarding ALDH activity as a universal CSC marker (Marcato et al., 2011a).

1.4.5.1 The use of ALDH to isolate CSCs

The activity of ALDH is now recognised as a universal marker for both normal and cancer SCs. Different assays have been described to study and measure the activity of ALDH including a spectrophotometric assay used to study the enzyme kinetics, where the rate of conversion of NAD^+ substrate to NADH by the activity of ALDH in the cell lysates can be measured at 37°C and a wavelength of 340 nm (Moreb et al., 1998). Western blot analysis has also been used to study ALDH in normal and cancer SCs (Giorgianni et al., 2000), although a limitation in the protein detection approach is that their enzymatic activity was not measured (Ma and Allan, 2011). Currently, the gold standard of studying the activity of ALDH in viable cells is the use of flow cytometry in combination with ALDH-specific fluorescent substrates as described below (Ma and Allan, 2011).

1.4.5.1.1 The ALDEFLUOR assay

The ALDEFLUOR assay has been shown to be an efficient strategy to isolate primitive haematopoietic SC (HSCs). This assay is based on the use of a fluorescent substrate, BODIPY aminoacetaldehyde (BAAA), which can passively diffuse into cells where it is converted by ALDH1 activity into a fluorescent green molecule (negatively-charged BODIPY aminoacetate (BAA-)). This fluorescent product accumulates in cells due to the presence of verapamil, an MDR1 inhibitor included in the assay buffer, which prevent active efflux of converted BAA-, allowing cells with high ALDH activity to be identified by flow cytometry (Alison et al., 2010). The addition of DEAB, an inhibitor of ALDH activity, which significantly reduces the fluorescence signal is used as a negative control to confirm that the isolated cells are $ALDH^+$ cells (Marcato et al., 2011a) (Figure 6).

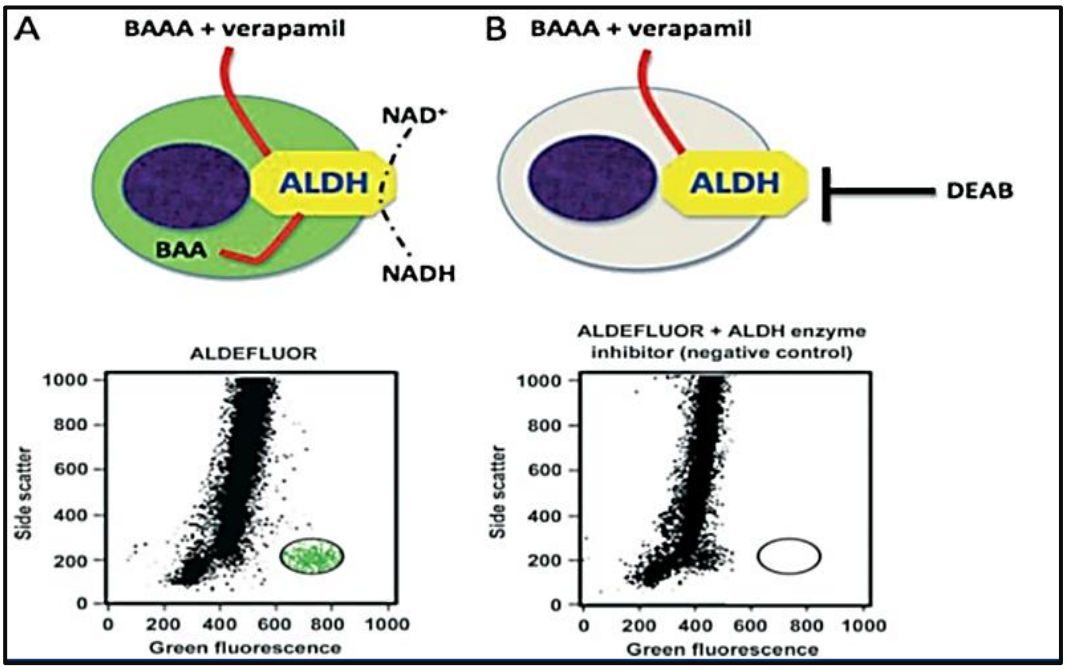

Figure 6 The basis of the ALDEFLUOR assay. Cells are incubated with BAAA in the presence of the MDR1 inhibitor, verapamil, enabling $ALDH^+$ cells to be detected (bottom left). When cells are treated with DEAB, ALDH activity is inhibited and no fluorescent subpopulation can be identified (bottom right). Adopted from (Alison et al., 2010) with License Number: 3833260321984.

1.4.5.1.2 The selectivity of the ALDEFLUOR assay

The ALDEFLUOR assay is a commercially available assay used to identify SCs. It is highly sensitive, reproducible, nontoxic, and easy to use. In addition, it does not involve antibody recognition or the use of DNA-intercalating dyes; hence it is a valuable method for live single cell isolation as the cytoplasmic enzyme activity detection is less likely to be damaged by enzymatic digestion and processing of the tissues (Minn et al., 2014, Dollé et al., 2015).

The ALDEFLUOR assay has been successfully employed for the isolation of viable haematopoietic SCs isolated from human umbilical cord blood cells (Storms et al., 1999, Hess et al., 2004). This assay has been reported to be specific to ALDH1A1 (Marcato et al., 2011a), however, recent information suggest it is not so specific, which may have implication for SC isolation (Levi et al., 2009, Marcato et al., 2011b). In a study conducted by Levi *et al.*, it was found that ALDH1A1 deficiency did not affect the haematopoietic and neural stem cell function, while no reduction in ALDEFLUOR activity was observed. Other ALDH isoforms (ALDH2, ALDH3A1 and ALDH9A1) have been detected and suggested to contribute to ALDEFLUOR activity (Levi et al., 2009). In a recent study conducted by Van den Hoogen *et al.* (van den Hoogen et al., 2010), the ALDEFLUOR assay was used to identify prostate CSCs. The study reported high expression of other ALDH isoforms and only low ALDH1A1 expression. In this study, ALDH7A1 was highly expressed in prostate cancer cells lines, prostate cancer tissue and matched bone metastasis samples, suggesting that ALDH7A1 might contribute to the ALDH

activity of these cells (van den Hoogen et al., 2010, van den Hoogen et al., 2011).

Marcato *et al.* also showed that at least for breast cancer, ALDH1A1 expression is not the primary determinant of ALDH activity. Instead, a better correlation has been suggested with ALDH1A3, ALDH2, ALDH4A1, ALDH5A1, ALDH6A1 and ALDH7A1. However, knockdown studies showed that only reduction in ALDH1A3 expression resulted in the reduction of ALDH activity in ALDEFLUOR positive cells (Marcato et al., 2011b). Moreb *et al.* also reported that the enzymatic activity of ALDH1A2 and ALDH2 was detected by ALDEFLUOR assay (Moreb et al., 2012).

Based on the aforementioned studies, it is becoming increasingly clear that the ALDH isoform(s) responsible for ALDEFLUOR activity is/are likely to vary depending on cancer type and tissue or cell origin. In addition, the tissue specificity of the ALDH isoforms may determine their pattern of expression in cancers, which may have potential to be used as biomarkers (Marcato et al., 2011a).

There is also a technical limitation for detection of ALDH activity using the ALDEFLUOR assay and a fluorescent green emission. Some organs (such as the liver) are rich in endogenous fluorophores (flavins and NADPH for example) that auto-fluoresce in the green wavelength (480 –580 nm). In addition, green emission reduces considerably the choice of combining fluorescently labelled antibodies to further fractionate the $ALDH^+$ population and preclude its use for cell isolation in tissues from green fluorescent protein (GFP) transgenic mice. An inevitable overlapping of green

fluorescence emission into other channels is also problematic, and therefore "contamination" of ALDH expressing cells in other lineages can be high (Minn et al., 2014, Dollé et al., 2015).

1.4.5.1.3 AldeRed-588-A: New red substrate for detecting ALDH activity

Recently, Minn and co-workers have described a new red-shifted fluorescent ALDH substrate (AldeRed-588-A) for labelling of viable $ALDH^+$ cells. The authors demonstrated that Aldefluor and AldeRed-588-A essentially have the same efficacy and efficiency for identifying $ALDH^+$ cells as both have a common substrate moiety; acetaldehyde (Figure 7A). In addition, by successfully mixing the two substrates, Minn and colleagues proved that the labelling technique does not impede the structural recognition of the substrate by ALDH enzyme and that cell isolation of ALDH expressing cells is feasible by a single-step isolation method (Aldefluor and AldeRed-588-A are incubated simultaneously), thus avoiding additional purification or enrichment steps in which cells can be lost or damaged. This technical innovation opens new avenues for stem cell research by offering a greater flexibility for $ALDH^+$ cell isolations (Minn et al., 2014, Dollé et al., 2015).

Minn and co-workers also proposed a protocol for using AldeRed-588-A to overcome the above mentioned problems associated with the ALDEFLUOR assay. In addition, the authors showed the possibility of synthesising functional substrates for ALDH enzymes (Figure 7B). One could thus generate a library of fluorescently distinct substrates able to discriminate and fractionate stem cell populations by flow cytometry based on expression of specific ALDH isoenzymes (Minn et al., 2014, Dollé et al., 2015). However,

ALDH selectivity of these chemical probes still appears to be an issue and therefore the true value of using such probes to isolate CSCs remains unclear.

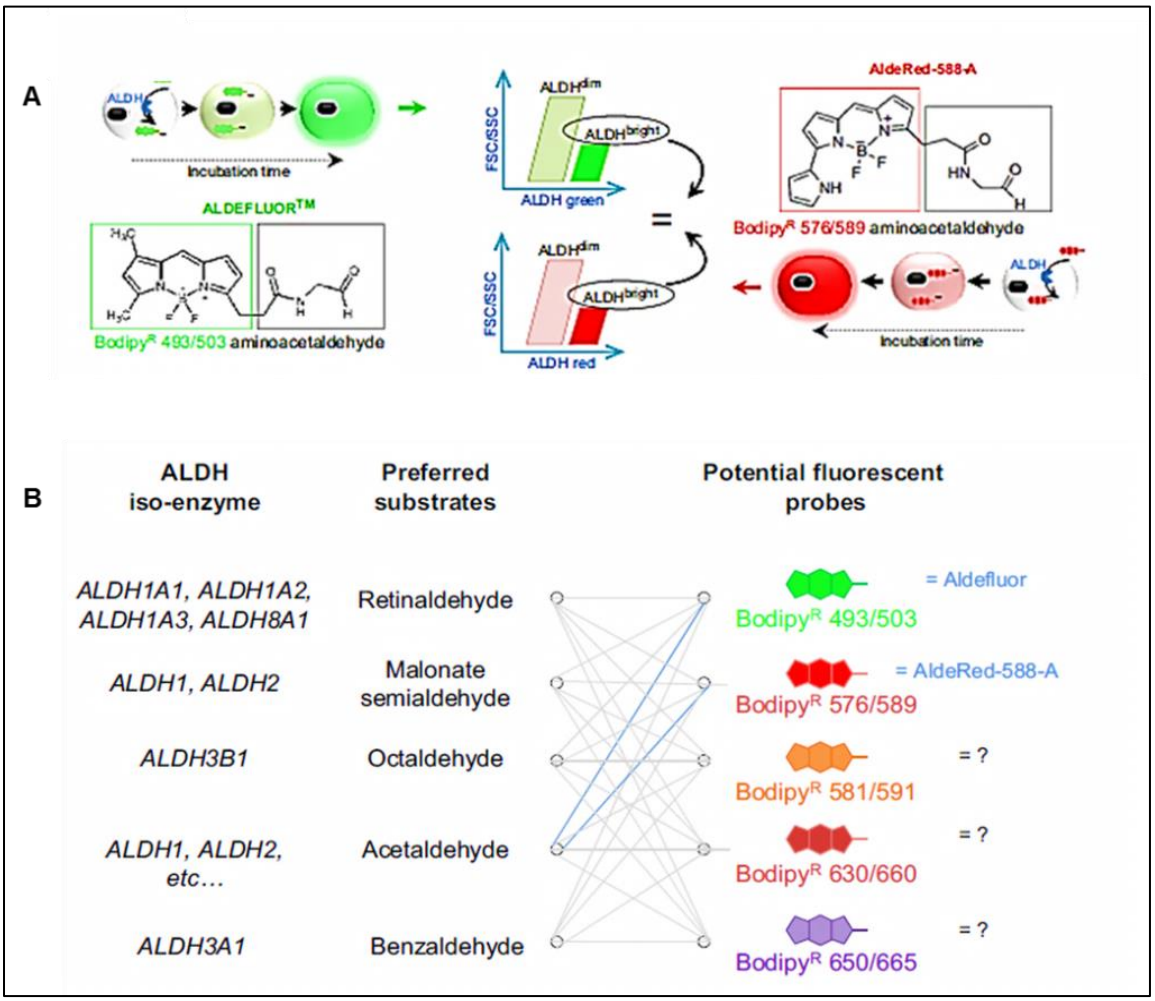

Figure 7 The Aldefluor and AldeRed-588-A substrates. Aldefluor and AldeRed-588-A have the same capacity to isolate an ALDHbright cell population enriched in stem cells from a heterogeneous mixture of cells (A). Emerging opportunities in generating preferred labeled substrates with different fluorescent probes (B). $ALDH^{bright}$, cells with high ALDH activity; $ALDH^{dim}$, low-ALDH-activity fraction. Adopted from (Dollé et al., 2015) and permission is not required for reuse in thesis.

1.5 The role of hypoxia in the regulation of ALDH expression

1.5.1 Hypoxia, oxidative stress and ALDH

Oxidative stress is defined as an imbalance between the production of free radicals and reactive metabolites, so-called oxidants or reactive oxygen species (ROS), and their elimination by protective mechanisms, referred to as antioxidants (Reuter et al., 2010). It is well known that high levels of ROS can occur in cancer cells as a result of increased basal metabolic activity, peroxisome activity, uncontrolled growth caused by cytokine signalling and oncogene activity (Fiaschi and Chiarugi, 2012). Enhanced activity of known ROS sources including NADPH oxidase or lipoxygenases were also described in cancer (Edderkaoui et al., 2005, Ushio-Fukai and Nakamura, 2008). In addition, low oxygen tension and hypoxia has been reported to be associated with an increase in ROS and oxidative stress that promotes tumour progression (Kondoh et al., 2013, Fiaschi and Chiarugi, 2012). The consequences of the production of oxygen radicals on cancer biology are pleiotropic and complex. ROS are reported to be tumorigenic by virtue of their ability to increase cell proliferation, survival and cellular migration (Reuter et al., 2010). Paradoxically high concentrations of ROS can trigger apoptotic or necrotic cell death (Reuter et al., 2010). ROS can initiate the oxidative degradation of biological membranes, known as lipid peroxidation (LPO) (Bartsch and Nair, 2006). In addition, it can attack DNA and proteins resulting in DNA strand breakage and enzyme inactivation, respectively (Fiaschi and Chiarugi, 2012). LPO is a self-perpetuating process and produces different types of aldehydes which can covalently bind biological

macromolecules producing similar damage such as caused by ROS (Bartsch and Nair, 2004). Aldehydes can also bind glutathione (GSH) causing depletion in GSH pools and as oxidative stress persists, cellular and intracellular redox balance becomes impaired (Brocker et al., 2011). Unhindered, the combined effects of ROS and LPO-derived aldehydes can significantly upset cellular homeostasis leading to apoptosis, cell cycle arrest and cellular senescence (Storz, 2005). Whether ROS promote tumour cell survival or are anti-proliferative depends on the cell and tissues, the location of ROS production, and the concentration of ROS produced (Storz, 2005).

Mounting evidence indicates that hypoxic cancer cells undergoing exposure to oxidative stress develop adaptive strategies to survive to the hostile milieu. These are indeed antioxidant responses that may result in increased aggressiveness (Fiaschi and Chiarugi, 2012). Examples of antioxidant systems that were found to be elevated in cancer include glutathione/glutathione peroxidase (GSH/GPX) (Fan et al., 2008), superoxide dismutase (SOD) and catalase enzymes (Hileman et al., 2004). These antioxidant mechanisms might also provide protection of cells against radiotherapy and chemotherapeutic drugs with activity mediated by production of ROS such as cisplatin, doxorubicin, and etoposide (Reuter et al., 2010, Balendiran et al., 2004, Storz, 2005). Genomic analysis showed that certain genes in the ALDH superfamily are also upregulated due to oxidative stress (Vasiliou and Nebert, 2005), which can explain the increased protection of the cell against oxidative insult by environmental chemicals and

drugs (Pappa et al., 2003a). Therefore, a possible link between ALDH and hypoxia signalling has been suggested (Kim et al., 2013).

1.5.2 Hypoxia and ALDH expression

Reisdorph and Lindahl studied the effects of hypoxia on constitutive and inducible ALDH3 gene expression (Reisdorph and Lindahl, 1998). It is known that ALDH3 gene is expressed differentially in a tissue-specific manner and occurring constitutively in some tissues like corneal epithelial cells. In addition, it is upregulated in tumours like hepatoma as a result of xenobiotic induction via the aryl hydrocarbon receptor (AhR)/ARNT pathway (Reisdorph and Lindahl, 1998). The results of this investigation showed that both constitutive and inducible ALDH3 expression can be downregulated by hypoxia. It has been speculated that this is due to limiting levels of ARNT (HIF-1β) being shared by two pathways, which under hypoxic condition forms heterodimers with HIF-1α and thus is not available to interact with critical xenobiotic response element (XREs) required for ALDH3 expression. Nonetheless, in a later study done by the same group, it was shown that ARNT is not the limiting transcription factor (Reisdorph and Lindahl, 2001). Therefore, further investigations are needed to explain the mechanism behind the down-regulation of ALDH3 under hypoxic conditions.

Recently, a link between ALDHs and hypoxia in CSCs has also been reported by Nagano *et al.* who showed that elevated ALDH activity may affect the proliferation and differentiation of mesenchymal SCs during hypoxia (Nagano et al., 2010). However, Hasmim *et al.* have examined the effect of hypoxia exposure of IGR-Heu, a NSCLC cell line on the expression

of ALDH1 and found that ALDH1 levels were not influenced by exposure to hypoxic stress (Hasmim et al., 2011). In a recent study conducted by Kim *et al.* the link between ALDH and hypoxia signalling was investigated in breast cancer (Kim et al., 2013). Exposure of breast cancer cells to hypoxia did not affect expansion of ALDEFLUOR$^+$ cells. In contrast, a robust increase in HIF-2α was reported in ALDEFLUOR$^+$ cells grown under normoxia. This elevation in expression was also observed under hypoxic conditions compared with ALDEFLUOR$^-$ cells. Further investigations showed that ALDH was highly correlated with the HIF-2α expression in breast cancer cell lines and primary tissues. Treatment of 4T1, a breast cancer cell line, with DEAB downregulated the expression of HIF-2α, leading to suppressed *in vitro* self-renewal ability and *in vivo* tumour initiation of ALDEFLUOR$^+$ cancer cells (Kim et al., 2013). Based on these results it was suggested that ALDH activity promotes cancer stemness through a novel mechanism that involves the upregulation of HIF-2α (Kim et al., 2013).

1.6 Aims and objectives

As reviewed in the preceding sections, much is to be understood about the impact of hypoxia on cancer aggressiveness and treatment outcome, which include identification and characterisation of TICs/CSCs that gives better understanding of drug resistance. ALDHs are emerging as a class of enzymes that appear to play a number of roles within the tumour microenvironment, but their expression and regulation is not well understood. The purpose of this study was to unravel the impact of hypoxia on ALDH expression and lay the foundation for future exploration of these enzymes in the stem cell component associated with CRC. The hypothesis is the expression of ALDH in cancer cell lines is modulated by hypoxia and may contribute to cell proliferation and migration. Specifically, the objectives of this research were:

1. To study the gene and protein expression of ALDH isoforms in CRC 2D/3D cancer models and xenograft tissues (Chapter 2).
2. To carry out siRNA knockdown studies of selected ALDH isoforms (ALDH1A3, 3A1 and 7A1) using both normoxic and hypoxic conditions, in an attempt for better understanding of their functional roles in CRC and drug treatment (Chapter 3).
3. To explore ALDH7A1 function using an isogenic lung cancer cell line pair (H1299/RFP and H1299/ALDH7A1-transfected) and identify small molecules that can be used to interrogate ALDH7A1 functional role (Chapter4).

Chapter 2: The impact of hypoxia on the expression of aldehyde dehydrogenases in 2D and 3D colorectal cancer models

2.1 Introduction

Colorectal cancer (CRC) is the second leading cause of cancer deaths with a worldwide cumulative incidence rate of 9.4%. In the UK, it is the third most common diagnosed type of cancer, with around 40,000 new cases diagnosed every year (Botchkina, 2013).

The colon (large intestine) refers to that part of the digestive system that is responsible for water absorption as the digested food passes through it and is divided into 5 parts; ascending, transverse, descending, sigmoid colon and the rectum (American Cancer Society, 2014). Cancer can occur in any part of the colon and starts in the innermost layer where most of the cancerous cells begin as a small growth on the lining wall called polyps or adenomas (Figure 8). These polyps are premalignant and if left untreated may become cancerous and grow into the muscle layers and penetrate the colon wall (Lee et al., 2006). The cancer can then invade into adjacent organs such as the bladder or prostate gland or it can spread through the lymphatic system to the lymph nodes such as the abdominal lymph nodes. CRC can also spread to other parts of the body through the bloodstream with the liver being the most common site of metastasis (Fidler, 2003).

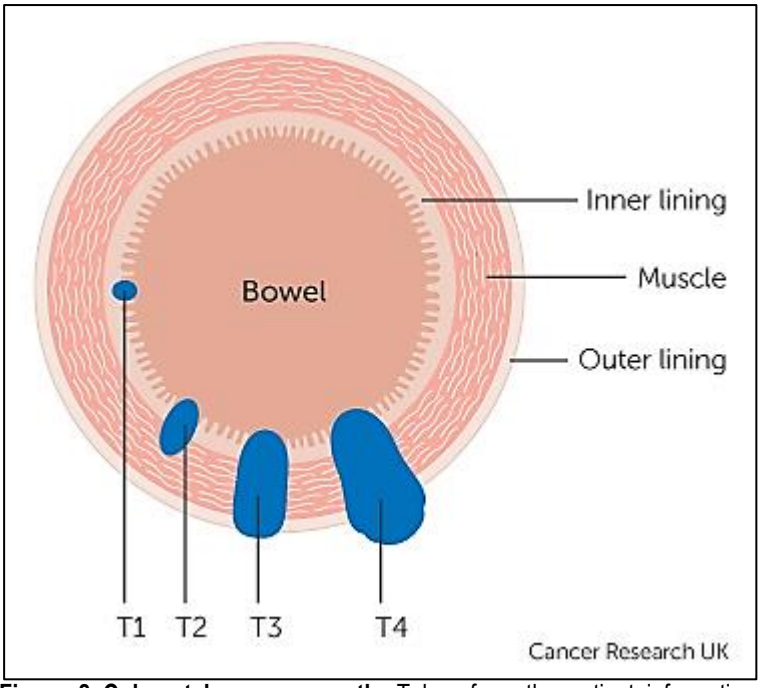

Figure 8 Colorectal cancer growth. Taken from the patient information website of Cancer Research UK with permission: http://www.cancerresearchuk.org/about-cancer/ (Cancer Research UK, 2016).

More than 95% of CRCs are adenocarcinomas that have originated in the glandular cells of the wall lining, although other types of cancer can also occur such as squamous cell carcinoma, carcinoid or sarcoma (Cuffy et al., 2006). TNM is the most common staging system used for CRC and stands for tumour, node and metastasis, respectively (Quirke et al., 2007). This staging system describes the size of a primary tumour (T), whether any lymph nodes contain cancer cells (N), and whether the cancer has spread to another part of the body (M) (Table 6). The number staging system is usually used by doctors to group CRC and contains 5 main stages (Puppa et al., 2010) (Table 7).

T	Describes the size of the tumour
T1	The tumour is only in the inner layer of the bowel.
T2	The tumour has grown into the muscle layer of the bowel wall.
T3	The tumour has grown into the outer lining of the bowel wall.
T4	The tumour has grown through the outer lining of the bowel wall. It may have grown into another part of the bowel, or other nearby organs or structures. Or it may have broken through the membrane covering the outside of the bowel (the peritoneum).
N	**Describes whether cancer cells are in the lymph nodes**
N0	There are no lymph nodes containing cancer cells.
N1	1 to 3 lymph nodes close to the bowel contain cancer cells.
N2	There are cancer cells in 4 or more nearby lymph nodes.
M	**Describes the presence of metastasis**
M0	The cancer has not spread to other organs.
M1	The cancer has spread to other parts of the body.

Table 6 TNM staging system of colorectal cancer. Taken from the patient information website of Cancer Research UK with permission: http://www.cancerresearchuk.org/about-cancer/ (Cancer Research UK, 2016).

Stage	Description
0	Carcinoma *in situ.*
1	The cancer has grown through the inner lining of the bowel, or into the muscle wall, but no further. There is no cancer in the lymph nodes (T1, N0, M0 or T2, N0, M0).
2	**2a**: the cancer has grown into the outer covering of the bowel wall but there are no cancer cells in the lymph nodes (T3, N0, M0). **2b**: the cancer has grown through the outer covering of the bowel wall and into tissues or organs next to the bowel (T4). No lymph nodes are affected (N0) and the cancer has not spread to another area of the body (M0).
3	**3a**: the cancer is still in the inner layer of the bowel wall or has grown into the muscle layer. Between 1 and 3 nearby lymph nodes contain cancer cells (T1, N1, M0 or T2, N1, M0). **3b**: the cancer has grown into the outer lining of the bowel wall or into surrounding body tissues or organs. Between 1 and 3 nearby lymph nodes contain cancer cells (T3, N1, M0 or T4, N1, M0). **3c**: the cancer can be any size and has spread to 4 or more nearby lymph nodes. The cancer has not spread to any other part of the body (any T, N2, M0).
4	The cancer has spread to other parts of the body (such as the liver or lungs) through the lymphatic system or bloodstream (any T, any N, M1).

Table 7 The number staging system of colorectal cancer. Taken from the patient information website of Cancer Research UK with permission: http://www.cancerresearchuk.org/about-cancer/ (Cancer Research UK, 2016).

.

Treatment of CRC relies mainly on the excision of the colon with the adjacent lymph nodes. However, neoadjuvant or adjuvant chemotherapy with or without radiotherapy are often required depending on the location of the tumour and its stage. Laparoscopic colectomy is the treatment of choice for patients with early stages (I or II) of CRC (Lacy et al., 2002). However, the benefit of including adjuvant therapy in stage II disease remains unclear and controversial but might be considered in patients at high risk. Patients presenting with regional or distal metastasis (stage III and IV), are usually treated with a combination of surgical and other therapeutic modalities (Kozovska et al., 2014).

When a chemotherapeutic regimen is indicated, a combination of conventional cytotoxic drugs including 5-Fluorouracil (5-FU)/ leucovorin with oxaliplatin (FOLFOX) or irinotecan (FOLFIRI) is usually used (de Gramont et al., 2000, Douillard et al., 2000). Recently, targeted therapy has also been shown to be effective for CRC treatment. For example, cetuximab and panitumumab, two monoclonal antibodies that target the epidermal growth factor receptor (EGFR), have been shown to be effective in combination with chemotherapy or as single agents in patients with wild-type KRAS-CRC tumours (Lièvre et al., 2006). In addition, antiangiogenic therapy targeting vascular endothelial growth factor (VEGF) (e.g. bevacizumab) confers a benefit when used in combination with chemotherapy (Giantonio et al., 2007).

FOLFOX, FOLFIRI and the newer molecularly-targeted therapies only offer a modest improvement in overall survival rates in patients with

advanced/metastatic CRC. In part, this is due to the emergence of drug resistance and in part due to insufficient and/or selective delivery of the drugs. The failure rate in the adjuvant setting is 30% for high-risk stage II and stage III patients, and overall response rate is 60% for patients with stage IV CRC (Langan et al., 2013). In addition, nearly 50% of CRC patients develop recurrent disease, and patients with advanced and metastatic CRC still succumb to this disease. The major reason is ascribed to the heterogeneity of CRC and the presence of cancer stem cells (CSCs) in the tumour mass; the latter are essentially resistant to current therapeutic strategies due to their infrequent capacity to divide (Kumar et al., 2014). Therefore, significant advance in the treatment care of CRC patients could be realised by (i) the use of biomarkers that can accurately identify patients at-risk for disease recurrence and dissemination, along with those that fail to respond to systemic therapy (Langan et al., 2013), (ii) the development of highly selective therapies targeting oncogenic drivers such as BRAF and KRAS (Lièvre et al., 2006) and/or the CSC population (Pors and Moreb, 2014) and (iii) a better understanding of how and when to use the various treatment modalities in combination (Soreide et al., 2011).

There is accumulating evidence for the existence of CSCs in human CRC. Identification and isolation of CSCs in CRC is usually based on cell surface marker such as CD133 and CD44, though they are not specific (Horst et al., 2009, Shmelkov et al., 2008). Two transcription factors, Oct-4 and Sox2, may be more promising CSC markers as they have been found to be elevated in CRC, correlating with increased CSC proliferation and poor prognosis

(Saigusa et al., 2009). Recently, aldehyde dehydrogenase 1 (ALDH1) has been shown to be a specific marker for identifying, isolating, and tracking human colonic SCs during CRC development (Huang et al., 2009). Immunostaining showed that $ALDH1^+$ cells are sparse and limited to the bottom of normal crypts, where SCs reside. However, during progression from normal epithelium to mutant adenomatous polyposis coli (APC) epithelium to adenoma, $ALDH1^+$ cells increased in number and became distributed further up the crypt. In addition, flow cytometric isolation of cancer cells based on enzymatic activity of ALDH (ALDEFLUOR assay) and implantation of these cells in non-obese diabetic–severe combined immunodeficient mice resulted in the generation of xenograft tumours even after implantation of as few as 25 cells (Huang et al., 2009). Carpentino *et al*. showed that ALDH1 can be used as a marker for tumour-initiating cells (TICs) not only from colon cancer but also from colitis (Carpentino et al., 2009). Cells were isolated from patients with chronic ulcerative colitis using FACS and showed both their transition to cancer stem-like cells in xenograft studies as well as their ability to generate three-dimensional spheres *in vitro* (Carpentino et al., 2009).

Proteomic analysis of the secretomes of CSCs isolated from three distinct metastasised colon tumours has also shown that these cells secrete high levels of drug-metabolising enzymes, including ALDH1A1 (Emmink et al., 2013). This isoform has been shown to be involved in causing resistance to a number of anticancer agents (Chapter 1, Introduction, section 1.4.4) and extracellular detoxification of prodrugs of alkyating agents such as

maphosphamide and thus contributes to CSC-intrinsic drug-resistance (Emmink et al., 2013).

Most of these and other studies used the ALDEFLUOR assay and confirmed it as an effective method for detection and isolation of CSCs (Guo et al., 2014) (Chapter 1 Introduction, sections 1.4.5.1.1-2). In addition, the metabolic function of ALDH1A1 was proposed to confer the ‘‘stemness’’ properties of normal and cancer SCs. However, the identity of ALDH isoforms that contribute to the enhanced ALDH activity were not identified. Chen *et al*. examined the expression profile of ALDH1A1 and ALDH1B1 in human adenocarcinomas of colon and other cancer tissues (Chen et al., 2011). The immunohistochemical expression of ALDH1A1 or ALDH1B1 showed approximately a 5-fold higher expression score for ALDH1B1 in cancerous tissues than that for ALDH1A1 and 39/40 colonic cancer specimens were stained positive for ALDH1B1. The study demonstrated that ALDH1B1 rather than ALDH1A1 is a potential biomarker for human colon cancer (Chen et al., 2011).

In addition to the potential role of ALDH isoforms as a biomarker for CRC and stem cell isolation, recent studies also described the role of ALDH in CRC drug resistance and cancer recurrence. Touil *et al*. reported the upregulation of ALDH1A3 in 5-FU resistant cells compared to the parental HT29 cells (Touil et al., 2014), indicating that colon cancer cells may escape 5-FU chemotherapy-induced cell death by entering a stemness state. Deng *et al.* 2014 showed that ALDH1 is an independent prognostic factor for patients with stages II–III rectal cancer after receiving radio-chemotherapy.

Specifically, preoperative treatment of rectal cancer upregulated the expression of ALDH1, while high ALDH1 expression post-treatment predicted poor prognosis for patients after neoadjuvant therapy; 40% of the patients with high ALDH expression suffered recurrence during the follow-up compared to no recurrence in the patients with low ALDH expression (Deng et al., 2014).

ALDH has also been described to be involved in CRC metastases. Mechanically-induced colon cancer cells with increased metastatic potential revealed that ALDH3A1 but not ALDH1 was among the genes that were highly upregulated, correlating with cancer cell migration and invasion (Tang et al., 2014).

The tumour microenvironment, including stromal component, is a key player in stimulating tumour proliferation, aggressiveness and drug resistance (Mathonnet et al., 2014). The dynamic interactions between CSCs and the microenvironment result in a continuous remodelling of both compartments, promoting metastasis and development of chemoresistance (Maugeri-Saccà et al., 2011). Increasing reports indicate that hypoxia may serve as a critical regulator of the CSCs pool. It is well known that hypoxia activates hypoxia-inducible factors (HIFs), which trigger adaptive changes at multiple levels, including angiogenesis. However, the neovasculature is chaotic and dysfunctional and thus prohibits the accrual of optimal concentrations of chemotherapeutic agents within the tumour (Wilson and Hay, 2011). Besides this mechanistic hypoxia-mediated drug resistance, direct evidence also connects HIF and CSCs. Cancer cells cultured under low oxygen conditions

or low pH express higher levels of stem cell markers, which acquire a stem-like phenotype and overexpress stemness-related genes (Heddleston et al., 2010). Furthermore, it has been proposed that hypoxic areas within a tumour act as niche for CSCs (Maugeri-Saccà et al., 2011). Therefore, targeting these effectors will more effectively deplete the CSC pool and contribute to increased chemotherapeutic response (Maugeri-Saccà et al., 2011).

Given the importance of hypoxia on tumourigenesis and resistance, information about how selective ALDHs adapt to hypoxia and oxidative stress within the tumour microenvironment could have a profound impact on the understanding of drug resistance and the identification and characterisation of TICs/CSCs in CRC. The hypothesis of this Chapter is ALDH expression is modulated by tumour hypoxia and the objectives were:

1. To study the gene and protein expression of ALDH isoforms in a panel of CRC cell lines.
2. To evaluate the impact of hypoxia on the expression of ALDH in CRC monolayer cells.
3. To evaluate the expression of ALDH in CRC multicellular spheroids (MCS).
4. To evaluate the expression of ALDH in CRC xenografts.
5. To assess if HIF-1 or HIF-2 is responsible for inducing the expression of ALDH.

2.2 Materials and Methods

2.2.1 The expression of ALDH in a panel of colorectal cancer cell lines

2.2.1.1 Cell culture

Mammalian cancer cell lines were obtained from the American Type Culture Collection (ATCC). Cells were at passage 0 and grown in complete RPMI 1640 medium (Sigma) at 37^{o}C, 5% CO_2 and 100% humidity (Table 8). Passaging of these cells was carried out when the cells were 75% confluent. See Appendix I for the composition of the cell culture media.

Cell line	Origin of cell line	Culture medium	Frequency of subculture	Dilution upon subculture
DLD-1	Dukes' type C, colorectal adenocarcinoma, adult male.	RPMI 1640	4-5 days	1:10 - 2:10
HCT116	Primary colorectal carcinoma, adult male.	RPMI 1640	3-4 days	1:8 - 1:10
HT29	Primary colorectal adenocarcinoma, 44 years adult female, Caucasian.	RPMI 1640	4-5 days	1:10
SW480	Dukes' type B, colorectal adenocarcinoma, 50 years male, Caucasian	RPMI 1640	3-4 days	1:8 - 1:10

Table 8 Culture of colorectal cancer cell lines.

2.2.1.1.1 Passaging of mammalian cells

Prior to passaging the cells, the old medium was removed and discarded from each 75 cm^2 flask. The cells were washed twice with 10 ml of phosphate buffered saline (PBS) (Sigma), which was removed and discarded. A brief pre-treatment of the cells with 1 ml of 0.25% trypsin/EDTA (Sigma) was carried out when flasks were 75% confluent. In order to degrade the protein attachments between the cells and flask surface, a

further 2 ml of trypsin/EDTA was added to the flask and allowed to cover the cell surface to cause cell detachment. Flasks were incubated at 37^{o}C for about 5 min before the cells were checked under a light microscope to confirm that they were detached. Trypsin was inhibited by the addition of 8 ml complete RPMI medium to the flask. After gentle pipetting up and down several times, the content of the flask was added to a 20 ml universal tube and the cells were centrifuged at 1,000 rcf for 5 min. The medium was carefully discarded to prevent the loss of cell pellets and 10 ml of fresh medium was added and mixed vigorously by vortexing to re-suspend the cells. The required amount of cell suspension was added to 10 ml of fresh medium in a new 75 cm^{2} flask before incubation at 37^{o}C, 5% CO_2 and 100% humidity.

2.2.1.1.2 Determination of the cell concentration

To determine the cell concentration, the live cell number was counted using a haemocytometer. 100 µl of 0.4% Trypan Blue Stain (Sigma) and 100 µl of cell suspension were added to a 1.5 ml microcentrifuge tube and mixed vigorously by vortexing. 10 µl of cell /Trypan mixture was transferred to each chamber of the haemocytometer by pipetting under the cover slip and allowing the chamber to be filled by capillary action. Under the light microscope, using the 10× objective lens and focusing on the gridlines of the chamber, the live cells (not blue) were counted in the central and the four squares of the corners of each chamber. Cells that were on the lines were counted only if they lied on the top and right-hand lines of each square.

Cell concentration was calculated using this formula:

Cells/ml = Average number of cells in one large square × dilution factor* × 10^4**.

*Dilution factor was 2 (1 volume cell suspension: 1 volume of Trypan blue).

**10^4 is the conversion factor to convert 10^{-4} ml (volume of one large square) to 1 ml.

2.2.1.2 Exposure of CRC cell lines to hypoxia

The CRC cell lines were seeded at a concentration of 2×10^5 cells in 75 cm^2 flasks and incubated at normoxic conditions (37ºC, 5% CO_2 and 100% humidity). Subsequently, cells were incubated either at normoxic conditions (control) or exposed to hypoxia (0.1% O_2, 95% N_2, 5% CO_2 and 100% humidity) for 6h, 24h or 48h prior to cell harvesting for gene extraction and protein extraction. The medium was replaced with fresh RPMI, which had been adapted to hypoxic conditions overnight using a hypoxic chamber (Whitley H35 hypoxystation). Cell harvesting was done on day 5 when the cells were ≈ 75% confluent.

To see whether the cells were alive after exposure to hypoxia, cells in flasks were stained with haematoxylin. In brief, medium was removed and cells were fixed with 70% ethanol (1-2 min). Cells were then stained with Harris' haematoxylin (Sigma) for 5 min and washed in running tap water for 5 min. Photos were taken using 10 × objective lens on an inverted microscope (Nikon ECLIPSE TE2000-U).

2.2.1.3 Analysis of ALDH gene expression of CRC cell lines using quantitative real time polymerase chain reaction (qRT-PCR)

2.2.1.3.1 Cell harvesting

The CRC cell lines which were exposed to normoxic or hypoxic conditions were washed with PBS and detached from the flask surface after trypsinisation. 2×10^6 cells were collected in 20 ml universal tube and centrifuged at 1,000 rcf for 5 min. Medium was discarded and 1 ml of PBS was added to the cell pellet, mixed with cells by pipetting before the cells were collected in 1.5 ml microcentrifuge tube and centrifuged for 5 min at 3,000 rcf. After centrifugation, PBS was discarded and the dry pellet was then processed for RNA extraction.

2.2.1.3.2 RNA extraction and quantification

Total RNA was extracted from the pellets isolated from CRC cell lines (exposed to normoxic or hypoxic conditions) using RNeasy Mini Kit (QIAGEN) according to the manufacturer's instructions. In brief, cells were disrupted in the lysis buffer and homogenised using motor and pestle. 70% ethanol was added to the homogenised lysate and mixed well by pipetting. The supernatant was transferred to an RNeasy spin column (QIAGEN) placed in a 2 ml collection tube (QIAGEN) and centrifuged for 15 seconds (s) at 8,000 rcf. The spin column membrane was washed one time with RW1 buffer before doing on-column DNase digestion with the RNase-Free DNase set (QIAGEN). In brief, DNase I incubation mix was prepared from DNase I stock solution according to the manufacturer's instructions. The DNase I incubation mix was added directly to the RNeasy spin column membrane

and placed on the benchtop for 15 min. Next, the spin column membrane was washed several times to avoid carry over of ethanol. Finally RNA was eluted by adding 30 µl of RNase-free water and centrifuged for 1 min at 8,000 rcf. The quantity and quality of RNA was evaluated by measuring the absorbance of UV light and calculating the 260/280 ratio using NanoDrop™ 1000 spectrophotometer (Thermo Scientific). Subsequently, samples were used for complementary DNA (cDNA) synthesis and stored at -80ºC until required.

2.2.1.3.3 Complementary DNA synthesis

Single stranded cDNA was synthesised from total RNA in 20 µl reaction volumes using AffinityScript QPCR cDNA Synthesis Kit (Agilent Technologies) by adding the following component in order: RNase-free water, 10 µl first strand master mix (2x) containing optimised buffer, $MgCl_2$ and dNTPs, 3 µl of random primer (0.1 µg/µl), 1 µl AffinityScript reverse transcriptase/ RNase Block enzyme mixture and 1 µg of specimen RNA. Reactions were carried out in a MJ Research PTC-200 Peltier thermal cycler using the conditions listed in Table 9. The completed first-strand cDNA synthesis reaction was stored at -20ºC until required.

Step	Time	Temperature
Incubation/ primer annealing	5 min	25ºC
cDNA synthesis	15 min	42ºC
Enzyme inactivation	5 min	95ºC

Table 9 Cycling conditions of cDNA synthesis.

2.2.1.3.4 QRT-PCR primers design

QRT-PCR assays were designed by PrimerDesign Ltd. PrimerDesign provides custom designed qRT-PCR assays for human, mouse, rat and other species genes in addition to high quality qRT-PCR assays for housekeeping genes. Assays are available with PerfectProbe, Double-Dye (Taqman style) probe or as primer only kits for use with SYBR Green chemistry. Every assay was individually designed to custom requirements and after synthesis they were fully validated on relevant biologically derived cDNA for priming specificity and amplification efficiency at optimal concentrations to ensure that the kit worked to the highest standards. Here, custom designed homo sapiens qRT-PCR assays for use with SYBR Green were used. Detailed information of the qRT-PCR assays is listed in Appendix III.

2.2.1.3.5 QRT-PCR method

QRT-PCR was set up in 96-well plate (MicroAmp^{TM}) in triplicate for each gene of interest in a UV- irradiated hood on 7500 RT-PCR System (Applied Biosystem). The assay was performed using 20 µl reactions consisting of 1 µl of forward and reverse primers mix for the target genes ALDH1A1, 1A2, 1A3, 1B1, 2, 3A1, 7A1, VEGFA and β-actin (working concentration of primers = 300 nM), 10 µl of PrimerDesign 2x Precision^{TM} Mastermix, 4 µl of RNAse/DNAse free water (all from PrimerDesign) and 5 µl of diluted cDNA [cDNA reactions were diluted 1:10 (10µl of cDNA and 90µl of water)]. VEGFA was used as a positive control gene for hypoxic conditions and β-actin was used as a housekeeping gene for the normalisation of the reaction.

For each assay, “no reverse transcription” controls and “no template” controls were included as negative controls. For the cycling conditions, see Table 10. A post PCR run melt curve (dissociation curve) was used to prove the specificity of the primers.

Stage	Repetition	Step	Time	Temperature
1	1	Enzyme activation	10 min	95ºC
2	50	Denaturation	15s	95°C
		Data collection	60s	60°C
3	1	Melt curve	15s	95°C
			60s	60°C
			15s	95°C

Table 10 Q-RT-PCR cycling conditions.

2.2.1.3.6 Data analysis

The qRT-PCR assay chosen in this study is based on measuring fluorescence using fluorescent reporter molecule such as SYBR Green. The fluorescence intensity increases proportionally with each amplification cycle in response to the increased target concentration, with the RT-PCR instrument systems (7500 Applied Biosystem) collecting data for each sample during each PCR cycle. The first cycle at which the amplification generated fluorescence can be detected as being above the ambient background signal is called the “Ct” or threshold cycle. The numerical value of the Ct is inversely related to the amount of target in the reaction (i.e., the lower the Ct, the greater the amount of target) (Schmittgen et al., 2008).

Relative quantification was used to evaluate the expression of the gene of interest in comparison to the housekeeping gene β-actin. ΔCt method was used to calculate the relative expression of the gene of interest. This method uses Ct values and inversely correlates with gene expression (the highest ΔCt value is the lowest expression). The ΔCt values were calculated using the following equation and these values were compared between samples being analysed:

ΔCt (sample) = Ct gene of interest - Ct internal control gene

$2^{-\Delta\Delta Ct}$ method was used to compare the fold change of gene expression between cells exposed to hypoxic conditions and cells exposed to normoxic conditions (control cells). ΔCt value was firstly calculated for each sample or control cells using the following equation:

ΔCt (sample) = Ct gene of interest - Ct internal control gene

ΔCt (control cells) = Ct gene of interest - Ct internal control gene.

Next, the ΔΔCt value for each sample was calculated using the following equation:

ΔΔCt = ΔCt (sample) - ΔCt (control cells)

Finally the ΔΔCt formula was used to estimate the normalised fold differences between hypoxia and normoxia exposed cells (Fold change = $2^{-\Delta\Delta Ct}$).

2.2.1.3.7 Statistical analysis

The significance of results was assessed through a comparison of means using two-tailed student t-test. Results were expressed as the mean ± standard deviation. P values were calculated to determine statistical significance of the results.

2.2.1.4 Analysis of ALDH protein expression of CRC cell lines using western blot

2.2.1.4.1 Sample preparation

The selected CRC cell lines were cultured and exposed to hypoxia as outlined in section 2.2.1.2. After exposure to hypoxia, cells were harvested as described in section 2.2.1.3.1. The supernatant was removed and cells were resuspended in 300 µl RIPA lysis buffer (see Appendix IV for western blot buffers and solutions). Cell suspensions were kept on ice under constant agitation for 15-20 min, followed by sonication (10s, 3 cycles at power 10) twice; between the two sonication steps, samples were kept on ice for 30s. Next, samples were centrifuged at 13,200 rcf for 15 min at 4ºC. Supernatants were removed to new microcentrifuge tubes. The protein concentration was determined using BCA protein assay kit (Thermo Scientific Pierce). Samples were then resuspended in 4x Laemmli's loading buffer [Appendix IV, (2:3, sample: total volume)] containing β-mercapto ethanol (6 % v/v) and subsequently denatured at 95ºC for 5 min. Finally, the samples were allowed to cool down at room temperature and kept at -20ºC for later use.

2.2.1.4.2 Determination of protein concentration

Protein standards ranging from 0 mg/ml to 2 mg/ml were prepared by serial dilution of bovine serum albumin standard (BSA, 2 mg/ml) (Thermo Scientific Pierce) in distilled water. 10 µl of BSA dilutions were added to the standard wells of 96 well plates (Nure 96-well collection plates), 10 µl of distilled water were added to the blank wells and 2 µl of the cell lysate were added to the sample wells. 50 parts of reagent A and 1 part reagent B (both provided in Thermo Scientific Pierce BCA kit) were mixed vigorously and 200 µl of this mixture was added to each well. The plate was incubated for 30 min at room temperature before the absorbance was measured using a spectrophotometer. A standard curve was created for protein standards using SkanIt Software 2.4.4 RE for Multiskan Spectrum and the protein concentration of the samples in loading buffer was calculated.

2.2.1.4.3 Polyacrylamide gel preparation

The gel loading assembly (Bio-Rad) was cleaned with 70% ethanol and assembled as directed by the manufacturer's instructions. A 12% resolving gel was prepared and pipetted into the assembled apparatus (Appendix IV). 0.5 ml of 0.1% (w/v) sodium dodecyl sulphate (SDS) was added above the resolving gel which was allowed to set at room temperature for at least 1 h. After discarding the SDS, a 5% stacking gel was prepared and pipetted above the resolving gel (Appendix IV). A gel comb was inserted and the gel was allowed to set at room temperature for at least 30 min. The comb was then removed and the gel apparatus was transferred to an electrophoresis buffer tank (Bio-Rad) filled with 1x running buffer (Appendix IV). The

denatured samples containing 50 µg of protein were loaded in the gel wells as well as 8 µl of pre-stained protein ladder (Fermentas PageRuler™ Plus, Thermo Scientific Pierce). The gel was run at 70 volt for 1h followed by 120 volt for 1:30h.

2.2.1.4.4 Protein transfer to nitrocellulose membrane

Following electrophoresis, wet blotting was carried out using nitrocellulose membrane (GE health care Life Sciences) soaked up in 1x transfer buffer (Appendix IV). Transfer was carried out at 35 amps overnight.

2.2.1.4.5 Immunodetection of electrophoresed proteins after transfer to nitrocellulose membrane

Nitrocellulose membrane was placed over clean tissue and allowed to dry at room temperature (3 × 15 min) then washed in PBS Tween 20 (PBST, Appendix IV) for 10 min on a shaker (20 rpm). The membrane was then placed in 25 ml of 5% blocking solution (5% w/v non-fat milk:PBST, (Appendix IV) on a shaker. The blocking solution was discarded and replaced with 20 ml of 5% blocking solution containing one of the unconjugated primary antibodies (1A1, 1A2, 1A3, 3A1, 7A1 and LDH-A) (Table 15, Appendix V).

The membrane with the primary antibody was incubated at 4ºC on a shaker overnight. Next, the membrane was washed with PBST (3 × 5 min) and subsequently incubated with 20 ml of 5% blocking solution containing horseradish peroxidase (HRP) based secondary antibody (Table 15, Appendix V) for 1h on a shaker. Finally, the membrane was washed with PBST (3 × 5 min) and then prepared for the detection of the bands.

2.2.1.4.6 Enhanced chemiluminescent detection

The membrane was developed using the enhanced chemiluminescent system (Roche). The detection solution was prepared according to the manufacturer's instructions. The excess washing buffer was drained off and the prepared detection solution was pipetted on the membrane with the surface protein side up. After incubation at room temperature for 1 min, excess of detection reagent was removed and the membrane was placed on X ray film (Amersham hyperfilm^{TM} ECL, GE Healthcare) processor before being developed using Ilford developer and fixer solutions (Developing: 2 min, d.H_2O wash, Fixation: 2 min and final d.H_2O wash) (Appendix IV). The same membrane was washed with PBST (3 × 5 min) and re-blotted with primary and secondary antibodies to detect actin protein (Table 15, Appendix V).

2.2.1.4.7 Data analysis

Image J software was used to measure the intensity of detected bands. The expression level of a target protein was normalised to the actin protein of the same sample. In order to calculate the fold change in the expression of the target protein upon exposure to hypoxia, the expression level in hypoxic samples was normalised to normoxic controls.

2.2.2 The expression of ALDH in colorectal cancer spheroids

2.2.2.1 Spheroids culture

2.2.2.1.1 Spheroids formation

Three-dimension (3D) multicellular spheroids were generated from HT29 and DLD-1 CRC cell lines using the spinner flask culture technique (O'Connor, 1999). HT29 or DLD-1 cells were seeded in 250 ml spinner flasks at a concentration of 4×10^6 cells in 100 ml complete RPMI, incubated at 37ºC on a magnetic stirrer plate (Techne, Bibby Scientific Limited, Stafford, UK) and stirred at 60 rpm. Medium was added to make up 250 ml and renewed every two days. Photos were taken at 10 × objective lens on an inverted microscope (Nikon ECLIPSE TE2000-U).

2.2.2.1.2 Spheroids growth curve

The diameter of HT29 and DLD-1 spheroids was measured from day 3 and every other day during the culture period using calibrated graticule fixed to the light microscope at 10 × objective lens. Results were plotted as a graph with the mean of the diameters of at least 20 spheroids on the Y-axis and time (day) on the X-axis.

2.2.2.2 Histology of spheroids

2.2.2.2.1 Fixation

DLD-1 and HT29 spheroids were transferred from spinner flasks to a 20 ml universal tube. All medium was removed and replaced with the fixative agent Bouin's solution (Sigma). The spheroids were incubated in Bouin's solution for 75 min at room temperature and then washed in 70% ethanol to remove

excess fixative. The spheroids were left in 70% ethanol at room temperature until processing.

2.2.2.2.2 Processing

The 70% ethanol was replaced with 90% ethanol for 60 min at room temperature, which was discarded and replaced with 100% ethanol for 30 min (100% ethanol wash was repeated twice). Ethanol was then removed and replaced with xylene for 30 min (xylene wash was repeated one more time). The spheroids were transferred from the universal tube to an embedding mould. Any excess xylene was removed and the mould was filled with paraffin wax. The spheroids were allowed to settle down in the wax and incubated for 30 min at 68ºC in the warming oven. The waste wax was pipetted off and replaced with fresh wax and returned to the warming oven for another 30 min (repeated twice). The mould was then allowed to set on a cold stage.

2.2.2.2.3 Sectioning

The wax blocks were stored at -20ºC overnight. Sections (5 µm thick) of paraffin embedded spheroid blocks were cut using a microtome and mounted on Superfrost Plus slides (BDH, Poole, UK). Slides were allowed to dry on a heated stage at 37ºC for at least 2h. This was done to ensure that sections were fully attached to the slide surface to reduce the risk of sections dislodgement during subsequent use.

2.2.2.2.4 Haematoxylin and Eosin Staining

Sections were de-paraffinised with xylene (2 × 5 min) and 50% xylene/ethanol (1 × 5 min) then rehydrated using 100% ethanol (1 × 5 min,

1× 2 min), 90% ethanol (1 × 2 min) and 70% ethanol (1 × 2 min). Sections were then stained with Harris' haematoxylin (Sigma) for 10 min and washed in running tap water for 5 min. Excess stain was removed from the section by soaking in acid alcohol (0.5% HCl in 70% ethanol) for a few seconds before rinsing in running tap water for 5 min and immersing in Scott's Tap Water for 2 min to allow the colour to develop. Sections were counterstained in Eosin for 1 min before a final wash in running tap water. Finally, the sections were dehydrated using sequential ethanol (1 x 1 min, 1 x 3 min), 50% xylene/ethanol (1 × 3 min), xylene (1 × 3 min, 1 × 5 min) and mounted using diphenylxylene (BDH)

2.2.2.3 Hypoxia detection

2.2.2.3.1 Spheroids treatment with the hypoxic marker pimonidazole

Hypoxia detection was performed using Hypoxyprobe™-1 Green kit (HPI). Pimonidazole, the active compound of Hypoxyprobe, forms stable adducts with proteins in hypoxic cells. HT29 (day 10) and DLD-1 (day 15) spheroids were transferred to 1.5 ml microcentrifuge tubes. Spheroids were treated with pimonidazole dissolved in the culture media (100 μM) for 2h at 37°C.

2.2.2.3.2 Fixation and processing

After pimonidazole treatment, all medium was removed and spheroids were washed with PBS and transferred to an embedding mould. PBS was removed and spheroids were frozen using Cryo-Freeze Aerosol (Agar Scientific). Spheroids were embedded in OTC embedding matrix form (Cryoteck), sprayed with Cryo-Freeze Aerosol and then kept at -80ºC. Negative control samples (no pimonidazole treatment) were also processed.

2.2.2.3.3 Sectioning

Frozen blocks were transferred to -20ºC at least 1 day before sectioning. Spheroids were cryosectioned to 5 µm thickness using a microtome (LEICA1100). Sections were collected on APES coated slides.

2.2.2.3.3.1 APES coated slides

Superfrost Plus slides were immersed in clean acetone for 2 min and allowed to drain then immersed in a freshly prepared 4% (v/v) solution of 3-aminopropyltriethoxysilane (APES) (Sigma) in acetone for 2 min. Slides were then drained, washed twice in running tap water for 2 min. Finally, the slides were dried overnight and stored at room temperature.

2.2.2.3.4 Immunofluorescence staining

Frozen sections (5 µm thick) from the central regions of spheroids were fixed for 10 min in acetone at 4°C then washed with PBS for 10 min. Slides were blocked for 30 min in 4% (v/v) FBS, 5% (w/v) non-fat milk, and 0.1% (v/v) Triton X-100 (Sigma) in PBS. Pimonidazole adducts were detected by incubating sections with FITC conjugated MAb1 (monoclonal mouse antibody provided in the Hypoxyprobe™-1 Green kit, 1/150 dilution) for 2h at 37°C. After PBS washes (3 × 3 min), DNA was stained using DAPI (VECTASHIELD Mounting Medium with DAPI, Vector). FITC (green) and DAPI (blue) fluorescent signals for spheroids sections were acquired on a Leica microscope.

2.2.2.4 Isolation of cells residing in surface layer and hypoxic region of CRC spheroids

Cells from different depths within HT29 or DLD-1 spheroids were harvested by sequential trypsinisation techniques (Phillips et al., 1994). Spheroids were washed with PBS and treated with trypsin-EDTA for 2 min at room temperature under constant gentle agitation. After the sample was trypsinised, 10 ml of complete growth medium was added, and cells in suspension were separated from spheroids by sedimentation. Spheroids were washed again with medium, and free floating cells were recovered by centrifugation. Pellets of cells were immediately frozen in a dry ice bath and stored at -80ºC until required for RNA or protein extraction. This process was repeated several times until spheroids were completely stripped of the numerous cell layers. After each cell layer was stripped from the spheroid, the diameter remaining was measured using calibrated graticule fixed to the light microscope at 10 × objective lens.

2.2.2.5 Analysis of ALDH gene expression of CRC spheroids using qRT-PCR

RNA extraction, cDNA synthesis and qRT-PCR techniques for cells residing in the surface layer (SL) and hypoxic region (HR) of the spheroids were carried out as described in section 2.2.1.3. The cells of the SL of HT29 and DLD-1 MCS were at (0-10.8 µm) and (0-21 µm) depth, respectively, while the cell of the HR were at depth of (132-186 µm) and (133-150.7 µm), respectively.

2.2.2.6 Analysis of ALDH protein expression of CRC spheroids using western blot

Protein extraction and western blot analysis for cells residing in SL and HR of the spheroids were carried out as described in section 2.2.1.4. Image J software was used to measure the intensity of detected bands. The expression level of a target protein was normalised to the actin protein of the same sample. In order to calculate the fold change in the expression of the target protein in the SL or HR, the expression level in these samples was normalised to normoxic monolayer cells.

2.2.2.7 Immunohistochemistry staining

Paraffin embedded spheroids were sectioned and collected on APES coated slides as previously described in section 2.2.2.2.3. Slides were processed for the detection of ALDH1A1, 1A3, 3A1 and 7A1 and the hypoxic marker, carbonic anhydrase IX (CAIX).

2.2.2.7.1 Dewaxing and rehydration

Sections were de-paraffinised with xylene (2 x 5 min) and rehydrated using absolute ethanol (1 x 5 min, 1 x 2 min), 90% ethanol (2 min) and 70% ethanol (2 min) before being washed in distilled water (5 min).

2.2.2.7.2 Antigen retrieval

Heat induced antigen retrieval was carried out using citrate buffer (10 mM, pH 6.0, see Appendix VI) at medium-high power of microwave for appropriate time (Table 16, Appendix VI), after which slides were allowed to cool for 30 min at room temperature. Slides were rinsed in PBS (pH 7.4) for 10 min.

2.2.2.7.3 Blocking

Endogenous peroxidase activity was then blocked using 3% (v/v) H_2O_2 (Sigma) in 100% methanol (Sigma) for 15 min at room temperature and slides were washed in PBS for 10 min. Afterwards, slides were incubated with normal blocking serum (Table 16, Appendix VI) for 30 min at room temperature to block the non-specific binding. The blocking serum was chosen from species where the biotinylated secondary antibody was raised (Table 16, Appendix VI).

2.2.2.7.4 Antibodies and detection

The sections were incubated in a humidified chamber with 100 µl of the primary antibody at optimum dilution (diluted in blocking serum) for the optimised time and incubation conditions (Table 16, Appendix VI). Slides were washed in PBS (2 x 5 min) before the addition of 100 µl of the vector biotinylated secondary antibody (1:200, 30 min) at room temperature. Following this, slides were again washed in PBS (2 x 5 min) and sections were incubated with Avidin/Biotin Complex (ABC, Vectastain peroxidase standard kit) for 30 min at room temperature. This was followed by PBS wash (2 x 5 min) before sections were incubated with 3,3-diaminobenzidine (DAB, Vector Laboratories) for 2-10 min at room temperature, enabling the ABC reagent to break down the DAB to a brown precipitate at the location of the antigen. Sections were washed in running tap water for 5 min before being counterstained using Harris' haematoxylin for 20s, rinsed in tap water for 60s, and Scott's tap water for 2 min.

2.2.2.7.5 Dehydration

Sections were dehydrated using 70% ethanol (1 × 5 min), 90% ethanol (1 × 5 min), 100% ethanol (2 × 2 min), 50% xylene/ ethanol (1 × 2 min) and xylene (1 × 2 min, 1 × 5 min) series and finally mounted using diphenylxylene (BDH).

2.2.3 The expression of ALDH in colorectal cancer xenografts

The xenografts were previously prepared by Mrs Patricia Cooper at the Institute of Cancer Therapeutics. In brief, immunodeficient mice (aged six to eight weeks), were obtained from Harlan (Loughborough, UK), and injected subcutaneously with human CRC cell lines (HT29, HCT116, DLD-1, SW620 and COLO205). When the tumour size reached 500 mm^3, mice were sacrificed. The tumours were then excised, fixed in 10% formalin for 24h and processed for embedding in paraffin wax. All animal procedures were performed according to a protocol approved by the UK Home Office and in accordance with the UK National Cancer Research Institute Guidelines for the Welfare of Animals (Workman et al. 2010).

Paraffin embedded xenografts were sectioned, processed and stained according to the immunohistochemistry (IHC) protocol used to detect ALDH expression as previously described in section 2.2.2.7. The endogenous hypoxic marker, CAIX was used to detect hypoxic areas as previously described in section 2.2.2.7.

2.2.4 The role of HIF in the regulation of ALDH7A1 expression

2.2.4.1 Induction of HIF using cobalt chloride ($CoCl_2$)

Cobalt chloride ($CoCl_2$) is known as a chemical inducer of HIF-1α under normoxic conditions (Law et al., 2012) and in an attempt to evaluate whether the expression of ALDH is induced by HIF-1α, $CoCl_2$ treatment was carried out. To determine the non-toxic concentration that was required to induce HIF-1α, DLD-1 and HT29 cells were seeded into 96 well plates by adding 180 µl of cell suspension containing 2×10^3 cells to each well followed by incubation for 24h at 37ºC, 5% CO_2 and 100% humidity. Cells were treated with $CoCl_2$ (concentration range 10 µM to 500 µM) for 24h before the media was replaced with fresh media and the cells were incubated for further 72h, after which the anti-proliferative activity was evaluated using the 3-(4,5-dimethylthiazol-2-yl)-2,5-diphenyltetrazolium bromide (MTT) assay (Sieuwerts et al., 1995). See Appendix II for the composition of MTT assay solutions.

The medium was replaced with 200 µl MTT solution (0.5 mg/ml) and the cells were incubated for an additional 4h. The supernatant was removed and 150 µl of DMSO was added to each well and gently pipetted up and down to dissolve the blue formazan crystals. The absorbance of samples was measured in a microplate reader (Thermo Electron Corporation) at 540 nm.

Microsoft Excel 2010 was used for data analysis and the percentage of cell survival was calculated as follows:

Mean absorbance for wells containing cells (control or treated) or no cells (blank) was calculated. The true absorbance from the microplate reading was calculated from the following formula:

True absorbance = Mean absorbance (each drug concentration or control wells) – mean absorbance of blank wells.

Percentage of cell survival = (true absorbance of treated / true absorbance of control) × 100%

To induce HIF-1α expression, DLD-1 and HT29 cells were seeded into 75 cm^2 flasks at concentration of 2×10^5 cells/flask. Cells were incubated at 37ºC, 5% CO_2 and 100% humidity. Based on the results of the MTT assay, DLD-1 (100 and 150 µM $CoCl_2$) and HT29 cells (200 and 300 µM $CoCl_2$) were treated for 24h before being harvested for protein extraction. Western blot was carried out as previously described in section 2.2.1.4 using HIF-1α and ALDH7A1 antibodies (Table 15, Appendix V).

2.2.4.2 Knockdown of HIF-1α or HIF-2α using siRNA to evaluate their effect on ALDH7A1 expression

2.2.4.2.1 ALDH7A1 expression

The expression of ALDH7A1 was revaluated in DLD-1 cells upon incubation at normoxic or hypoxic conditions, as a part of optimising the conditions for knockdown experiments (see below). In brief, DLD-1 cells were seeded at a

concentration of 2.75 × 10^5 cells/25 cm^2 flask in 5 ml complete RPMI and incubated at 37˚C and 5% CO_2 for 24h. Cells were transferred to the hypoxic chamber with medium being replaced with hypoxic preconditioned medium. The cells were incubated for a further 24h, 48h and 72h before being harvested for RNA and protein extraction. Normoxic cells were included as controls at each time point. ALDH7A1 expression was evaluated at the gene and protein levels as previously described (Sections 2.2.1.3-4).

2.2.4.2.2 Preparation of siRNA solution

siRNA duplexes against HIF-1α or HIF-2α were designed, synthesised and validated by Ambion/Life Technologies. See Appendix VII for siRNA information.

Stock solution: 20 µM siRNA solutions of HIF-1α or HIF-2α siRNAs were prepared by dissolving 20 nmol of each siRNA (Ambion/Life Technologies) in 1 ml of 1x Dharmacon siRNA re-suspension buffer. 2 µM of siRNA was also prepared as a working stock solution. Both concentrations of siRNA were stored in aliquots at -80˚C.

2.2.4.2.3 Transfection with siRNA

DLD-1 cells in early passage number (2-4) were seeded at a concentration of 2.75 × 10^5 cells/25 cm^2 flask in 5 ml complete RPMI and incubated at 37˚C and 5% CO_2 for 24h. Cells were checked under the microscope to make sure that they were 20-30% confluent and evenly distributed throughout the flask surface. For single siRNA transfection, siRNA was prepared in 1.5 ml microcentrifuge tube by adding 30 µl of 2 µM siRNA stock solution into 525 µl Optimem (Gibco). For dual transfection, 15 µl of each siRNA (2 µM stock)

were added into 525 µl Optimem. 45 µl of diluted oligofectamine solution (1:5 oligofectamine (Life Technologies) in Optimem was prepared and incubated for 30 min at room temperature) was added to siRNA mix (final concentration = 7.5% v/v) and was thoroughly mixed by pipetting (20-30 times). The mix was incubated for 45 min inside the cell culture safety cabinet. A control solution with the liposome carrier was prepared by adding 45 µl of diluted oligofectamine solution into 555 µl Optimem. During the incubation time, medium was removed from the flasks and 5 ml of Optimem was added to each flask for washing before being discarded. 2 ml of fresh Optimem was then added to each flask. After 45 min of incubation, 500 µl of siRNA mix was added to relevant flasks (final concentration of each siRNA in single or co-transfection is 20 or 10 nM respectively). For liposome control cells, 500 µl of control solution was added to each flask. For mock-transfected cells, 500 µl of Optimem only was added to each flask. Cells were incubated at 37ºC and 5% CO_2 for 4h before being exposed to hypoxia (0.1% O_2); 2.5 ml preconditioned hypoxic 2x RPMI was added to each flask. Normoxic mock samples were also included as a control and 2.5 ml of 2x RPMI was added to each flask. Cells were then incubated for 48h or 72h before being harvested for RNA or protein extraction. The expression of HIF-1α, HIF-2α and ALDH7A1 was evaluated at both the gene and protein levels as previously described in sections 2.2.1.3-4 (Table 15, Appendix V for antibodies information).

2.3 Results

2.3.1 Analysis of ALDH expression in CRC cell lines

2.3.1.1 Gene expression using q-RT-PCR

2.3.1.1.1 ALDH gene expression profiling of CRC cell lines under normoxic conditions

ALDH gene expression levels were evaluated for seven selected ALDH isoforms ALDH1A1, 1A2, 1A3, 1B1, 2, 3A1 and 7A1 in four CRC cell lines (DLD-1, HCT116, HT29 and SW480). These isoforms were selected as they have been found to play various roles in cancer; ALDH1A1 and 1A3 in CSCs, 1A2 as TSG in prostate cancer, 1B1 as a potential biomarker for CRC, 2 in oesophageal carcinoma, 3A1 in drug resistance and 7A1 as a contributing mediator of prostate cancer metastasis (Chapter 1 Introduction, section 1.4.3-5).

As shown in Figure 9A, qRT-PCR of DLD-1 cells revealed high gene expression of ALDH1B1, 2, 3A1 and 7A1 compared to ALDH1A3, while ALDH1A1 and 1A2 showed the lowest expression. Similar analysis was performed in HCT116 cells and revealed high endogenous levels of ALDH1A3, 1B1, 2 and 7A1 compared to ALDH3A1, while ALDH1A1 and 1A2 were expressed at the lowest levels (Figure 9B). A similar pattern of expression was also found in SW480 (Figure 9D). In contrast to other CRC cell lines examined, qRT-PCR of HT29 showed that there was less differential expression between the ALDHs, with ALDH1A2 exhibiting the lowest expression (Figure 9C).

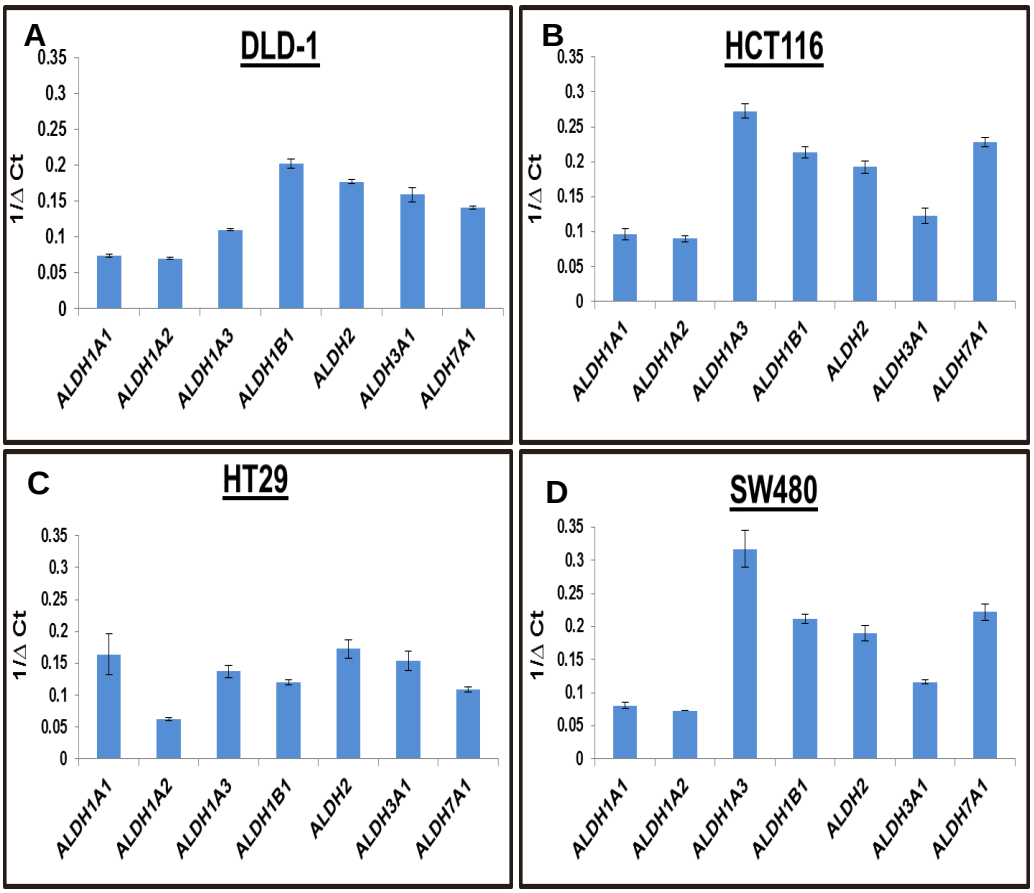

Figure 9 Expression profiling of ALDH1A1, 1A2, 1A3, 1B1, 2, 3A1 and 7A1 mRNAs in CRC monolayer cells. DLD-1 (A), HCT116 (B), HT29 (C) and SW480 (D). Values are the mean of 3 independent experiments and error bars are SD. ΔCt= Ct (target gene) – Ct (actin).

2.3.1.1.2 ALDH genes expression profiling under hypoxic conditions

The CRC cell lines were exposed to hypoxic conditions and stained with Haematoxylin as previously described (Material and Methods, section 2.2.1.2), which revealed cells were still viable and attached to the flask surface (Figure 10).

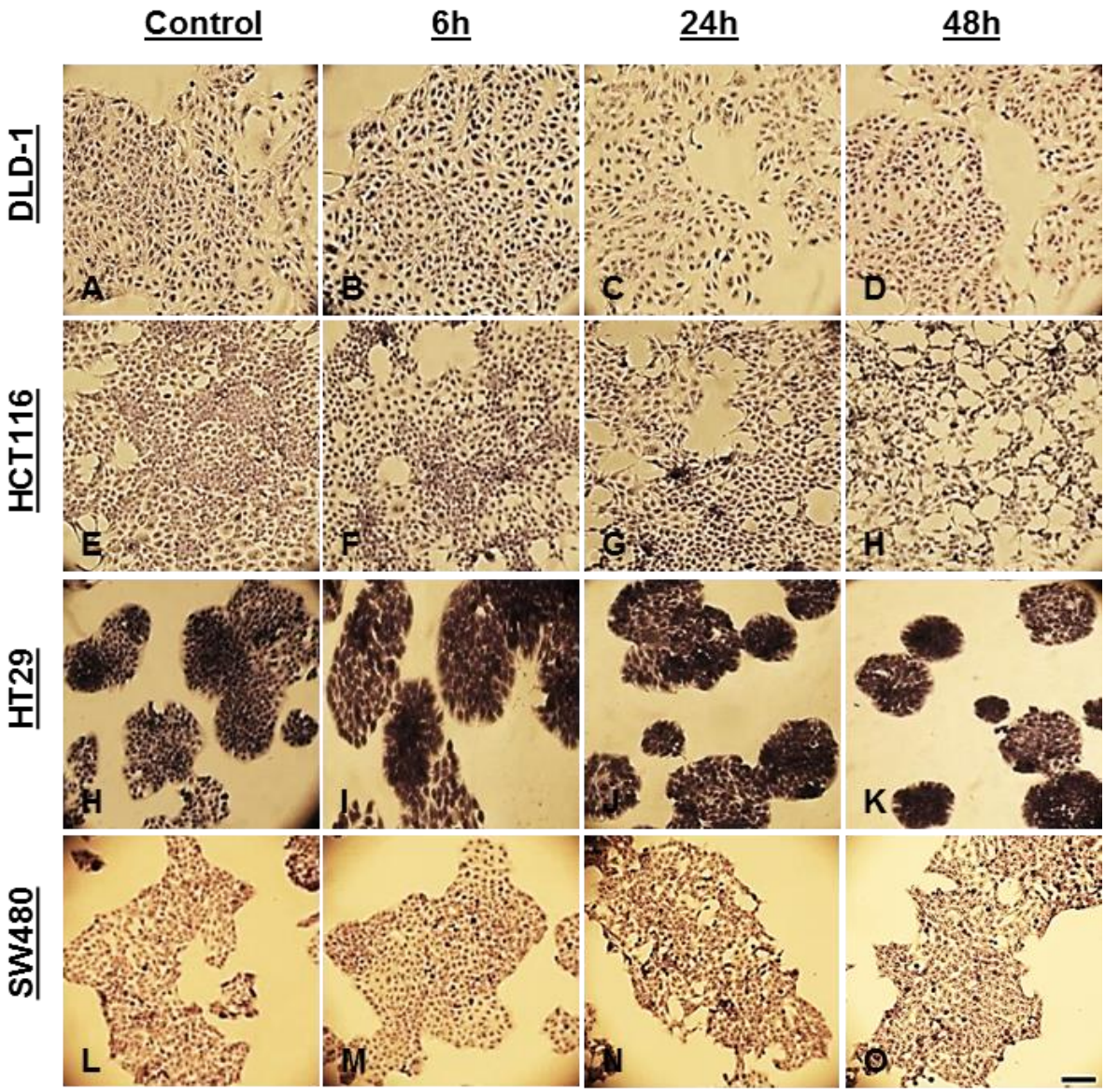

Figure 10 Histology of DLD-1 (A-D), HCT116 (E-H), HT29 (I-L) and SW480 (M-P) CRC monolayer cells. Normoxic conditions (A,E,I,M), Hypoxic conditions [6h (B, F,J,N), 24h (C, G,K,O), 48h (D,H,L,P)]. Scale bar = 100 µm at 10x objective lens.

Gene expression analysis of ALDH isoforms was evaluated using qRT-PCR (Materials and Methods, section 2.2.1.3).

In order to evaluate whether the selected exposure times to hypoxic conditions were enough to induce changes at the gene level, VEGFA gene expression was used as a positive control. As shown in Figure 11, VEGFA gene expression was induced in DLD-1 cells upon exposure to 24h and 48h of 0.1% O_2. In contrast, only the expression of ALDH1A2 and ALDH7A1 was found to be upregulated about a 3-fold in response to the same hypoxic conditions.

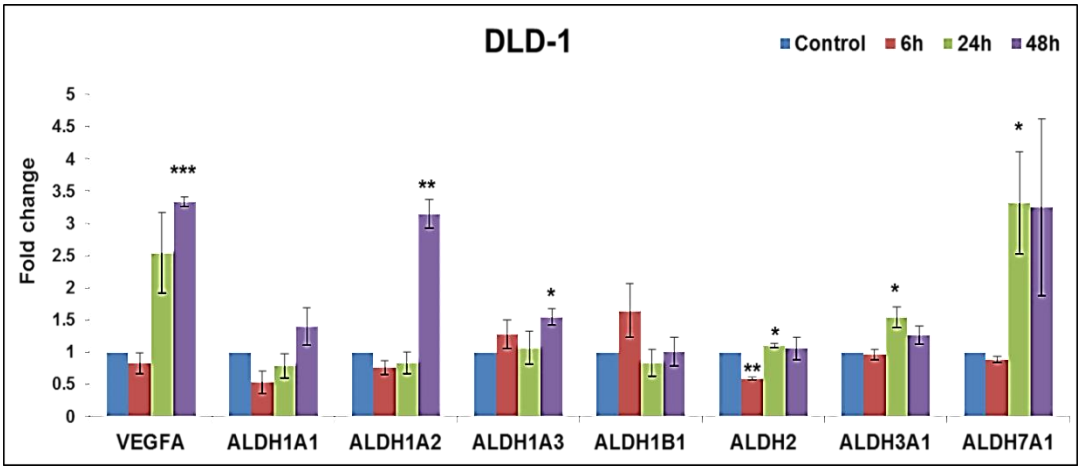

Figure 11 Influence of hypoxia on the expression of ALDH mRNA in DLD-1 cells. VEGFA was used as positive control and β-actin as internal control gene. ALDH gene expression analysis was performed under normoxic (control, blue bar) and hypoxic conditions (0.1% O_2; 6h (red bar), 24h (green) and 48h (purple)). Values are the mean of 3 independent experiments and error bars are SD. P values: * $p<0.05$, ** $p<0.01$, *** $p<0.001$. For Raw data, see Appendix IX.

The same analysis was carried out in HCT116 cells (Figure 12). All examined ALDH isoforms showed similar response to hypoxia exposure: downregulation after transient exposure to hypoxia (6h) and an increase in expression after 48h with the exception of ALDH2 and ALDH7A1, which at the last time point had not yet recovered to normoxic expression levels.

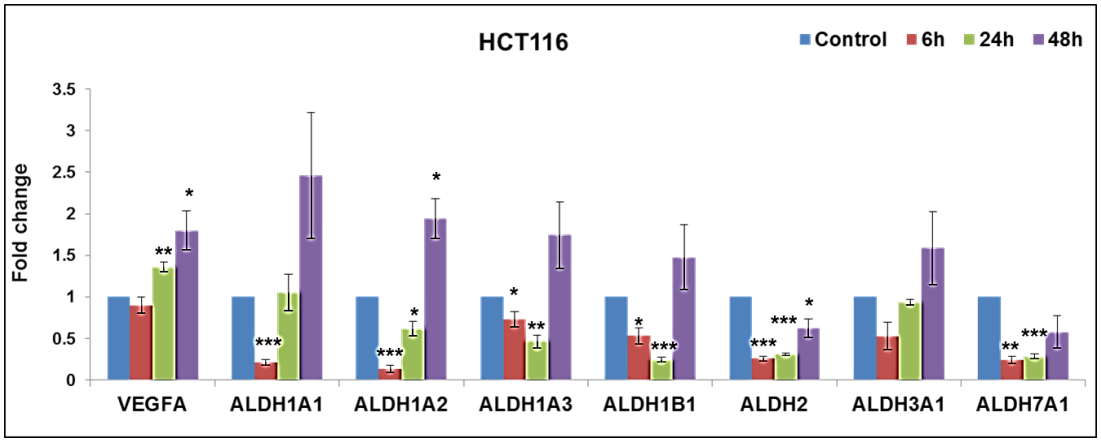

Figure 12 Influence of hypoxia on the expression of ALDH mRNA in HCT116 cells. VEGFA was used as positive control and β-actin as internal control gene. ALDH gene expression analysis was performed under normoxic (control, blue bar) and hypoxic conditions (0.1% O_2; 6h (red bar), 24h (green) and 48h (purple)). Values are the mean of 3 independent experiments and error bars are SD. P values: * p<0.05, ** p<0.01, *** p<0.001.

Figure 13 shows that VEGFA was upregulated in HT29 cells in response to hypoxia reaching 5-fold after 48h. The results of ALDH gene expression analysis revealed that ALDH1A1, 1A2 and 7A1 were upregulated after 48h of exposure to hypoxia reaching 5, 9 and 6-fold, respectively. The expression of ALDH1B1 was also increased, however this elevation was not correlated with hypoxia exposure time.

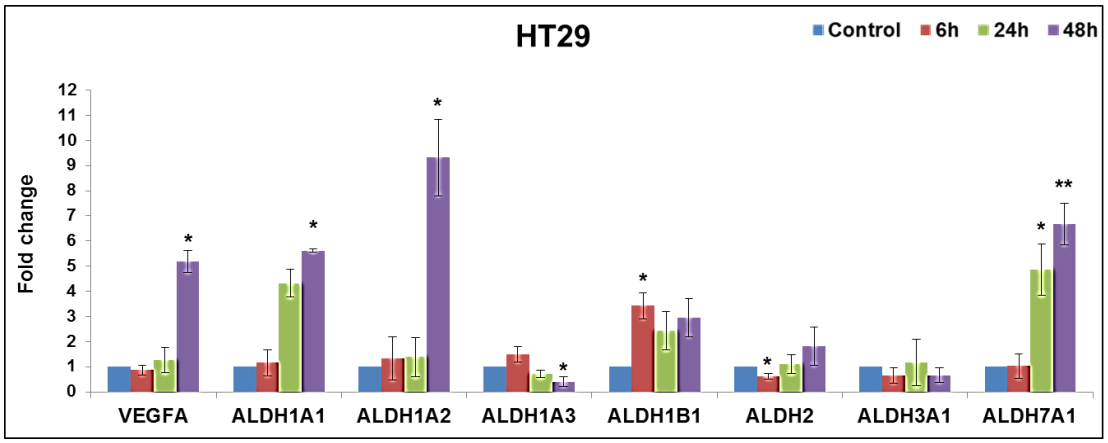

Figure 13 Influence of hypoxia on the expression of ALDH mRNA in HT29 cells. VEGFA was used as positive control and β-actin as internal control gene. ALDH gene expression analysis was performed under normoxic (control, blue bar) and hypoxic conditions (0.1% O2; 6h (red bar), 24h (green) and 48h (purple)). Values are the mean of 3 independent experiments and error bars are SD. P values: * p<0.05, ** p<0.01.

Exposure of SW480 cells to hypoxia (6h) resulted in 3-fold increase of ALDH1A1 and 1A2 expression, however, the upregulation was transient and the expression levels declined as the exposure times increased reaching the same levels as under normoxic conditions (Figure 14). Only ALDH1A3 was found to be upregulated upon 48h exposure to hypoxia, while ALDH1B1, 2 and 7A1 were downregulated in response to low oxygen tensions.

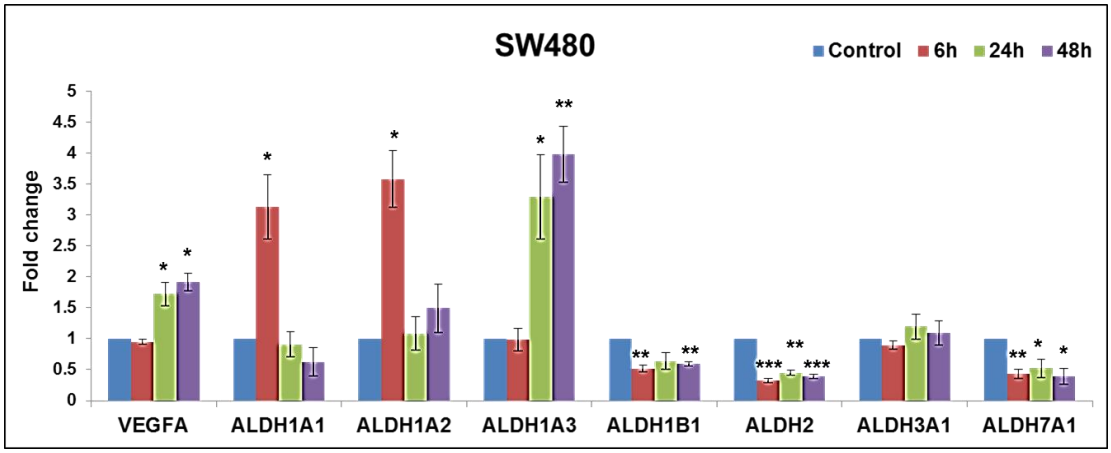

Figure 14 Influence of hypoxia on the expression of ALDH mRNA in SW480 cells. VEGFA was used as positive control and β-actin as internal control gene. ALDH gene expression analysis was performed under normoxic (control, blue bar) and hypoxic conditions (0.1% O_2; 6h (red bar), 24h (green) and 48h (purple)). Values are the mean of 3 independent experiments and error bars are SD. P values: * p<0.05, ** p<0.01, *** p<0.001.

2.3.1.2 Analysis of ALDH protein expression using western blot

The protein expression levels of selected ALDH isoforms 1A1, 1A2, 1A3, 3A1 and 7A1 were evaluated in CRC cell lines 48h after exposure to normoxic conditions or 0.1% O_2 using western blot. ALDH1B1 and 2 were not selected for protein analysis as these isoforms were not shown to be significantly affected by exposure to low oxygen tension over 48h. All cell lines were probed for target ALDH expression after they were loaded to the same gel. Here lactate dehydrogenase A (LDH-A) protein was used as a

positive control because the VEGFA antibody was not producing clear bands in contrast to LDH-A that gave reliable bands.

The expression of ALDH1A1, 1A2, and 1A3 at the protein level was not detectable in the DLD-1 cell line (Figure 15B-D). This observation is consistent with the gene expression data where these isoforms were expressed at low level compared to other isoforms (Figure 9, section 2.3.1.1.1). Even after 48h exposure to hypoxia (0.1% O_2), no variation in the expression was observed. In contrast, the positive control protein LDH-A was found to be upregulated 6-fold after 48h exposure to hypoxia (0.1% O_2) (Figure 15A). ALDH3A1 was largely unaffected (Figure 15E), while ALDH7A1 was found to be upregulated by 25% after exposure to hypoxia (Figure 15F) indicating good correlation between the gene (Figure 11, section 2.3.1.1.2) and protein expression patterns.

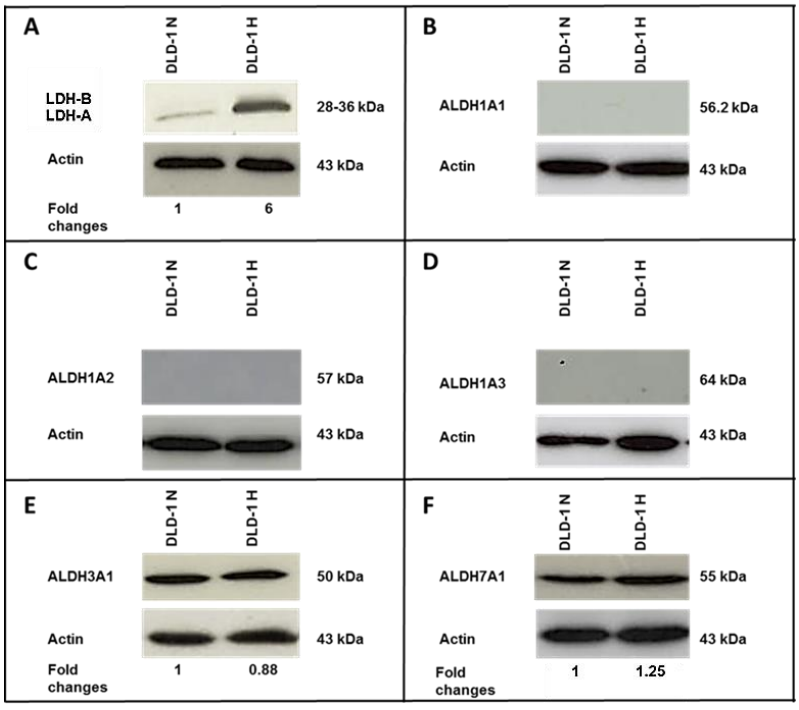

Figure 15 Western blot analysis of ALDH in DLD-1 cell line under normoxic (N) and hypoxic conditions (H) (48h exposure to 0.1% O_2). LDH-A (A), 1A1 (B), 1A2 (C), 1A3 (D), 3A1 (E) and 7A1 (F).

ALDH1A3 was observed to be increased to 1.3-fold after hypoxia exposure (Figure 16D) while ALDH7A1 was slightly reduced in HCT116 cells (Figure 16F). ALDH1A1, 1A2 and 3A1 were not expressed in normoxic or hypoxic cells (Figure 16B, C and E respectively), which is in agreement with gene expression data (Figure 9 and 12, section 2.3.1.1.1-2). LDH-A was upregulated in hypoxia exposed cells (Figure 16A).

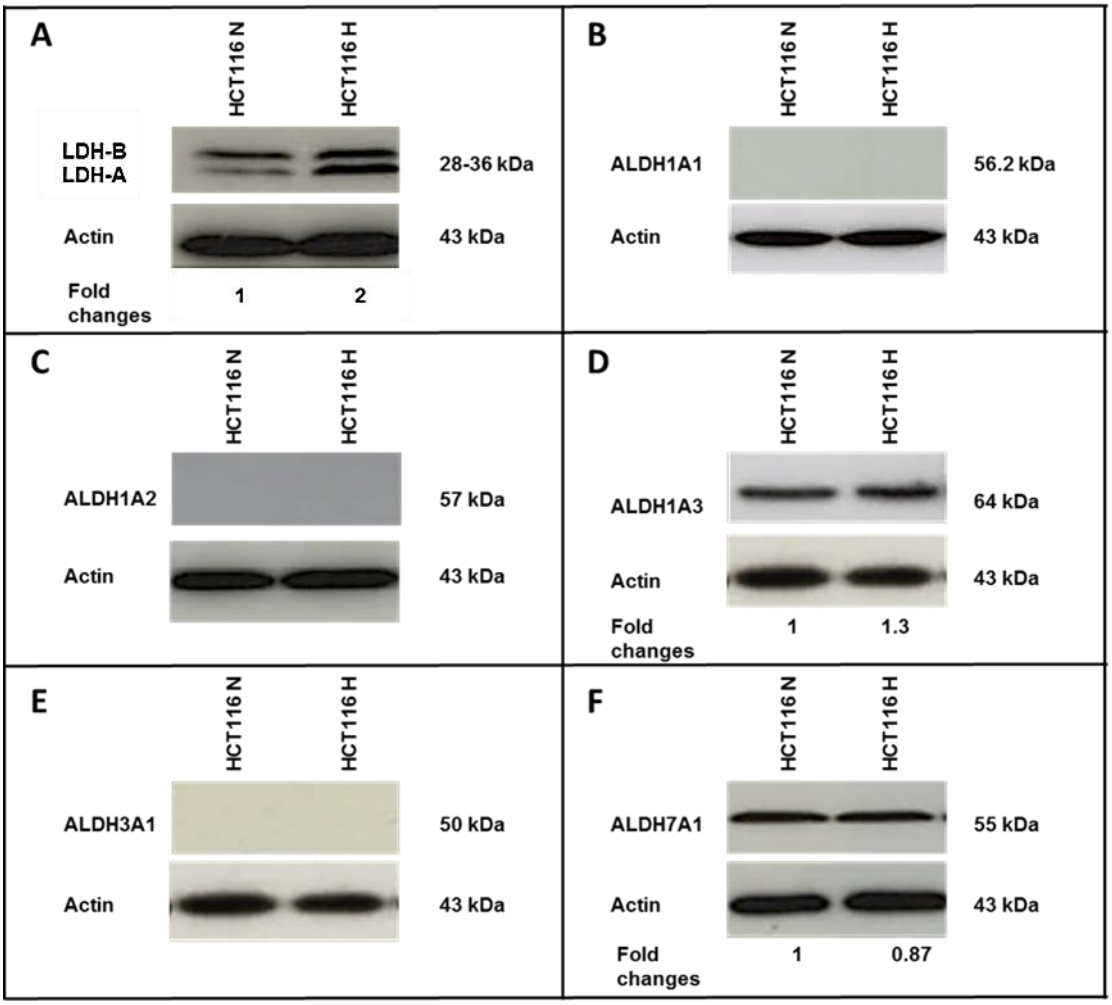

Figure 16 Western blot analysis of ALDH in HCT116 cell line under normoxic (N) and hypoxic conditions (H) (48h exposure to 0.1% O_2). LDH-A (A), 1A1 (B), 1A2 (C), 1A3 (D), 3A1 (E) and 7A1 (F).

Among the three ALDH1 isoforms examined in HT29 cells, only ALDH1A1 was detected in normoxic cells. However, no major variation in its expression between normoxic and hypoxic cells was detected (Figure 17B), which was in contrast to LDH-A that was induced a 3-fold (Figure 17A). ALDH3A1 and 7A1 were also expressed in cells grown under normoxic conditions (Figure 17E and F). ALDH3A1 expression was slightly reduced in hypoxic cells (Figure 17E), however, ALDH7A1 was upregulated 1.34-fold (Figure 17F). These findings confirm the modulation of ALDH expression that was observed in hypoxic cells at the gene level (Figure 13, section 2.3.1.1.2).

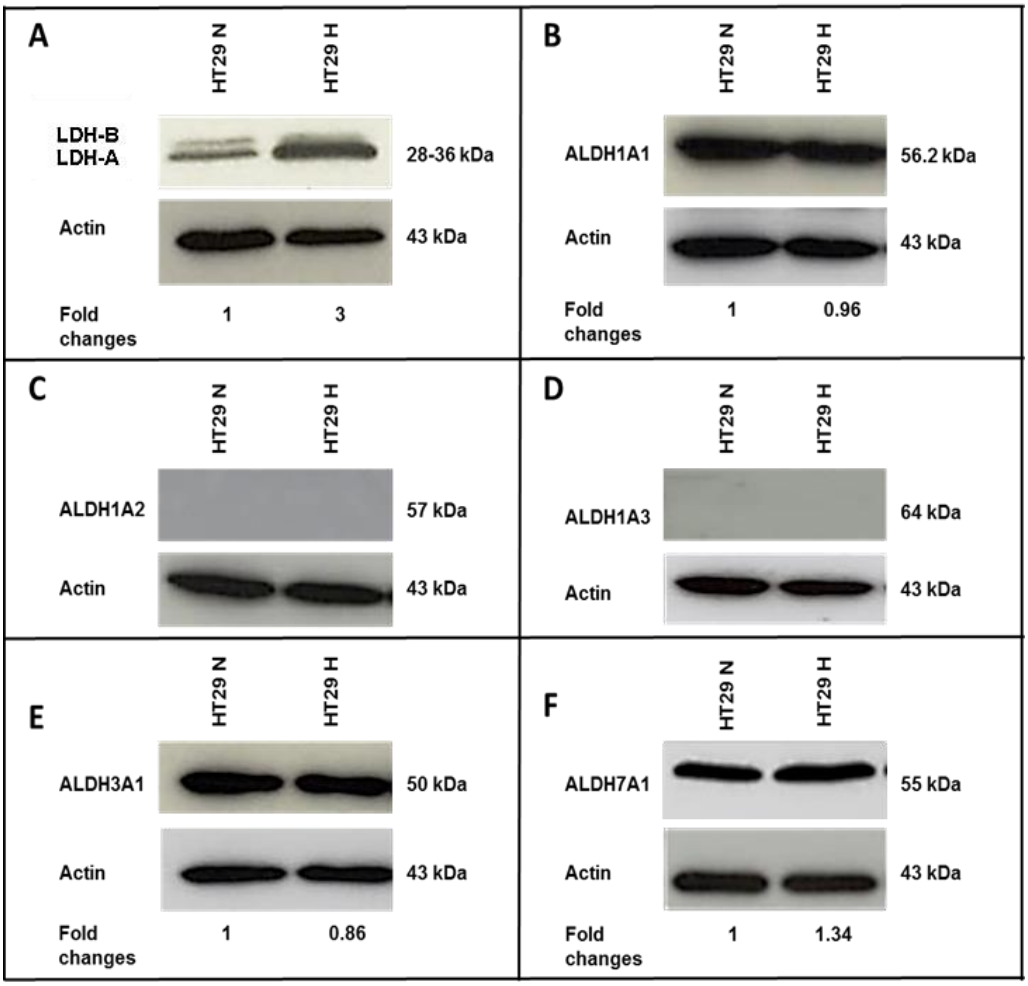

Figure 17 Western blot analysis of ALDH in HT29 cell line under normoxic (N) and hypoxic conditions (H) (48h exposure to 0.1% O_2). LDH-A (A), 1A1 (B), 1A2 (C), 1A3 (D), 3A1 (E) and 7A1 (F).

Figure 18 shows the ALDH protein expression of SW480 cells which showed a similar pattern of expression as observed in HCT116 cells. LDH-A was upregulated 1.3-fold under hypoxic conditions (Figure 18A), however ALDH 1A1, 1A2 and 3A1 were not detected under normoxic or hypoxic conditions (Figure 18B, C and E). In contrast, the ALDH1A3 protein was detected in normoxic cells and a 2.17-fold induction was observed upon hypoxia exposure (Figure 18D). ALDH7A1 was also detected in control cells and its level was found to be slightly downregulated under hypoxic conditions (0.85-fold) (Figure 18F). These findings are consistent with the gene expression data (Figure 14, section 2.3.1.1.2).

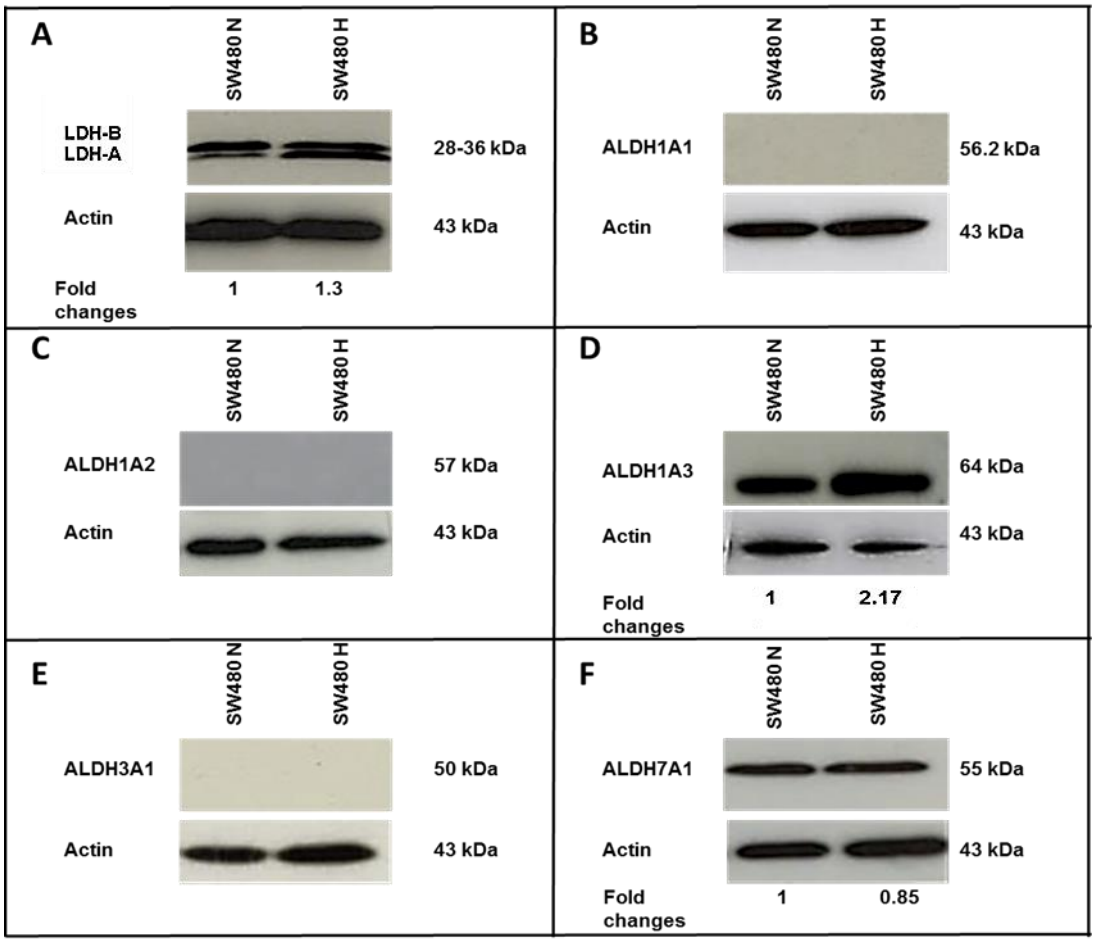

Figure 18 Western blot analysis of ALDH in SW480 cell line under normoxic (N) and hypoxic conditions (H) (48h exposure to 0.1% O_2). LDH-A (A), 1A1 (B), 1A2 (C), 1A3 (D), 3A1 (E) and 7A1 (F).

Table 11 shows summary of the findings of ALDH expression at both the mRNA and protein levels upon exposure to 0.1% O_2 for 48h in DLD-1, HCT116, HT29 and SW480 cell lines.

	mRNA level	**Protein level**
ALDH1A1		
DLD-1	No major difference	Not detected
HCT116	No major difference	Not detected
HT29	Upregulated	No major difference
SW480	No major difference	Not detected
ALDH1A2		
DLD-1	Upregulated	Not detected
HCT116	Upregulated	Not detected
HT29	Upregulated	Not detected
SW480	No major difference	Not detected
ALDH1A3		
DLD-1	No major difference	Not detected
HCT116	Upregulated	Upregulated
HT29	Downregulated	Not detected
SW480	Upregulated	Upregulated
ALDH3A1		
DLD-1	No major difference	No major difference
HCT116	No major difference	Not detected
HT29	Downregulated	Downregulated
SW480	No major difference	Not detected
ALDH7A1		
DLD-1	Upregulated	Upregulated
HCT116	Downregulated	Downregulated
HT29	Upregulated	Upregulated
SW480	Downregulated	Downregulated

Table 11 Summary of ALDH1A1, 1A2, 1A3. 3A1 and 7A1 expression at the mRNA and protein levels upon exposure to 0.1% O_2 for 48h.

2.3.2 Analysis of ALDH expression of colorectal spheroids

2.3.2.1 Spheroids culture

2.3.2.1.1 Spheroids generation

The DLD-1 and HT29 CRC cell lines were incubated in a spinner flask as previously described in Materials and Methods, section 2.2.2.1. As shown in Figure 19A, HT29 cells were able to form spheroids when incubated in spinner flasks. Small spheroids were visible after 3 days of incubation and their diameter was increasing as the period of incubation was prolonged.

The growth of the spheroids was monitored by taking the average diameter and plotting it against the time of incubation. Figure 19B reveals the diameter of HT29 multicellular spheroids (MCS) increasing proportionally with the incubation time, reaching approximately 1200 µm after 17 days.

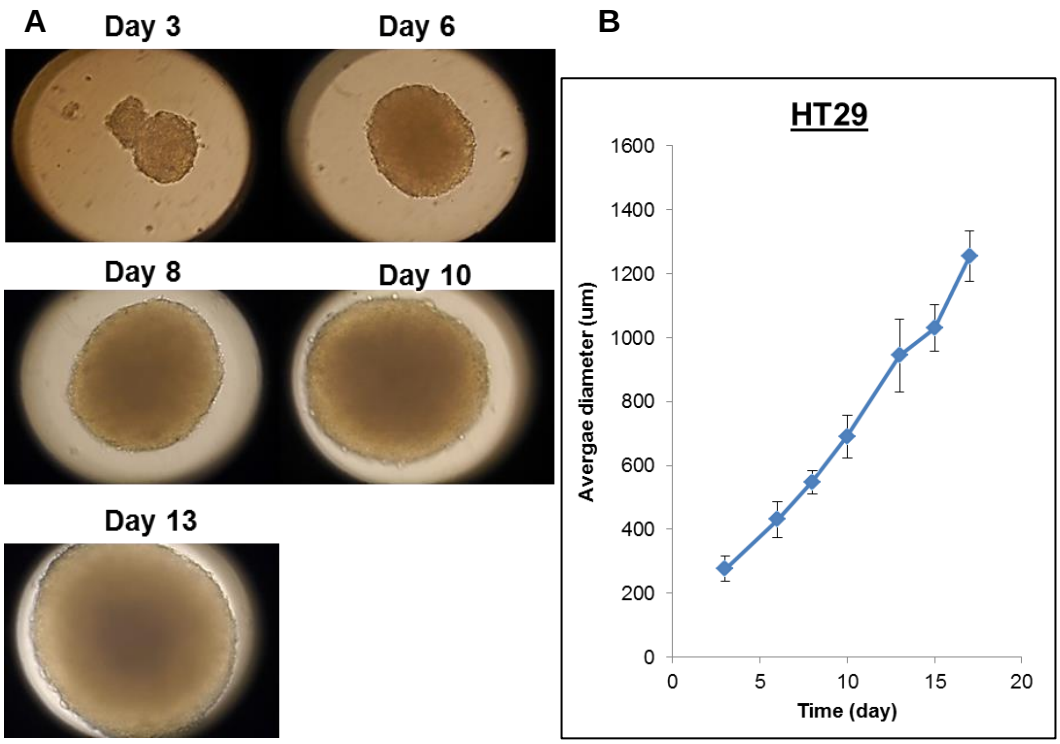

Figure 19 HT29 spheroids growth using spinner flasks. Photos of HT29 MCS at 10x objective lens (A). Growth curve of HT29 MCS (B). Points represent the average of at least 20 spheroids and error bars are SD.

Figure 20A shows that DLD1 cells were able to form small spheroids after 3 days of incubation in a spinner flask. In addition, the diameter was increasing proportionally with the incubation time, albeit slower than the HT29 spheroids. The growth curve shows that DLD-1 spheroids were growing exponentially reaching approximately 600 µm after 15 days of incubation (Figure 20B).

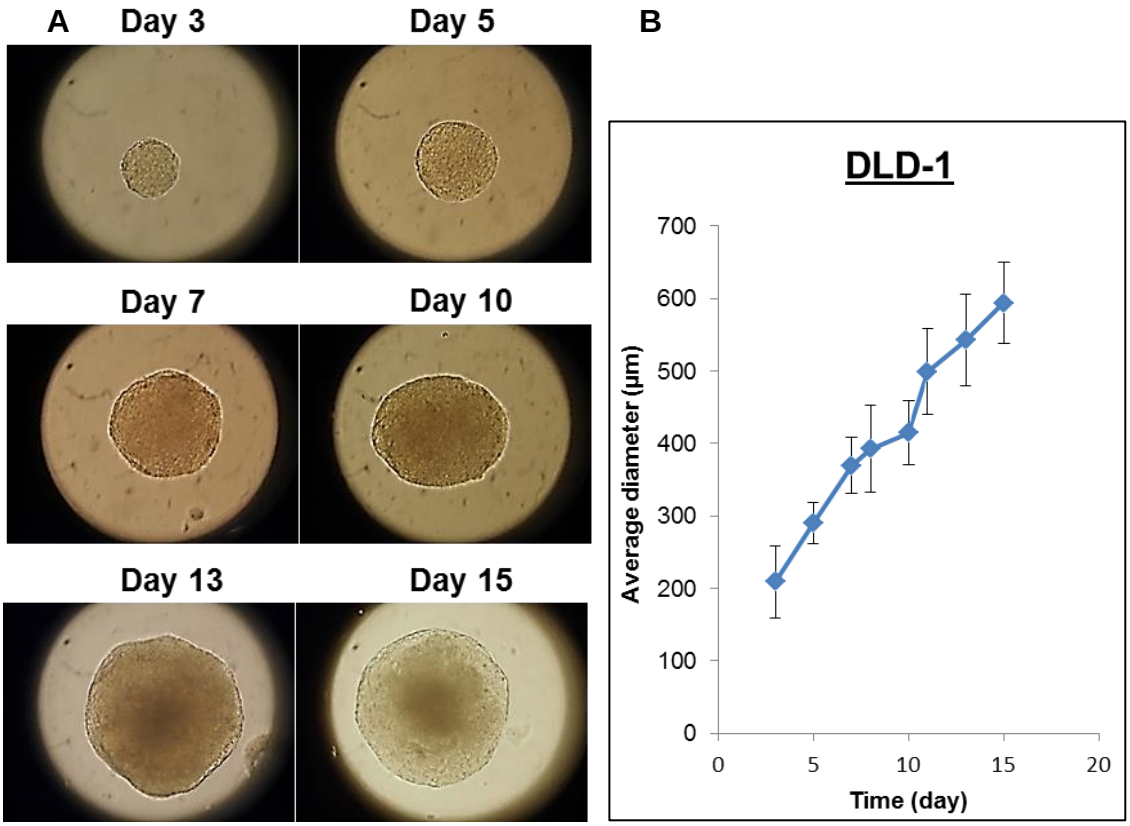

Figure 20 DLD-1 spheroids growth using spinner flasks. Photos of DLD-1 MCS at 10x objective lens (A). Growth curve of DLD-1 MCS (B). Points represent the average of at least 20 spheroids and error bars are SD.

2.3.2.1.2 Characterisation of Spheroids

In order to investigate the HT29 cells residing in the inner hypoxic regions and the outer peripheral layers, spheroids were sectioned and stained with H & E (Materials and Methods, section 2.2.2.2). As shown in Figure 21, the size of spheroids increased proportionally with incubation time. The necrotic (inner) core was only observed after 10 days of incubation when the diameter reached approximately 600 μm (Figure 21E). In addition, as the spheroids increased in size, the necrotic core also increased.

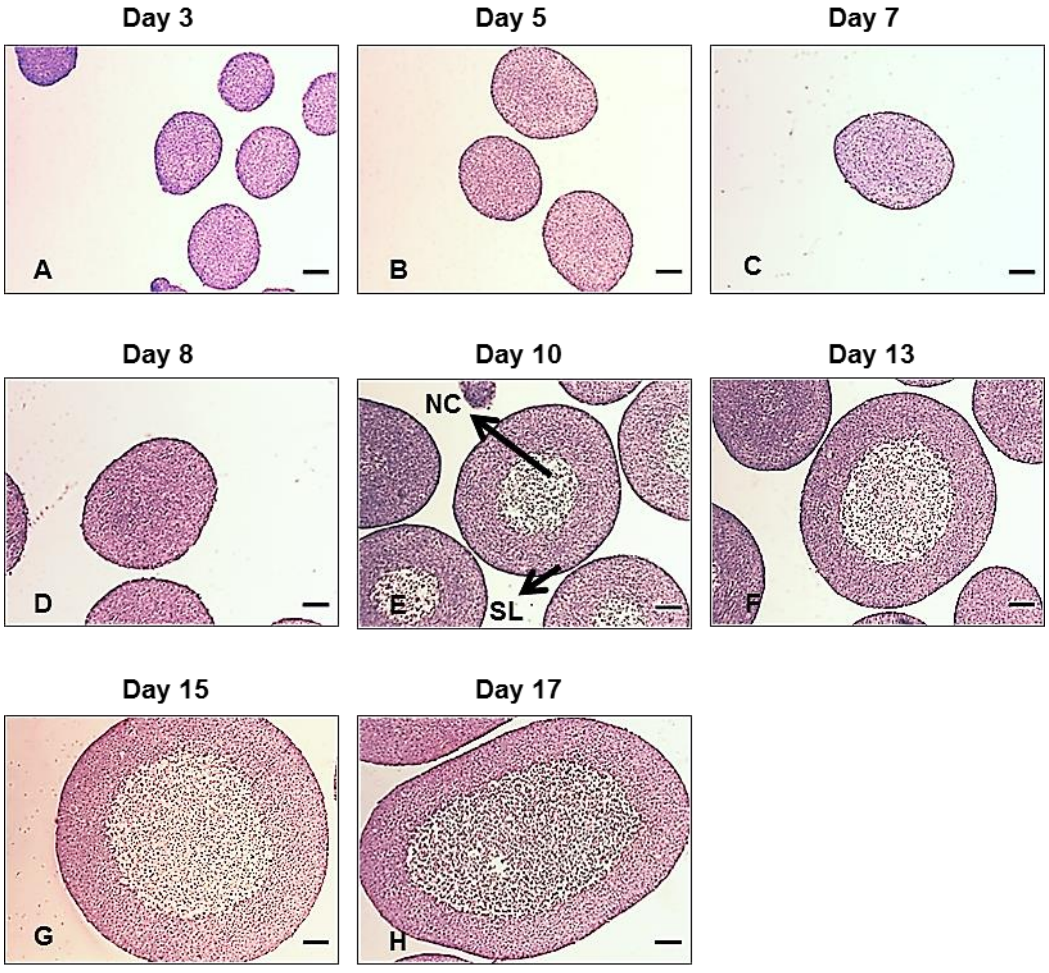

Figure 21 Histology of HT29 spheroids. Spheroids were processed and stained with H & E staining (day 3 (A), day 5 (B), day 7 (C), day 8 (D), day 10 (E), day 13 (F), day 15 (G) and day 17 (H)). Surface layer (SL), Necrotic core (NC). Scale bar = 100 μm at 10x objective lens.

Similar histology experiments were conducted using DLD-1 spheroids. As illustrated in Figure 22, the necrotic core was visible after 15 days of incubation when the spheroid diameter reached approximately 600 µm and this increased in size after a further 2 days of incubation.

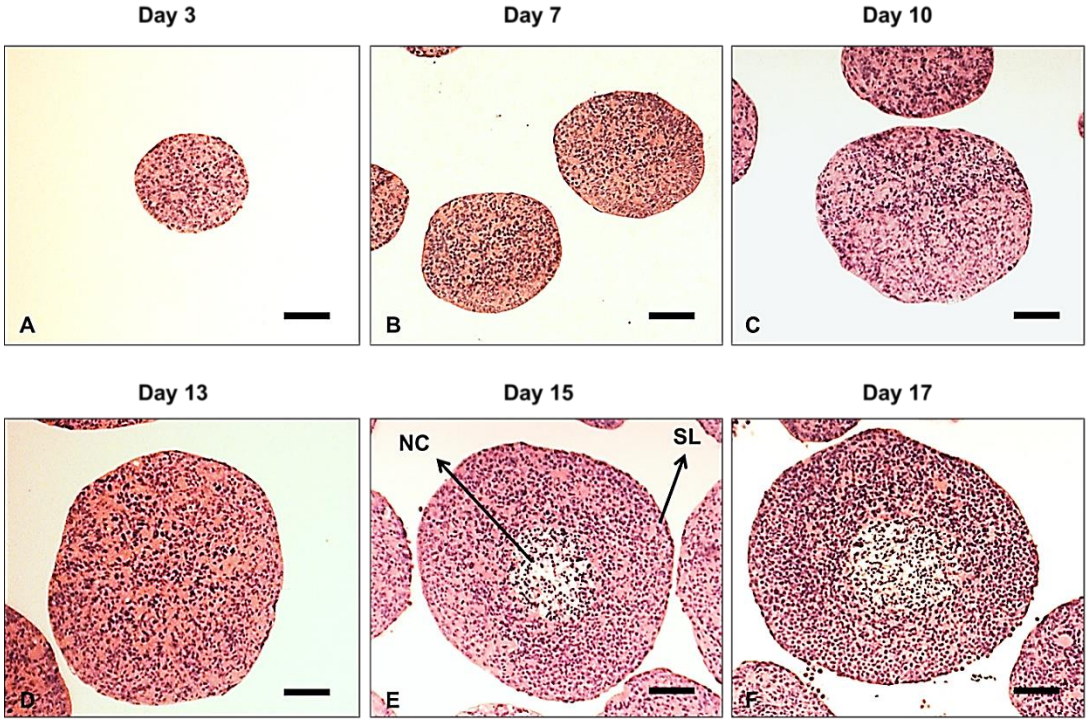

Figure 22 Histology of DLD-1 spheroids. Spheroids were processed and stained with H&E staining (day 3 (A), day 7 (B), day 10 (C), day 13 (D), day 15 (E), day 17 (F)). Surface layer (SL), Necrotic core (NC). Scale bar = 100 µm at 10x objective lens.

2.3.2.1.3 Detection of the hypoxic region of MCS

Pimonidazole, a hypoxic marker, is reductively activated in an oxygen dependent manner and is covalently bound to thiol-containing proteins in hypoxic cells (Varia et al., 1998). Pimonidazole–protein adducts can be detected by means of immunohistochemistry, immunofluorescence and flow cytometry (Varia et al., 1998). In this study, when the necrotic cores of HT29 and DLD-1 MCS were observed for the first time they were treated with pimonidazole on day 10 and 15, respectively, followed by immunofluorescence as described in Materials and Methods, section 2.2.2.3.

Figures 23A and B show the necrotic cores in the centre of the HT29 and DLD-1 spheroids, respectively. Cells directly around the necrotic core have very bright green fluorescence, which decreases gradually as the distance to the surface layer cells of the spheroids becomes smaller. The peripheral cells residing in the surface layer were only stained with DAPI.

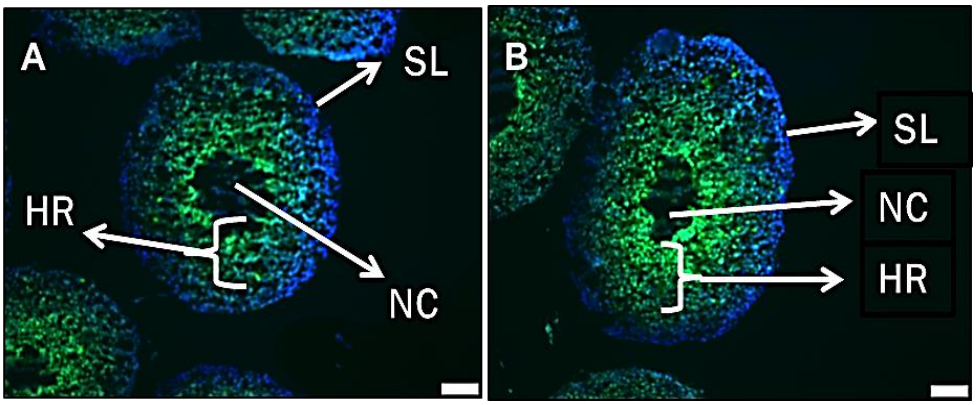

Figure 23 Hypoxia detection in HT29 (A) and DLD-1 (B) MCS. Hypoxic regions are stained by pimonidazole (green) and nuclei are stained using DAPI (blue). Surface layer (SL), Necrotic core (NC), Hypoxic region (HR). Scale bar = 100 µm at 10x objective lens.

2.3.2.1.4 Isolation of different layers from MCS

A total of 6 layers of cells were stripped and isolated from HT29 MCS and 7 layers were isolated from DLD-1 MCS. The change in diameter of spheroids for each layer of cells removed is presented in Figure 24 (HT29 (A), DLD-1(B)).

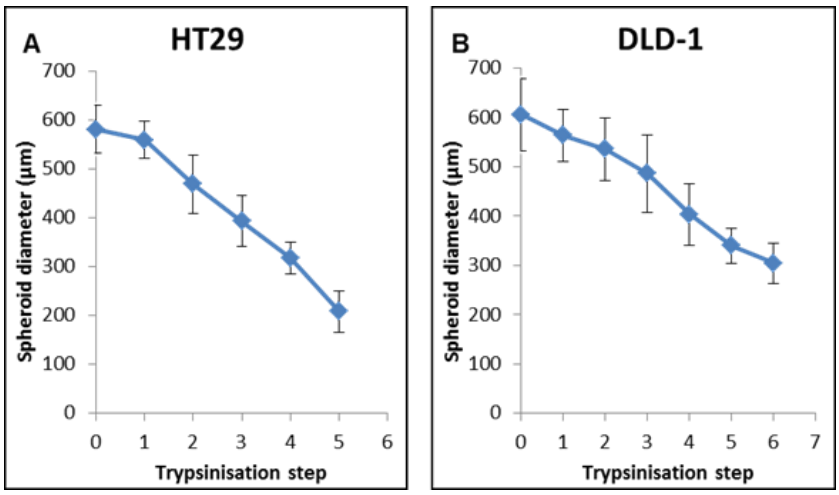

Figure 24 Isolation of cells from different depths within MCS by sequential trypsinisation. HT29 (A) and DLD-1 (B) spheroid diameters after trypsinisation. Points represent the mean of at least 30 spheroids and error bars are SD.

2.3.2.2 Expression profiling of ALDH genes and proteins of cells residing in the surface layer and the hypoxic region of MCS

The gene and protein expression was analysed in cells residing in the surface layer (depth ≈ 0-10.8 µm) and hypoxic region (depth ≈ 132-186 µm) of HT29 spheroids.

The results of qRT-PCR (Figure 25) shows that VEGFA (positive control) is highly upregulated in the hypoxic region (HR) compared to surface layer (SL) or monolayer (ML) cells. The expression of ALDH1A1 and 1A2 was enhanced in SL but reduced as the depth increased toward the HR. However, both layers showed higher expression in comparison to monolayer.

ALDH1B1 also showed increased expression in SL compared to the HR, which was shown to have the same expression level as in monolayer cells. ALDH1A3 and 3A1 were slightly downregulated in SL and that was more pronounced as the depth increased toward the HR. ALDH2 showed upregulation in the HR compared with both the SL and the monolayer cells. The SL showed 5-fold upregulation of ALDH7A1 compared to monolayer and the expression was elevated more in the HR (7-fold).

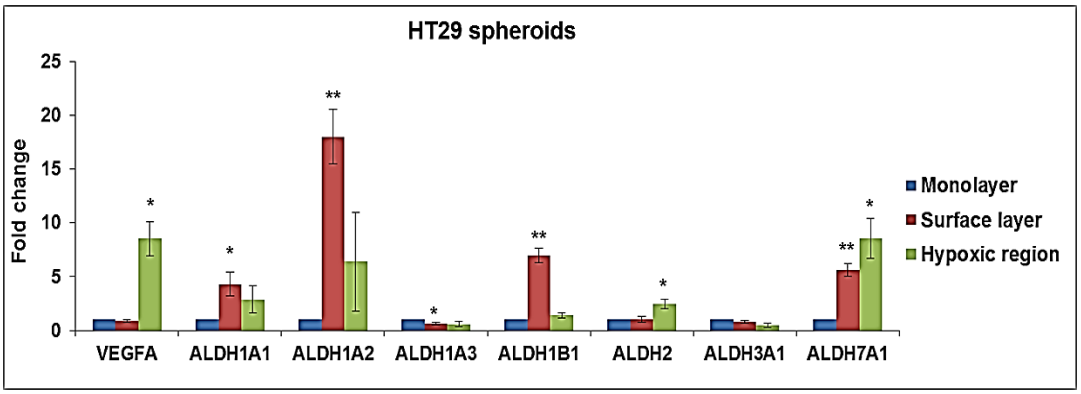

Figure 25 The expression of ALDH mRNA in HT29 MCS. Gene expression analysis was carried out using q-RT-PCR. VEGFA was used as positive control and β-actin as internal control gene. Values are the mean of 3 independent experiments and error bars are SD. P values: * $p<0.05$, ** $p<0.01$.

To evaluate whether these observations were translated to the protein level, western blot was carried out and protein expression was analysed in SL and HR cells and compared to monolayer cells. Figure 26 shows that ALDH1A1 was upregulated in SL (1.4-fold) and HR (1.8-fold) compared to monolayer cells. The expression of ALDH1A2 and 1A3 was not detected in spheroids nor in monolayer cells. No major difference was observed in ALDH3A1 expression in SL compared to monolayer, however, the expression was reduced in HR cells, which is in agreement with gene analysis results. ALDH7A1 showed 1.9-fold increase in SL and 4.6-fold in the HR compared to monolayer cells.

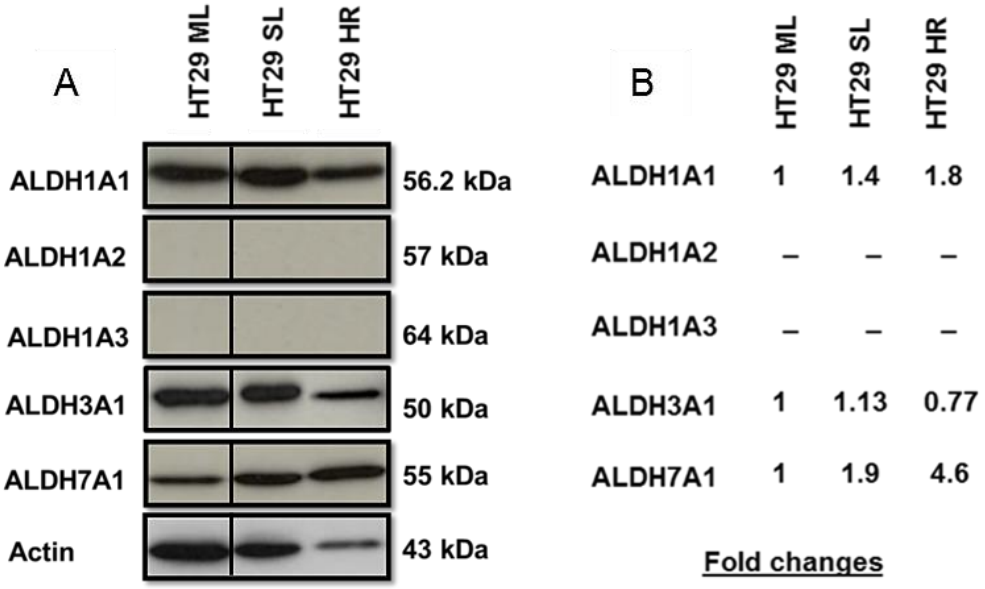

Figure 26 ALDH protein expression profiling of HT29 MCS. Western blot (A), Fold changes of protein level (B). Protein expression analysis was carried out using western blot. Actin was used as internal control protein. Monolayer (ML), Surface layer (SL) and Hypoxic region (HR).

Similar analysis was carried out in DLD-1 spheroids. The gene and protein expression was analysed in cells residing in the surface layer (depth ≈ 0-21 µm) and hypoxic region (depth ≈ 133-150.7 µm) of DLD-1 spheroids.

Figure 27 shows the results of qRT-PCR. The positive control gene VEGFA was upregulated in the hypoxic region but not in the surface layer, confirming the presence of hypoxia in the deep layer of DLD-1 spheroids but not in the surface layer. Slight upregulation of ALDH1A1 was observed in SL, however this was significantly elevated in the HR (5-fold). No major variation was detected in other ALDH1 isoforms (1A2, 1A3 and 1B1). ALDH2 and 3A1 showed elevated level of expression in the HR compared to SL, while ALDH7A1 was found to be elevated in both SL (2-fold) and HR (3-fold) layers compared to monolayer cells.

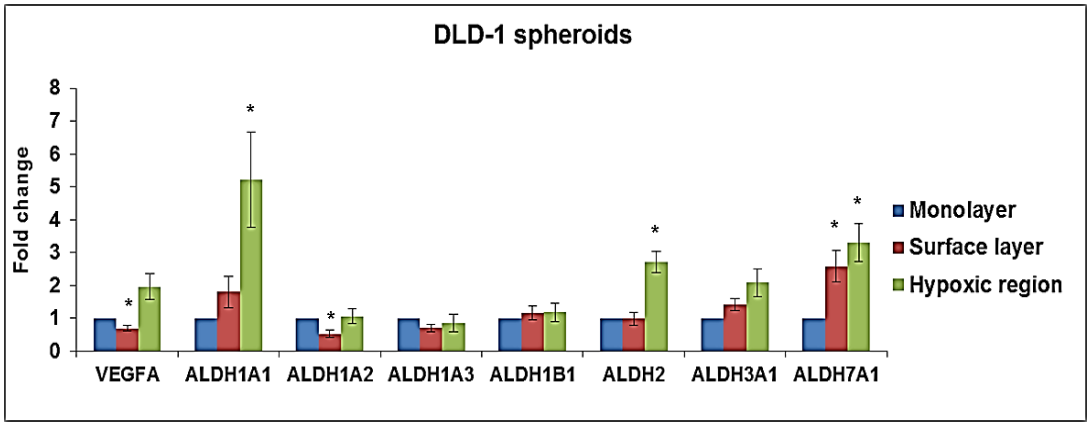

Figure 28 The expression of ALDH mRNA in DLD-1 MCS. Gene expression analysis was carried out using q-RT-PCR. VEGFA was used as positive control and β-actin as internal control gene. Values are the mean of 3 independent experiments and error bars are SD. P values: * $p<0.05$.

Western blot analysis was carried out to see whether these observations were translated to protein level (Figure 28). ALDH1 isoforms were not detected in SL or in HR. ALDH3A1 was found to be upregulated in HR compared to monolayer (ML) (1.8-fold) with no major difference in expression between SL and ML, while ALDH7A1 was found to be elevated in SL and HR compared to ML (2.7 and 3-fold, respectively).

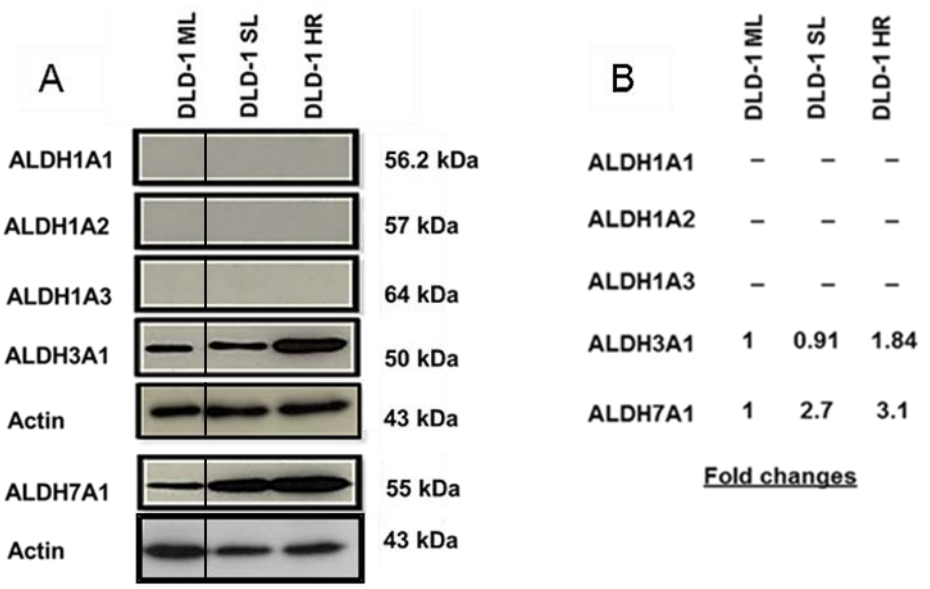

Figure 27 ALDH protein expression profiling of DLD-1 MCS. Western blot (A), Fold changes of protein level (B). Protein expression analysis was carried out using Western blot. Actin was used as internal control protein. Monolayer (ML), Surface layer (SL) and Hypoxic region (HR).

2.3.2.3 Evaluation of ALDH expression in colorectal cancer MCS and tumour xenograft models

To evaluate the distribution of ALDH and their cellular localisation, protein expression was evaluated in colon cancer MCS and tumour xenograft models using IHC staining as previously described in Materials and Methods, section 2.2.2.7.

Figure 29A shows that ALDH1A1 is uniformly expressed in HT29 MCS with the main expression occurring in the cytoplasm, although some cells show nuclear staining as well. Furthermore, some cells residing in the necrotic core were also expressing ALDH1A1. DLD-1 MCS showed positive staining in the deeper hypoxic region, while surface layers showed faint staining indicating less expression compared to hypoxic region (Figure 29B).

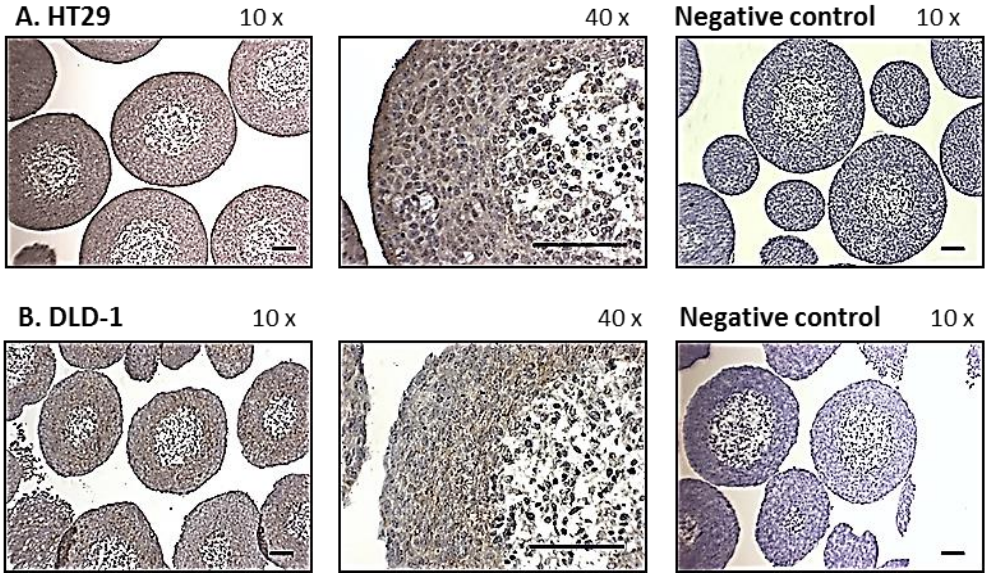

Figure 29 Immunohistochemistry of ALDH1A1 in HT29 (A) and DLD-1 (B) MCS. Brown colour indicates positive staining and ALDH1A1 expression. Scale bar = 100 µm at 10x and 40x objective lens.

Figure 30A shows high expression of ALDH1A1 in the HT29 xenograft with staining primarily in the cytoplasm and some cells showing positive nuclear expression. The COLO205 xenograft also had high expression of ALDH1A1 in both cytoplasmic and nuclear compartments (Figure 30E). The DLD-1 xenograft showed moderate cytoplasmic expression of ALDH1A1 (Figure 30B), while the HCT116 and SW620 xenografts had the lowest cytoplasmic expression of ALDH1A1 amongst the xenografts models investigated (Figure 30C and D, respectively).

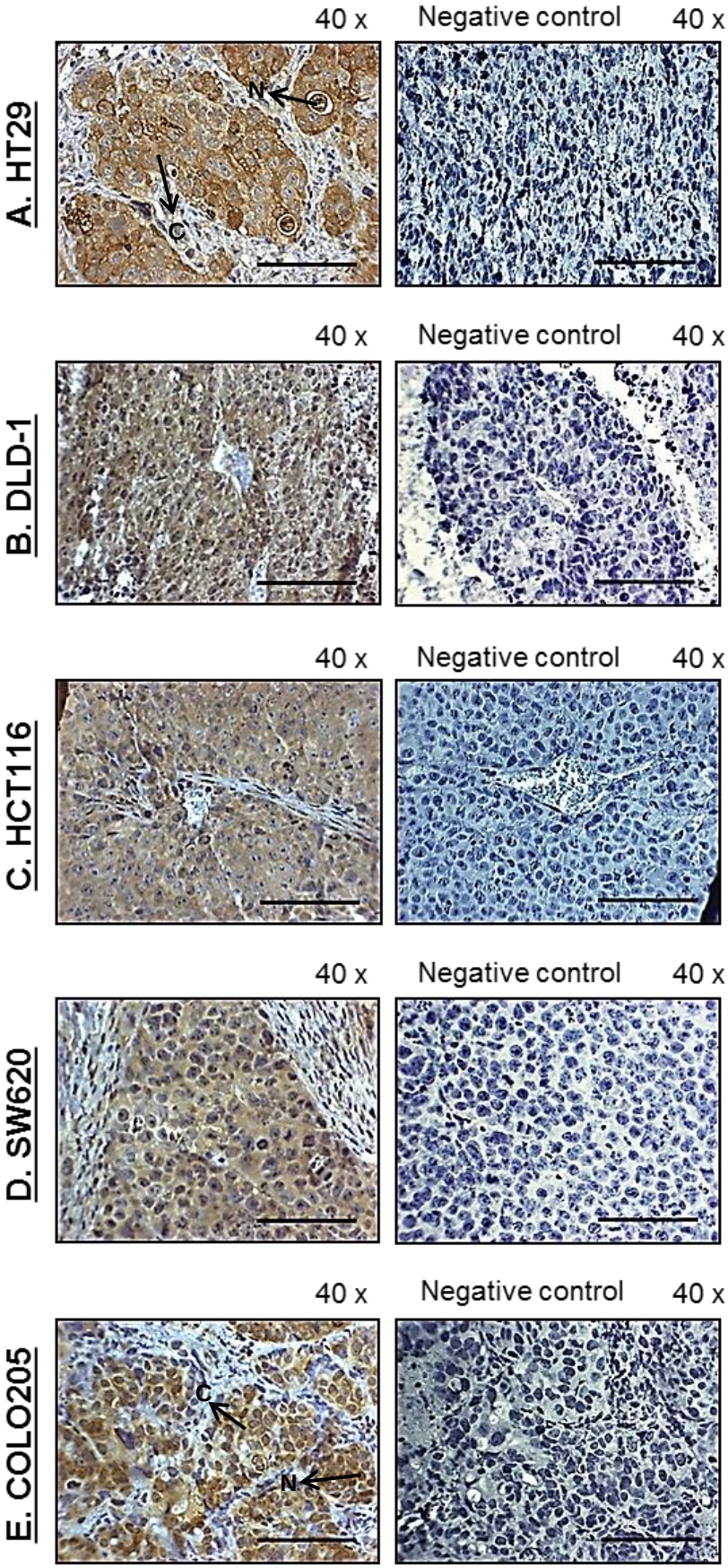

Figure 30 Immunohistochemistry of ALDH1A1 in colon cancer xenografts. HT29 (A), DLD-1 (B), HCT116 (C), SW620 (D) and COLO205 (E). Brown colour indicates positive staining and ALDH1A1 expression. Nuclear staining (N) and cytoplasmic staining (C). Scale bar = 100 μm at 40x objective lens.

\\

Figure 31 shows that both HT29 and DLD-1 MCS do not express ALDH1A3 confirming the results from western blot (Figure 26 and 28, section 2.3.2.2). IHC of xenografts are shown in Figure 32. Only stromal cells in HT29 xenograft have weak detectable expression of ALDH1A3, while tumour cells were negative. The DLD-1 and SW620 xenografts showed weak, primarily cytoplasmic expression, while COLO205 xenografts were shown to express both weak cytoplasmic and nuclear ALDH1A3 expression. HCT116 showed the highest expression, primarily in the cytoplasm although some cells also showed nuclear expression.

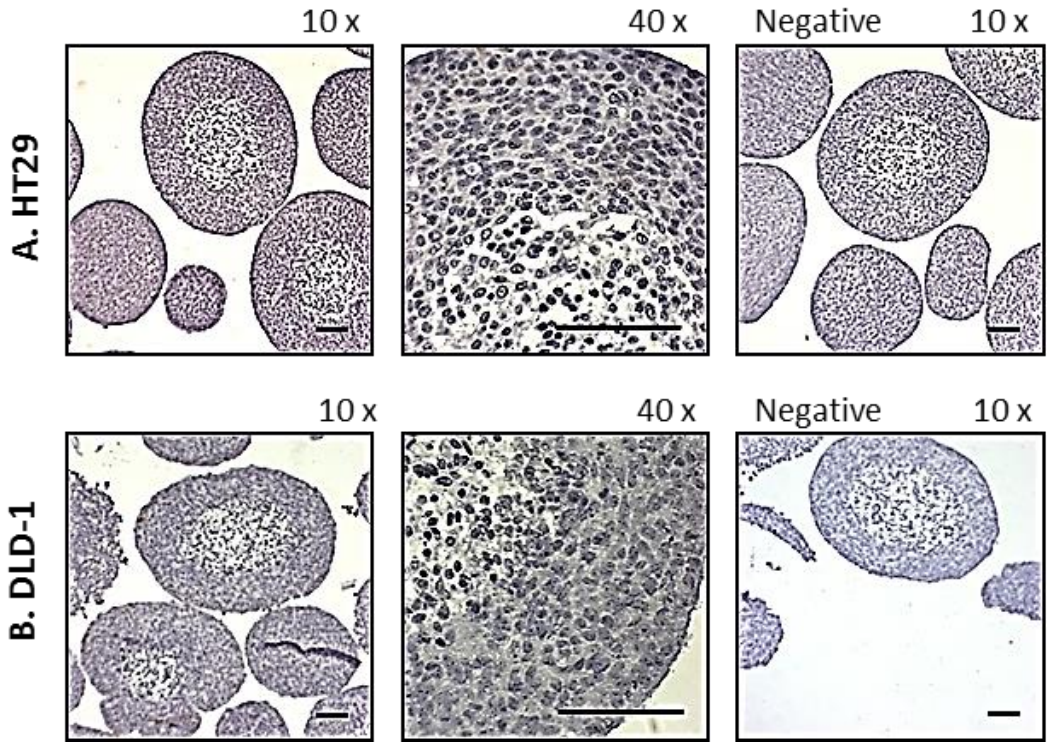

Figure 31 Immunohistochemistry of ALDH1A3 in HT29 (A) and DLD-1 (B) MCS. Both spheroids were negative for ALDH1A3 expression (no brown colour was detected). Scale bar = 100 µm at 10x and 40x objective lens.

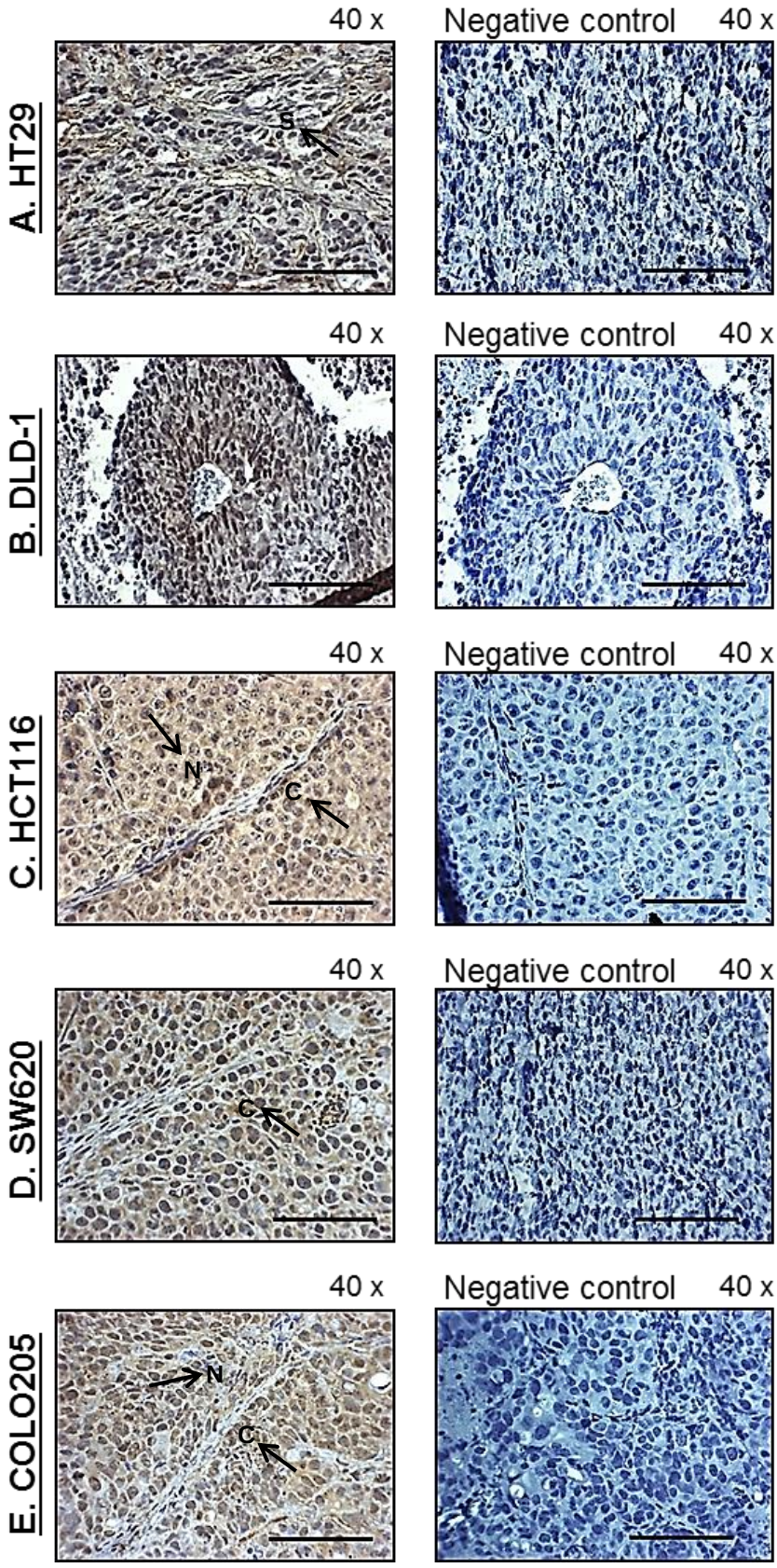

Figure 32 Immunohistochemistry of ALDH1A3 in colon cancer xenografts. HT29 (A), DLD-1 (B), HCT116 (C), SW620 (D) and COLO205 (E). Brown colour indicates positive staining and ALDH1A3 expression. Nuclear staining (N), cytoplasmic staining (C) and stromal staining (S). Scale bar = 100 μm at 40x objective lens.

IHC staining of ALDH3A1 showed high expression in both HT29 and DLD-1 MCS (Figure 33). The expression was mainly cytoplasmic in HT29 but both cytoplasmic and nuclear in DLD-1 MCS. Interestingly, cells in the necrotic core of both spheroids showed positive nuclear staining of ALDH3A1.

All tested xenograft models showed weak, primarily cytoplasmic expression of ALDH3A1 with the exception to COLO205, which showed high nuclear expression as well (Figure 34).

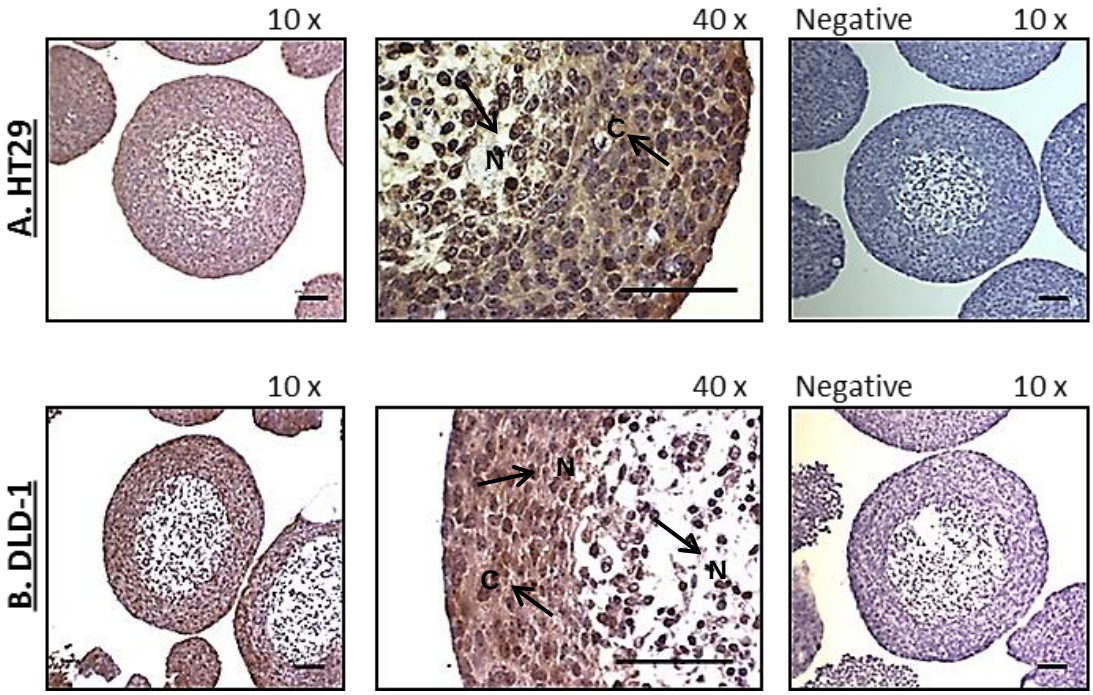

Figure 33 Immunohistochemistry of ALDH3A1 in HT29 (A) and DLD-1 (B) MCS. Brown colour indicates positive staining and ALDH3A1 expression. Nuclear staining (N) and cytoplasmic staining (C). Scale bar = 100 µm at 10x and 40x objective lens.

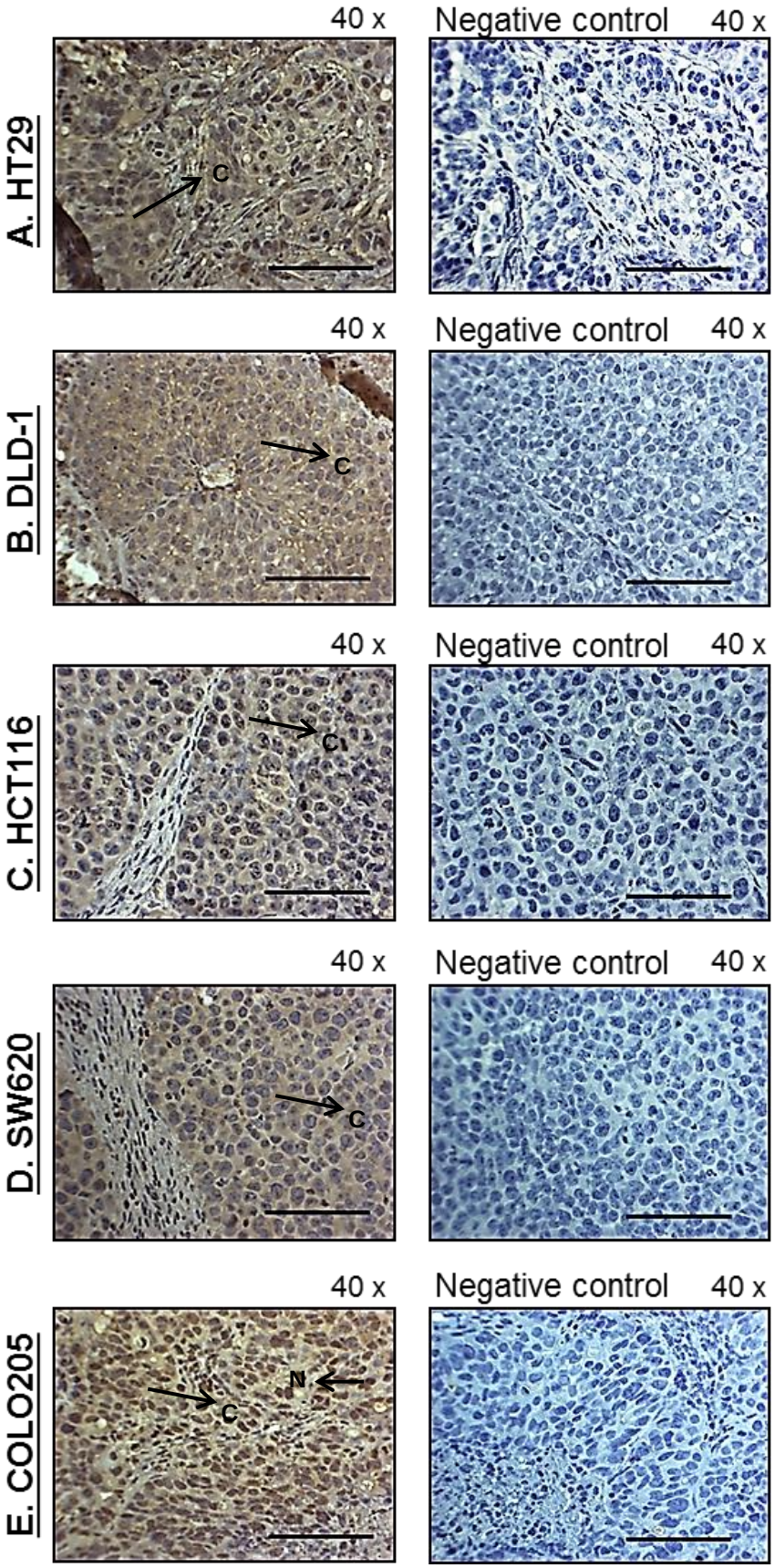

Figure 34 Immunohistochemistry of ALDH3A1 in colon cancer xenografts. HT29 (A), DLD-1 (B), HCT116 (C), SW620 (D) and COLO205 (E). Brown colour indicates positive staining and ALDH3A1 expression. Nuclear staining (N) and cytoplasmic staining (C). Scale bar = 100 µm at 40x objective lens.

Figure 35 shows the expression of ALDH7A1 in MCS. Both spheroids were shown to possess high expression of this isoform in the hypoxic regions, which gradually reduced with distance to the peripheral surface layers. This finding confirms that ALDH7A1 is upregulated in hypoxic areas. The expression was both cytoplasmic and nuclear in HT29 MCS. In contrast, the DLD-1 surface layer cells showed only cytoplasmic staining while inner layers showed both cytoplasmic and nuclear. Some cells in the necrotic core of both MCS models were stained positive for ALDH7A1.

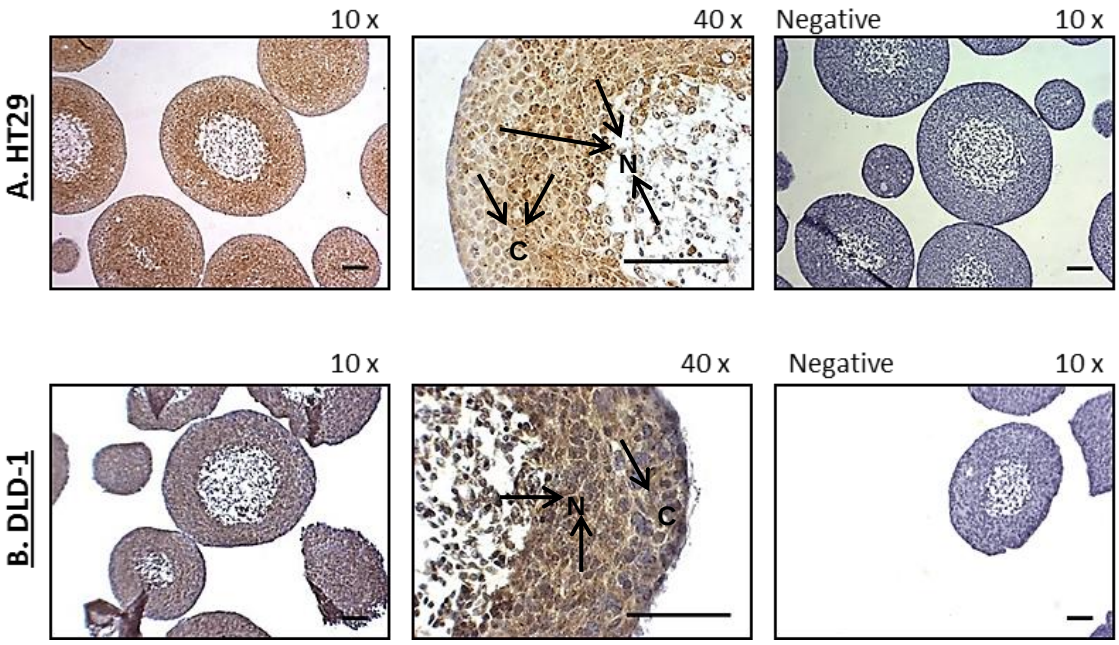

Figure 35 Immunohistochemistry of ALDH7A1 in HT29 (A) and DLD-1 (B) MCS. Brown colour indicates positive staining and ALDH7A1 expression. Nuclear staining (N) and cytoplasmic staining (C). Scale bar = 100 µm at 10x and 40x objective lens.

Figure 36 shows that ALDH7A1 is highly expressed in all examined xenograft models. Its expression is mainly cytoplasmic, although some cells showed nuclear expression as well.

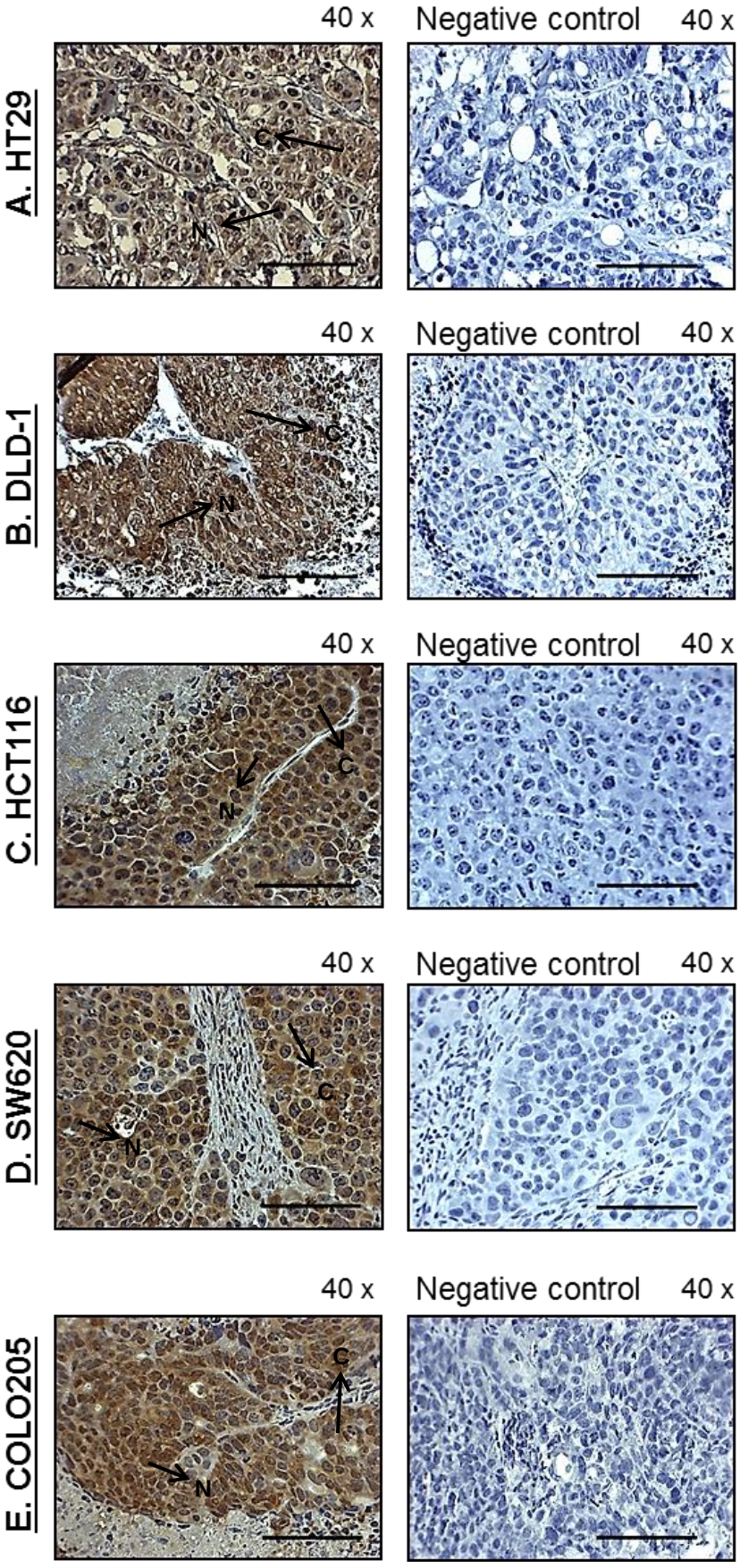

Figure 36 Immunohistochemistry of ALDH7A1 in colon cancer xenografts. HT29 (A), DLD-1 (B), HCT116 (C), SW620 (D) and COLO205 (E). Brown colour indicates positive staining and ALDH7A1 expression. Nuclear staining (N) and cytoplasmic staining (C). Scale bar = 100 µm at 40x objective lens.

2.3.2.4 Detection of hypoxia in MCS and xenograft models

The areas of hypoxia were identified in HT29 MCS using the hypoxic marker carbonic anhydrase IX (CAIX). Figure 37 shows the hypoxic region of HT29 MCS that were stained with CAIX (brown) where CAIX is mainly located in the cellular membrane of HT29 cells, although some cytoplasmic expression was also observed. In comparison, cells residing in the outer layers showed no expression, suggesting that these cells were not hypoxic. The expression of ALDH7A1 as previously described is significantly elevated in the hypoxic region of HT29 MCS compared to the outer viable rim, indicating that low oxygen tensions may modulate ALDH7A1 expression. In contrast, localisation of the hypoxic regions in DLD-1 MCS and xenografts were unsuccessful with anti-CAIX antibody, although different incubation conditions were carried out and HT29 spheroids were included as controls.

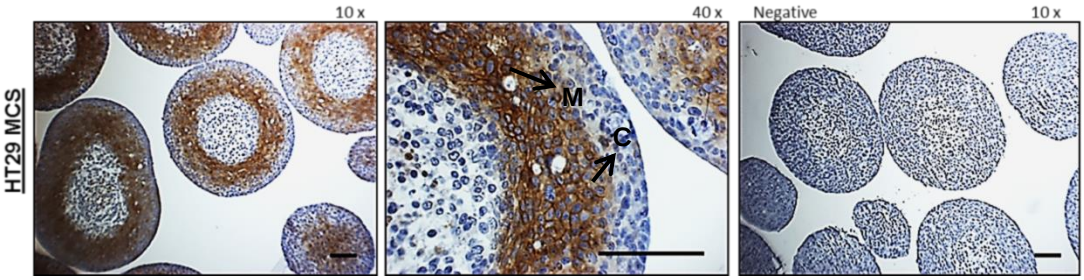

Figure 37 Immunohistochemistry of CAIX in HT29 MCS. Brown colour indicates positive staining and CAIX expression. Membranous staining (M) and cytoplasmic staining (C). Scale bar = 100 µm at 10x and 40x objective lens.

2.3.3 Regulation of ALDH7A1 expression by HIF

2.3.3.1 HIF-1α induction using $CoCl_2$ treatment

Results from 2D and 3D experiments showed that ALDH7A1 is upregulated under hypoxia in both HT29 and DLD-1 cells. To understand whether the expression of ALDH7A1 was regulated by HIF-1α, cells were treated with $CoCl_2$, which is known as an inducer of HIF-1α protein (Piret et al., 2002).

The concentration of $CoCl_2$ was selected based on the results of the MTT assay. Figure 38 shows the dose response curve of DLD-1 and HT29 cells that were treated with $CoCl_2$ for 24h. 100 and 150 µM were chosen to treat DLD-1 cells while 200 and 300 µM were chosen to treat HT29 cells.

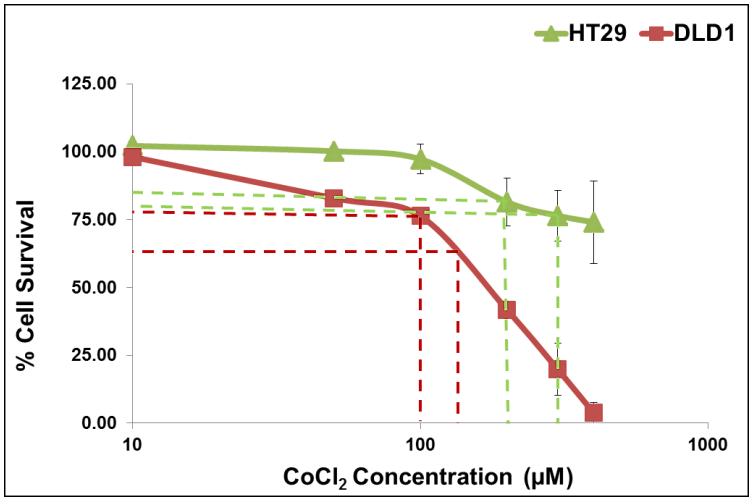

Figure 38 Dose response curve of 24h $CoCl_2$ treatment in HT29 and DLD-1 cell lines using the MTT assay. Values are the mean of 3 independent experiments and error bars are SD.

$CoCl_2$ treatment induced significant expression of HIF-1α but not ALDH7A1 in both DLD-1 and HT29 cell lines (Figure 39), which point towards ALDH7A1 being independent of the HIF-1α key regulator.

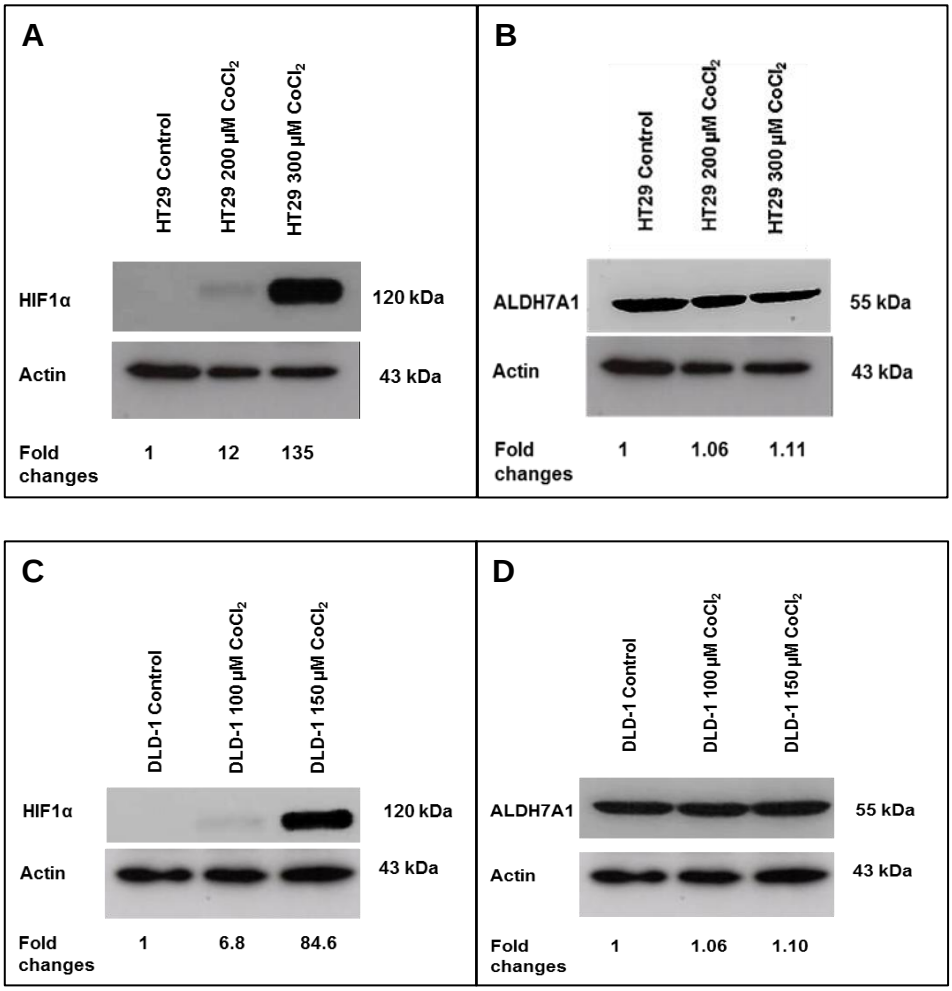

Figure 39 Western blot analysis of HIF-1α and ALDH7A1 protein expression upon treatment with $CoCl_2$ in HT29 cells (A,B) and DLD-1 cells (C,D). Actin was used as internal control protein.

2.3.3.2 Knockdown of HIFs and their effect on ALDH7A1 expression

The expression of ALDH7A1 was measured in DLD-1 cells after 24h, 48h and 72h exposure to hypoxia, revealing an upregulation at each time point at both the gene and protein levels (Figure 40). This preliminary finding reconfirms that ALDH7A1 was upregulated under hypoxic conditions.

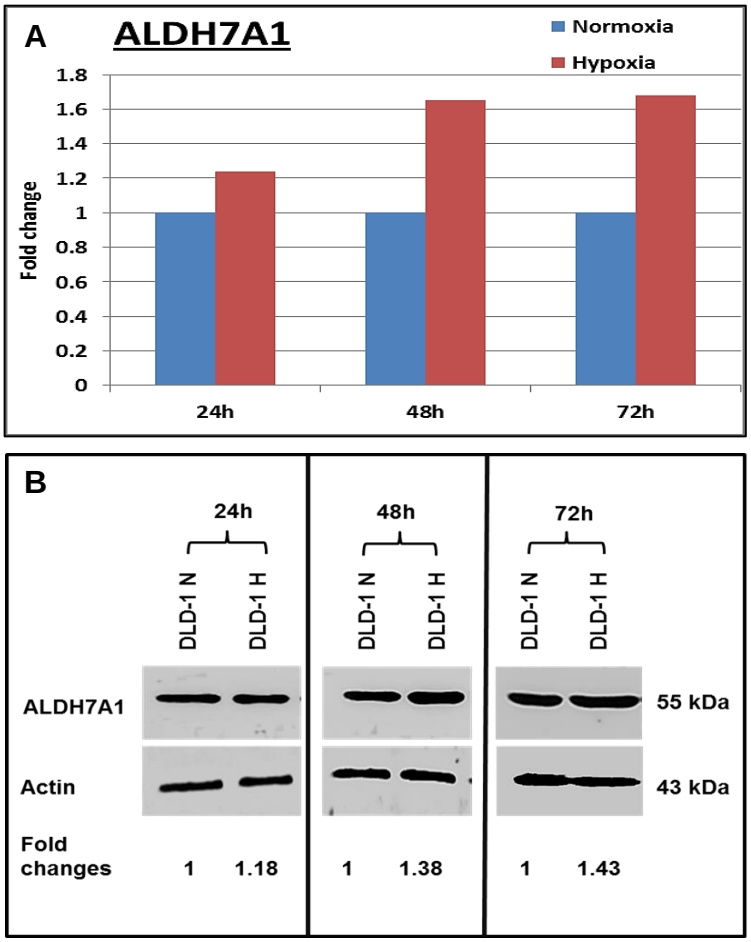

Figure 40 ALDH7A1 expression in DLD-1 cells upon exposure to hypoxia for 24h, 48h and 72h. ALDH7A1 mRNA expression using qRT-PCR (A). ALDH7A1 protein expression using western blot (B). Results represent one experiment.

The previous experiment using $CoCl_2$ treatment, however, showed no difference in ALDH7A1 expression upon induction of HIF-1α. Accordingly, to confirm this observation and to evaluate whether HIF-2α might have a regulatory role, single and dual knockdown experiments of HIF-1α and HIF-2α were carried out under hypoxic conditions.

Figure 41 shows the preliminary result with significant reduction in HIF-1α and HIF-2α gene expression was achieved after 48h and 72h of single or dual siRNAs transfection. However, it was not possible to confirm this at the protein level as no bands were detected using western blot.

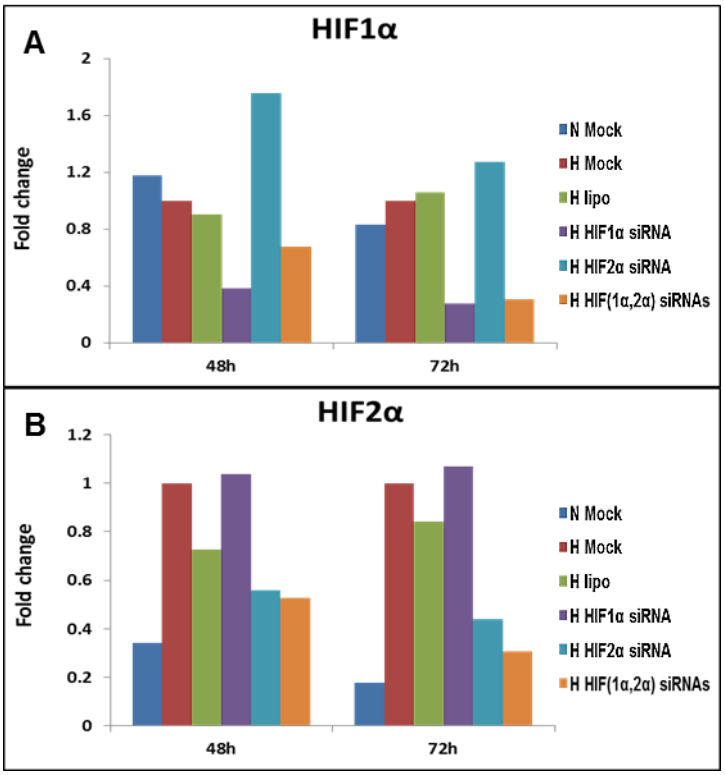

Figure 41 The expression of HIF1-α and HIF2-α mRNA in DLD-1 cells using qRT-PCR upon HIFs knockdown. HIF1-α (A), HIF2-α (B), Normoxia (N), Hypoxia (H). Results represent one experiment.

Nevertheless, gene analysis of ALDH7A1 in HIF-α knockdown cells was carried out. The preliminary results showed that ALDH7A1 gene expression was not affected after 48h or 72h of single HIF-α knockdown. On the other hand, dual knockdown of HIF-1α and HIF-2α after 72h resulted in 50% reduction of ALDH7A1 expression at the mRNA level (Figure 42A). The results of ALDH7A1 protein expression, however, revealed that it was not significantly affected upon HIF knockdown (Figure 42B).

The aforementioned findings suggest that ALDH7A1 expression under hypoxic conditions is HIF1α/2α independent.

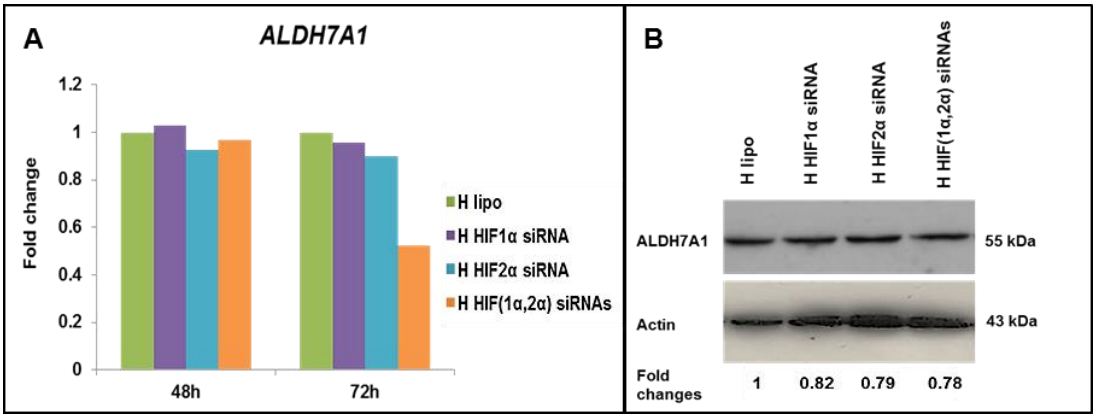

Figure 42 The expression of ALDH7A1 after HIF knockdown. ALDH7A1 mRNA expression using qRT-PCR after 48h and 72h of HIF-α knockdown (A). ALDH7A1 protein expression using western blot after 72h of HIF knockdown (B). Results represent one experiment.

2.4 Discussion

Some evidence suggests that certain ALDH isoforms may play important roles in the aggressiveness of colorectal cancer. ALDH1A1 has been shown to act as a stem cell marker (Emmink et al., 2013), while 1B1 in one study was shown to be highly expressed in clinical tissue and on this basis was suggested to be a potential colon cancer biomarker (Chen et al., 2011). In addition, it has been demonstrated that ALDH1A3 and 3A1 are involved in drug resistance and metastasis, respectively (Touil et al., 2014, Tang et al., 2014) (for further details, see Introduction, section 2.1).

Given the role of the tumour microenvironment and hypoxia in the aggressiveness of CRC and drug resistance (Mathonnet et al., 2014), this study was designed to explore the link between hypoxia and ALDH expression. Specifically, the impact of hypoxia on the expression of selected ALDH isoforms (1A1, 1A2, 1A3, 1B1, 2, 3A1 and 7A1) that have been linked to cancer pathogenesis was evaluated. ALDH7A1 was of particular interest due to its role in protection against oxidative stress (Brocker et al., 2011). It was envisaged that this line of investigation would subsequently aid in determining the suitability of using ALDHs as biomarker(s) and/or therapeutic target(s).

To interrogate ALDH expression, a panel of CRC cell lines (DLD-1, HT29, HCT116 and SW480) were exposed to very low oxygen level (0.1%) and compared to cells grown under normoxia. Although an oxygen gradient exists across a solid tumour, 0.1% O_2 was chosen in this study as it is a physiologically relevant level that is associated with induction of HIF-1

activation (Wilson and Hay, 2011) and likely to support an aggressive microenvironment.

Gene expression profiling of ALDH was evaluated by measuring the level of mRNA using qRT-PCR (Ginzinger, 2002), while protein expression was evaluated using western blot (Mahmood and Yang, 2012). VEGFA gene was used as a positive control because it is known to be upregulated under hypoxic conditions (Bergers and Benjamin, 2003). However, the antibody of VEGFA for western blot did not work consistently in all experiments and therefore, LDH-A was also used as a positive control to validate the hypoxia-related experiments (Firth et al., 1995). In this study, all cell lines showed upregulation of VEGFA gene and LDH-A protein in hypoxic samples, confirming that cells were exposed to hypoxic conditions capable of inducing changes at the gene and protein levels.

The CSC marker ALDH1A1 was found to be expressed at low level in all examined normoxic cell lines except HT29 cells. Exposure of these cells to hypoxia resulted in upregulation of ALDH1A1 in both HCT116 and HT29 cells. However, at the protein level, only HT29 cells showed expression of ALDH1A1 but without significant change upon exposure to hypoxia. This finding supports the result of Hasmim *et al.* study, where the expression of ALDH1 in NSCLC was found not to be affected by hypoxia (Hasmim et al., 2011).

ALDH1A2 gene was found to have the lowest level of expression amongst all seven ALDH isoforms evaluated and its expression was upregulated upon exposure to hypoxia in all cell lines except SW480. However, this isoform

was not detected at the protein level. As a previous study showed that this isoform act as TSG in prostate cancer, where it was found to be epigenetically silenced (Kim et al., 2005), it might suggest that ALDH1A2 expression is also under epigenetic control in CRC. However, further work such as DNA methylation analysis in both normal and cancerous colon cells is required to confirm this observation.

In the current study, ALDH1A3 was found to be highly expressed in HCT116 and SW480 cell lines at the mRNA level. In addition, it was only detected in these two cell lines at the protein level. The change in expression upon exposure to hypoxia revealed that only the aforementioned cell lines showed significant upregulation of ALDH1A3. A previous study reported that ALDH1A3 is upregulated in 5-FU resistant cells (Touil et al., 2014). In addition, hypoxia has been shown to induce drug resistance against 5-FU in a wide panel of cells (Ahmadi et al., 2014). Therefore, the upregulation of ALDH1A3 might be one of the mechanisms that contribute to drug resistance observed in hypoxic cells. However, more experiments are needed to confirm this is indeed the case.

ALDH1B1 was the last ALDH1 isoform evaluated in this study and was found to be highly expressed in all cell lines with the exception of HT29. However, as hypoxia exposure showed no major effect on ALDH1B1 gene expression, the protein expression was not evaluated. The abundance of ALDH1B1 is in agreement with immunohistochemical studies that showed expression of this isoform in 98% of colon cancer samples (Chen et al., 2011). Although very little is understood about what regulates ALDH1B1, its high and reliable

expression in clinical samples could be used to ascertain the presence of CRC.

Little is known regarding the expression of ALDH2 in CRC. ALDH2 gene was found to be highly expressed in the four CRC cell lines that showed similar levels of expression. However, hypoxia resulted either in its downregulation (HCT116 and SW480) or no major changes (HT29 and DLD-1), hence the protein expression was not evaluated.

The third family that was investigated was ALDH3. ALDH3A1 has been shown to be amongst the genes that were highly upregulated in a mechanically-induced colon cancer cell population, which correlated with cancer cell migration and invasion (Tang et al., 2014). In this study, DLD-1 and HT29 showed similar level of 3A1 gene expression which was higher than what was found in HCT116 and SW480 cells. ALDH3A1 protein expression was only detectable in HT29 and DLD-1 cells. However, only HT29 showed slight, insignificant reduction of 3A1 expression at both the gene and protein levels. The findings presented here is in line with previously published data, which indicated that hypoxia exerts downregulation of both the constitutive and inducible ALDH3 expression and the effect is cell line specific (Reisdorph and Lindahl, 1998). It has been speculated that this was due to limiting levels of ARNT (HIF-1β) being shared by two pathways, which under hypoxic conditions forms heterodimers with HIF-1α and thus was not available to interact with critical xenobiotic response elements (XREs) required for ALDH3 expression (Reisdorph and Lindahl, 1998). Nonetheless, in a later study conducted by the same group, it was shown that ARNT was

not the limiting transcription factor and thus it was concluded that further investigations were urgently needed to explain such findings (Reisdorph and Lindahl, 2001).

ALDH7A1 was the final ALDH isoform investigated in this study. Human ALDH7A1 protects against hyperosmotic stress presumably through the generation of betaine, an important cellular osmolyte, formed from betaine aldehyde (Brocker et al., 2010). In addition, it was found that ALDH7A1 may possess important antioxidant activity that attenuate reactive aldehyde and oxidative stress induced cytotoxicity (Brocker et al., 2011). Abnormally high expression of ALDH7A1 has been found in ovarian cancer (Saw et al., 2012), prostate cancer and matched bone metastasis samples (van den Hoogen et al., 2010, van den Hoogen et al., 2011), while its expression in NSCLC patients has been linked with increased incidence of cancer recurrence (Giacalone et al., 2013). However, the role of ALDH7A1 in CRC is unexplored. In the present study, ALDH7A1 was found to be expressed in all cell lines at both the gene and protein levels. Exposure of these cells to hypoxia resulted in significant upregulation in HT29 and DLD-1 cells at both the gene and protein levels. As previous studies reported the role of ALDH7A1 as an antioxidant enzyme (Brocker et al., 2011), it suggests that hypoxic cells might enhance the expression of this enzyme in order to protect themselves against ROS and oxidative stress. Accumulating evidence has shown that hypoxic cells undergoing exposure to oxidative stress develop adaptive responses to survive in the aggressive environment (Fan et al., 2007) (Chapter 1 Introduction, section 1.5.1). In fact, these might include

antioxidant responses such as the GSH–GPX antioxidant system (Fan et al., 2008). In the present study, one of these adaptive responses may be the upregulation of the antioxidant enzyme, ALDH7A1. Brocker *et al*. showed that ALDH7A1 enzyme activity is cytoprotective under oxidative conditions where LPO and subsequent aldehyde levels are elevated. Mechanistically, it has been shown that the removal of LPO-derived aldehydes by ALDH7A1 could have multiple cytoprotective functions; ALDH7A1 metabolic activity could reduce the need for GSH conjugation and help maintain intracellular GSH levels counteracting the damaging effects of oxidative stress (Brocker et al., 2011).

The data presented in this study using 2D models demonstrated that the selected panel of ALDHs are expressed in CRC cell lines at different levels but there is no clear distinction between these cells based on the ALDH expression pattern. To our knowledge, this is the first study to report findings on the role of hypoxia in modulating the aforementioned isoforms with the exception to ALDH1A1 and 3. The findings of the current study suggested that hypoxia has an impact on ALDH expression although this is cell line specific. In addition, the upregulation of ALDH1A3 and 7A1 upon exposure to hypoxia suggests that these isoforms might have important roles in cell survival and aggressiveness of hypoxic cells of CRC. However, more work is required to clarify their roles.

The impact of hypoxia on ALDHs in 3D multicellular spheroids (MCS) models of DLD-1 and HT29 CRC cell lines was also explored. Although they do not have an existing vasculature system, MCSs are good representatives of

micro-metastases prior to vascularisation due to their 3D nature (Hirschhaeuser et al., 2010) and lack of abundant oxygen and nutrients (Waleh et al., 1995). Therefore, it was of great interest to study the selected ALDHs in cells that reside in the hypoxic region of the MCS as well as cells in the outer viable rim; the latter has access to molecular oxygen and nutrients in contrast to the former which is starved of both. To our knowledge, only few studies have explored the expression of ALDH in 3D spheroids. ALDH1 was reported to be upregulated in CRC spheroids (HT29) (Fan et al., 2011), while ALDH1A1 isoform was found to be highly expressed in ovarian cancer MCS where it was directly connected to key elements of the β-catenin pathway (Condello et al., 2015). However, these studies did not explore the expression of ALDH at different depth within MCS which may affect enzyme expression and function.

Spheroids were generated using the spinner flask technique (O'Connor, 1999) and hypoxia was detected using the hypoxic marker, pimonidazole (Laurent et al., 2013). It was found that cells residing in the outer layers were not hypoxic, while the intensity of pimonidazole staining increased toward the inner layers surrounding the necrotic cores. These cells were stripped from HT29 and DLD-1 MCSs using sequential trypsinisation technique as previously described (Phillips et al., 1994). Results from gene and protein expression of DLD-1 and HT29 MCS models, revealed that ALDH1A1 was upregulated in HT29 MCS compared to monolayer normoxic cells which supports the findings of Fan et al. study (Fan et al., 2011). However, no major difference in ALDH1A1 expression between peripheral layer and

hypoxic region of MCS was observed. In contrast, ALDH7A1 expression was found to be increased in the peripheral layers of both DLD-1 and HT29 spheroids compared to normoxic monolayer cells, while hypoxic regions showed more pronounced upregulation. Variable responses were observed for other ALDH examined in this study (See Results, section 2.3.2.2). Given the role of ALDH7A1 in oxidative stress, the coexistence of hypoxia and ALDH7A1 may provide a signature of the aggressiveness of CRC.

Immunohistochemistry (IHC) studies were also carried out to assess the distribution of ALDH7A1 through different depth of MCS as well as its cellular localisation (Schacht and Kern, 2015). Interestingly, the expression of ALDH7A1 was highly elevated in the hypoxic region of both MCS compared to the outer layer, indicating that this isoform might be an important player in the CRC microenvironment. In addition, cytoplasmic and nuclear expression was evident, suggesting that ALDH7A1 might have a role in cell cycle progression. Chan *et al*. studies showed that ALDH7A1 was upregulated and accumulated in the nucleus during G1/S phase transition in both the human embryonic kidney HEK293 cells and liver WRL68 cells. Knockdown experiments showed modulation in the levels of several key cell cycle-regulating proteins .(Chan et al., 2011). For further investigation of ALDH7A1 role in CRC, analysis of cell cycle phases upon ALDH7A1 knockdown will be carried out and discussed in the next chapter.

To further evaluate the abundance of ALDH7A1 in CRC, the expression was explored in 5 CRC xenografts (HT29, DLD-1, SW620, HCT116 and COLO205) using IHC and it was found to be highly expressed in all

examined xenografts. IHC were also carried out to assess ALDH7A1 distribution in correlation with hypoxia using an intrinsic marker of tumour hypoxia, CAIX, which is a membrane-associated zinc metalloenzyme that has a key role in pH regulation and one of HIF-1α targets (Loncaster et al., 2001). In this study, the expression of CAIX was only detected in the inner layers of HT29 MCS confirming that these cells were hypoxic. As ALDH7A1 was found to be highly expressed in these layers, this supports the potential role of hypoxia in the modulation of ALDH7A1 expression. The use of CAIX to locate hypoxia in DLD-1 MCS and xenograft tumour models was however, unsuccessful and other markers such as glucose transporter-1 (Glut-1) will be considered for future work (Airley et al., 2003).

Results from 2D and 3D culture models of HT29 and DLD-1 cell lines strongly supports the evidence that hypoxia modulates the expression of ALDH7A1. It is well known that tumour cells adapt to deprivation in oxygen through the stabilisation of hypoxia inducible factors (Sutherland, 1998). In order to investigate whether HIF-1α and/or HIF-2α are involved in the transcriptional regulation of ALDH7A1 expression, induction of HIF-1α using $CoCl_2$ and downregulation of these HIFs using knockdown experiments were carried out. $CoCl_2$ is known to cause stabilisation of HIF-1α under normoxic conditions (Piret et al., 2002, Law et al., 2012). In this study $CoCl_2$ was found to intensely induce HIF-1α protein expression in both DLD-1 and HT29 cells. However, no variation in the expression level of ALDH7A1 was observed. This suggests that the expression of ALDH7A1 under hypoxic conditions is

HIF-1α independent. Therefore, knockdown studies of both HIF-1α and/or HIF-2α were carried out to confirm this finding.

The expression of ALDH7A1 in DLD-1 cells was revaluated after 24h, 48h and 72h of incubation under hypoxia and it was found to be increased at both the gene and protein levels. Knockdown studies using small interfering RNAs (siRNAs) against HIF-1α and/or HIF-2α were carried out and their effect on ALDH7A1 expression was evaluated. Significant and specific knockdown of HIF-1α and HIF-2α expression was achieved after 48h and 72h at the gene level. Although different incubation conditions for western blot were used, results were not confirmed at the protein level as no bands were detected. Nevertheless, the expression of ALDH7A1 was only downregulated by 50% after 72h of HIF-1α/2α dual knockdown at the gene level, while less than 22% reduction occurred at the protein level. This suggests that ALDH7A1 expression in hypoxia is HIF-1α/HIF-2α independent and might be controlled by another cellular mechanism. Although the major hypoxia-regulated transcription factor is HIF, tumour cells can also adapt to hypoxic microenvironment through other hypoxia inducible transcriptional factors such as nuclear factor κB (NF-κB), activator protein I (AP-I) and p53 (Carroll and Ashcroft, 2005). Therefore, these factors might be involved in the regulation of ALDH7A1 expression upon exposure to hypoxia, however, further work is needed to confirm this.

In summary, the expression of ALDHs was assessed in CRC at both the gene and the protein levels using 2D and 3D models. ALDH7A1 was found to be highly expressed in CRC xenografts, while this isoform was found to be

sensitive to hypoxia exposure in HT29 and DLD-1 cell lines. In addition, this enzyme was highly expressed in the hypoxic region of 3D MCS models of these cell lines compared to surface layer cells. Given the role of hypoxia in mediating the adaptive strategies in cells undergoing exposure to oxidative stress, upregulation of ALDH7A1 as antioxidant enzyme was suggested. However, knockdown experiments suggested that HIF-1α/HIF-2α were not important for inducing ALDH7A1 expression and hence this enzyme is controlled by another cellular mechanism. Accordingly, ALDH7A1 was further explored and the data from knockdown studies and isogenic cell line pair is reported in Chapter 3 and 4, respectively.

The main findings of this Chapter were:

- ALDH1A2 is expressed at very low level in the four cell lines examined in this study.
- ALDH1A3 expression was found to be upregulated upon exposure to hypoxia in both HCT116 and SW480 cell lines at both the mRNA and protein levels.
- ALDH7A1 expression was found to be upregulated upon exposure to hypoxia in both HT29 and DLD-1 cell lines at both the mRNA and protein levels. Its expression was also increased at the hypoxic regions of MCS of both cell lines.

Chapter 3: Probing the functional roles of selected ALDH isoforms in colorectal cancer using siRNA knockdown

3.1 Introduction

Previous studies reported various roles for particular ALDH isoforms in CRC. These include ALDH1B1 as a potential biomarker (Chen et al., 2011), ALDH1A1 as stem cell marker (Emmink et al., 2013), ALDH1A3 associated with drug resistance (Touil et al., 2014) and ALDH3A1 involved in mediating metastasis (Tang et al., 2014). In addition, results from Chapter 2 revealed ALDH7A1 expression in four CRC cell lines and its expression was shown to increase upon exposure to hypoxia in both HT29 and DLD-1 cell lines. Furthermore, cells residing in the surface layer of MCS models were shown to possess high expression of ALDH7A1 that also increased toward the hypoxic region at both the gene and protein levels compared with monolayer cells. Paraffin-embedded sections of MCS showed clear increased staining for ALDH7A1 in hypoxic regions, while it was also shown that ALDH7A1 was expressed in 5/5 CRC xenografts. Whilst the current literature indicates a role for ALDH1A1, 1A3, 1B1 and 3A1 in CRC, the novel data generated in Chapter 2 suggests that ALDH7A1 might also play an important role in CRC particularly in the context of the hypoxic tumour microenvironment.

Human ALDH7A1 plays a major role in lysine catabolism in the pipecolic acid pathway where it catalyses the oxidation of alpha-aminoadipic semialdehyde (AASA) to alphaaminoadipate. Mutation in ALDH7A1 has been linked to pyridoxine-dependent epilepsy (PDE) as a result of defective lysine catabolism (Mills et al., 2010). In addition, Broker *et al.* reported that human ALDH7A1 plays an important role in protecting cells and tissues from hyperosmotic stress presumably through the generation of betaine, an

important cellular osmolyte, formed from betaine aldehyde (Brocker et al., 2010). Recent investigation showed that this isoform also has protective role against oxidative stress and lipid peroxidation (Brocker et al., 2011).

Increased expression of ALDH7A1 has been reported in different cancer types. Hoogen *et al.* has shown high expression of ALDH7A1 in prostate cancer and matched bone metastasis samples, where it has been validated to be involved in mediating metastasis (van den Hoogen et al., 2010, van den Hoogen et al., 2011). In melanoma, ALDH7A1 was found to be expressed in nodular melanoma (NM), the most aggressive form of melanoma, but not in superficial spreading melanoma (SSM) (Rose et al., 2011). Furthermore, ALDH7A1 was discovered to be upregulated in human papilloma virus-16 (HPV-16)-immortalised cervical epithelial cells, Ecto1 and E6E7, upon treatment with nicotine-derived carcinogen (Prokopczyk et al., 2009). Prokopczyk *et al.* proposed that ALDH7A1 might contribute to malignant transformation of HPV-16-immortalised cervical cells to cervical carcinoma through ALDH7A1 mediated metabolism of 4-(methylnitrosamino)-1-(3-pyridyl)- 1-butanone (Prokopczyk et al., 2009). Significant overexpression of ALDH7A1 has also been observed in ovarian tumours relative to normal ovarian tissue (Saw et al., 2012). A recent study also found the expression of ALDH7A1 to be associated with recurrence in patients with surgically resected NSCLC (Giacalone et al., 2013). More recently, proteomic studies showed that ALDH7A1 was upregulated in DU145 cells resistant to zoledronic acid, pointing to a potential role of ALDH7A1 in drug resistance (Milone et al., 2015).

The above-mentioned investigations and studies presented in Chapter 2 concern the expression of ALDH7A1, however, relatively little is known regarding its biological functions and roles in mediating cancer progression. Therefore, in an attempt to understand the biological significance of ALDH7A1 in CRC, this Chapter interrogates ALDH7A1 function *in vitro* using RNA interference (RNAi). Specifically, RNAi is the process by which expression of a target gene can be effectively silenced or knocked down by the selective degradation or inhibition of translation of its corresponding mRNA by double-stranded RNA (dsRNA) (Rao et al., 2009, Davidson and McCray, 2011). RNAi is activated by dsRNA species delivered to the cytoplasm of cells. The silencing mechanisms can either lead to the degradation of a target mRNA using small interfering RNAs (siRNAs) or short hairpin RNAs (shRNAs), or the suppression of translation of specific mRNAs, as induced by microRNA (miRNA) (Davidson and McCray, 2011). This in turn blocks further expression/accumulation of the target protein, causing a decrease in its levels, and eventual knockdown at the protein level (Davidson and McCray, 2011).

Two key approaches to RNAi that have gained important interest for use in gene silencing are the double-stranded small interfering RNAs (siRNAs) and the vector-based short hairpin RNAs (shRNAs) (Rao et al., 2009). While both siRNAs and shRNAs can be used for experimental knockdown studies, there are differences in their mechanisms of action (Figure 43) (Rao et al., 2009). siRNAs are short duplexes of about 21 base pairs (bps) that are introduced directly into cells where they accumulate in the cytoplasm and get

incorporated into the RNA-induced silencing complex (RISC), which is composed of endoribonuclease Argonaute-2 (Ago-2), Dicer (a dsRNA-specific RNAse III enzyme) and TAR-RNA-binding protein (TRBP). The RNA duplex is separated and one strand is removed from the complex. The strand with the lowest duplex stability at its 5'-end is selected for stable incorporation into the RISC. As a moiety of the RISC, the siRNA binds to the target mRNA in a sequence-specific manner that is mediated by complementary base pairing, leading to cleavage of the target RNA phosphate backbone near the centre of the duplex via the action of Ago-2 (Allison and Milner, 2014). This process is illustrated in Figure 43.

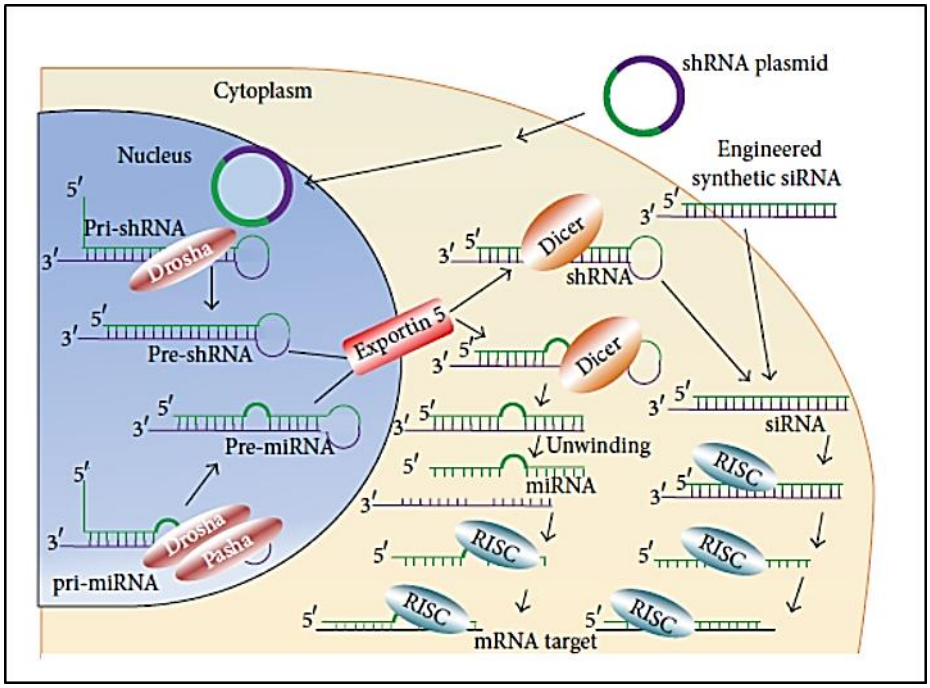

Figure 43 RNAi mechanism. Differences between siRNA, shRNA, and miRNA. Adopted from Torrecilla *et al*. 2014 (Open access article distributed under the Creative Commons Attribution License, which permits unrestricted use, distribution, and reproduction in any medium, provided the original work is properly cited).

shRNAs are synthesised in the nucleus of transfected/transduced cells and form hairpin structures that consist of a stem region of paired antisense and sense strands connected by unpaired nucleotides that make up a loop. shRNAs are introduced into the nuclei of target cells using either bacterial or viral vectors that, in some cases, can stably integrate into the genome. shRNAs are transcribed by either RNA polymerase II or III, depending on the promoter driving their expression (Rao et al., 2009). These initial precursors are processed by Drosha and its dsRNA-binding partner DGCR8, resulting in species known as pre-shRNAs before being exported to the cytoplasm by Exportin-5. The pre-shRNA is then cleaved by Dicer and TRBP/PACT, removing the hairpin and creating a double-stranded siRNA with a length of 20-25 nucleotides. This active siRNA is then loaded onto the RISC complex. Once loaded onto the RISC, the process of targeting mRNA recognition and degradation by both shRNA and siRNA is essentially the same (Rao et al., 2009).

shRNA has an advantage over siRNA because of the ability to use viral vectors for delivery to overcome the difficulty of transfecting certain cell types, however a drawback with shRNA is the need for it to be delivered into the cell nucleus to be processed (Torrecilla et al., 2014). In addition, shRNA can cause oversaturation of the endogenous RNAi machinery, which can result in non-physiological and off-target effects and induce cellular stress. On the other hand, siRNA oligomers can be chemically modified in order to reduce direct off-target effects (Rao et al., 2009). Accordingly, in this study ALDH7A1 siRNA was used to downregulate the expression of ALDH7A1,

while ALDH1A3 and ALDH3A1 siRNAs were employed as controls to help understand specificity of any ALDH7A1 knockdown and associated biological consequences.

The hypothesis of this Chapter was that ALDH7A1 is involved in CRC cell proliferation, migration and reduction in ROS generation. The aims and objectives of this Chapter were:

1. To carry out siRNA knockdown studies of ALDH7A1, ALDH3A1 and ALDH1A3 in DLD-1 cells using both normoxic and hypoxic conditions.
2. To evaluate the effect of ALDH knockdown using the following endpoints:
    - Cell proliferation using the trypan blue assay.
    - Cell migration using the scratch assay.
    - Reactive oxygen species (ROS) generation.
    - DNA damage using phosphorylated H2AX as a marker of dsDNA breaks.
    - Drug cytotoxicity of three CRC anticancer drugs; oxaliplatin, 5-FU and irinotecan using the trypan blue assay.

3.2 Material and Methods

3.2.1 Target mRNA knockdown using siRNA

3.2.1.1 Cell seeding

DLD-1 cells in early passage number (2-4) were seeded at concentration of 2.75×10^5 cells/ 25 cm^2 flask in 5 ml complete RPMI medium (for gene and protein expression, cell proliferation assay, cell cycle and ROS detection experiments) or at concentration of 1.1×10^5 cells/ well (2 ml complete RPMI) in 6 well plates (for migration and trypan blue cytotoxicity assays). Cells were incubated at 37˚C and 5% CO_2 for 24h.

3.2.1.2 Preparation of siRNAs

siRNA duplexes against ALDH1A3, 3A1 and 7A1 were designed, synthesised and validated by Ambion/Life Technologies. See appendix VII for siRNA information.

Stock solution: 20 µM of siRNA solution (ALDH1A3, ALDH3A1 and ALDH7A1 siRNAs) was prepared by dissolving 20 nmol of each siRNA (Ambion/Life Technologies) in 1 ml of 1x Dharmacon siRNA resuspension buffer. 2 µM of siRNA was also prepared as a working stock solution. Both concentrations of siRNA were stored in aliquots at -80˚C.

3.2.1.3 Transfection with siRNA

After 24h of incubation at 37˚C and 5% CO_2, the cells were checked under the microscope to make sure that they were 20-30% confluent and evenly distributed on the flask surface. For single siRNA transfection, siRNA was prepared in 1.5 ml microcentrifuge tube by adding 30 µl of 2 µM siRNA stock

solution (ALDH1A3, ALDH3A1 or ALDH7A1 siRNAs) into 525 µl Optimem (Gibco). For ALDH3A1 and ALDH7A1 siRNAs cotransfection, 15 µl of ALDH3A1 siRNA (2 µM stock) and 15 µl of ALDH7A1 siRNA (2 µM stock) were added into 525 µl Optimem. 45 µl of diluted oligofectamine solution (1:5 oligofectamine (Life technologies) in Optimem was prepared and incubated for 30 min at room temperature) was added to siRNA mix (final concentration = 7.5% v/v) and was mixed by pipetting 20-30 times. The mix was incubated for 45 min inside the cell culture safety cabinet. Control solution with the liposome carrier only was prepared by adding 45 µl of diluted oligofectamine solution into 555 µl Optimem. During the incubation time, medium was removed from flasks and 5 ml of Optimem was added to each flask for washing before it was discarded (or 2 ml of Optimem in 6 well plates). 2 ml of fresh Optimem was added to each flask (or 800 µl of Optimem in 6 well plates). After 45 min of incubation, 500 µl of siRNA mix (or 200 µl to 6 well plates) was added to relevant flasks (final concentration of each siRNA in single or cotransfection was 20 or 10 nM respectively). For liposome control cells, 500 µl of control solution was added to each flask (or 200 µl to 6 well plates). For mock transfected cells, only 500 µl of Optimem was added to each flask (or 200 µl to 6 well plates). Cells were incubated at 37˚C and 5% CO_2 for 4h before 2.5 ml of 2x RPMI was added to each flask (or 1ml to 6 well plates). Next, cells were incubated at 37˚C and 5% CO_2 for 24h, 48h or 72h before being harvested for RNA or protein extraction. For knockdown studies under hypoxic conditions, the same steps were carried out until the end of the 4h incubation, after which flasks or plates were incubated in the

hypoxic chamber (0.1% O_2) and preconditioned hypoxic 2x RPMI was added. Normoxic mock samples were also included as a control.

3.2.1.4 Cells harvesting

To evaluate whether there were any obvious phenotypic changes due to transfection, bright field images were taken for flasks containing mock and liposome controls, ALDH1A3 siRNA, ALDH3A1 siRNA, ALDH7A1 siRNA and co-transfection (ALDH3A1 and ALDH7A1 siRNAs) at 24h, 48h and 72h time points. To harvest cells, the medium was removed into 20 ml universal tube and 5 ml PBS was used to wash the cells. Next, cells were trypsinised and detached from the flask surface before all contents were transferred to a 20 ml universal tube and centrifuged at 1,000 rcf for 5 min. Media was then discarded and the cell pellet was washed with 1 ml PBS. The PBS containing the cells was collected in 1.5 ml microcentrifuge tube and centrifuged for 5 min at 3,000 rcf. Finally, PBS was discarded and the cell pellet was kept at -80˚C for RNA or protein extraction.

3.2.2 ALDH gene expression analysis after knockdown

RNA extraction and cDNA synthesis was carried out as previously described (Chapter 2, Material and Methods, section 2.2.1.3) Gene expression analysis was carried out using qRT-PCR (Chapter 2, Material and Methods, section 2.2.1.3) and the fold change in the expression of the target gene was calculated for siRNA transfected samples and liposomes control samples in comparison to mock controls

3.2.3 ALDH protein expression analysis after knockdown

Protein extraction was carried out as previously described (Chapter 2, Material and Methods, section 2.2.1.4). Protein expression analysis was carried out using western blot technique (Chapter 2, Material and Methods, section 2.2.1.4) and Image J was used to calculate the fold change in the expression of the target protein in siRNA transfected samples and liposomes control samples in comparison to mock controls.

3.2.4 Cell proliferation and viability

To evaluate whether ALDHs are involved in the regulation of cellular proliferation, cells were seeded into 25 cm^2 flasks and transfected with siRNAs as described in sections 3.2.1.1-3. After 24h, 48h and 72h, cell proliferation and viability was evaluated using the trypan blue assay. In brief, cells were trypsinised and centrifuged to obtain the cell pellet, which was then re-suspended in RPMI. 100 µl of cell suspension was mixed with 100 µl of trypan blue dye before the total number of live cells was counted. Cell number on the Y-axis was then plotted against the incubation time post transfection on the X-axis.

3.2.5 Cell cycle analysis

DLD-1 cells were seeded into 25 cm^2 flasks and transfected as previously described (Sections 3.2.1.1-3). After 24h, 48h or 72h of siRNA transfection, cells were harvested for ethanol fixation and cell cycle analysis. In brief, cells were trypsinised and both adherent and floating cells were collected. After centrifuge at 1,000 rcf for 5 min, the cell pellet was washed twice with ice cold PBS to remove serum proteins present in the culture media. Cells were

then re-suspended in 1 ml ice cold PBS in a 15 ml Falcon tube and vortexed while 4 ml of 90% -20ºC chilled ethanol was added dropwise before the samples were left on ice for 1h. Next, the samples were stored at 4ºC until processed for propidium iodide staining. The fixed cells were centrifuged at 1,000 rcf for 5 min at 4ºC. Ethanol was then carefully aspirated and discarded. The cell pellet was re-suspended in 5 ml ice cold PBS and re-centrifuged at 1,500 rcf for 5 min (this was done twice). The residual PBS was carefully removed and cells were gently re-suspended in 500 µl PBS (at room temperature) containing 20U/ml RNase (Sigma) and incubated at 37ºC for 15 min. 500 µl of propidium iodide (60 µg/ml diluted in PBS) (Sigma) was then added, mixed well by pipetting and cells left for 30 min at room temperature. Occasionally, tubes were flicked to keep cells in suspension. Subsequently, samples were incubated overnight at 4ºC after which the cell cycle analysis was carried out using FACS and detection of propidium iodide fluorescence using the FL2-A channel (red channel).

Propidium iodide is the most commonly used dye to quantitatively assess DNA content of cells. It binds DNA stoichiometrically by intercalating in the DNA double helix, however it will also bind to dsRNA. Treatment with RNase is therefore necessary to degrade dsRNA (Krishan, 1975).

3.2.6 Detection of reactive oxygen species (ROS)

DLD-1 cells were seeded in phenol red free RPMI medium (Gibco, Appendix I) into 25 cm^2 flasks and transfected with siRNAs to knockdown ALDH1A3, ALDH3A1 and ALDH7A1 as well as co-knockdown of ALDH3A1 and ALDH7A1 as described previously in sections 3.2.1.1-3. After 48h of

transfection, 1 flask with cells was treated with 250 µM H_2O_2 (in 5 ml phenol red free RPMI) and used as a positive control for ROS detection. After 72h of transfection, medium was transferred to 20 ml universal tube and cells were washed with PBS and removed to the universal tube. Trypsin was added to detach the cells and were inhibited by the addition of phenol red free RPMI and all cells were collected into the universal tube. Cells were centrifuged at 1,000 rcf for 3 min and media was discarded. 5 ml of PBS at room temperature was added to wash the cell pellet and centrifuged at 1,000 rcf for 3 min before being discarded. Next, 2 ml of phenol red free RPMI containing 5 µM of 6-carboxy-2',7'-dichlorodihydrofluorescein diacetate (carboxy-H2DCFDA, Fisher scientific) was added to the cell pellet and the mixture was mixed gently with pipetting. The medium containing the cells was transferred to 1 well of a 6 well plate and incubated at 37ºC for 30 min with gentle shaking every 6 min to prevent cell attachment.

Carboxy-H2DCFDA is a chemically reduced, acetylated form of fluorescein used as an indicator for ROS in cells. Carboxy-H2DCFDA is readily converted to a green-fluorescent form when the acetate and ester groups are removed by intracellular oxidation (e.g. by the activity of ROS). The carboxylated H2DCFDA has two negative charges at physiological pH and upon cleavage carboxydichlorofluorescein is produced, which has additional negative charges that impede its leakage out of the cell. Fluorescence can be monitored using a flow cytometer at Ex/Em: ~492–495/517–527 nm (Eruslanov and Kusmartsev, 2010).

After 30 min of incubation, cells were removed to a 20 ml universal tube and centrifuged at 700 rcf for 3 min. The cell pellet was then washed with 5 ml PBS and centrifuged at 1,000 rcf for 3 min. To enable fluorescence analysis, the cell pellet was re-suspended in 0.5 ml PBS and analysed with FACS using the FL1H channel (green channel).

3.2.7 Detection of double strand DNA breaks

In order to study the potential protective role of the ALDH7A1 enzyme against DNA damage that might be caused by ROS, the effect of ALDH knockdown on phosphorylated H2AX expression was evaluated. In brief, DLD-1 cells were seeded into 25 cm^2 flasks, transfected with siRNAs for 72h under normoxic conditions and harvested for protein extraction as described previously in section 3.2.1. Western blot was carried out as described previously in section 3.2.3 using rabbit anti phosphorylated H2AX primary antibody and HRP based anti-rabbit secondary antibody (Table 15, Appendix V)

3.2.8 Cell migration

A scratch assay was used to evaluate the role of ALDH in cell migration. The scratch assay is an easy, low-cost and well-developed method to measure cell migration *in vitro* (Liang et al., 2007). In brief, DLD-1 cells were seeded and transfected in 6 well plates as described in sections 3.2.1.1-3. After 72h of transfection, confluent cells were scraped in a straight line to create a "scratch" with a p200 pipet tip. The cells were then washed to remove the debris and smooth the edge of the scratch using 1 ml of RPMI. Next, 2 ml of RPMI containing 2% FBS was added to each well. Photos were taken at time

0 (initial scratch before migration) as well as after 24h of incubation at 37ºC and 5% CO_2 (24h after migration). To compare the cell migration under normoxic and hypoxic conditions, only mock samples were included; cells were incubated in the hypoxic chamber directly after the scratch had been created. Preconditioned hypoxic media containing 2% FBS was added afterwards. Image J was used for migration analysis by calculating the cell free area (at t = 0 and 24h) and quantifying the migration rate of the cells after 24h.

3.2.9 Drug cytotoxicity

DLD-1 cells were seeded and transfected in 6 well plates as described in sections 3.2.1.1-3. After 48h of transfection, cells were treated with 2 ml of RPMI containing oxaliplatin (75 µM), irinotecan (75 µM) or 5-FU (100 µM) for 48h. Control cells were treated with 0.1% DMSO. The total number of live cells was calculated using the trypan blue assay as previously described in Chapter 2, Material and Methods, section 2.2.1.1.2. The same experiments were also carried out under hypoxic conditions using ALDH7A1 siRNA transfected cells. The percentage of live cells was calculated as following:

% Live cells = Total number of live cells (treated)/ Total number of live cells (Control).

3.2.10 Statistical data analysis

The significance of results was assessed through a comparison of means using two-tailed student t-test. Results were expressed as the mean ± standard deviation. P values were calculated to determine statistical significance of the results.

3.3 Results

3.3.1 Phenotypic appearance of DLD-1 cells after siRNA transfection and culture under normoxic conditions

Cell images were taken 24h, 48h and 72h following siRNA transfection and this showed that there were no obvious phenotypical differences between siRNA transfected cells, liposome controls and mock cells (Figure 44).

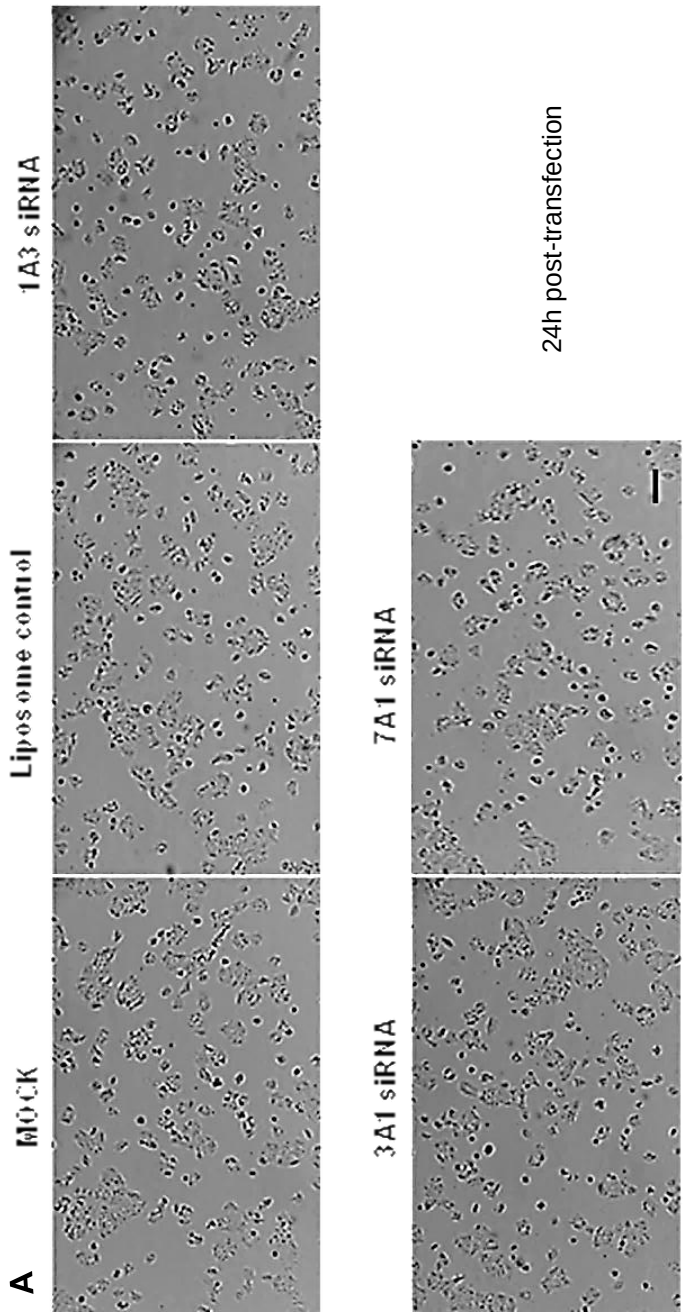

Figure 44 Phenotypic appearance of DLD-1 cells after ALDH Knockdown. 24h (A), 48h (B) and 72h (C) post-transfection. Photos are at 10x lens and scale bar= 100 µm.

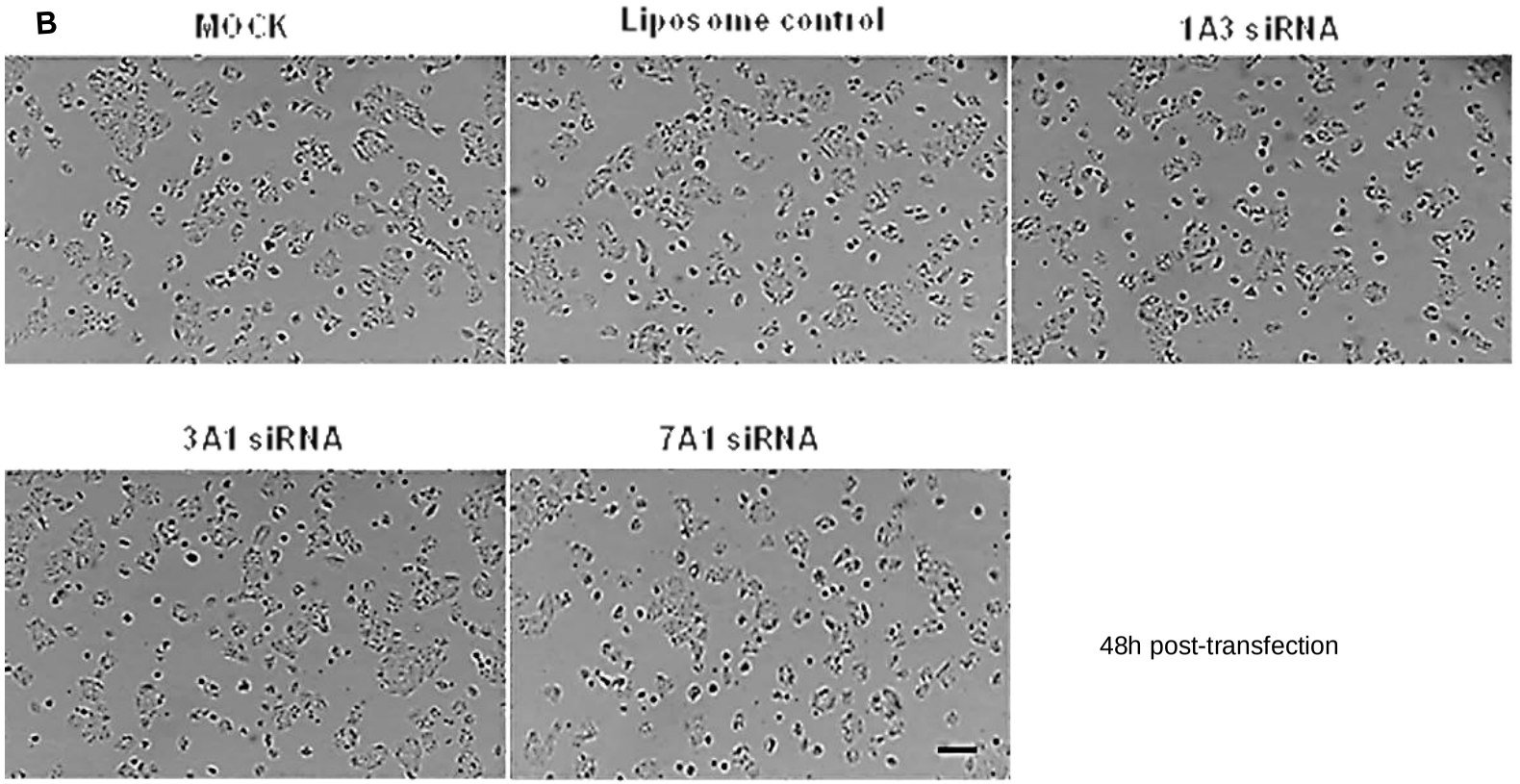

Figure 44 Phenotypic appearance of DLD-1 cells after ALDH Knockdown. 24h (A), 48h (B) and 72h (C) post-transfection. Photos are at 10x lens and scale bar= 100 µm.

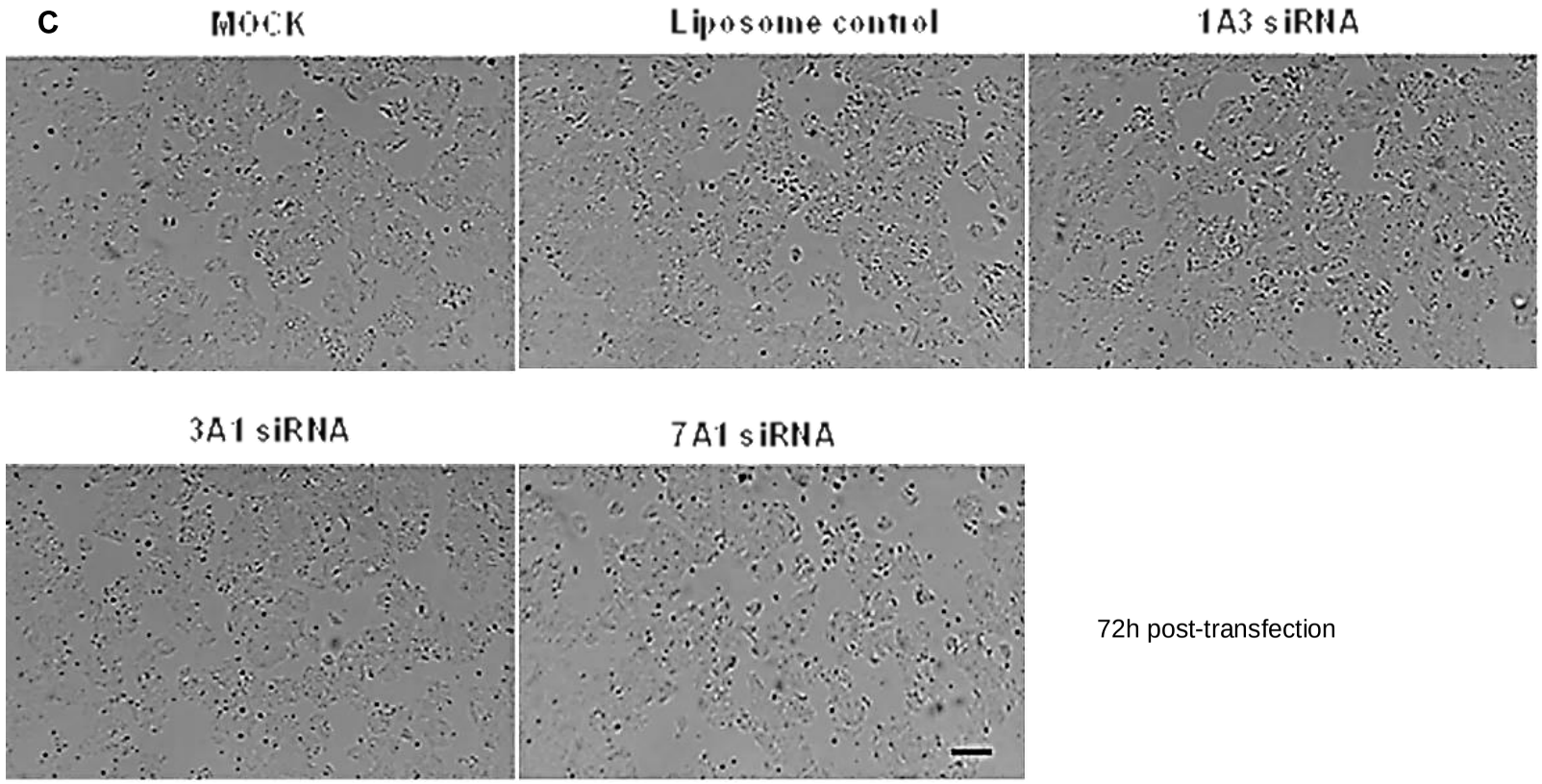

Figure 44 Phenotypic appearance of DLD-1 cells after ALDH Knockdown. 24h (A), 48h (B) and 72h (C) post-transfection. Photos are at 10x lens and scale bar= 100 µm.

3.3.2 Evaluation of ALDH mRNAs and protein expression after siRNA transfection and culture under normoxic conditions

Gene and protein expression was evaluated using qRT-PCR and western blot, respectively as described previously in Materials and Methods, sections 3.2.2-3.

Figure 45 shows the preliminary finding that ALDH1A3 siRNA resulted in a 60-75% reduction in ALDH1A3 mRNA levels compared to mock transfected cells. However, expression of ALDH1A3 protein could not be detected using western blot and hence the effect of the mRNA knockdown on protein levels could not be determined.

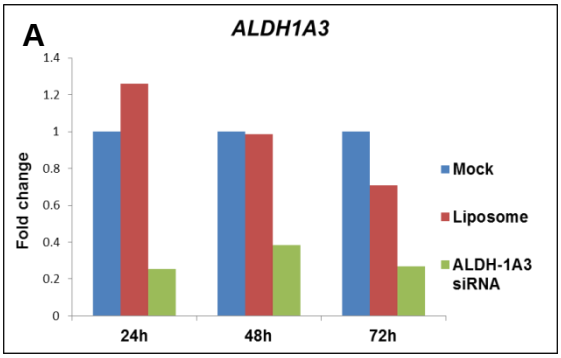

B

% *ALDH1A3* expression

	24h	48h	72h
Mock	100	100	100
Liposome	126	98.5	70.8
ALDH1A3 siRNA	25.5	38.5	26.8

Figure 45 ALDH1A3 mRNA expression in ALDH1A3 siRNA transfected DLD-1 cells after 24h, 48h and 72h of transfection. The fold change of ALDH1A3 gene expression using qRT-PCR (A) and the percentage of ALDH1A3 gene expression (B). Results represent 1 experiment.

Figure 46A and B shows the preliminary finding of 60-75% knockdown in the expression of the ALDH3A1 mRNA after ALDH3A1 siRNA transfection with levels most reduced at 72h post-transfection. ALDH3A1 was also reduced at the protein level with the decrease in protein levels correlating with the length of time after siRNA transfection (Figure 46C).

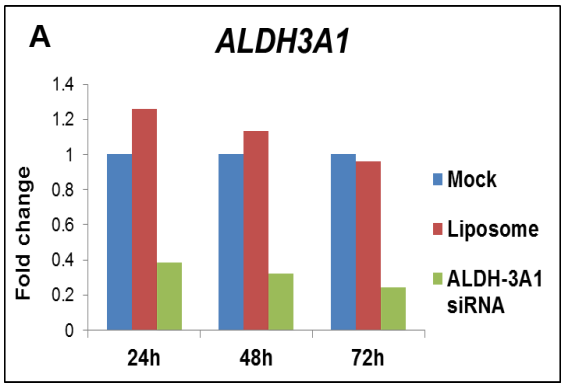

B % *ALDH3A1* expression

	24h	48h	72h
Mock	100	100	100
Liposome	126	113	96
ALDH3A1 siRNA	38	32	24

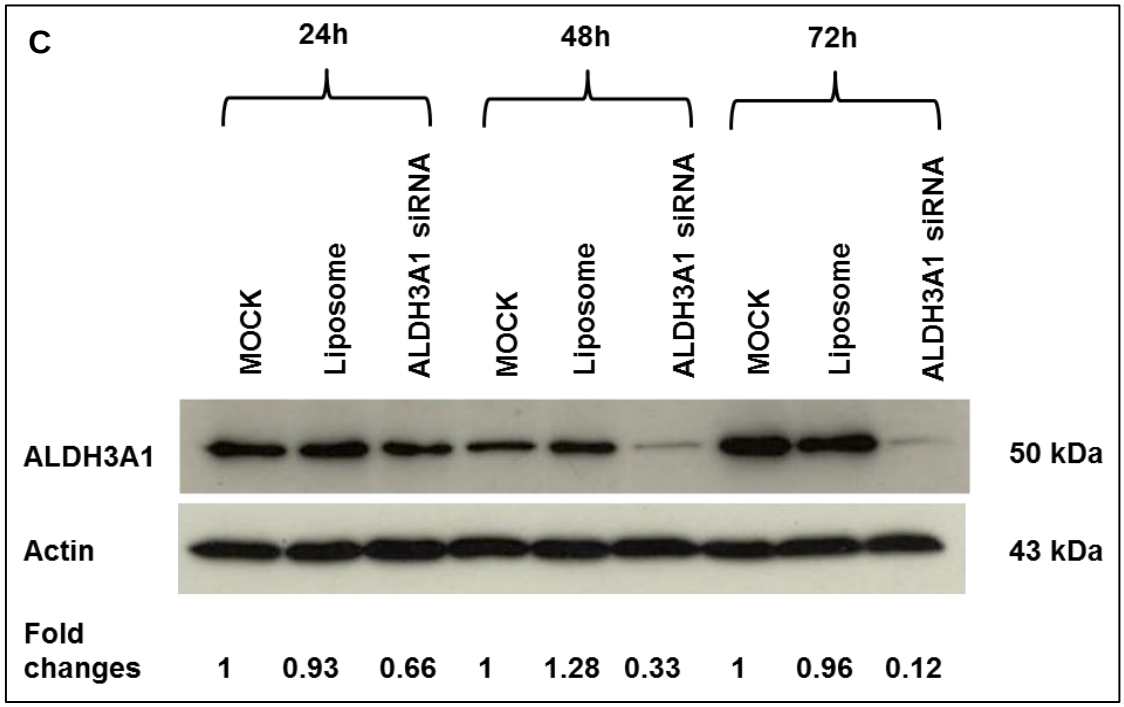

Figure 46 ALDH3A1 mRNA and protein expression in ALDH3A1 siRNA transfected DLD-1 cells after 24h, 48h and 72h of transfection. Fold change of ALDH3A1 gene expression using qRT-PCR (A), the percentage of ALDH3A1 gene expression (B) and ALDH3A1 protein expression using western blot (C). Results represent 1 experiment.

Figure 47 shows that ALDH7A1 mRNA levels were reduced by 75-82% after ALDH7A1 siRNA transfection and ALDH7A1 protein levels by 60-90%.

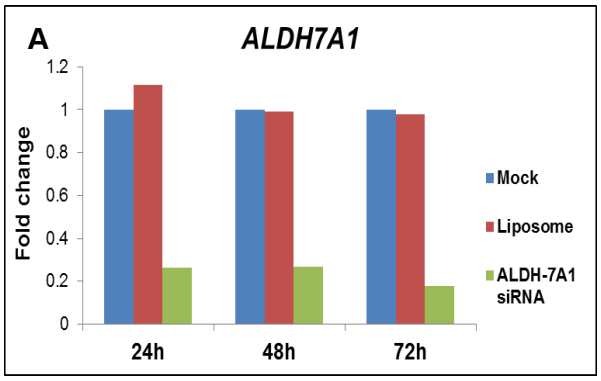

B

% *ALDH7A1* expression

	24h	48h	72h
Mock	100	100	100
Liposome	111	99	97
ALDH7A1 siRNA	26.2	26.6	17.8

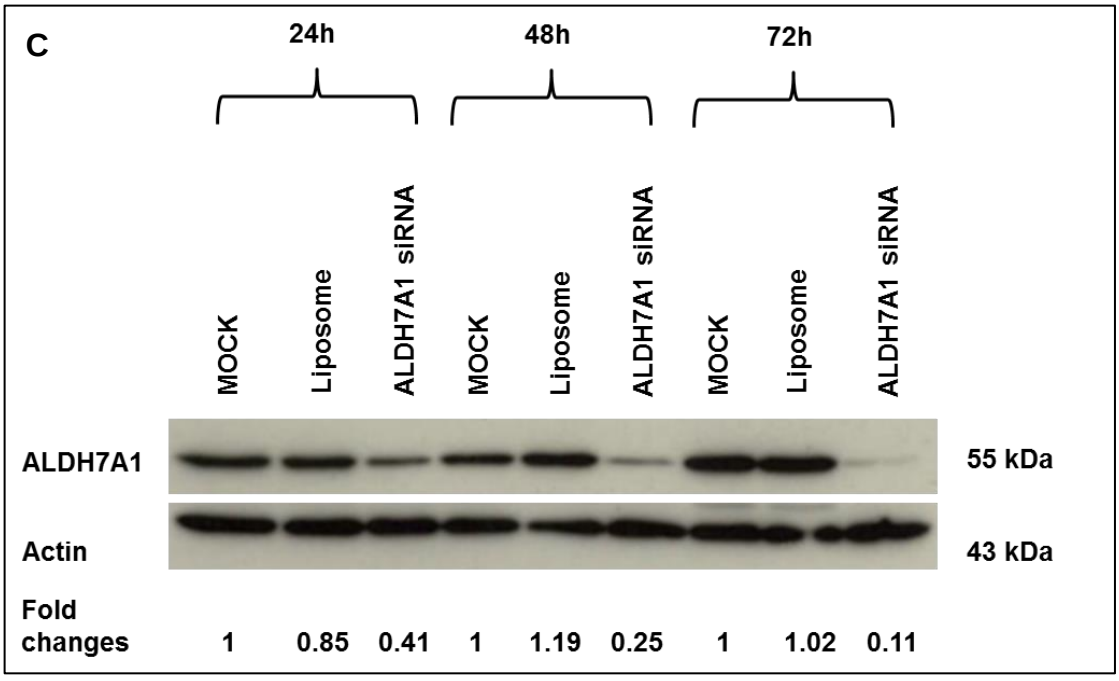

Figure 47 ALDH7A1 gene and protein expression in ALDH7A1 siRNA transfected DLD-1 cells after 24h, 48h and 72h of transfection. The fold change of ALDH7A1 gene expression using qRT-PCR (A), the percentage of ALDH7A1 gene expression (B) and ALDH7A1 protein expression using western blot (C). Results represent 1 experiment.

To evaluate the specificity of target siRNA and to assess whether there was cross talk between different ALDH isoforms, analysis of the effect of ALDH isoform knockdown on other selected members of the ALDH family was carried out. Figure 48 shows the preliminary findings that significant and specific knockdown of each isoform mRNA can be achieved. However,

ALDH7A1 siRNA also resulted in consistent upregulation of both ALDH3A1 mRNA and protein. This may be a compensatory response to reduced 7A1 levels but indicates crosstalk between different ALDH isoforms and that 7A1, directly or indirectly, can influence expression of 3A1

Accordingly, co-transfection experiments were carried out to reduce the expression of both ALDH7A1 and ALDH3A1 in DLD-1 cells. Experiments were carried out as described in Materials and Methods, section 3.2.1.

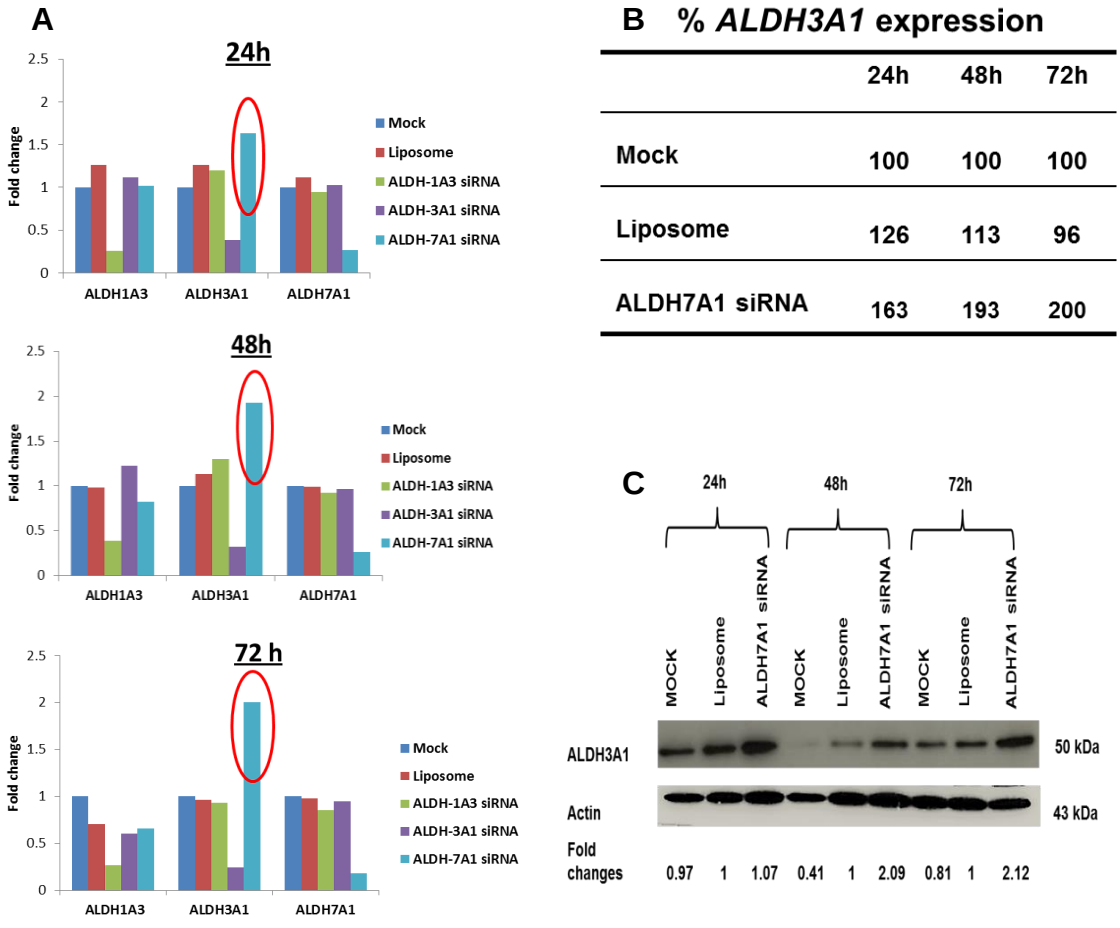

Figure 48 ALDH 1A3, 3A1 and 7A1 expression in ALDH (1A3, 3A1 or 7A1) siRNAs transfected DLD-1 cells after 24h, 48h and 72h of transfection. The fold change of ALDH (1A3, 3A1 and 7A1) gene expression using qRT-PCR (A), the percentage of ALDH3A1 gene expression in ALDH7A1 siRNA transfected cells (B) and ALDH3A1 protein expression in ALDH7A1 siRNA transfected cells (C). Results represent 1 experiment.

3.3.3 Phenotypic appearance of co-transfected DLD-1 cells cultured under normoxic conditions

Figure 49 shows that the phenotypic appearance at 10x objective lens of mock, liposome control and co-transfected cells 24-72h after transfection were similar. No morphological differences were detectable when viewing at higher magnification (40x or 100 x objective lens).

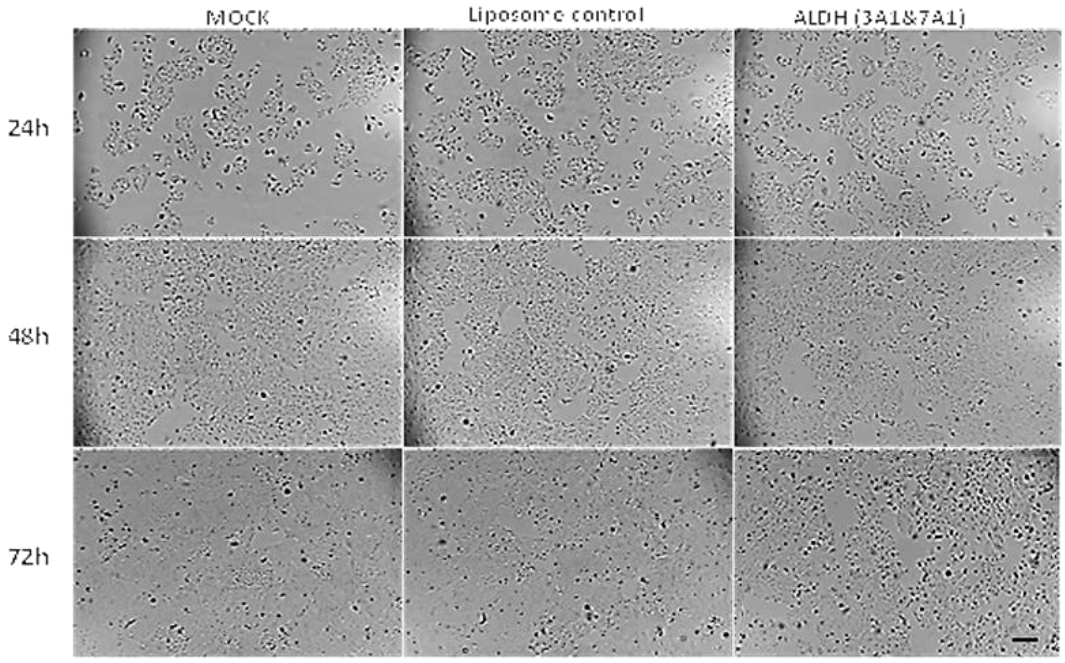

Figure 49 Phenotypic appearance of DLD-1 cells after ALDH3A1 and 7A1 co-knockdown. Photos were taken 24h, 48h and 72h post-transfection at 10x lens and scale bar= 100 µm.

3.3.4 Evaluation of ALDH mRNA and protein expression in co-transfected cells cultured under normoxic conditions

As ALDH7A1 knockdown resulted in upregulation of ALDH3A1 at both the gene and protein levels, cells were transfected with ALD3A1 and 7A1 siRNAs in order to try and knockdown both ALDH3A1 and 7A1 isoforms. Figure 50A and B show the preliminary finding that the co-transfection resulted in a reduction of both ALDH3A1 and ALDH7A1 mRNAs by 50-60%

and 65%, respectively relative to mock-transfected cells. Figure 50C shows that ALDH3A1 and ALDH7A1 proteins were also significantly reduced, confirming that the co-transfection and mRNA knockdown resulted in effects at the level of protein expression.

A

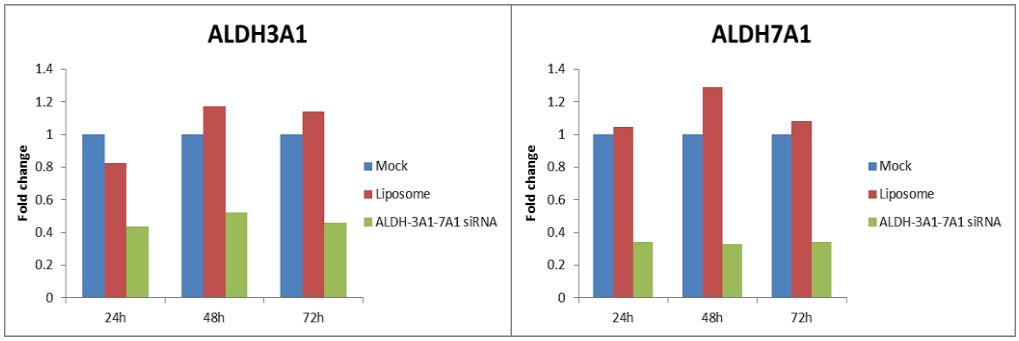

B

% *ALDH3A1* expression				% *ALDH7A1* expression			
	24h	48h	72h		24h	48h	72h
Mock	100	100	100	Mock	100	100	100
Liposome	82	117	114	Liposome	104	129	108
Co-transfection	43.8	52	46	Co-transfection	34	33	34

C

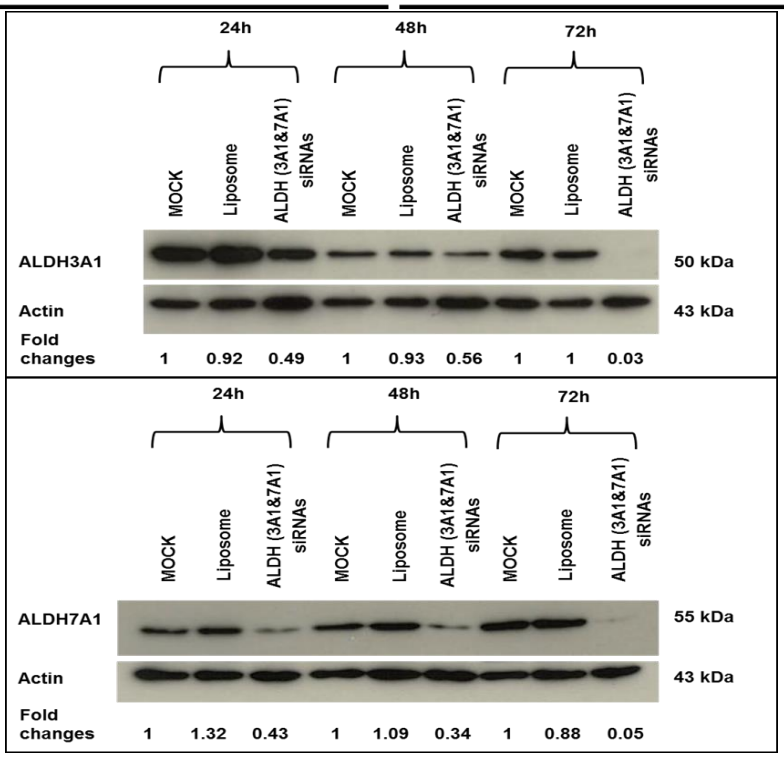

Figure 50 ALDH7A1 and ALDH3A1 expression in co-transfected DLD-1 cells (ALDH3A1&7A1 siRNAs) after 24h, 48h and 72h of transfection. The fold change of ALDH (3A1 and 7A1) gene expression using qRT-PCR (A), the percentage of ALDH3A1 and ALDH7A1 gene expression in co-transfected cells (B) and the protein expression of ALDH3A1 and ALDH7A1 in co-transfected cells (C). Results represent 1 experiment.

3.3.5 Phenotypic appearance after RNAi and culture of cells under hypoxic conditions

The role of ALDH7A1 was also studied under hypoxic conditions and protocols were used as already described in Materials and Methods, section 3.2.1. As observed under normoxic conditions, no discernible difference was observed on cells morphology after siRNA transfection, however, all cells cultured in hypoxic conditions grew more slowly compared to normoxic mock cells; resulting in reduced confluency which was most apparent 72h post-transfection (Figure 51).

3.3.6 Evaluation of ALDH mRNA and protein levels after siRNA transfection and culture under hypoxic conditions

ALDH1A3, ALDH3A1 and ALDH7A1 mRNA and protein expression levels were determined 24h, 48h and 72h post-siRNA transfection. As shown in Figure 52, the preliminary result shows that ALDH1A3 mRNA levels were slightly lower in both mock and liposome hypoxic controls whilst ALDH1A3 siRNA resulted in 65% reduction in ALD1A3 mRNA relative to normoxic mock control cells.

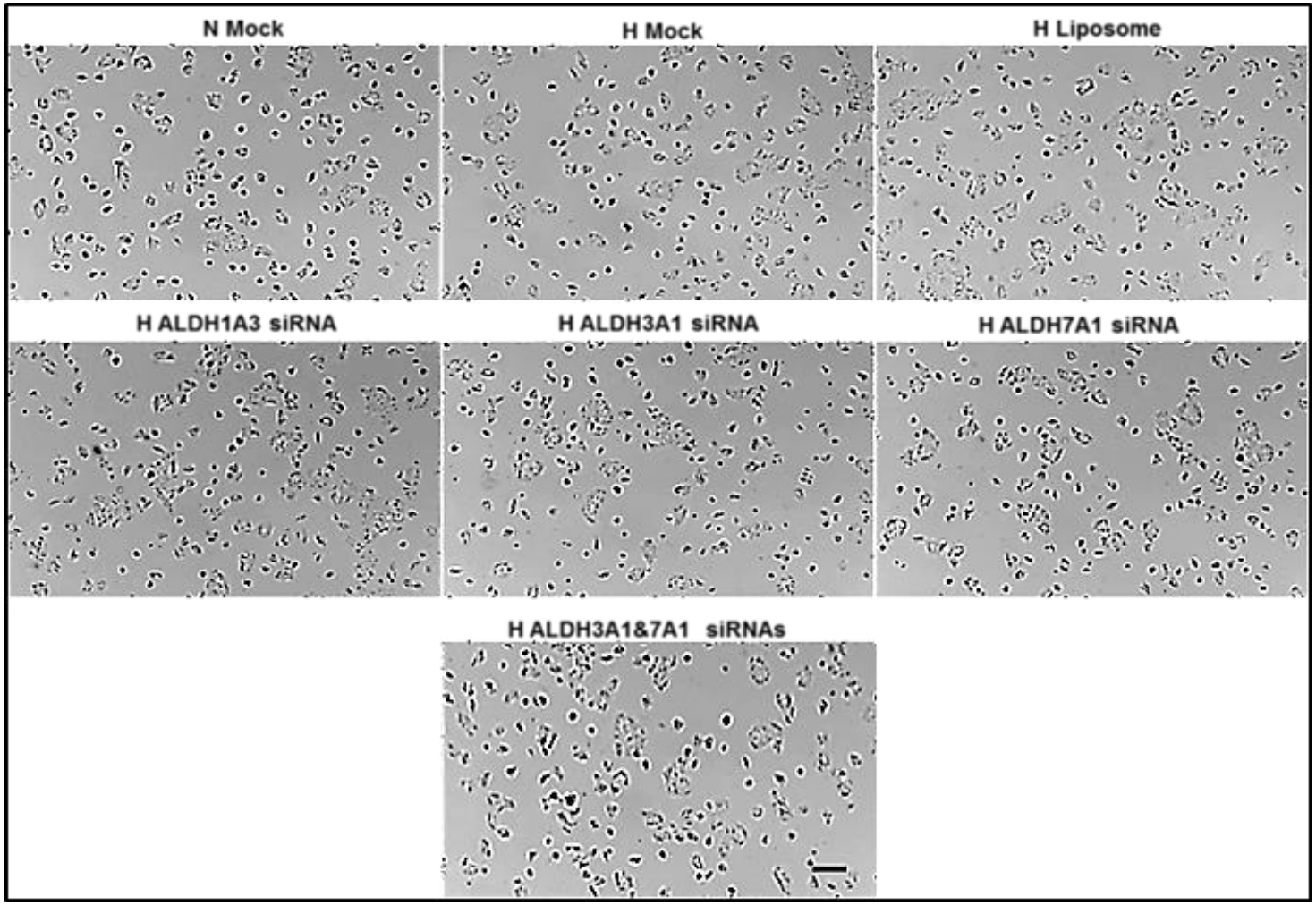

Figure 51 Phenotypic appearance of DLD-1 cells after ALDH Knockdown under hypoxic conditions. Photos were taken 24h (A), 48h (B) and 72h (C) post-transfection at 10x lens and scale bar= 100 µm. Normoxia (N), Hypoxia (H).

B

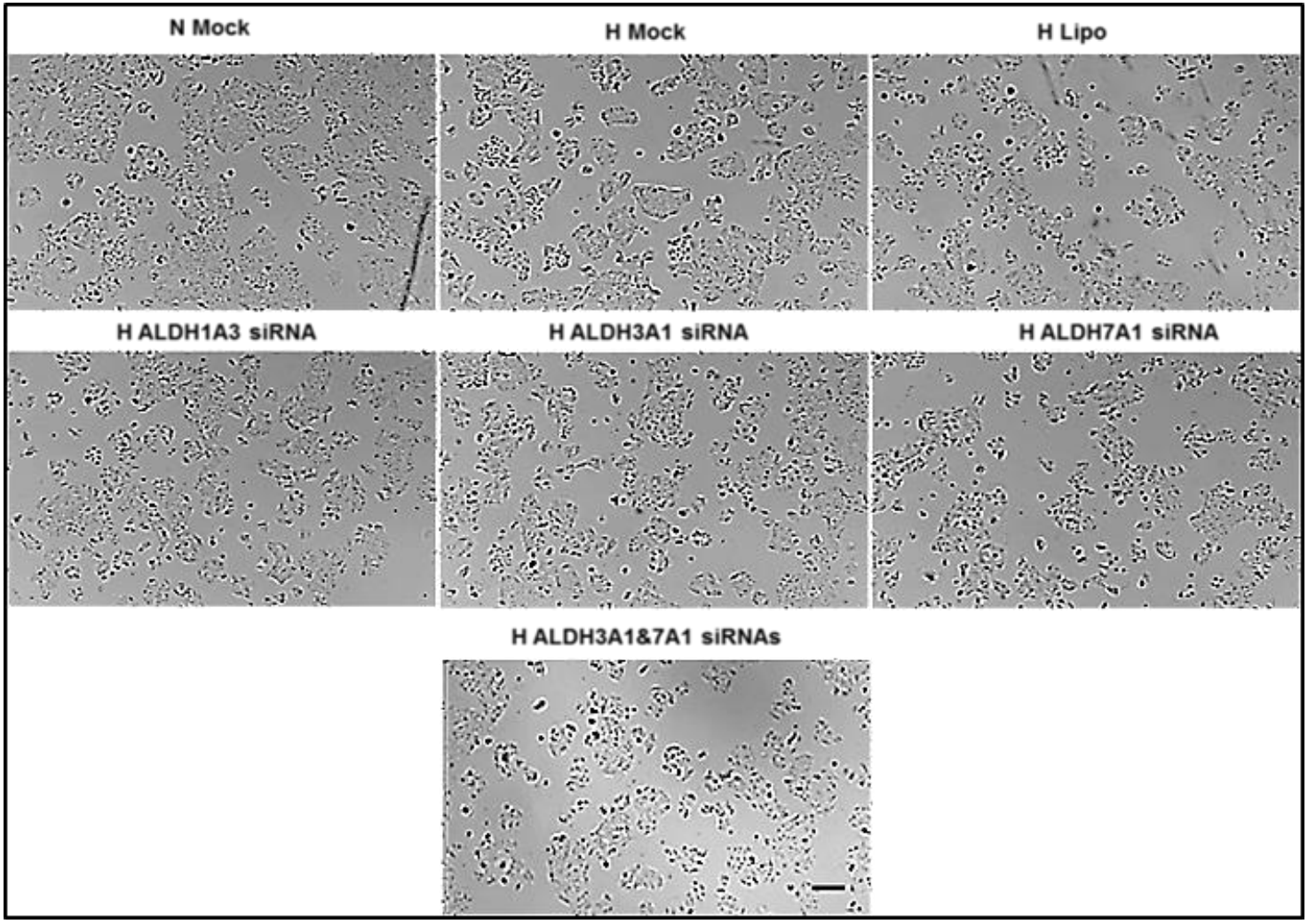

Figure 51 Phenotypic appearance of DLD-1 cells after ALDH Knockdown under hypoxic conditions. Photos were taken 24h (A), 48h (B) and 72h (C) post-transfection at 10x lens and scale bar= 100 µm. Normoxia (N), Hypoxia (H).

C

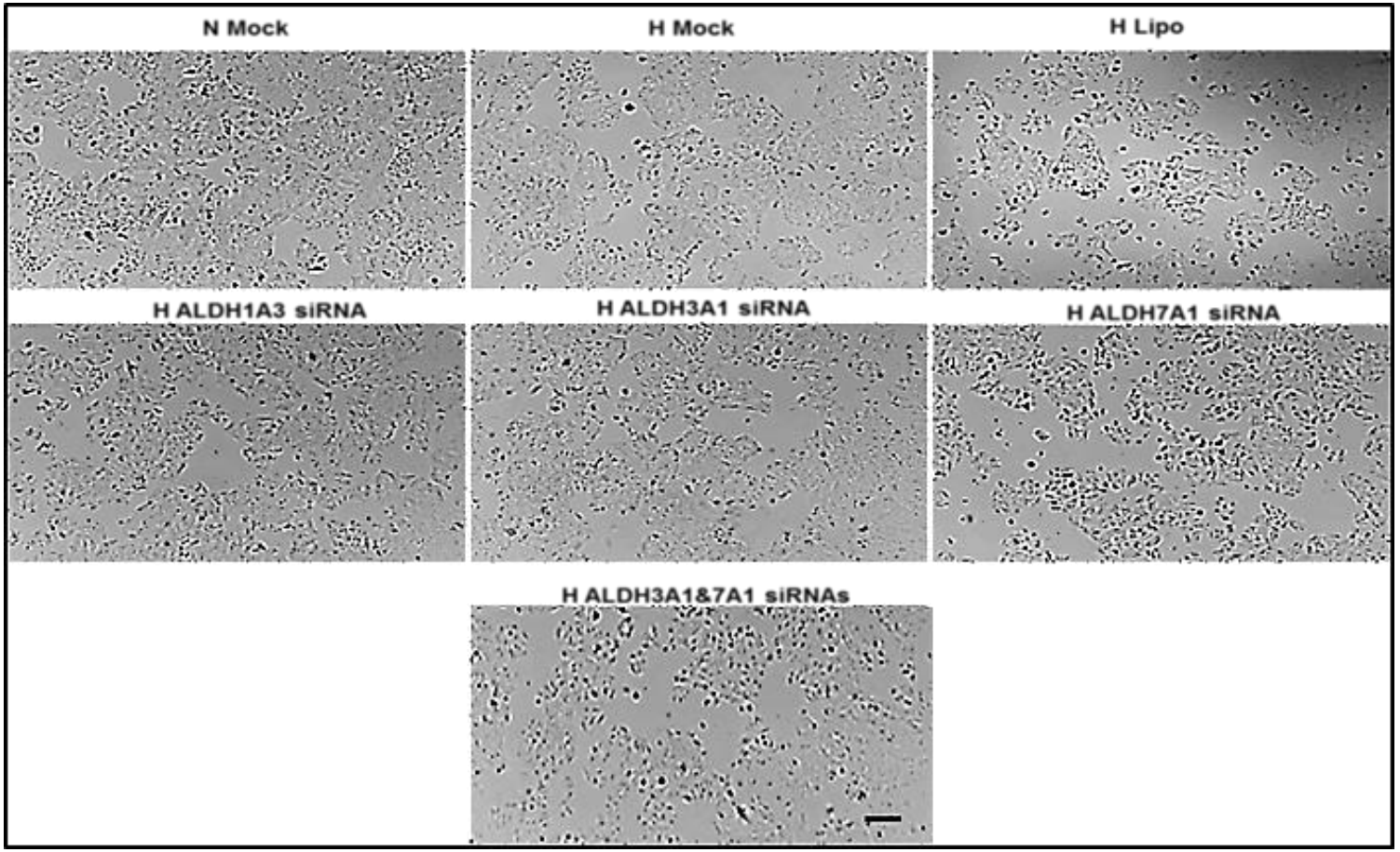

Figure 51 Phenotypic appearance of DLD-1 cells after ALDH Knockdown under hypoxic conditions. Photos were taken 24h (A), 48h (B) and 72h (C) post-transfection at 10x lens and scale bar= 100 µm. Normoxia (N), Hypoxia (H).

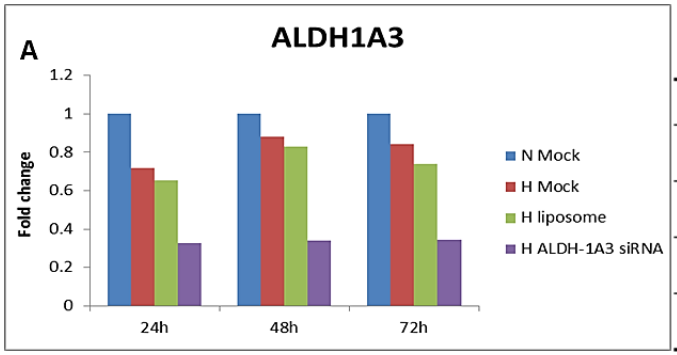

B % *ALDH1A3* expression

	24h	48h	72h
N Mock	100	100	100
H Mock	71.8	88	84
H Liposome	65	82	73.7
H ALDH1A3 siRNA	32.7	34	34.4

Figure 52 ALDH1A3 mRNA expression in ALDH1A3 siRNA transfected DLD-1 cells after 24h, 48h and 72h of transfection under hypoxic conditions. The fold change of ALDH1A3 gene expression using qRT-PCR (A), the percentage of ALDH1A3 gene expression (B). Normoxia (N), Hypoxia (H). Results represent 1 experiment.

ALDH3A1 mRNA was increased under hypoxic conditions (at 48h & 72h) compared to normoxia (Figure 53A and B). Significant knockdown of ALDH3A1 mRNA and protein was also observed relative to the elevated levels observed in hypoxic control cells (Figure 53C).

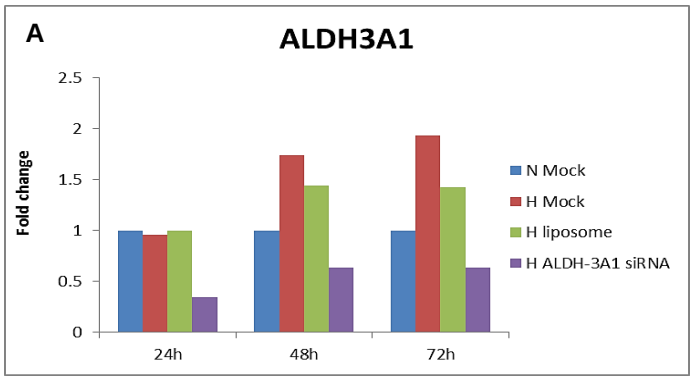

B

% *ALDH3A1* expression

	24h	48h	72h
N Mock	100	100	100
H Mock	96	174	193.5
H Liposome	99.6	144	142
H ALDH3A1 siRNA	34	63.6	63.2

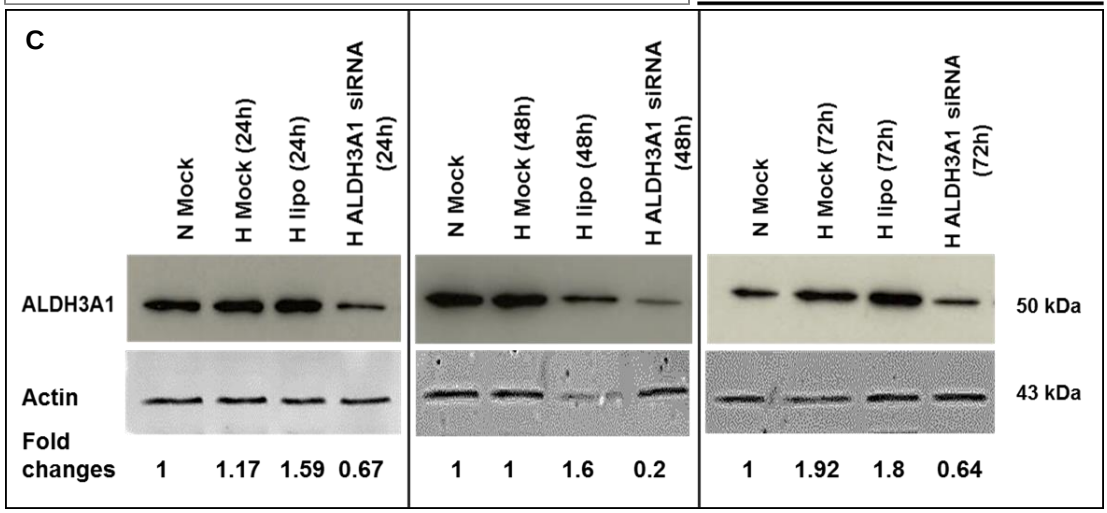

Figure 53 ALDH3A1 mRNA and protein expression in ALDH3A1 siRNA transfected DLD-1 cells after 24h, 48h and 72h of transfection under hypoxic conditions. The fold change of ALDH3A1 gene expression using qRT-PCR (A), the percentage of ALDH3A1 gene expression (B) and ALDH3A1 protein expression using western blot (C). Normoxia (N), Hypoxia (H). Results represent 1 experiment.

the preliminary findings revealed that ALDH7A1 mRNA and protein levels were increased 1.7-fold and 1.4-fold, respectively in response to prolonged hypoxia exposure (48h & 72h), as indicated in Figure 54. ALDH7A1 siRNA reduced mRNA expression by approximately 35% relative to normoxic controls and 60% relative to hypoxic controls after 48h and 72h transfection (Figure 54A and B). Protein expression was also significantly reduced at all time points. After 72h transfection, protein levels were reduced by 78% relative to normoxic controls and 85% relative to hypoxic controls (Figure 54C).

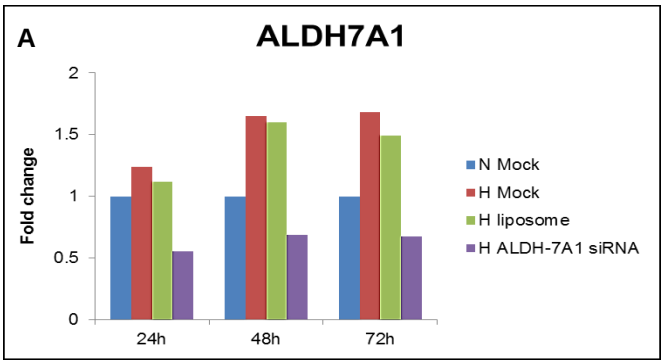

B % *ALDH7A1* expression

	24h	48h	72h
N Mock	100	100	100
H Mock	124	165	168
H Liposome	112	160	149
H ALDH7A1 siRNA	55.6	68.7	67.6

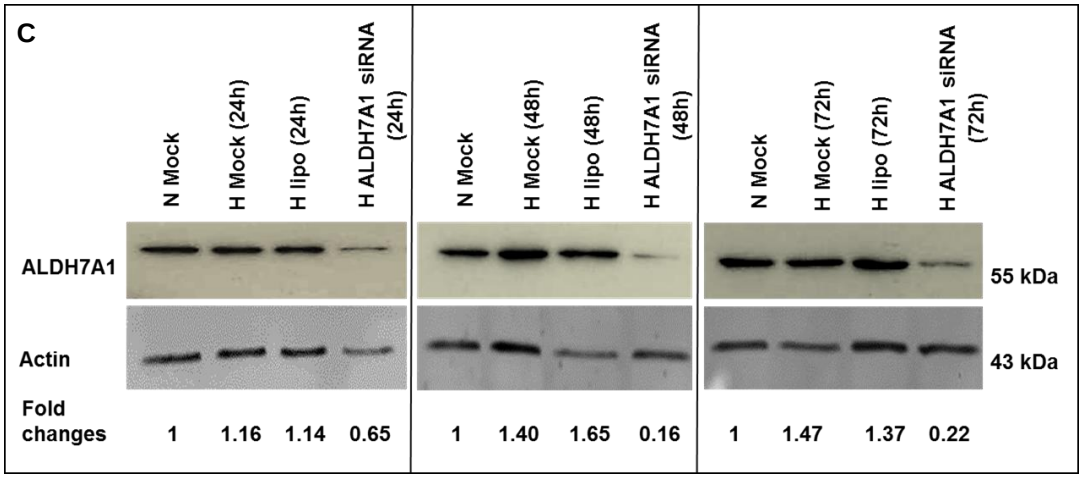

Figure 54 ALDH7A1 mRNA and protein expression in ALDH7A1 siRNA transfected DLD-1 cells after 24h, 48h and 72h of transfection under hypoxic conditions. The fold change of ALDH7A1 gene expression using qRT-PCR (A), the percentage of ALDH7A1 gene expression (B) and ALDH7A1 protein expression using western blot (C). Normoxia (N), Hypoxia (H). Results represent 1 experiment.

As indicated in Figure 48, ALDH7A1 knockdown in normoxic conditions resulted in increased levels of ALDH3A1. To assess whether this is also the case under hypoxia, the expression of ALDH3A1 following ALDH7A1 knockdown in hypoxic DLD1 cells was evaluated. Figure 55 shows the preliminary findings that ALDH7A1 knockdown in hypoxic conditions also resulted in the upregulation of ALDH3A1, particularly after 48h and 72h of siRNA transfection; supporting existence of a regulatory link or crosstalk between these two isoforms. Accordingly, co-transfection experiments using both ALDH3A1 and ALDH7A1 siRNAs were carried out, as was previously done for cells cultured under normoxic conditions. Figure 56 shows a reduction in both ALDH7A1 and 3A1 mRNAs and proteins with co-transfection.

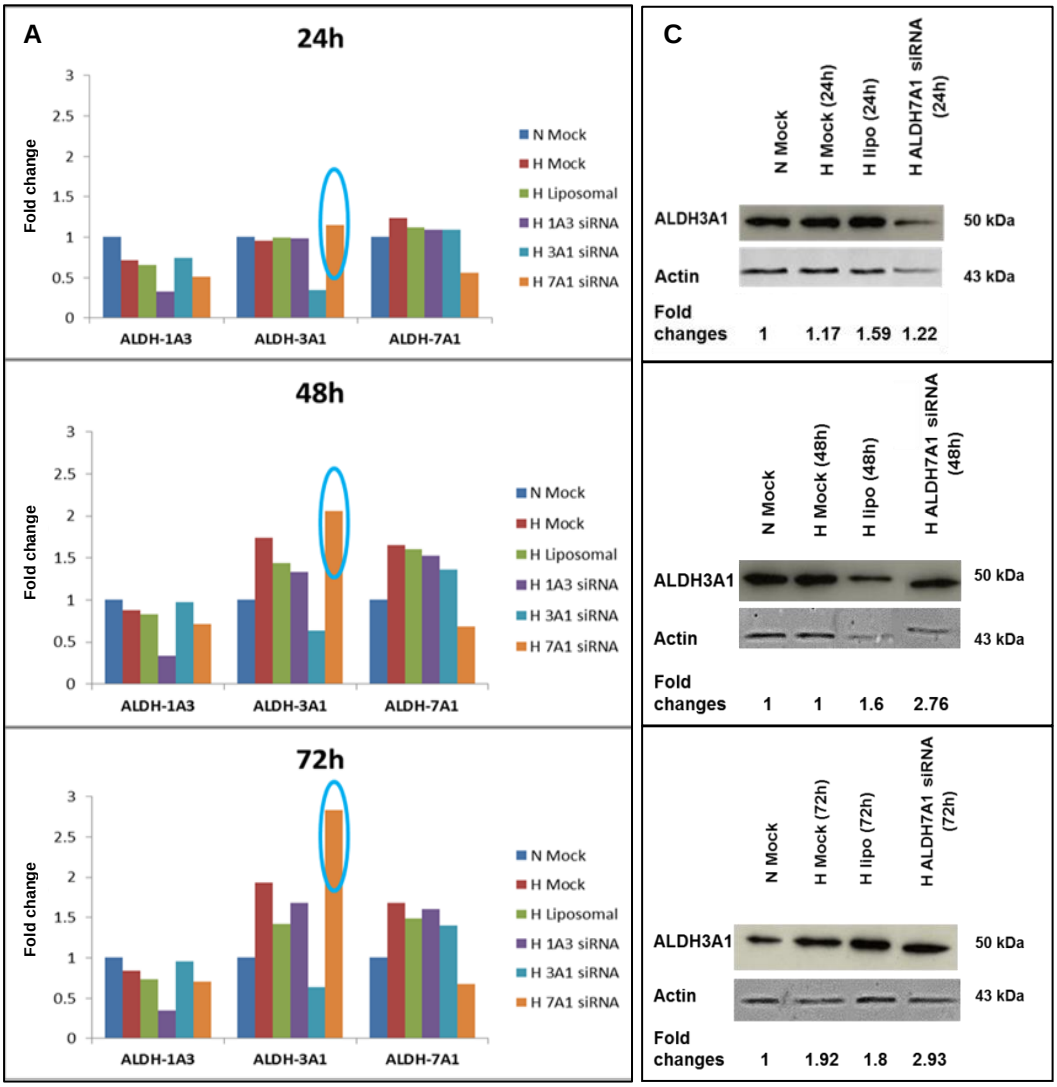

B % *ALDH3A1* expression

	24h	48h	72h
N Mock	100	100	100
H Mock	96	174	193
H Liposome	99.6	144	142
H ALDH7A1 siRNA	115	206	283

Figure 55 ALDH1A3, 3A1 and 7A1 expression in ALDH1A3, 3A1 or 7A1 siRNAs transfected DLD-1 cells after 24h, 48h and 72h of transfection under hypoxic conditions. The fold change of ALDH1A3, 3A1 and 7A1 gene expression using qRT-PCR (A), the percentage of ALDH3A1 gene expression in ALDH7A1 siRNA transfected cells (B) and ALDH3A1 protein expression in ALDH7A1 siRNA transfected cells (C). Normoxia (N), Hypoxia (H). Results represent 1 experiment.

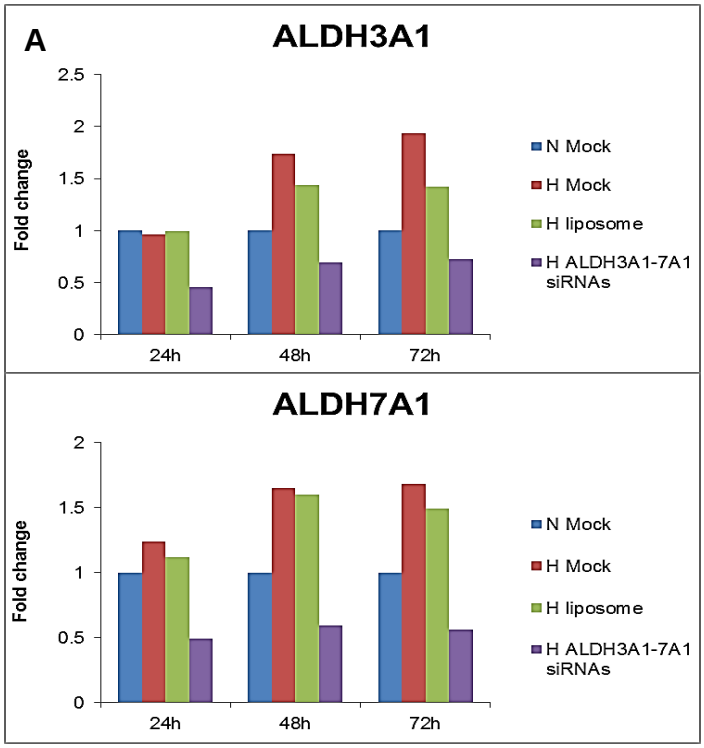

B

% *ALDH3A1* expression

	24h	48h	72h
N Mock	100	100	100
H Mock	96	174	193
H Liposome	99.6	144	142
H Co-transfection	45	69	72

% *ALDH7A1* expression

	24h	48h	72h
N Mock	100	100	100
H Mock	124	165	168
H Liposome	112	160	149
H Co-transfection	49.5	59	56

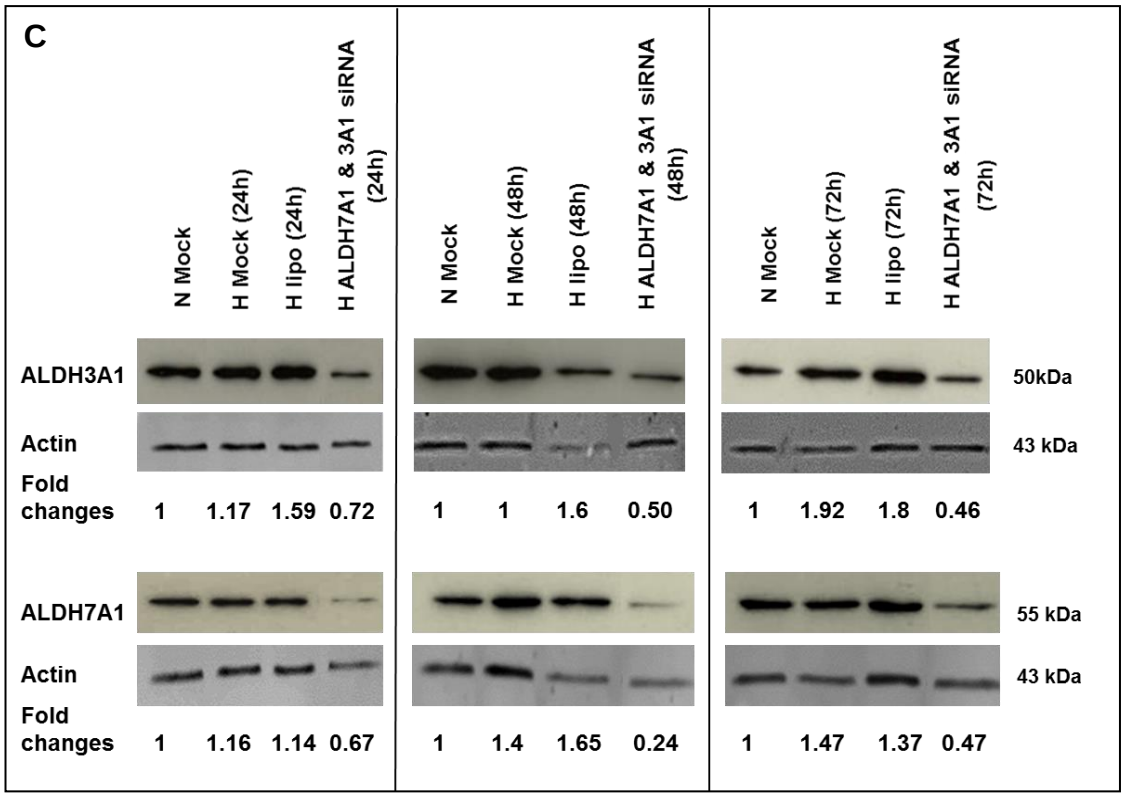

Figure 56 ALDH7A1 and ALDH3A1 expression in co-transfected DLD-1 cells (ALDH3A1&7A1 siRNAs) after 24h, 48h and 72h of transfection under hypoxic conditions. The fold change of ALDH3A1 and 7A1 gene expression using qRT-PCR (A), the percentage of ALDH3A1 and 7A1 gene expression in cotransfected cells (B) and the protein expression of ALDH3A1 and 7A1 in cotransfected cells using western blot (C). Results represent 1 experiment.

3.3.7 The role of ALDH isoforms in cell proliferation

Recent studies have reported a role of ALDH7A1 in mediating cell survival and proliferation in prostate cancer (van den Hoogen et al., 2011). To assess whether ALDH7A1 may have a similar function in CRC, cell proliferation and survival in ALDH7A1 knockdown cells was evaluated using the trypan blue exclusion assay.

Figure 57A shows that no major difference in the total number of live cells was observed between mock-transfected cells, liposome control cells, or ALDH1A3 siRNA-transfected cells under normoxic conditions at all time points. ALDH3A1 siRNA-transfected cells showed less cell number only after 24h of transfection relative to mock cells (P value= 0.007). In comparison, ALDH7A1 siRNA-transfected cells appeared to proliferate at a slower rate with fewer live cells at all time points. This was found to be statistically significant with P values = 0.007, 0.02 and 0.02 for 24h, 48h and 72h, respectively. This was also observed to a similar extent in ALDH7A1 and 3A1 siRNAs co-transfected cells, where the reduction in cell number was presumed to be due to reduced ALDH7A1 expression. No clear differences in dead cell number was observed using positive staining for trypan blue indicating effects of ALDH7A1 on cell proliferation but no apparent effects on cell survival.

Similar experiments were also carried out under hypoxic conditions (Figure 57B). The rate of cell proliferation was a lot lower under hypoxia as evident from comparing cell number for cells cultured under hypoxia versus normoxia. This is consistent with many other studies showing that hypoxia

can significantly reduce cell proliferation (Goda et al., 2003). Nonetheless, total live cell number at 24h and 48h post-transfection was reduced in ALDH7A1 siRNA-transfected cells, compared to hypoxic mock control cells supporting a role for this isoform in promoting cell proliferation both under normoxic and hypoxic conditions in DLD-1 cells.

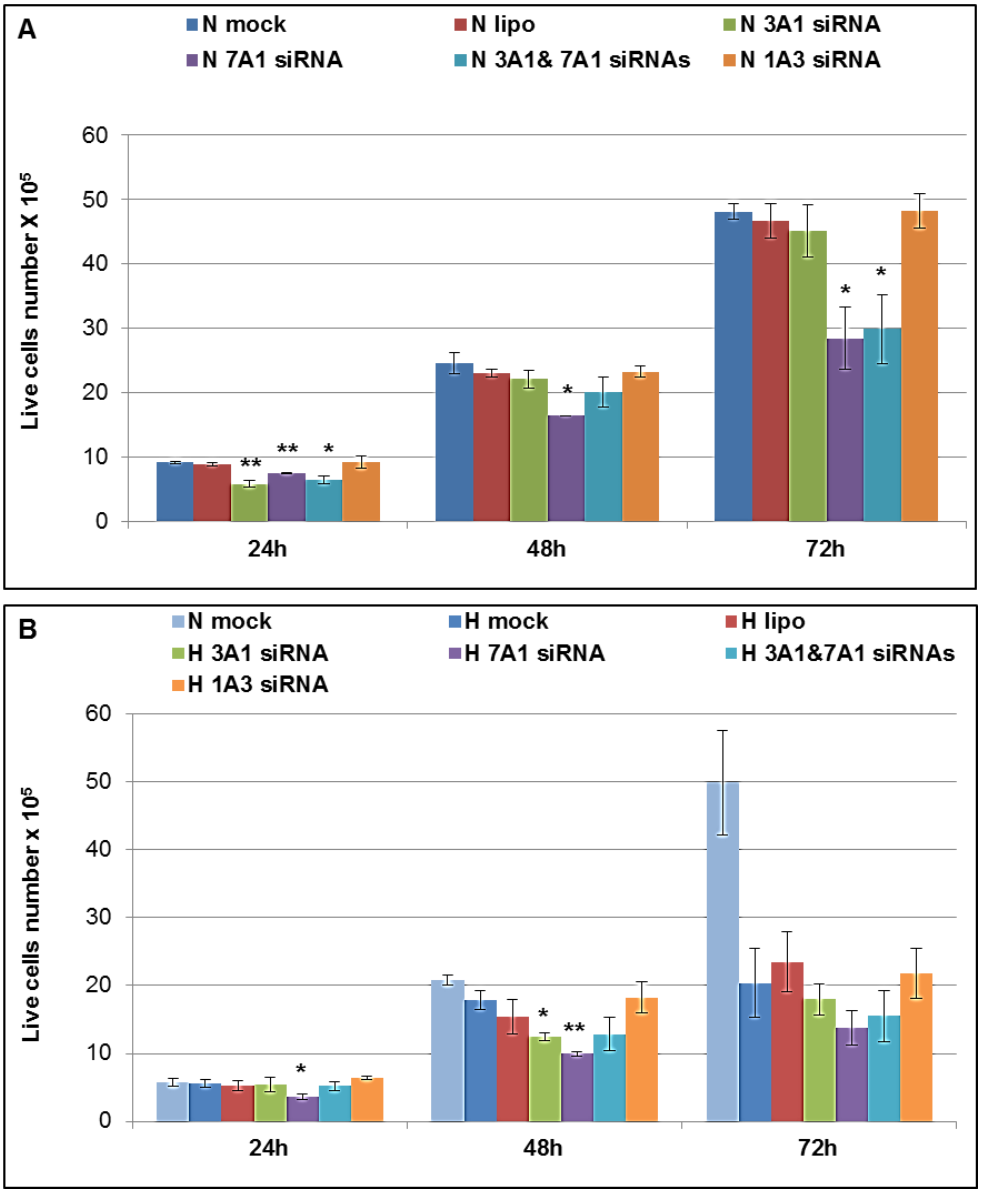

Figure 57 Live cells number using trypan blue assay after ALDH knockdown under normoxic conditions (A) or hypoxic conditions (B). Normoxia (N), Hypoxia (H). Values are the mean of 3 independent experiments and error bars are SD. Live cell number was compared to N mock in A and H mock in B. P values: * $p<0.05$, ** $p<0.01$.

3.3.8 Effects of ALDH isoforms on the cell cycle

To assess whether ALDH7A1 knockdown might exert its effects on cell proliferation via effects on the cell cycle, cell cycle analysis were performed. The preliminary data revealed no obvious changes in cell cycle distribution with either ALDH1A3 or ALDH7A1 knockdown (Figure 58), suggesting that ALDH7A1 knockdown inhibited cell proliferation through mechanism other than cell cycle arrest.

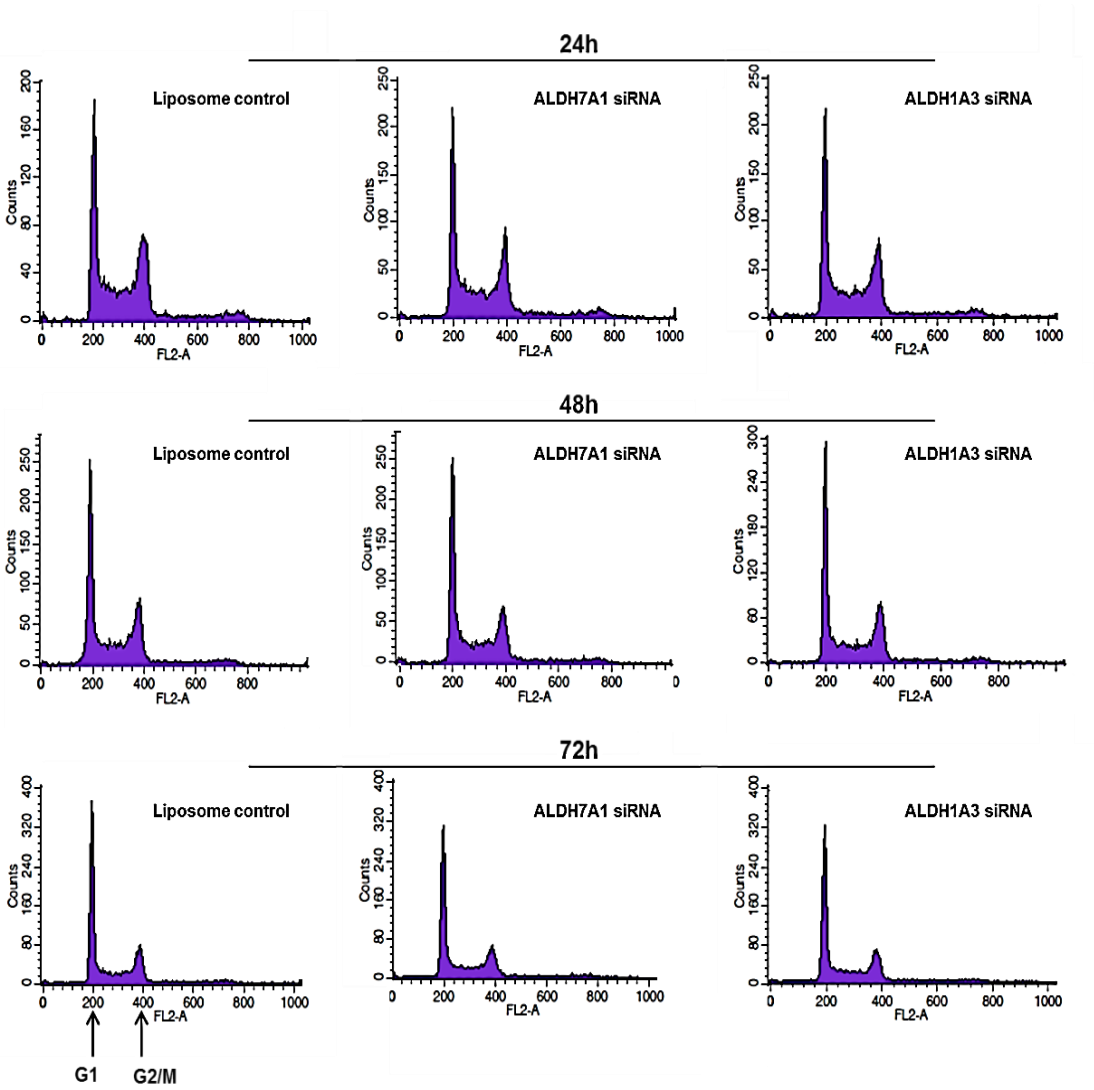

Figure 58 Cell cycle analysis in ALDH7A1 or ALDH1A3 siRNAs transfected DLD-1 cells after 24h, 48h, and 72h of transfection. Cell cycle analysis was performed using FACS. Results represent 1 experiment.

3.3.9 The role of ALDH isoforms in ROS generation

The literature has described the role of ALDH3A1 as an antioxidant and how it promotes resistance to UV and 4-HNE-induced oxidative damage in the cornea (Marchitti et al., 2011). Emerging evidence also points towards antioxidant properties of ALDH7A1, which in part offers protection to normal tissues from oxidative stress induced by ROS (Brocker et al., 2011). However, no reports are available to describe its role in the protection of cancer cells against cell death caused by ROS. Accordingly, DLD-1 cells were transfected with ALDH1A3, ALDH3A1 and ALDH7A1 siRNAs as single transfection and co-transfection (ALDH3A1 and ALDH7A1) and flow cytometry was employed to detect the generation of ROS compared to liposome controls as previously described in Material and Methods, section 3.2.6.

Hydrogen peroxide (H_2O_2) was used as a positive control for ROS induction (Figure 59A, curve shifted to right). ALDH1A3 knockdown resulted in reduction of ROS formation (Figure 59B, curve shifted to left) while ALDH3A1 knockdown had no effect on the ROS generation (Figure 59C). In contrast, ALDH7A1 knockdown resulted in an increase in ROS compared to control cells (Figure 59D), suggesting that ALDH7A1 in CRC DLD-1 cells has antioxidant properties; a similar finding was observed in co-transfected cells (Figure 59E). The fold change of ROS generation between siRNA transfected cells is illustrated in Figure 59F.

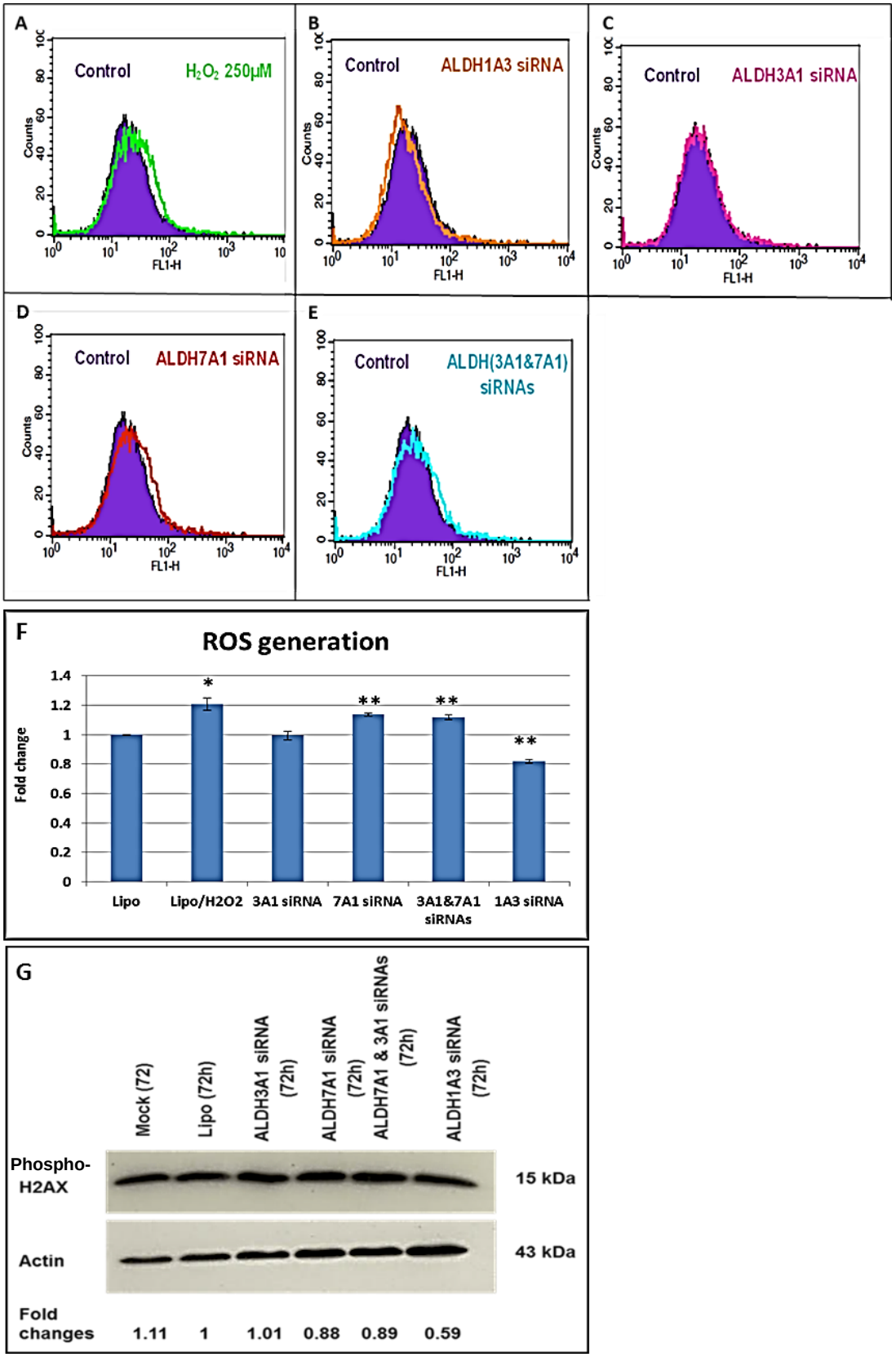

Figure 59 Detection of reactive oxygen species (ROS) generation in DLD-1 siRNA transfected cells after 72h of transfection under normoxic conditions. ROS generation curves (A-E), Fold change of ROS generation using the geometric means of area under the curve (F) and phosphorylated H2AX expression in knockdown samples (G). Values are the mean of 3 independent experiments and error bars are SD. P values: * $p<0.05$, ** $p<0.01$. For raw data, see Appendix X.

Direct effects of ROS, generally attributed to their high concentrations, include single strand (ss) or double strand (ds) DNA breaks that ultimately might cause cell death (Li et al., 1994). Accordingly, experiments were conducted to evaluate the effect of ROS on phosphorylated histone protein H2AX, which is a marker for dsDNA damage (KUO and YANG, 2008). However, no major difference in phosphorylated H2AX expression was observed for ALDH7A1 knockdown cells. ALDH1A3 knockdown cells showed lower levels of phosphorylated H2AX. This is consistent with the reduced ROS levels observed upon ALDH1A3 knockdown, suggesting that ALDH1A3 might have pro-oxidant activity in these cells (Figure 59G).

Similar experiments were carried out under hypoxic conditions and showed that H_2O_2 treatment (positive control) resulted in increased ROS generation compared to control cells (curve shifted to right, Figure 60A and B). Hypoxic cells were shown to have less ROS compared to normoxic samples (curve shifted to left, Figure 60A and C) which is in agreement with previous studies (Lopez-Barneo, 2001, Liu et al., 2004). Comparison between hypoxic knockdown samples and hypoxic liposome control, showed no major difference between ALDH1A3 or ALDH3A1 knockdown. However, ALDH7A1 knockdown either alone or when combined with ALDH3A1 knockdown showed more formation of ROS (curve shifted to right, Figure 60A and E), again pointing to an antioxidant role for ALDH7A1 under both normoxic and hypoxic conditions.

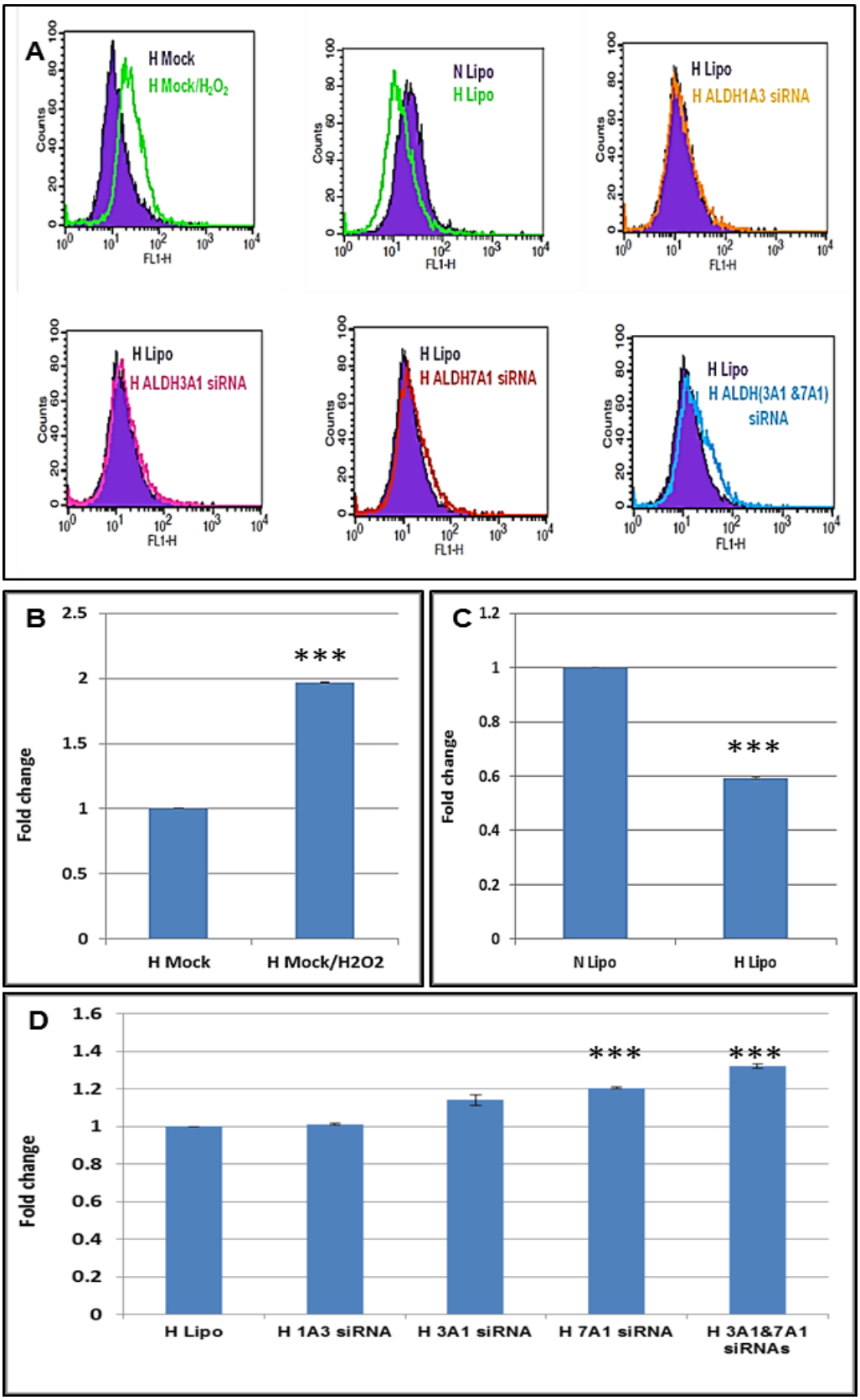

Figure 60 Detection of reactive oxygen species (ROS) generation in DLD-1 siRNA transfected cells after 72h of transfection under hypoxic conditions. ROS generation curves (A), Fold change of ROS generation using the geometric means of area under the curve (B,C,D). Values are the mean of 3 independent experiments and error bars are SD. P values: *** p<0.001.For Raw data, see Appendix X.

3.3.10 The role of ALDH in cell migration

Given a role for ALDH7A1 in mediating cell migration in prostate cancer has recently been described (van den Hoogen et al., 2011); studies were performed to determine if ALDH7A1 might have a similar function in CRC. Accordingly, the migratory ability of ALDH-knockdown cells was evaluated. Figure 61 reveals that single knockdown of ALDH3A1 or ALDH7A1 resulted in a small reduction in DLD-1 cell migration but this was not found to be statistically significant (P value = 0.091 and 0.095, respectively).

The literature has described how hypoxia often contributes to the aggressiveness of cancer cells, however there is controversy regarding its impact on cell migration (Qu et al., 2005, Fujiwara et al., 2007). Therefore, migration of normoxic and hypoxic mock cells were studied. Results showed less migratory ability of hypoxic cells compared to normoxic even after 40h (Figure 62). Consequently, no evaluation of migration in hypoxic knockdown cells was carried out.

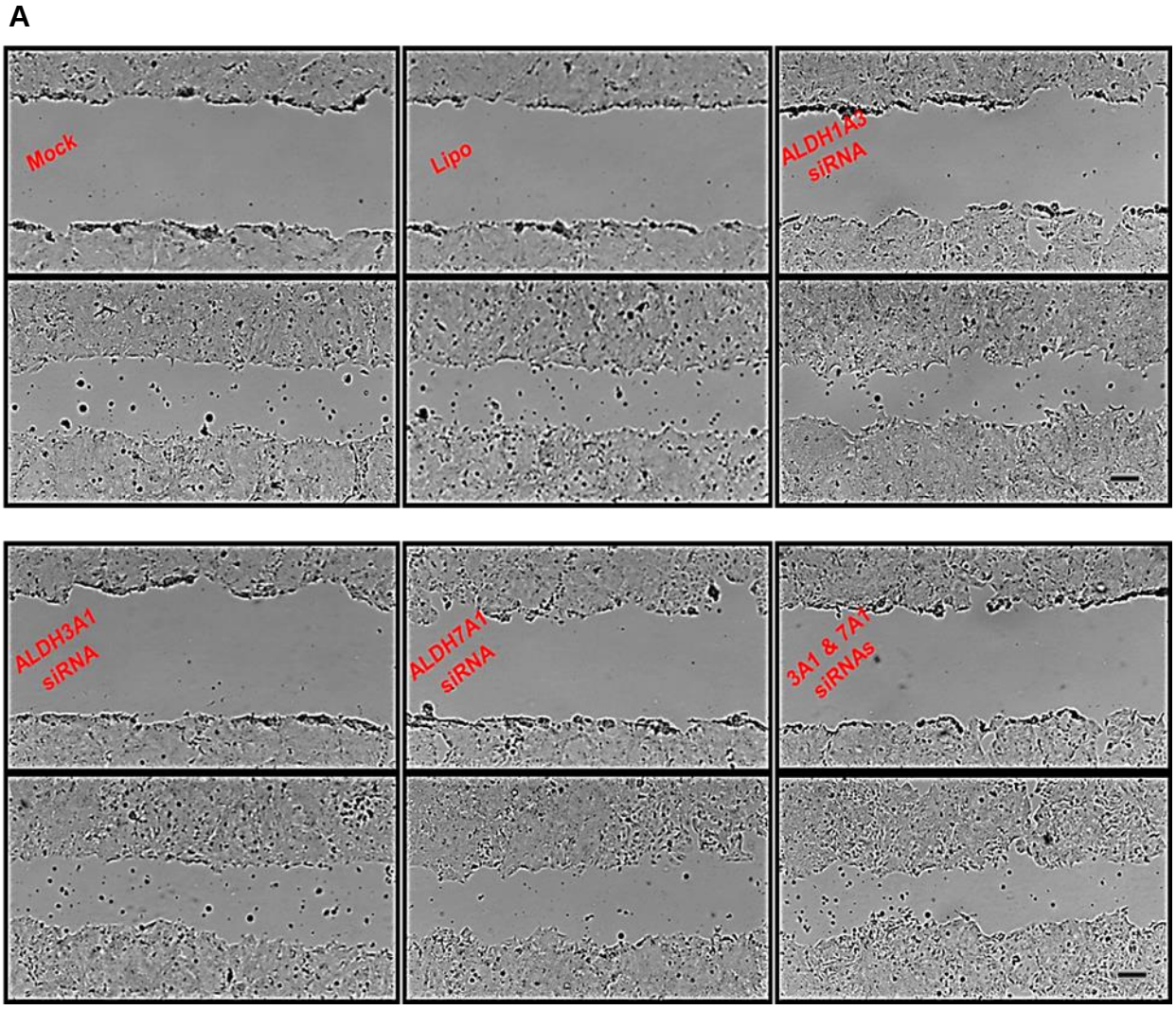

Figure 61 DLD-1 cell migration after 72h of ALDH knockdown using scratch assay. Initial scratch (0h) and after 24h of migration (A), Migration rate after 24h (B). Values are the mean of 3 independent experiments and error bars are SD. Photos are at 10x lens and scale bar = 100 µm.

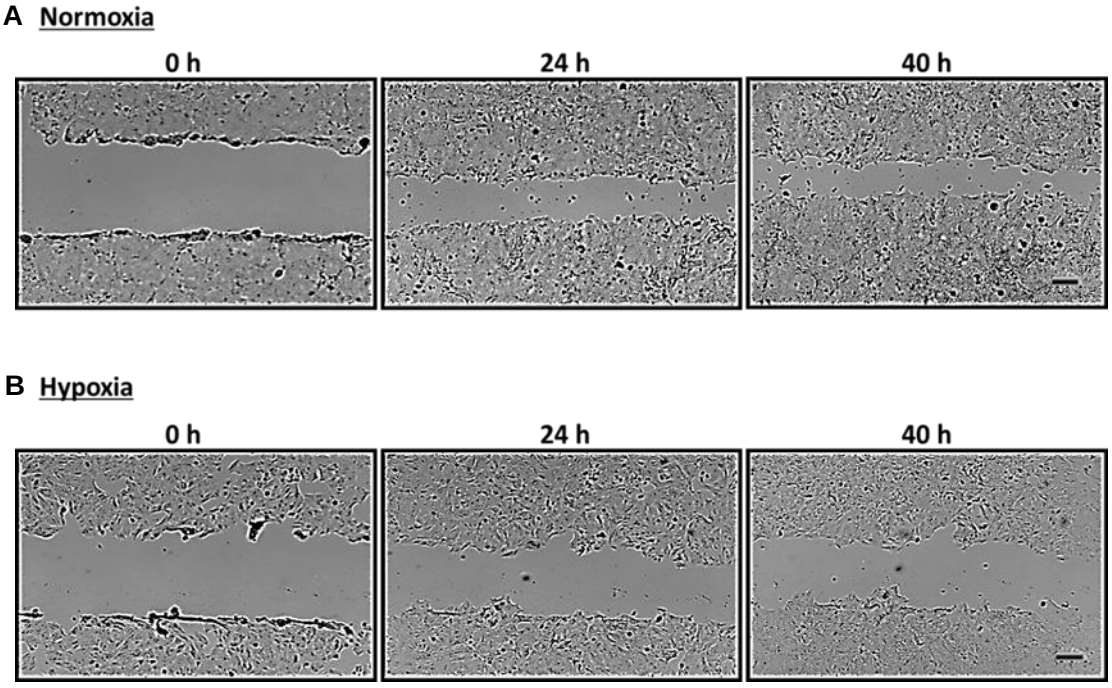

Figure 62 DLD-1 cell migration under normoxic (A) or hypoxic conditions (B) using scratch assay. Photos are at 10x lens and scale bar = 100 µm.

3.3.11 Impact of ALDH expression on cell sensitivity to colon cancer drugs

The expression of ALDHs has been correlated with drug resistance to several anticancer drugs (Chapter 1, Introduction, section 1.4.4). Accordingly, it was desirable to measure the potency of oxaliplatin, 5-FU and irinotecan in ALDH1A3, ALDH3A1 or ALDH7A1 siRNA, single or co-transfected DLD-1 cells.

Figure 63A shows that oxaliplatin treatment (75 µM, 48h) of mock cells resulted in 70% cell kill. ALDH1A3 and ALDH7A1 knockdown resulted in the same level of sensitivity to oxaliplatin treatment. While ALDH3A1 and ALDH3A1/7A1 co-transfected cells showed a slight increase in the percentage of cell survival compared to mock or liposome treated cells this was not found to be significant (P values= 0.13 and 0.46, respectively). In

contrast, co-transfection resulted in an insignificant increase in sensitivity to 5-FU treatment (P value= 0.08) (Figure 63B), while all other treated samples showed no difference upon knockdown. Figure 63C shows that irinotecan caused 80% cell kill in all samples without any difference between knockdown, liposome or mock treated cells.

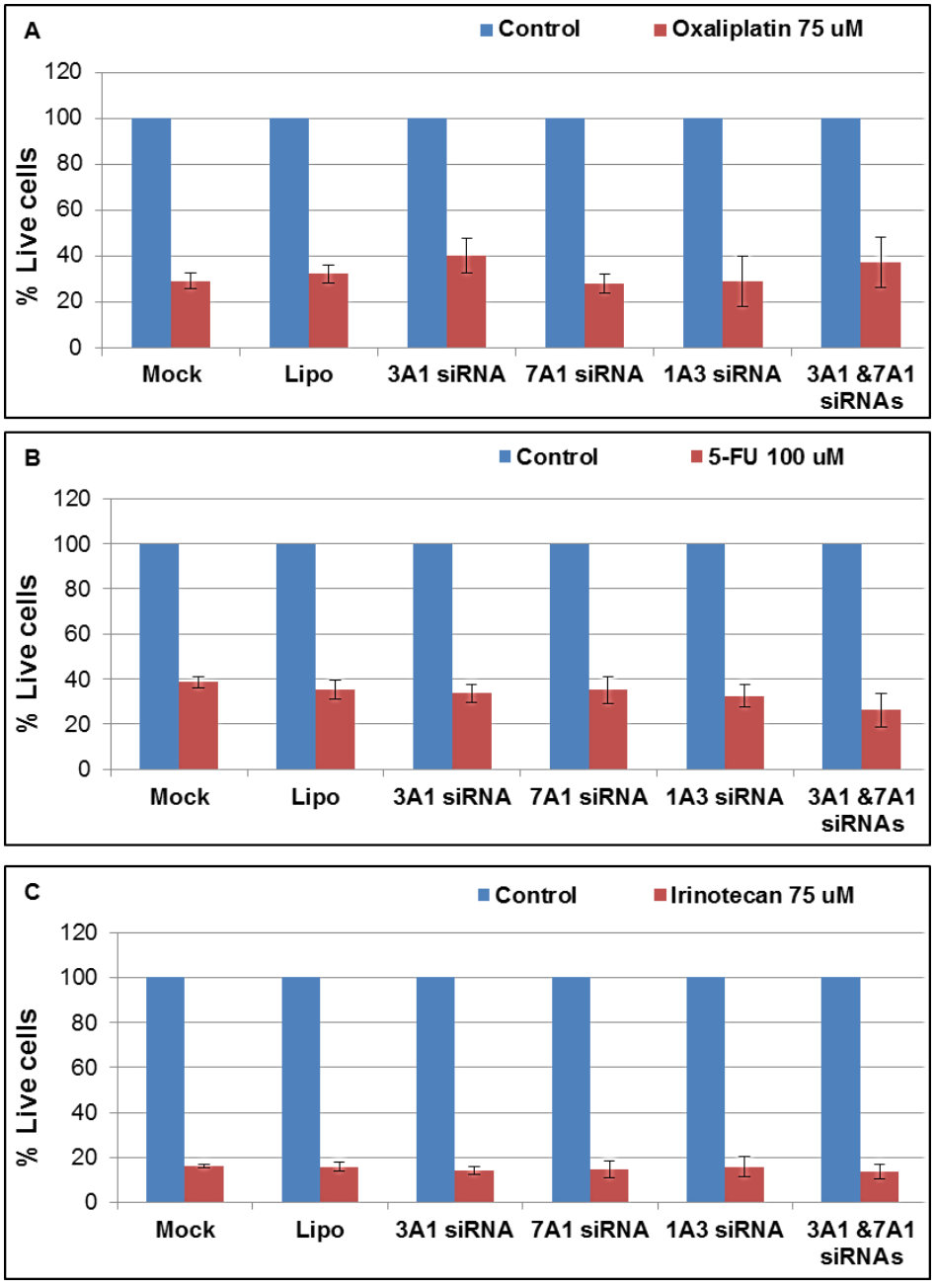

Figure 63 The cell survival of DLD-1 knockdown cells upon drug treatment under normoxic conditions using the trypan blue assay. Cells were treated with oxaliplatin (A), 5-FU (B) and irinotecan (C) for 48h. Values are the mean of 3 independent experiments and error bars are SD.

A recent study reported the role of hypoxia in mediating 5-FU drug resistance (Ahmadi et al., 2014). Accordingly, evaluation of drug sensitivity was also carried out under hypoxic conditions. ALDH7A1 knockdown experiment was also included to assess whether ALDH7A1 was involved in drug resistance. Figure 64 shows that hypoxia caused drug resistance to the three anticancer drugs evaluated in this study. Upon exposure to hypoxic conditions (0.1% O_2), the percentage of cell survival was increased from 24% to 87% for oxaliplatin, 30% to 66% for 5-FU and 20% to 77% for irinotecan. However, no significant difference was observed in sensitivity of drug treated cells transfected with ALDH7A1 siRNA versus liposome control cells under hypoxic conditions (P values= 0.91, 0.23 and 0.13 for oxaliplatin, 5-FU and irinotecan, respectively).

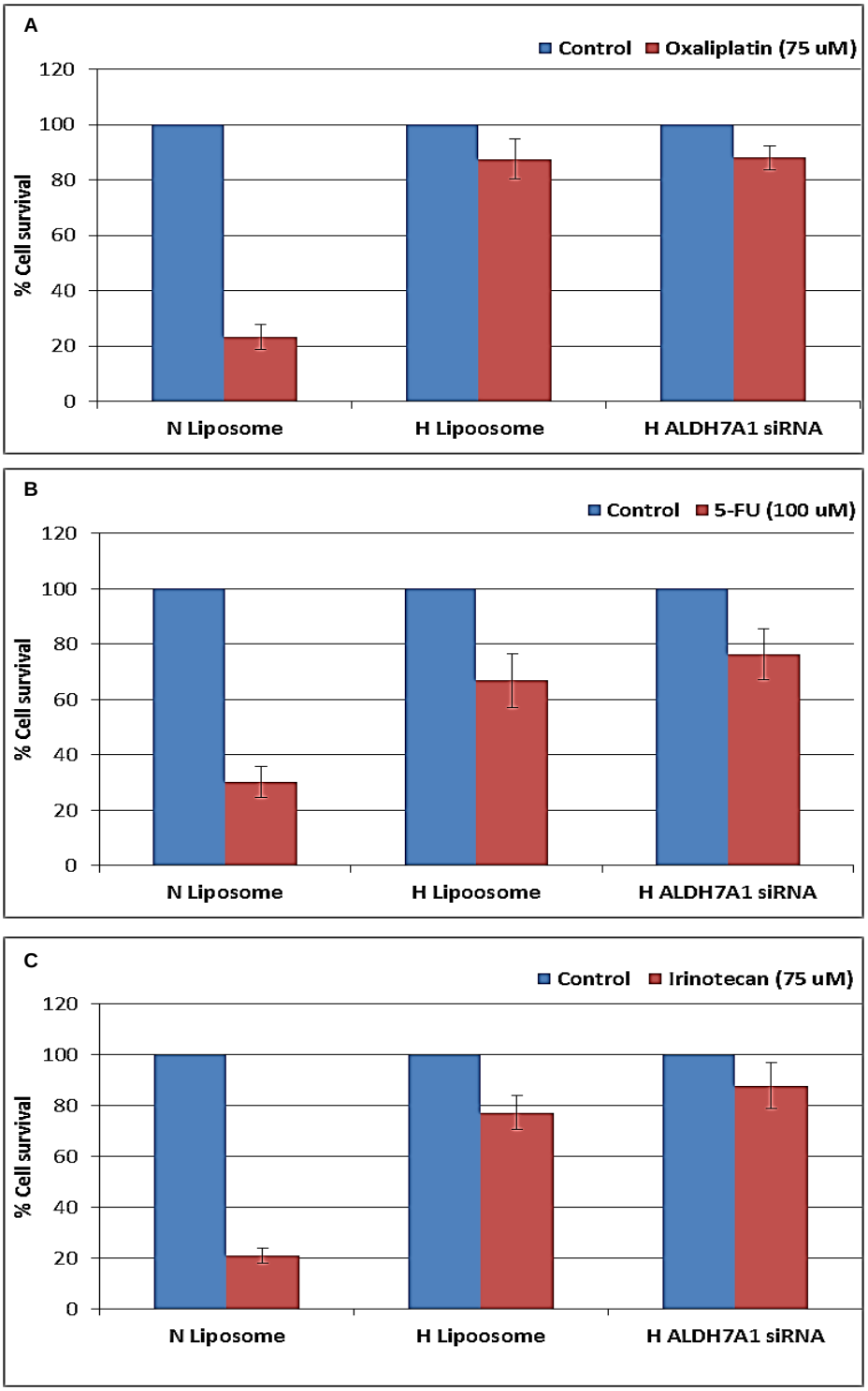

Figure 64 The cell survival of DLD-1 knockdown cells upon drug treatment under hypoxic conditions using the trypan blue assay. Cells were treated with oxaliplatin (A), 5-FU (B) and irinotecan (C) under normoxic (N) and hypoxic (H) conditions. Values are the mean of 3 independent experiments and error bars are SD.

3.4 Discussion

In this study, siRNA knockdown was used to assess the functional role of ALDH7A1 in CRC, in order to gain insight into its biological importance in CRC progression and drug resistance. DLD-1 cells were chosen for knockdown studies as they showed high expression of ALDH7A1. In addition, ALDH7A1 was upregulated in DLD-1 cells under hypoxic conditions and in the hypoxic regions of DLD-1 spheroids (Chapter 2). Similar observations were also found in HT29, however this cell line is not migratory and hence was not employed for siRNA studies. siRNAs against ALDH1A3 and ALDH3A1 were employed as controls to help understand specificity of ALDH7A1 knockdown and associated biological consequences.

Knockdown of ALDH3A1 and ALDH7A1 isozymes were successfully achieved resulting in abolishment of up to 70% of target ALDH expression in DLD-1 cells at both the gene and protein levels. The efficiency of ALDH1A3 knockdown was only evaluated at the gene level, as it was not detectable in DLD-1 cells at the protein level.

Interestingly, silencing of ALDH7A1 resulted in the upregulation of ALDH3A1 expression, which might suggest a compensatory mechanism when ALDH7A1 is suppressed. Accordingly, simultaneous dual knockdown of ALDH3A1 and 7A1 was carried out, which resulted in knockdown of both targets at both the gene and protein levels. Knockdown experiments were also carried out under hypoxic conditions as upregulation of ALDH7A1 upon exposure to hypoxia in both monolayer and MCS models were observed (Chapter 2). Significant and specific knockdown was also achieved. In

addition, the role of ALDH7A1 knockdown in the upregulation of ALDH3A1 was also observed under hypoxic conditions supporting the suggested compensatory mechanism or cross-talk between these two isoforms.

ALDH7A1 has been shown to be involved in mediating cell growth and enhancing clonogenicity in prostate cancer (van den Hoogen et al., 2011). Accordingly, the effect of ALDH7A1 knockdown on cell viability and proliferation was assessed using the trypan blue assay. Trypan blue is a cell membrane impermeable molecule which only enters cells with compromised membranes (dead cells), binds to intracellular proteins and renders the cells a bluish colour. This assay allows for a direct identification and enumeration of live (unstained) and dead (blue) cells in a given population (Strober, 2001). Using the trypan blue assay, marked reduction of live cell number of DLD-1 cells was observed upon knockdown of ALDH7A1 (P value< 0.05), supporting the findings of Hoogen *et al.* study, where ALDH7A1 knockdown led to significantly decreased prostate cancer cell growth and clonogenicity (van den Hoogen et al., 2011). Although these results suggest that ALDH7A1 may promote CRC cell proliferation, no difference in the number of dead cells was observed, indicating that ALDH7A1 does not affect cell survival or apoptosis. To confirm this, future work will include evaluation of the effect of ALDH knockdown on cell proliferation using cell proliferation assays such as ATP bioluminescence (Crouch et al., 1993) and the effect on cell apoptosis using Annexin V/Propidium Iodide apoptosis assay (Rieger et al., 2011).

Similar results were also observed when knockdown experiments were carried out under hypoxic conditions. All hypoxic cells had reduced live cell

numbers compared to normoxic cells, which is in agreement with the reported role of extreme hypoxia in arresting cell proliferation (Åmellem and Pettersen, 1991, Goda et al., 2003). Here, hypoxic cells with ALDH7A1 knockdown had the lowest live cell number among all other samples, providing further support for the potential role of ALDH7A1 in cell proliferation.

The role of ALDH7A1 in cell cycle progression is still not fully understood. Chan *et al*. has shown that ALDH7A1 has a role in cell cycle progression through its upregulation and accumulation in the nucleus during the G1/S phase transition in both the human embryonic kidney HEK293 cells and liver WRL68 cells. Knockdown studies resulted in changes in the levels of several key cell cycle-regulating proteins including upregulation of cyclin E, cyclin D1 and E2F-1 while the level of cyclin A decreased (Chan et al., 2011). In this work, nuclear staining of ALDH7A1 in MCS and xenograft models were demonstrated (Chapter 2). Accordingly, to understand if ALDH7A1 mediated cell growth through a role in cell cycle progression, analysis of the cell cycle phases upon ALDH7A1 knockdown using flow cytometry was carried out. However, no difference was observed compared to controls. Das *et al.* showed that inhibition of cell proliferation and growth rate can be caused by increase in cell doubling time without being triggered by cell death or cell cycle arrest (Das et al., 2012). This might be the reason for the findings observed in this study, however, further investigations are needed to confirm this such as using BrdU labelling Assay (Weber et al., 2014).

The detoxification capacity of ALDHs has been suggested to be one of the important factors governing CSC longevity and protect them against oxidative insults that are markedly increased in cancer (Reuter et al., 2010, Klaunig et al., 2010, Dando et al., 2015). Oxidative stress is caused by increased production of reactive oxygen intermediates that in part cause peroxidation of lipids (Brocker et al., 2011). This in turn can increase the production of aldehydes which can be directly toxic through the formation of adducts that damage DNA and inactivate enzymes (Comporti, 1998). In this study, it was expected that ALDH7A1 might enhance cell growth through its role in the protection against oxidative stress as previously observed (Brocker et al., 2011). It has been shown that stable expression of ALDH7A1 in Chinese hamster ovary (CHO) cells provides significant protection against treatment with the LPO-derived aldehydes hexanal and 4HNE (Brocker et al., 2011). In addition, a significant increase in cell survival was observed when cells were treated with increasing concentrations of hydrogen peroxide (H_2O_2), implicating a protective function for the enzyme during oxidative stress (Brocker et al., 2011). However, the antioxidant properties of 7A1 have not been investigated in cancer under normal basal growth conditions; in the absence of any external source of oxidative stress. Accordingly, the ROS levels in siRNA transfected cells was measured and compared to liposome control. Higher ROS levels were specifically detected in DLD-1 cells in which 7A1 expression was reduced by siRNA silencing. This advocates potential antioxidant properties of ALDH7A1, at least in DLD-1 CRC cells and supports the findings of Brocker *et al.* study (Brocker et al., 2011). Although ALDH3A1 has been described as ROS scavenger (Lassen

et al., 2007), no difference in ROS levels was observed upon its knockdown. In contrast, ALDH1A3 knockdown cells showed lower levels of ROS suggesting that 1A3 might have a pro-oxidant role in CRC DLD-1 cells. This would represent a novel function for 1A3, although the mechanism for its apparent pro-oxidant activity is presently unclear.as this role has not been described before.

ROS detection was also evaluated under hypoxic conditions as there is controversy regarding its level in hypoxic cells and tumour microenvironment (Liu et al., 2004, Kondoh et al., 2013). It is well known that oxygen pressure (pO_2) is a critical culture parameter which can cause oxidative stress (Ross et al., 2001). In this study, hypoxic cells were found to generate less ROS compared to normoxic cells, which is in agreement with previous studies (Fan et al., 2007, Fan et al., 2008). Fan *et al*. demonstrated that hypoxia effectively reduced intracellular ROS levels by downregulating NADPH oxidase expression (Fan et al., 2007). In addition, the analysis of glutathione redox status and ROS products showed less superoxide and H_2O_2 generation in hypoxia compared to normoxia (Fan et al., 2008). In order to evaluate whether the upregulation of ALDH7A1 observed upon hypoxia exposure (Chapter 2) also contributes to reduction of ROS generation in hypoxic cells, knockdown experiments were carried out. It was found that ALDH7A1 knockdown (single or in combination with ALDH3A1 knockdown) had more ROS generation. These findings support its potential role as antioxidant enzyme and suggest that hypoxia might reduce ROS generation, in part through upregulation of antioxidant enzymes such as ALDH7A1.

The role of ALDH7A1 in mediating prostate cancer metastasis has been reported (van den Hoogen et al., 2011). However, evaluation of DLD-1 cell migration using the scratch assay (Liang et al., 2007) showed that ALDH3A1 or 7A1 knockdown resulted in insignificant suppression of cell migration.

The migration ability of DLD-1 cells under normoxic and hypoxic conditions was also investigated as there is a controversy regarding the relation between hypoxia and cell migration (Turner et al., 1999, Qu et al., 2005, Fujiwara et al., 2007, Chen et al., 2009). It was found that DLD-1 cells incubated under hypoxia lost their migration ability. This might be due to changes in the cellular metabolism that can supress cell migration or through downregulation of migration-related genes, such as matrix metalloproteinases (MMPs) as previously reported in other studies (Turner et al., 1999, Qu et al., 2005).

Finally, the effect of ALDHs on the cytotoxicity of the clinically used colon cancer drugs; oxaliplatin, irinotecan and 5-FU was evaluated using the trypan blue assay. The activity of ALDHs has been shown to have a crucial role in causing resistance to a number of cancer therapeutics (Chapter 1, Introduction, section 1.4.4). However, little is known regarding the role of ALDH7A1 in drug resistance. Only one recent study using proteomics analysis revealed, incidentally, high expression of ALDH7A1 in DU145 prostate cancer cell line resistant to zoledronic acid (ZOL), nitrogen-containing bisphosphonates (Milone et al., 2015). In this study, the doses of oxaliplatin, irinotecan and 5-FU that were used caused 70%, 80% and 60% cell kill, respectively. However, no significant difference in drug sensitivity

was observed at these doses between knockdown and control cells, suggesting that ALDH7A1 is not involved in mediating resistance to these drugs.

The role of hypoxia in mediating drug resistance to certain conventional cytotoxic drugs as well as tyrosine kinase inhibitors (TKIs) is well established (Brown, 2002, Ahmadi et al., 2014). In this study, it was found that hypoxia resulted in resistance to oxaliplatin, irinotecan and 5-FU which supports previous reports (Luo et al., 2010, Chintala et al., 2010, Ahmadi et al., 2014). To evaluate whether ALDH7A1 upregulation in hypoxia might contribute to this observation, knockdown studies and drug treatment were carried out under hypoxic conditions. However, hypoxic cells with supressed ALDH7A1 expression upon knockdown showed the same response to these drugs as in hypoxic control cells, suggesting that ALDH7A1 is not involved in causing resistance to these drugs.

In summary, the data generated in this Chapter revealed that ALDH7A1 is involved in the reduction of ROS in CRC under both normoxic and hypoxic conditions. This is the first study to report on ALDH7A1 and hypoxia in cancer, indicating that the expression of ALDH7A1 in hypoxic cells might have an impact on CRC cell proliferation and its protection against cell death caused by oxidative stress. In order to further study the role of ALDH7A1, similar experiments will be carried out using an isogenic cell line pair and are described in Chapter 4.

The main findings of this Chapter were:

- Significant and specific knockdown of ALDH1A3, 3A1 and 7A1 was achieved.
- ALDH7A1 is involved in increased live cell number of DLD-1 cells under normoxic and hypoxic conditions.
- ALDH7A1 is involved in reducing the level of ROS in DLD-1 cells under normoxic and hypoxic conditions.

Chapter 4: Towards identifying small molecules to clarify the functional role of ALDH7A1

4.1 Introduction

The work described in Chapter 2 using 2D and 3D CRC cell culture models showed that ALDH7A1 expression was increased upon exposure to low oxygen level. Recent reports in the literature have linked ALDH7A1 with prostate cancer and matched bone metastasis (van den Hoogen et al., 2011), ovarian cancer (Saw et al., 2012) and recurrence in patients with non-small-cell lung carcinoma (Giacalone et al., 2013), further confirming a role for this enzyme in some cancer types. The pilot study using siRNA in the DLD-1 colorectal cancer cell line showed that ALDH7A1 increased the live cell number (Chapter 3), although further RNAi studies in additional CRC cell lines are required. Effects observed in the DLD-1 cells revealed the first demonstration that ALDH7A1 is involved in the reduction of ROS level in a cancer setting (Chapter 3, Results, section 3.3.9), which is in agreement with a reported protective role against oxidative stress (Brocker et al., 2011). However, ALDH7A1 had no apparent effect on the DLD-1 cell sensitivity of oxaliplatin, 5-FU and irinotecan (Chapter 3, Results, section 3.3.11). In an attempt to further unravel the role of ALDH7A1 in cancer, an isogenic cell line pair was acquired as a gift from Professor Jan Moreb (University of Florida). Specifically, the H1299 NSCLC cell line was employed due to its low endogenous ALDH expression (Moreb et al., 2012) and hence was deemed a good cell line to stably transfect with ALDH7A1, enabling an isogenic cell line pair to be used for investigation in this chapter.

In collaboration with Dr Zoe Cournia (Athens Academy Biomedical Research Foundation), a Maybridge database consisting of 24,000 compounds were included in a virtual screen against the ALDH7A1 protein structure. Several constraints were set including filters for solubility (QPlogS> -6.5), cell permeability (QPCaco> 22 nm), and number of metabolites (<7) compounds while Lipinski's rule of five (Lipinski, 2004) was adhered to (Maybridge UK, 2015). Nine compounds (BTB10142, HAN00316, RJC00145, DSHS00561, HC00017, KM06288, BTB04710, SEW03901 and SO6259) with the highest binding affinity for ALDH7A1 were purchased from Maybridge and were used to probe ALDH7A1 activity. The optimised binding model of HAN00316 compound is illustrated in Figure 65.

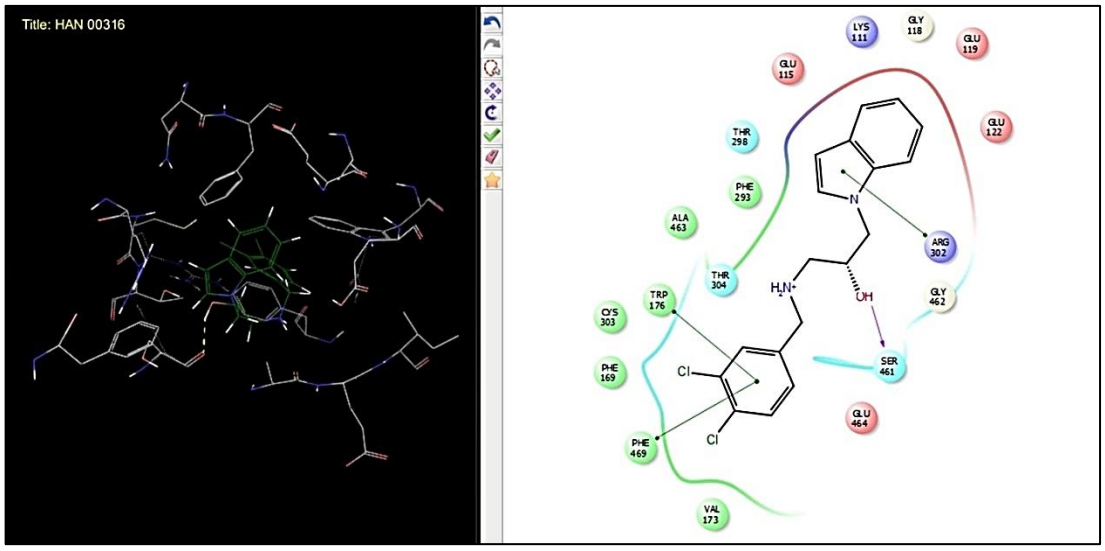

Figure 65 The optimised binding model of HAN00316 compound to ALDH7A1. The binding model is obtained from Dr Zoe Cournia.

The hypothesis of this Chapter is: ALDH7A1 expression in NSCLC affects cell proliferation and migration and small molecule agents can be used to clarify its functional role. The aim of this chapter was to explore ALDH7A1 function using lung H1299 cancer cell lines. The specific objectives were:

1. To study the role of ALDH7A1 in mediating cell proliferation, migration, spheroid formation and invasion.
2. To evaluate the effect of ALDH7A1 overexpression on ROS level.
3. To evaluate ALDH7A1 role in osmoregulation.
4. To evaluate ALDH7A1 effect on the sensitivity of conventional cytotoxic drugs and molecularly-targeted agents.
5. To evaluate computationally designed compounds with potential of inhibiting ALDH7A1 activity to find a compound that might act as a starting point for further chemical tool discovery to study the role of ALDH7A1 in cancer.

4.2 Material and Methods

4.2.1 Cell culture

The human non-small cell lung carcinoma cell line, H1299, derived from the metastatic lesion in the lymph node was originally obtained from ATCC. These are known to have no significant ALDH activity by the ALDEFLUOR assay and western blot (Moreb et al., 2012). Cells were transduced with lentiviral vectors containing the full cDNA for ALDH7A1 or red fluorescent protein RFP (used as a control) (Personal communication, Prof Jan Moreb). The cells were cultured and maintained in complete RPMI 1640 culture medium (Table 12) containing 1x penicillin/streptomycin antibiotic (Sigma) and used for the experiments when they were 70% confluent.

Cell line	Culture medium	Frequency of subculture	Dilution upon subculture
H1299/RFP	RPMI	5-6 days	1:10-1:20
H1299/ALDH7A1	RPMI	5-6 days	1:10- 1:20

Table 12 Maintenance of H1299 cell lines.

4.2.2 Evaluation of ALDH gene expression

To evaluate the gene expression of ALDH in both H1299/RFP and H1299/ALDH7A1 cell lines, cells were seeded into 75 cm^2 flasks at a concentration of 2×10^5 cells/flask. After 5 days of incubation at 37ºC, 5% CO_2 and 100% humidity, cells were harvested for RNA extraction and cDNA synthesis as previously described (Chapter 2, Materials and Methods, section 2.2.1.3.1-3). Gene expression analysis of ALDH1A1, 1A2, 1A3, 1B1, 2, 3A1, 7A1 and β-actin (internal control gene) was carried out as previously described (Chapter 2, Materials and Methods, section 2.2.1.3.5-6).

4.2.3 Evaluation of ALDH7A1 protein expression

Cells were seeded into 75 cm^2 flasks at a concentration of 2×10^5 cells/flask. After 5 days of incubation at 37ºC, 5% CO_2 and 100% humidity, cells were harvested for protein extraction. Protein expression analysis of ALDH7A1, 2, 1A3 and actin (internal control protein) was carried out using western blot as previously described (Chapter 2, Materials and Methods, section 2.2.1.4).

4.2.4 Evaluation of ALDH activity using the ALDEFLUOR assay

ALDH activity was assessed using the ALDEFLUOR Assay System (StemCell Technologies) according to the manufacturer's recommendations. This system uses an immunofluorescent method to detect intracellular enzyme activity of ALDH (Chapter 1, Introduction, section 1.4.5.1.1). Single cells obtained by trypsinisation from fresh H1299/RFP and H1299/ALDH7A1 cell cultures (70% confluent) were washed in PBS and re-suspended in 1 ml of ALDEFLUOR™ assay buffer. This suspension was divided equally in two microcentrifuge tubes (test sample and control sample) and ALDEFLUOR™ DEAB inhibitor was added to control sample to block ALDH activity. 2.5 µl of the fluorescent-activated ALDEFLUOR™ reagent, BAAA, was then added to each sample. The "test" and "control" samples were incubated for 30-40 min at 37°C. Following incubation, samples were centrifuged for 5 min at 250 rcf and supernatants were discarded. Samples were then re-suspended in 0.5 ml of ALDEFLUOR™ assay buffer and placed immediately on ice. Samples were washed and analysed with a flow cytometer. Each FACS analysis was performed on at least 10,000 events. First the mean number of ALDH positive cells was calculated for each cell line using the following formula:

Mean $ALDH^+$ = Mean $ALDH^+$ of t sample – Mean $ALDH^+$ of control sample

The fold change of ALDH activity between H1299/RFP and H1299/ALDH7A1 cells was calculated using the following formula:

ALDH activity (fold change) = Mean $ALDH^+$ (H1299/ALDH7A1)/ Mean $ALDH^+$ (H1299/RFP)

4.2.5 Effect of ALDH7A1 overexpression on cell proliferation

The cell lines were seeded in six 96-well microtitre plates by adding 200 µl of 5×10^3 cells/ml cell suspension to the relevant wells (1×10^3 cells/well). 200 µl of cell free media was added to blank wells. Plates were incubated at 37ºC, 5% CO_2 and 100% humidity until ready to be assayed by the MTT assay on day 1, 3, 4, 5 and 6. See Appendix II for the composition of MTT assay.

On day 0, the 96-well plate was centrifuged at 1000 rcf for 5 min. The supernatants were removed carefully and 200 µl of MTT (Sigma) solution (0.5 mg /ml) was added to each well. The plate was incubated for 4h at 37ºC, 5% CO_2 and 100% humidity before being centrifuged at 1,000 rcf for 5 min to pellet down the cells. Supernatants were carefully removed and 150 µl of DMSO (Sigma) was added to each well and gently pipetted up and down to dissolve the formazan blue crystals. The absorbance of each well was determined using a plate reader (Thermo Electron Corporation) at 540 nm. On day 1, 3, 4, 5 and 6, one plate was removed on the relevant day. The MTT assay was carried out as described above but without centrifugation.

The mean of the absorbance values for each cell concentration minus the mean of the blank absorbance values was calculated. Results were generated in Microsoft Excel 2010 and plotted as a histogram with the mean absorbance values on the Y-axis and time (days) on the X-axis.

4.2.6 Effect of ALDH7A1 overexpression on cell migration

Cells were seeded in 6 well plates at a concentration of 7×10^5 cells/well in 2 ml RPMI. After 24h of incubation at 37ºC, 5% CO_2 and 100% humidity, the cells formed monolayer and were scraped in a straight line to create a "scratch" with a p200 pipet tip. The cells were then washed to remove the debris and smooth the edge of the scratch using 1 ml of RPMI. Next, 2 ml of RPMI containing 2% FBS was added to each well. Photos were taken at time 0 (initial scratch before migration) as well as after 15h of incubation at 37˚C and 5% CO_2. Image J was used for migration analysis by calculating the cells free area and quantify the migration rate of the cells.

4.2.7 Effect of ALDH7A1 overexpression on reactive oxygen species (ROS) generation

In order to study the antioxidant activity of ALDH7A1 enzyme, the effect of ALDH7A1 overexpression on ROS generation was evaluated using FACS. The cells were seeded in phenol red free RPMI medium (Gibco) into 25 cm^2 flasks at a concentration of 2×10^5 cells/flask and incubated at 37˚C and 5% CO_2. After 72h of incubation, the cells were harvested and treated with carboxy-H2DCFDA (Fisher scientific) as previously described in Chapter 3, Materials and Methods, section 3.2.6 before ROS analysis was carried out using FACS.

4.2.8 Effect of ALDH7A1 overexpression on double strand DNA damage

The possible protective role of ALDH7A1 against DNA damage that might be caused by ROS was evaluated using phosphorylated H2AX as a marker of cellular dsDNA damage (KUO and YANG, 2008). In brief, the cells were seeded and harvested for protein extraction as previously described in section 4.2.3. Western blot was carried out as previously described (Chapter 2, Materials and Methods, section 2.2.1.4) using rabbit anti phosphorylated H2AX primary antibody (New England Biolabs, concentration: 1:1000) and HRP based antirabbit secondary antibody (Dako, concentration: 1:2500).

4.2.9 Effect of ALDH7A1 overexpression on osmoregulation

H1299 cells were seeded into 96-well plates by adding 180 µl of cell suspension with a concentration of 0.55×10^4 cells/ml (1×10^3 cells/well) to each well. Plates were incubated for 24h at 37ºC, 5% CO_2 and 100% humidity. The following day, medium was removed and cells were treated with NaCl or sucrose dissolved in RPMI by adding 200 µl of working solutions to the relevant wells (final NaCl concentrations in wells were 12.5:200 mM, final sucrose concentrations in the wells were 18.75:300 mM). The control cells and blank wells were treated only with complete RPMI medium. Plates were incubated for 24h at 37ºC, 5% CO_2 and 100% humidity. The next day, medium was removed and replaced with fresh RPMI medium. The cells were incubated for further 72h before the cell survival was measured using the MTT assay as previously described (Chapter 2, Materials and Methods, section 2.2.4.1)

4.2.10 Effect of ALDH7A1 overexpression on spheroids formation

Spheroids were generated from H1299/RFP and H1299/ALDH7A1 cells using a hanging drop technique (Del Duca et al., 2004). In brief, 4×10^3 cells in 40 µl of complete RPMI media containing 20% (v/v) methylcellulose (Sigma) (Appendix VIII) were seeded as drops on the inner side of the lid of a 10 cm Petri dish using 200 µl tips. PBS was added to the dish below the drops to maintain a humidified atmosphere and to prevent dehydration. The dish was gently covered with the lid and incubated at 37°C and 5% CO_2 for 48h. The diameter of the spheroids was measured using calibrated graticule fixed to the light microscope at 10 × objective lens.

4.2.11 Effect of ALDH7A1 overexpression on spheroids invasion

After 48h of cell seeding for spheroid formation, H1299/RFP and H1299/ALDH7A1 spheroids were embedded in collagen matrix to evaluate their invasion ability. In brief, collagen matrix was prepared on ice by dissolving collagen stock solution (collagen type 1 rat tail, Corning) in 5x PBS, NaOH (1M) and distilled water (Appendix VIII). 75 µl of invasion collagen matrix (pH 7.4) was added to each well of flat bottomed 96 well plates and allowed to set at 37°C for 30 min. Next, one spheroid in 2 µl medium was transferred to each well, which was allowed to settle down and covered with another layer of collagen matrix (75 µl). The plate was incubated at 37°C for 30 min after which 150 µl of RPMI containing 40%, 20%, and 4% of FBS was added to relevant wells to obtain final

concentration of 20%, 10% and 2% FBS, respectively. The plate was then incubated at 37°C, 5% CO_2 and 100% humidity. Spheroid invasion was visualised at 0h and 48h after incubation. Photographs were taken at 10 × objective lens using Lumascope 500 microscope and data analysis was performed using Image J software.

4.2.12 Effect of ALDH7A1 overexpression on the anti-proliferative activity of anticancer drugs

4.2.12.1 Drug stock solution

H1299 cells were treated with anticancer drugs and compounds listed in Table 13. Cytotoxic drugs (cisplatin, doxorubicin, paclitaxel (Avachem scientific), oxaliplatin, irinotecan and 5-FU (Sigma)), molecularly-targeted drugs (gefitinib, sunitinib, dasatinib, masitinib, imatinib and vandetinib (LC laboratories)), ALDH inhibitors (DEAB, disulfiram, pargyline and salinomycin (Sigma)) and Maybridge compounds (BTB10142, HAN00316, RJC00145, DSHS00561, HC00017, KM06288, BTB04710, SEW03901 and SO6259) were dissolved in DMSO (Sigma). The stock solutions were kept at -20ºC and working solutions were prepared in complete RPMI medium (Sigma) immediately prior to use.

Drug category	example	Mode of action
Cytotoxic drugs	Cisplatin	Platinum compounds/intra-strand DNA crosslinking
	Doxorubicin	Anthracycline antibiotic/topoisomerase II inhibitor
	Paclitaxel	Taxanes/microtubule polymer stabilisation and prevention from disassembly
	Oxaliplatin	Platinum compounds inter- and intra-strand DNA crosslinking
	Irinotecan	topoisomerase 1 inhibitor
	5-Flurouracil	Antimetabolite/pyrimidine analogue
Targeted drugs	Gefitinib	EGFR inhibitor
	Sunitinib	PDGF-Rs, VEGFRs, c-Kit, RET and others
	Dasatinib	BCR/Abl (the "Philadelphia chromosome"), Src, c-Kit, ephrin receptors inhibitor
	Masitinib	c-Kit, PDGFR, and FGFR inhibitor
	Imatinib	BCR/Abl, PDGFR, and c-Kit inhibitor
	Vandetanib	VEGFR, EGFR and RET inhibitor
Non-selective inhibitors	DEAB	ALDH1, 2 and 7A1 inhibitor
	Disulfiram	ALDH1A1 and 2 inhibitor
	Pargyline	Non-selective monoamine oxidase (MAO) inhibitor
	Salinomycin	Induce apoptosis, potassium ionophore (Kills CSCs)
ALDH7A1 inhibitors	BTB10142	ALDH7A1 inhibitors
	HAN00316	
	RJC00145	
	DSHS00561	
	HC00017	
	KM06288	
	BTB04710	
	SEW03901	
	SO6259	

Table 13 Drug category, examples and mode of action.

4.2.12.2 Drug treatment using the MTT assay

Cells were seeded into 96-well plates by adding 180 µl of cell suspension with a concentration of 0.55×10^4 cells/ml (1×10^3 cells/well) to each well. Plates were incubated for 24h at 37ºC, 5% CO_2 and 100% humidity to enable the cells to attach to the plastic surface. Next, 20 µl of working solutions of drug in appropriate concentration range were added to the wells. The control cells were treated with 20 µl of DMSO in complete RPMI medium (final concentration in wells: less than 0.1 % v/v), while blank wells contained cell free media. Plates were incubated for 96h at 37ºC, 5% CO_2 and 100% humidity. After exposure, the chemosensitivity was evaluated by the MTT assay as previously described (Chapter 2, Materials and Methods, section 2.2.4.1). Additionally, the cells were treated with the Maybridge compounds and DEAB for 24h to assess the non-toxic concentrations, which were used to probe the importance of ALDH7A1 in the isogenic H1299/RFP and H1299/ALDH7A1 cell line pair.

4.2.13 Effect of Maybridge compounds on ROS generation

The cells were seeded in phenol red free RPMI medium (Gibco) into 25 cm^2 flasks at a concentration of 2×10^5 cells/flask and incubated at 37˚C and 5% CO_2. After 48h of incubation, the cells were treated with DEAB (200 µM), HAN00316 (20 µM), KM06288 (20 µM), DSHS00561 (25 µM) or DMSO (0.1% v/v) for 24h. Next, the cells were harvested and treated with carboxy-H2DCFDA (Fisher scientific) as previously described in section 4.2.7 and the ROS formation was evaluated using FACS.

4.2.14 Effect of Maybridge compounds on cell migration

The migration assay was carried out using the scratch assay as previously described in section 4.2.6. 2 ml of 2% RPMI containing DEAB (100 µM), HAN00316 (10 µM), KM06288 (10 µM), DSHS00561 (20 µM) or DMSO (0.1% v/v) was added to wells after creating the scratch. Photos were taken at time 0 (initial scratch before migration) as well as after 15h of treatment (15h after scratch). Image J was used for migration analysis by calculating the cells free area and quantify the migration rate of the cells.

4.2.15 Statistical data analysis

The significance of results was assessed through a comparison of means using two-tailed student t-test. Results were expressed as the mean ± standard deviation. P values were calculated to determine statistical significance of the results.

.

4.3 Results

4.3.1 ALDH expression analysis

Figure 66A shows the ALDH gene expression analysis of H1299/RFP cells. ALDH 1A1, 1A2, 1A3, 1B1, 2, 3A1, and 7A1 genes were expressed at low level. As expected, the expression of ALDH7A1 was induced 85-fold at the gene level (Figure 66B) and 9-fold at the protein level (Figure 66C) compared to H1299/RFP (control).

The effect of ALDH7A1 overexpression on other members of the ALDH family was also explored. Figure 66D shows that the ALDH7A1 transfection also had effect on inducing ALDH1A3 (4-fold) and ALDH2 (1.8-fold) at the gene level compared to H1299/RFP cells. However, the expression of these isoforms was not detected at the protein level (Figure 66E).

4.3.2 ALDH activity

The ALDEFLUOR assay was employed to detect the intracellular enzymatic activity of ALDH in both H1299 cell lines. Figure 67 shows that H1299/ALDH7A1 cells had 17-fold increase in ALDEFLUOR activity compared to H1299/RFP cells. The detection of higher ALDEFLUOR activity in H1299/ALDH7A1 cells combined with significant ALDH7A1 expression, suggests that ALDH7A1 might be the isoform responsible for the reported activity.

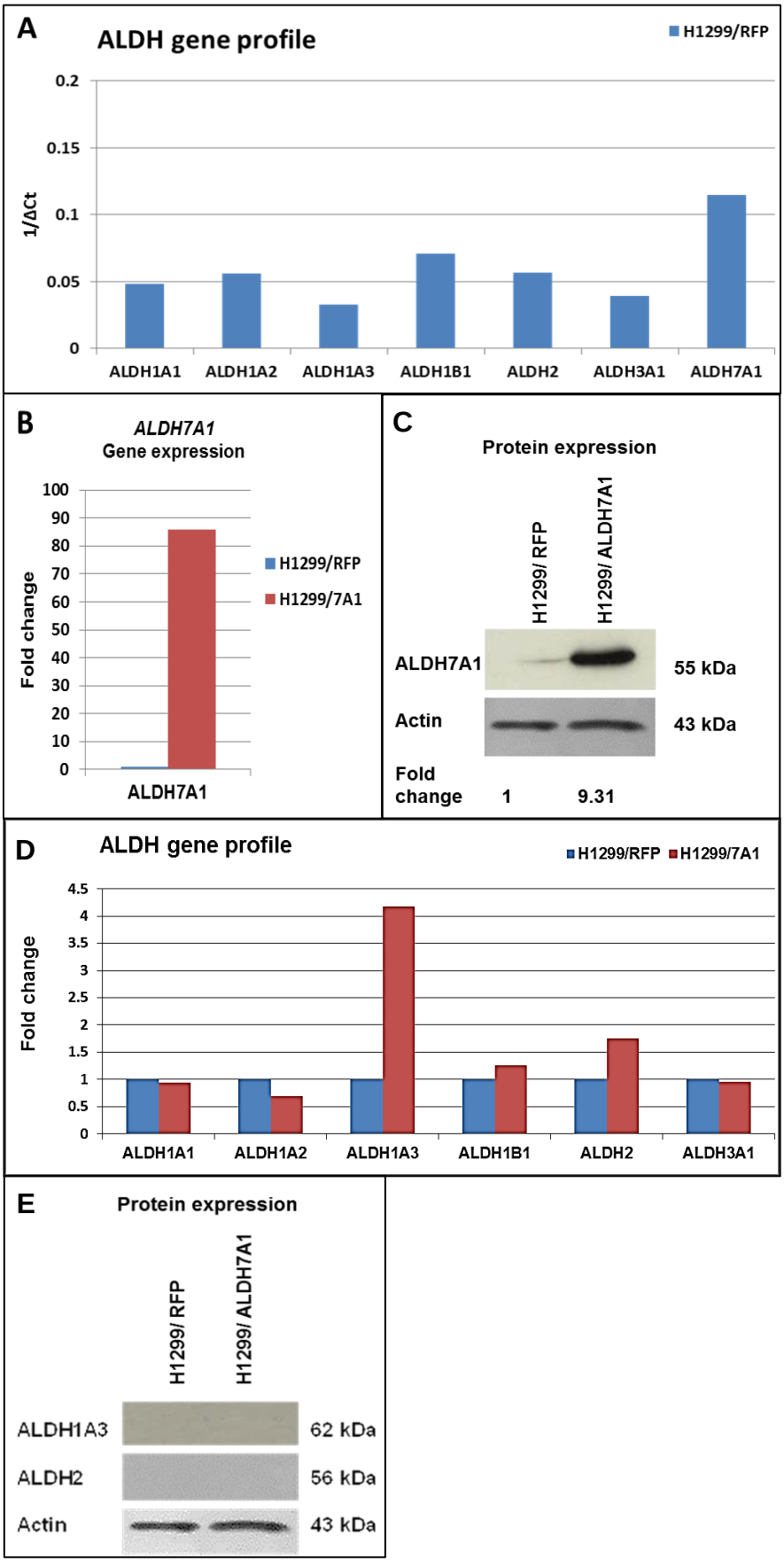

Figure 66 The expression of ALDH in H1299/RFP and H1299/ALDH7A1 cells. ALDH gene expression analysis in H1299/RFP using qRT-PCR (A), ALDH7A1 gene expression using qRT-PCR (B), ALDH7A1 protein expression using western blot (C), comparison of ALDH gene expression using qRT-PCR (D) and protein expression of ALDH1A3 and 2 (E). Results represent 1 experiment.

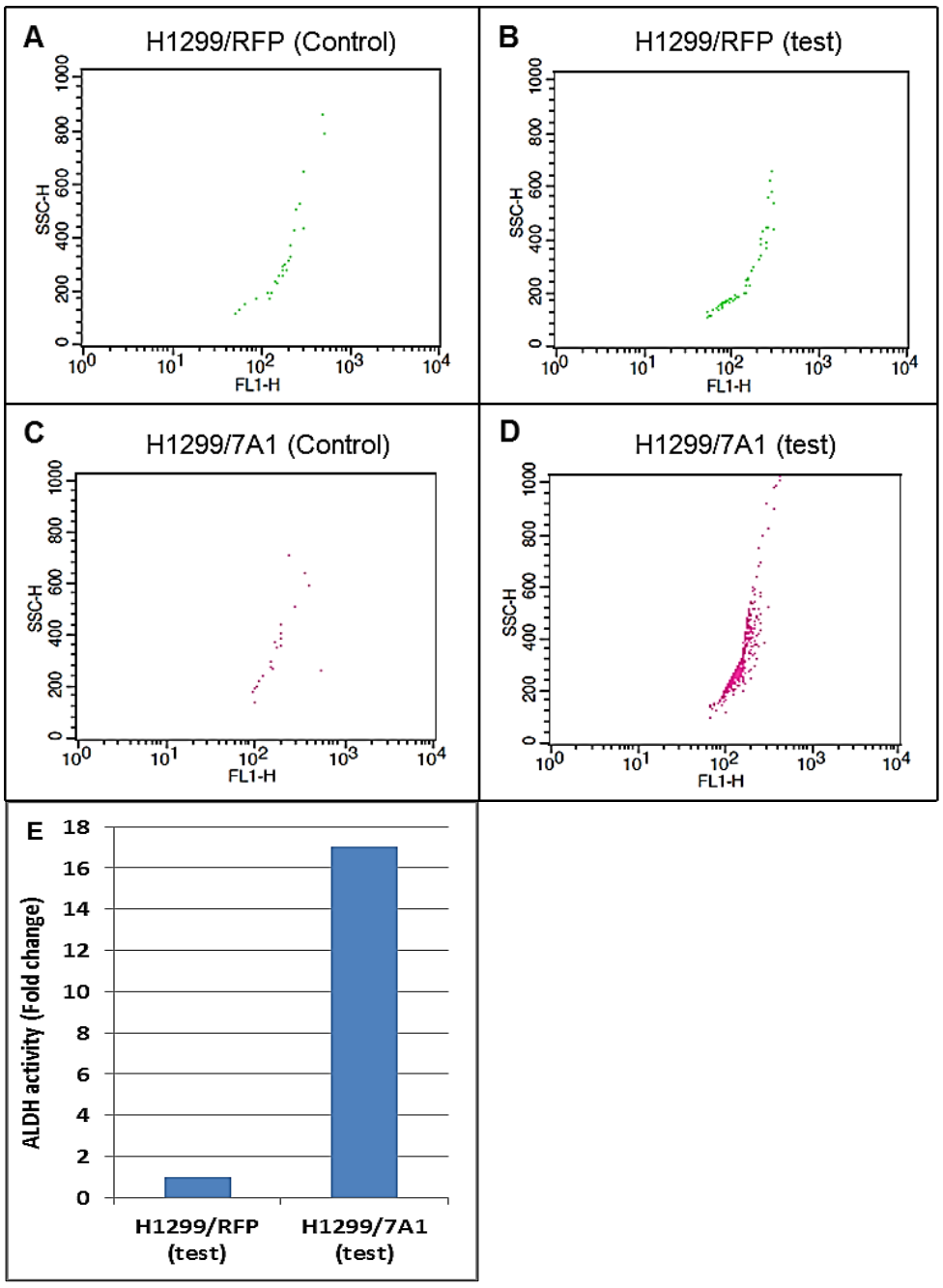

Figure 67 ALDH activity detection in H1299 isogenic cell pair using the ALDEFLUOR assay. H1299/RFP (Control) (A), H1299/RFP (test) (B), H1299/7A1 (Control) (C), H1299/7A1 (test) (D). Fold change of ALDH activity (E). Dots represent ALDEFLUOR positive cells and values are the mean of 2 experiments.

4.3.3 Effects of ALDH7A1 overexpression on cell proliferation

Results from Chapter 3 showed that knockdown of ALDH7A1 resulted in reduction of DLD-1 live cell number, which is in agreement with ALDH7A1's effect on cell proliferation and clonal efficiency in prostate cancer (van den Hoogen et al., 2011). Here, the cell proliferation was evaluated using the MTT assay to detect differences in daily cell growth. Overexpression of ALDH7A1 increased the proliferation rate compared to H1299/RFP cells (Figure 68).

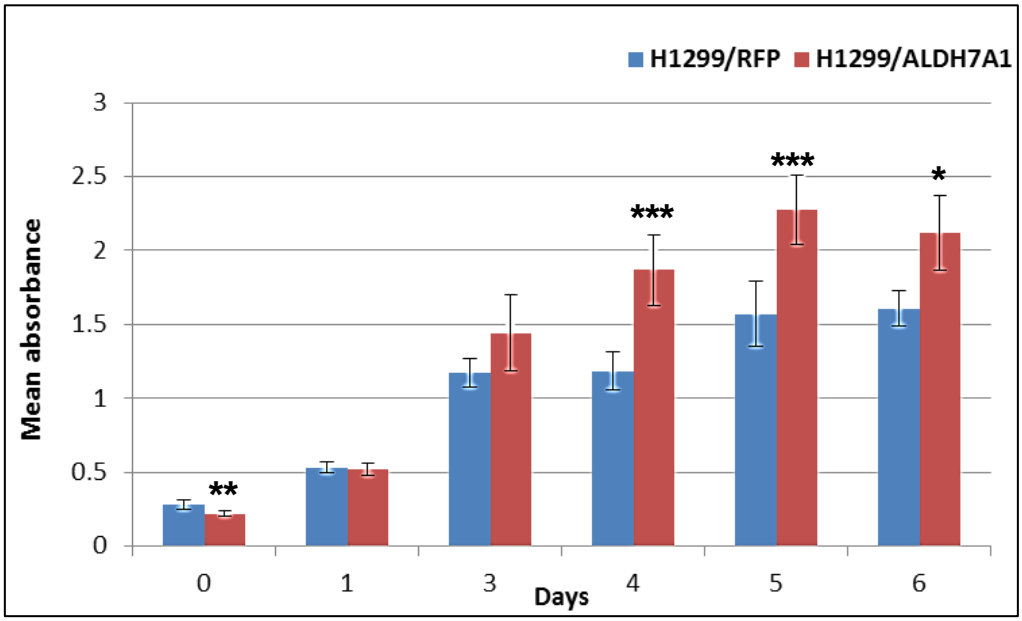

Figure 68 The effect of ALDH7A1 overexpression on H1299 cell proliferation using the MTT assay. Values are the mean of at least 3 experiments and error bars are SD. P values: * p< 0.05, ** p<0.01, *** p<0.001.

4.3.4 Effects of ALDH7A1 overexpression on cell migration

The effect of ALDH7A1 overexpression on H1299 cells migration was explored using the scratch assay. ALDH7A1 increased the migration rate by 10% as compared to H1299/RFP (Figure 69A and B).

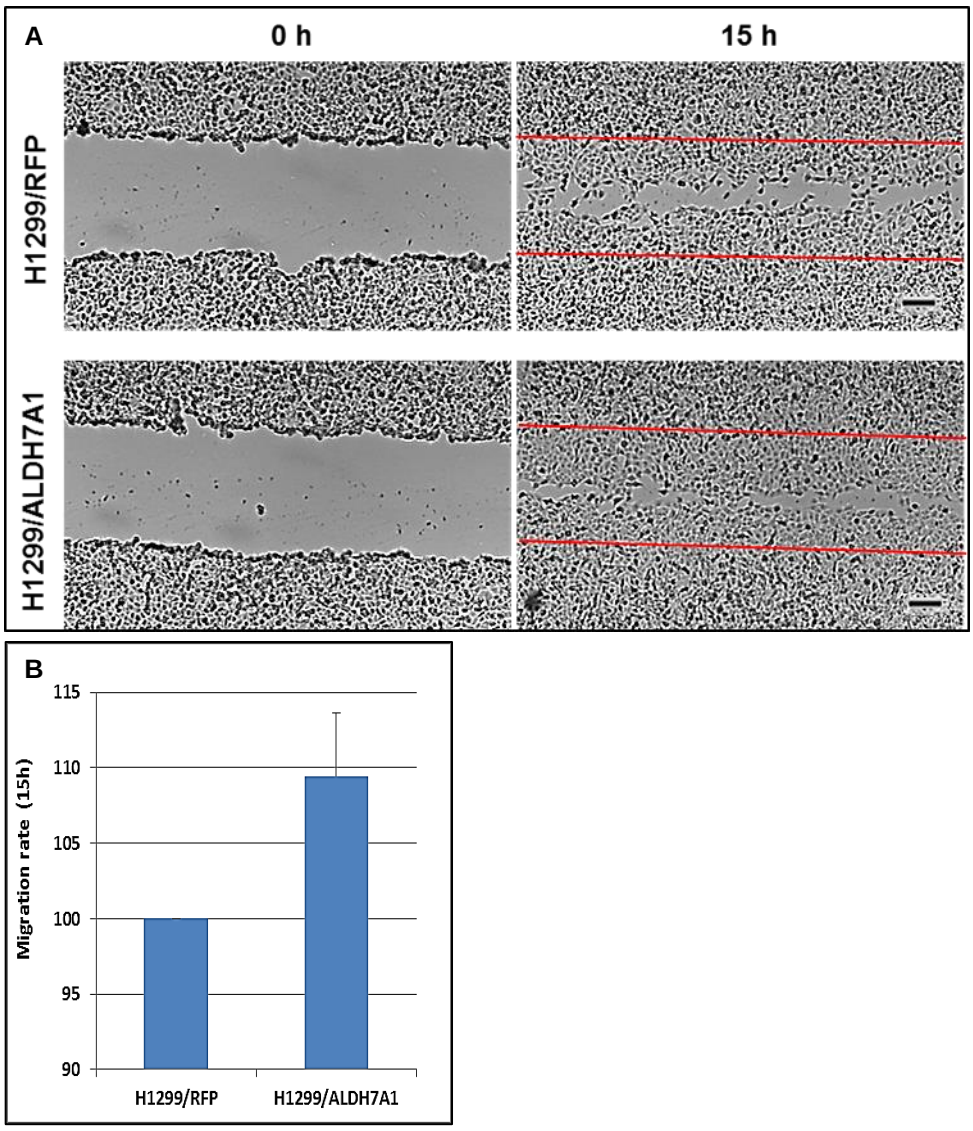

Figure 69 The effect of ALDH7A1 overexpression on H1299 cell migration using the scratch assay. Photos of H1299/RFP cells and H1299/ALDH7A1 cells at initial scratch (0h) and after 15h of migration (A), Migration rate after 15h of initial scratch (B). Values are the mean of 3 independent experiments and error bars are SD. P value: * $p<0.05$. Photos are at 10x lens and scale bar = 100 µm.

4.3.5 Effect of ALDH7A1 overexpression on reactive oxygen species (ROS) generation and DNA damage

The role of ALDH7A1 on ROS generation was explored using FACS. Figure 70A and B shows that ALDH7A1 overexpression resulted in significantly less ROS formation compared to H1299/RFP (curve shifted to left) with more than 90% reduction in ROS generation.

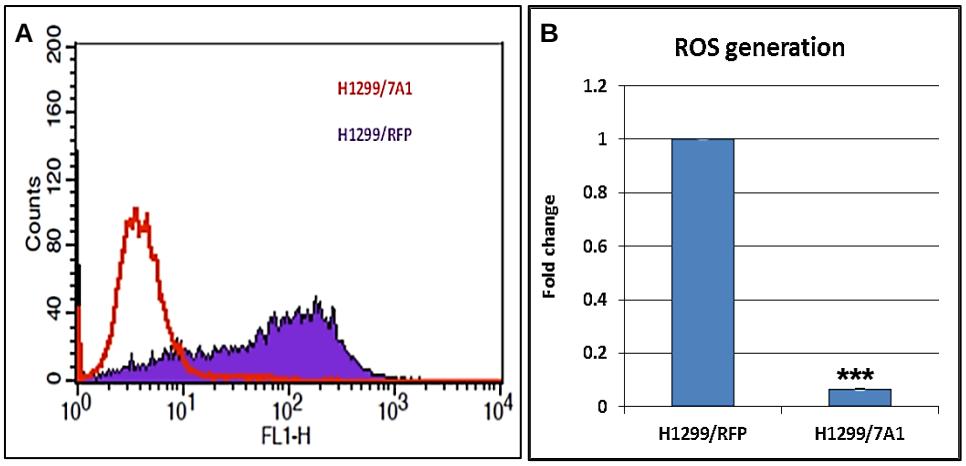

Figure 70 The antioxidant properties of ALDH7A1 in H1299 isogenic cell pair. ROS generation curves in H1299/RFP and H1299/ALDH7A1 cells using FACS (A), and fold change of ROS generation using the geometric means of area under the curve (B). Values are the mean of 3 independent experiments and error bars are SD. P value: *** p<0.001.

Direct effects of ROS include dsDNA breaks that might cause cell death (Li et al., 1994) and hence the expression of phosphorylated histone protein, H2AX was evaluated as a marker of dsDNA damage (KUO and YANG, 2008). Figure 71 shows that overexpression of ALDH7A1 has a protective role against the dsDNA breaks that might be caused by ROS. The expression level of phosphorylated H2AX was significantly downregulated in H1299/ALDH7A1 cells with approximately 70% reduction in its expression compared to H1299/RFP.

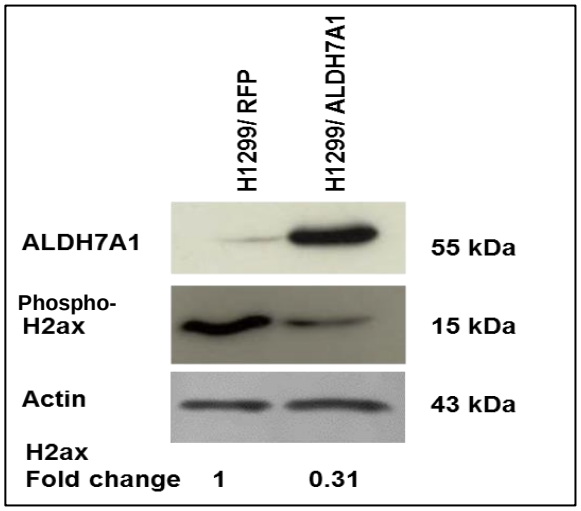

Figure 71 Evaluation of phosphorylated H2AX as a marker of dsDNA damage in H1299/RFP and H1299/ALDH7A1 cells.

4.3.6 Effect of ALDH7A1 overexpression on osmoregulation

The effect of ALDH7A1 overexpression on osmoregulation was evaluated as recent study showed that ALDH7A1 has potential protective role against osmotic stress (Brocker et al., 2010). The two H1299 cell lines were treated with NaCl or sucrose and the effect on cell survival was evaluated using MTT assay as previously described in section 4.2.9. However, both H1299/RFP and H1299/ALDH7A1 cells showed similar response to NaCl and sucrose treatment (Figure 72A and B, respectively).

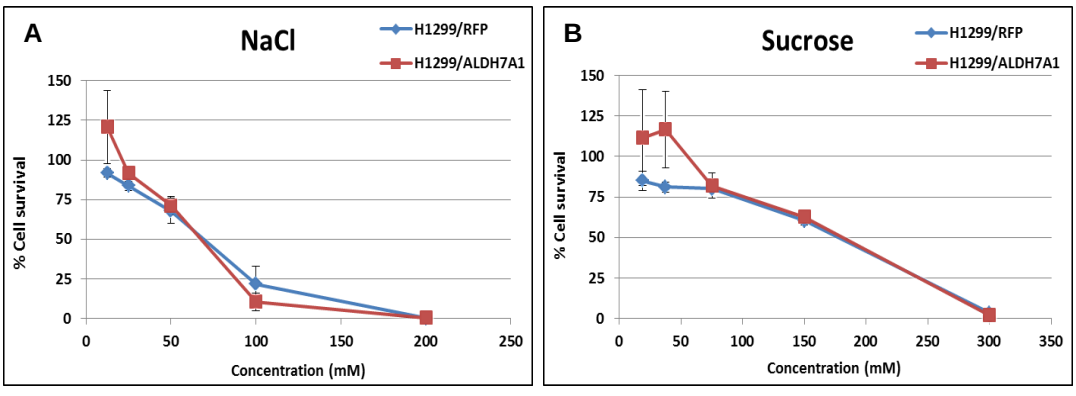

Figure 72 Cell survival of H1299 cell lines using the MTT assay after 24h of treatment with NaCl (A) or Sucrose (B). Values are the mean of 3 independent experiments and error bars are SD.

4.3.7 Effect of ALDH7A1 overexpression on spheroids formation and invasion

Both H1299/RFP and H1299/ALDH7A1 cell lines were able to form compact spheroids using a hanging drop technique (Figure 73). The diameter of formed spheroids after 48h of cell seeding was 320 µm and 380 µm for H1299/RFP and H1299/ALDH7A1, respectively.

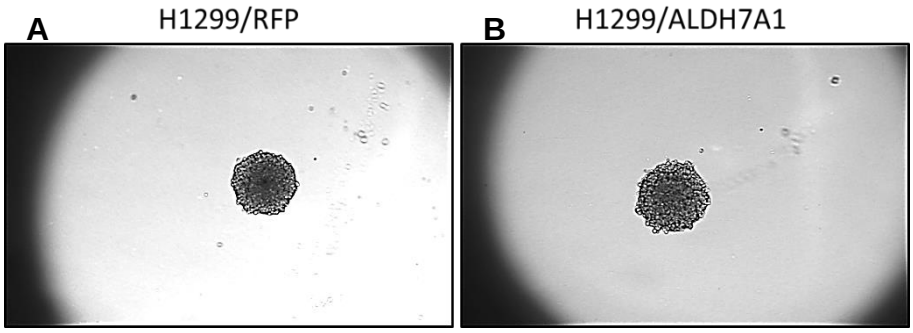

Figure 73 H1299 spheroids using the hanging drop technique after 48h of cell seeding. H1299/RFP spheroids (A), and H1299/ALDH7A1 spheroids (B). Images are at 10x objective lens.

Next, the ability of H1299/RFP and H1299/ALDH7A1 spheroids to invade in 3D ECM-like environment was evaluated. After 48h of embedding, both spheroids were able to invade through the collagen matrix (Figure 75). Figure 74 shows the analysis of spheroid invasion. The percentage of area before and after migration was calculated using Image J and the percentage of invasion after migration was calculated using the following equation:

% of invasion = B – A

A is the % area before migration and B is the % area after migration.

Figure 75 shows that the invasion rate was also directly correlated with the concentration of FBS in the growth medium.

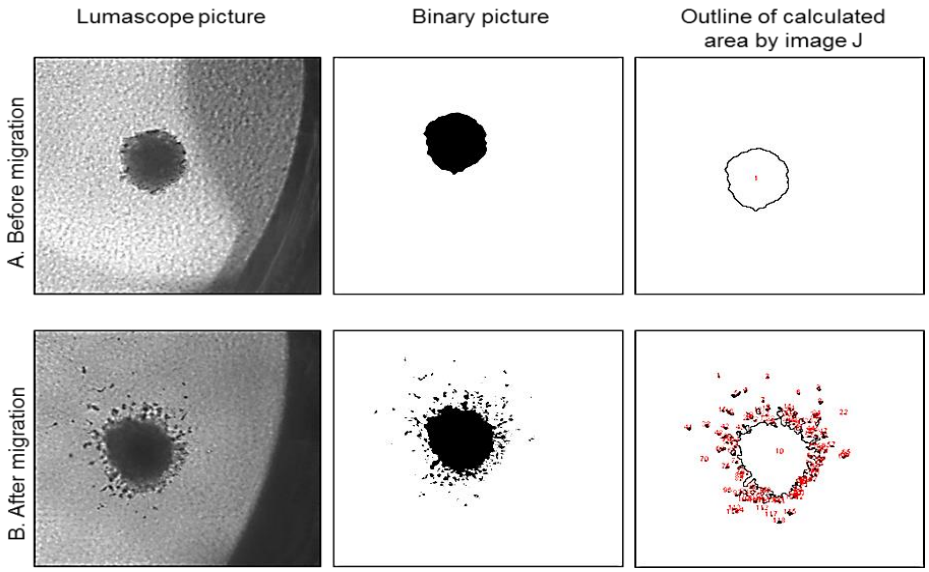

Figure 74 Analysis of spheroids invasion. Images were taken using Lumascope 500 microscope and changed into binary before calculating the total invasion area using Image J software. Images are at 10x objective lens.

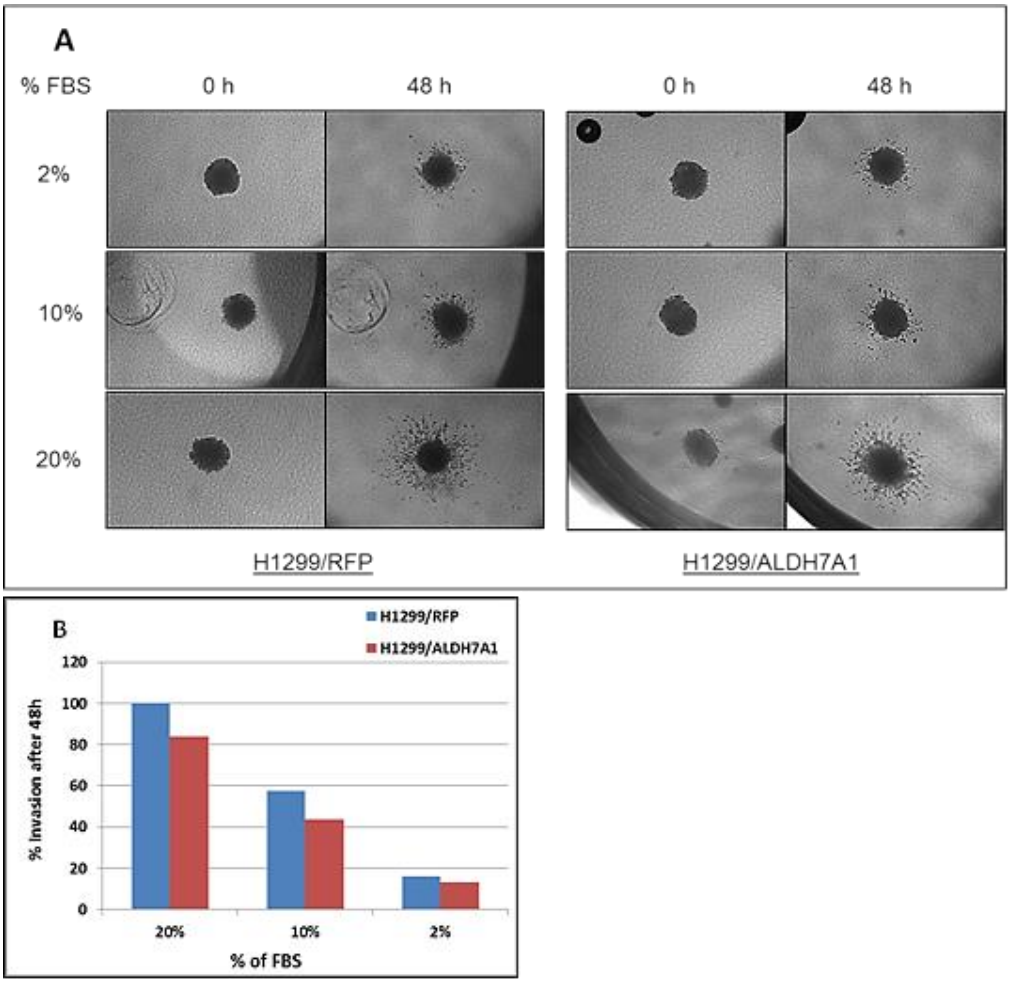

Figure 75 H1299 spheroids invasion after 48h of embedding in collagen matrix. Images of H1299/RFP and H1299/ALDH7A1 spheroids invasion at 10x objective lens (A) and analysis of invasion rate normalised to H1299/RFP spheroids with 20% FBS (B). Values are the mean of two independent experiments.

4.3.8 Effect of ALDH7A1 overexpression on anticancer drugs sensitivity

To examine the *in vitro* anti-proliferative activity of conventional anticancer drugs and molecularly-targeted drugs, the H1299 cell lines were exposed to various concentrations of these drugs for 96h. The MTT assay was employed to measure the antiproliferative effects. The dose-response curves obtained for 96h exposure for conventional anticancer drugs (Figure 76) and molecularly-targeted drugs (Figure 77) essentially reveal that ALDH7A1 overexpression had no effect on treatment outcomes.

4.3.9 H1299 cell survival upon treatment with non- specific ALDH inhibitors

The H1299 cell lines were also treated with disulfiram (ALDH inhibitor), salinomycin (stem cell-targeting agent) and parygline (non-specific monoxidase/ALDH inhibitor), however no difference in treatment outcome was observed (Figure 78).

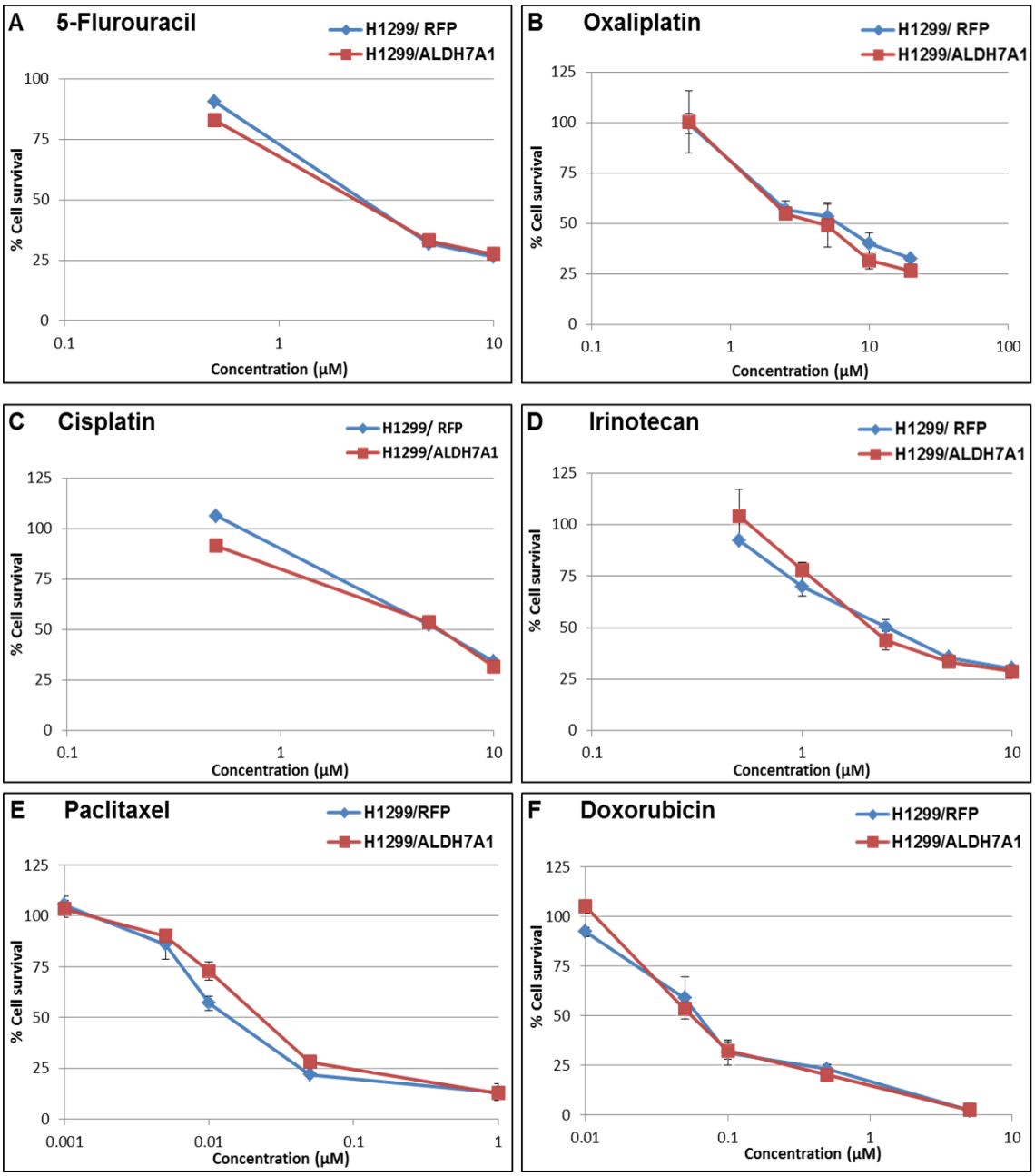

Figure 76 The cell survival of H1299 isogenic cell pair after 96h exposure to conventional anticancer drugs using the MTT assay. 5-FU (A), Oxaliplatin (B), Cisplatin (C), Irinotecan (D), Paclitaxel (E) and Doxorubicin (F). Values are the mean of 3 independent experiments with the exception to A and C and error bars are SD.

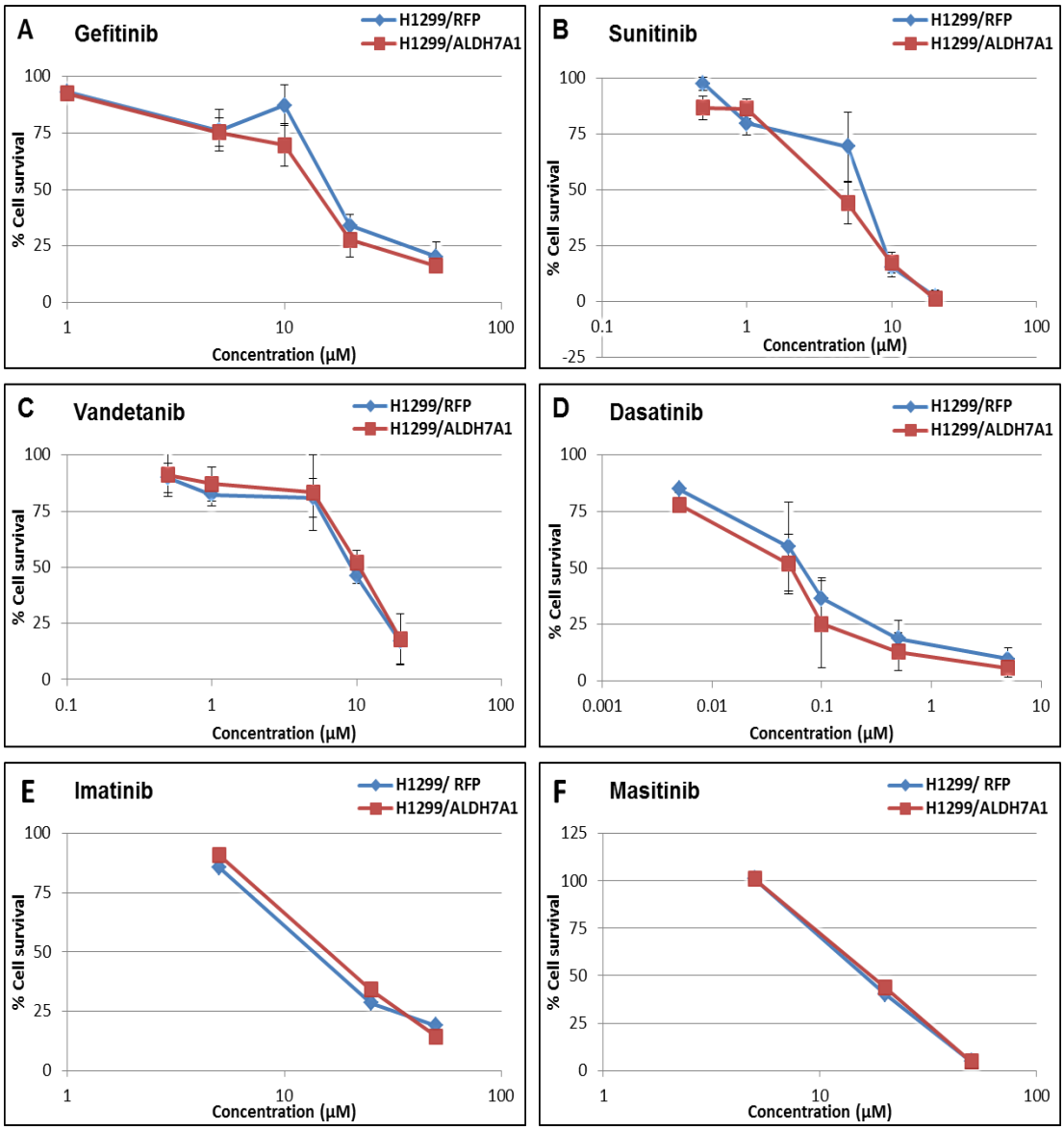

Figure 77 The cell survival of H1299 isogenic cell pair after 96h exposure to targeted anticancer drugs (TKIs) using the MTT assay. Gefitinib (A), Sunitinib (B), Vandetanib (C), Dasatinib (D), Imatinib (E) and Masitinib (F). Values are the mean of 3 independent experiments with the exception to E and F and error bars are SD.

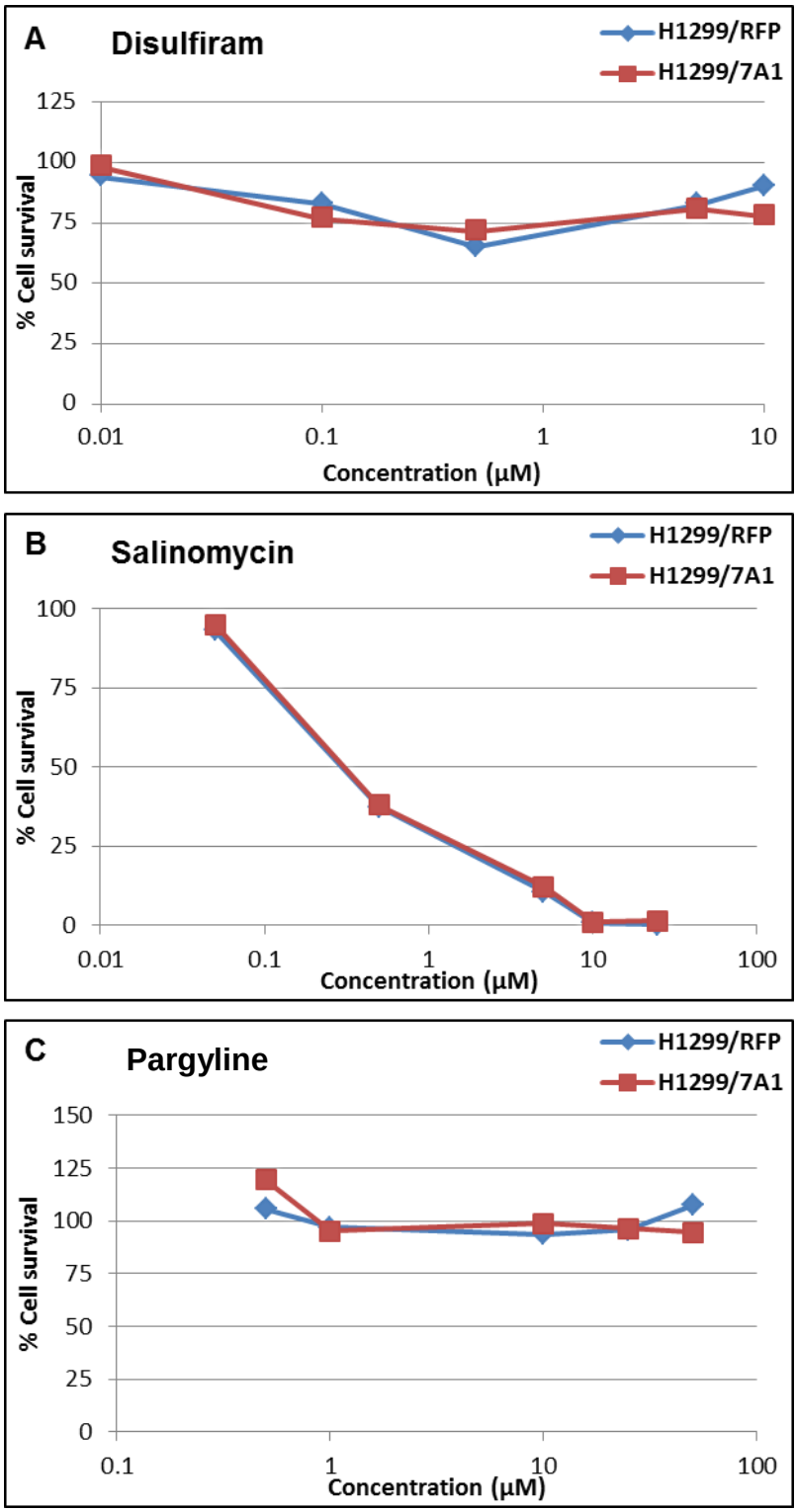

Figure 78 The cell survival of H1299 isogenic cell pair after 96h exposure to Disulfiram (A), Salinomycin (B) and Pargyline (C) using the MTT assay. Values represent 1 experiment.

4.3.10 Targeting ALDH7A1 activity using Maybridge compounds

4.3.10.1 H1299 cell survival using the MTT assay

The H1299 cell lines were treated with 9 compounds purchased from Maybrige/UK (Table 13, section 4.2.12). At first, the effect of these compounds on cell survival was evaluated after 96h of treatment using the MTT assay. H1299/ALDH7A1 cells were slightly more sensitive to HAN00316 compared with H1299/RFP cells (Figure 79A) and accordingly it was chosen for further investigation. KM06288 and DSHS00561 were used as controls (Figure 79C and D, respectively). Cells were treated with HAN00316, KM06288, DSHS00561 and DEAB for 24h. DEAB was chosen because a recent study showed that it acts as an irreversible inhibitor to ALDH7A1 activity (Luo et al., 2015). The 24h treatment was carried out in order to choose a non-toxic concentration for further evaluation of the effect of these compounds on ALDH7A1 activity (Figure 80).

.

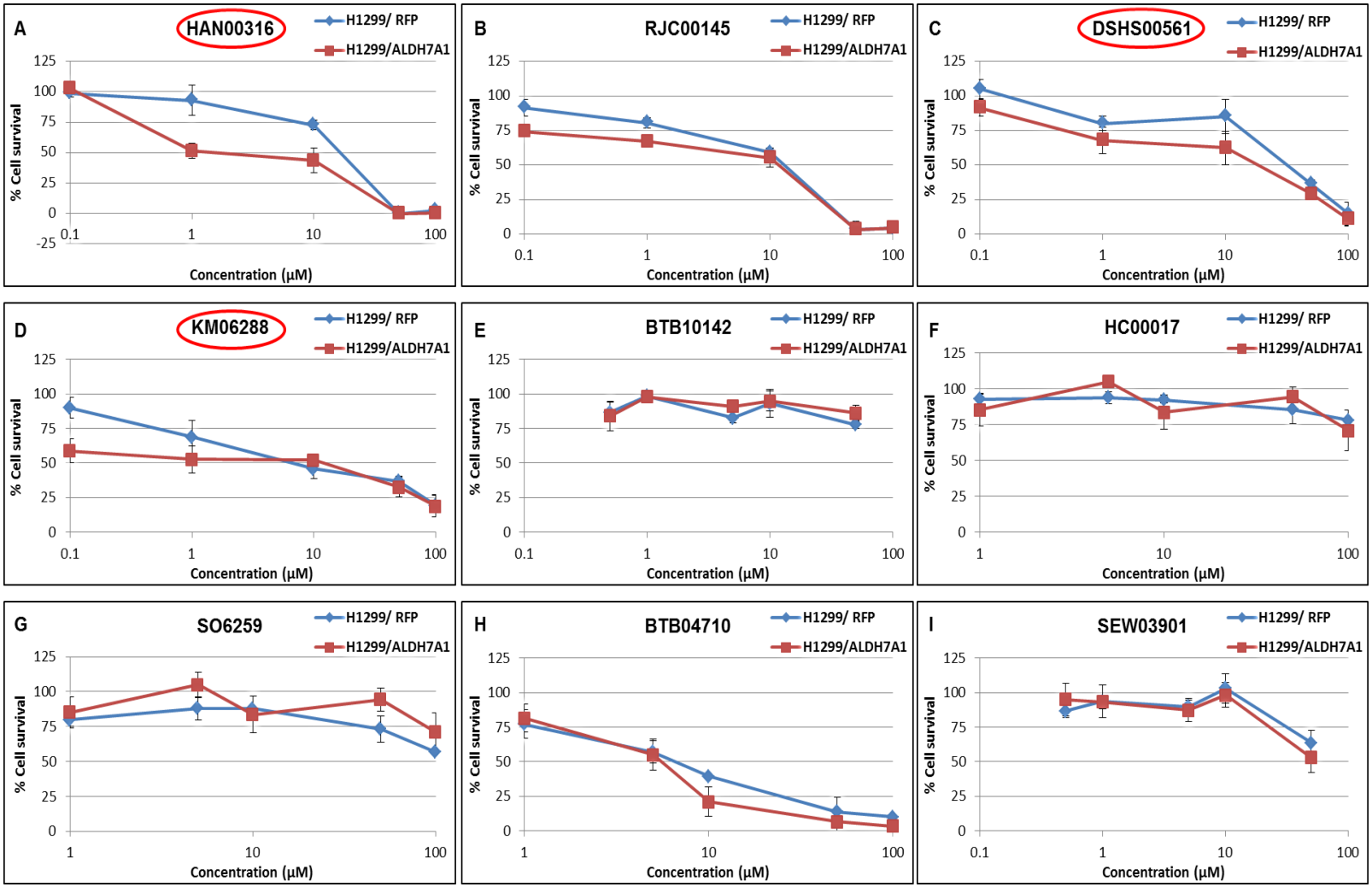

Figure 79 The cell survival of H1299 isogenic cell pair after 96h treatment with Maybridge compounds using the MTT assay. Values are the mean of 3 independent experiments and error bars are SD.

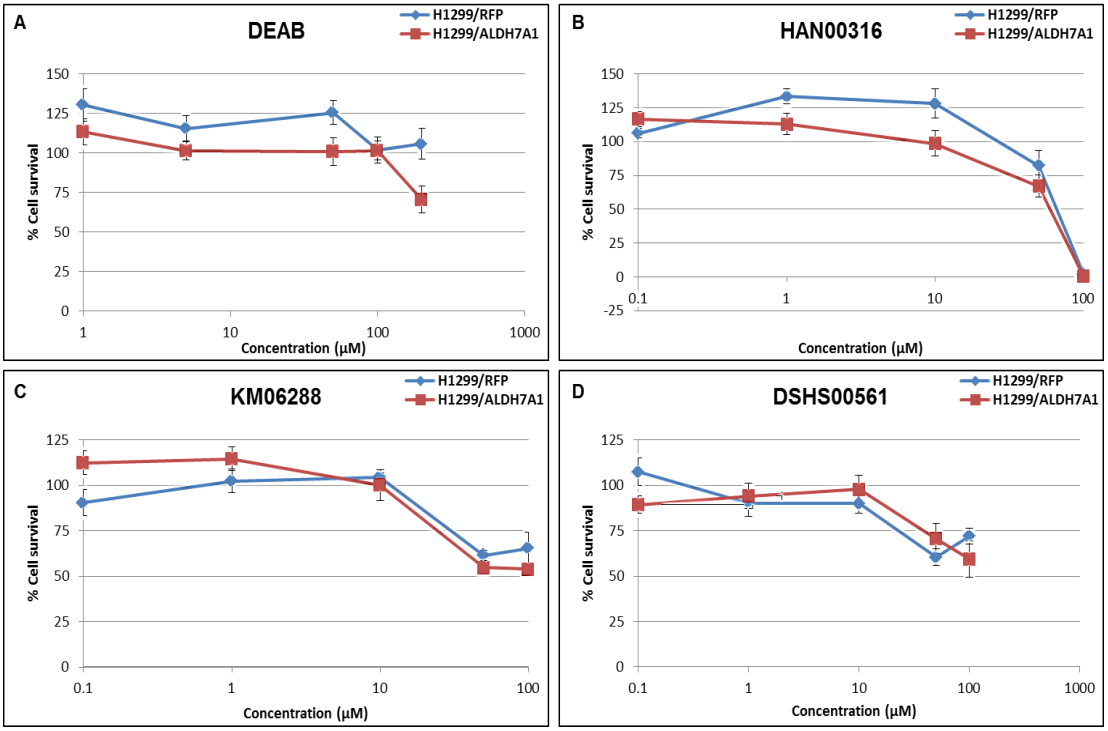

Figure 80 The cell survival of H1299 isogenic cell pair after 24h treatment with DEAB (A), HAN00316 (B), KM06288 (C) and DSHS00561 (D) using the MTT assay. Values are the mean of 3 independent experiments and error bars are SD.

4.3.10.2 The effect of Maybridge compounds on ROS generation

H1299/ALDH7A1 cells showed significantly less ROS generation compared to H1299/RFP cells (Figure 70, section 4.3.5). To evaluate the possibility of inhibiting ALDH7A1 activity, the H1299 cell lines were treated with HAN00316 (20 µM), KM06288 (20 µM), DSHS00561 (25 µM), DEAB (200 µM) or only DMSO (control, 0.1% v/v) for 24h before evaluation of ROS generation. Results obtained from H1299/RFP are illustrated in Figure 81A-E and showed that neither DEAB nor HAN00316 had any effect on ROS generation in comparison to DMSO control cells. In contrast, both DSHS00561 and KM06288 reduced the generation of ROS.

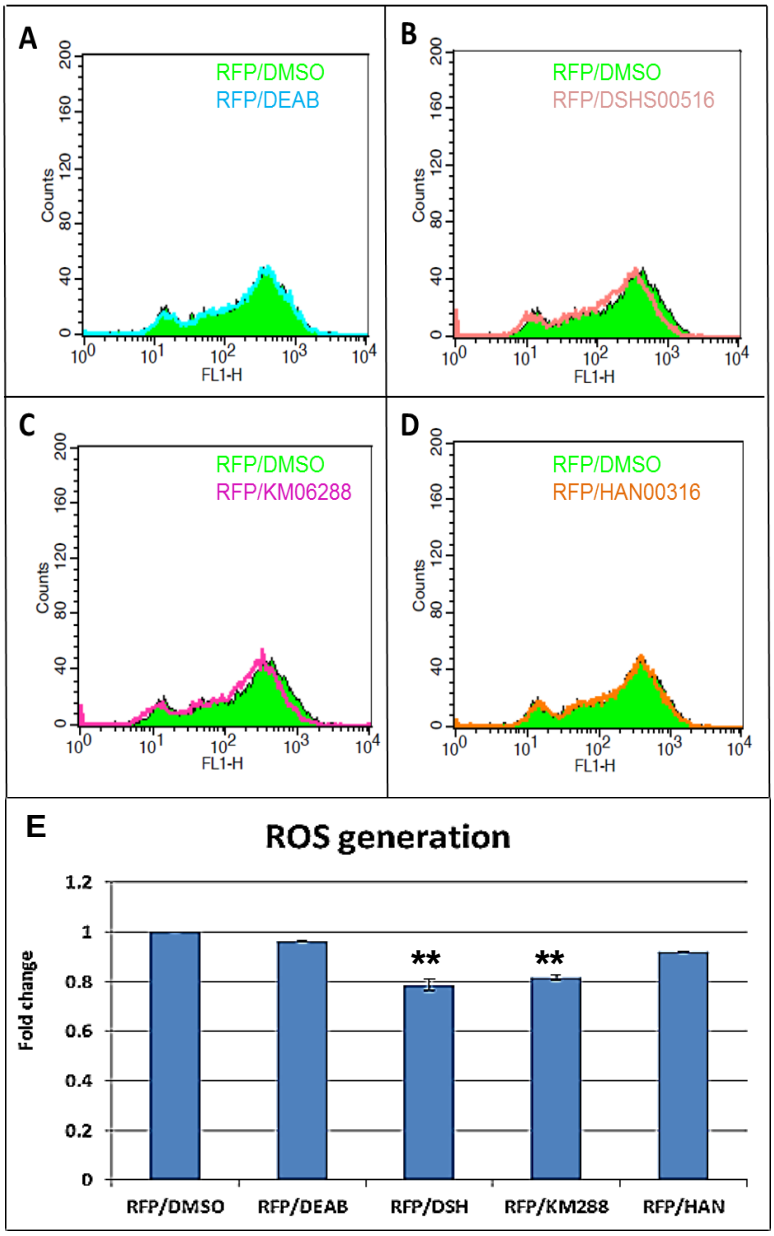

Figure 81 The effect of Maybridge compounds on ROS generation in H1299/RFP cells. ROS generation curves of DEAB (A), DSHS00561 (B). KM06288 (C) and HAN00316 (D), and fold change of ROS generation (E). Values are the mean of 3 independent experiments and error bars are SD. P values: ** $p<0.01$. For raw data, see Appendix XI.

Next, the effect of these compounds on ROS generation was evaluated in H1299/ALDH7A1 cells. Figure 82A shows that DEAB treatment resulted in more ROS in comparison to DMSO treated cells. HAN00316 was also found to increase the generation of ROS (Figure 82D). This was observed selectively in the 7A1 overexpressing cells suggesting that DEAB and

HAN00316 may promote ROS generation through inhibition of 7A1 antioxidant activity. The generation of ROS may also contribute to the cytotoxic effects of DEAB and HAN00316 observed by MTT (Figure 79, section 4.3.10.1). In contrast, neither DSHS00561 nor KM06288 showed any difference in ROS generation compared with DMSO treated cells (Figure 82B and C, respectively).

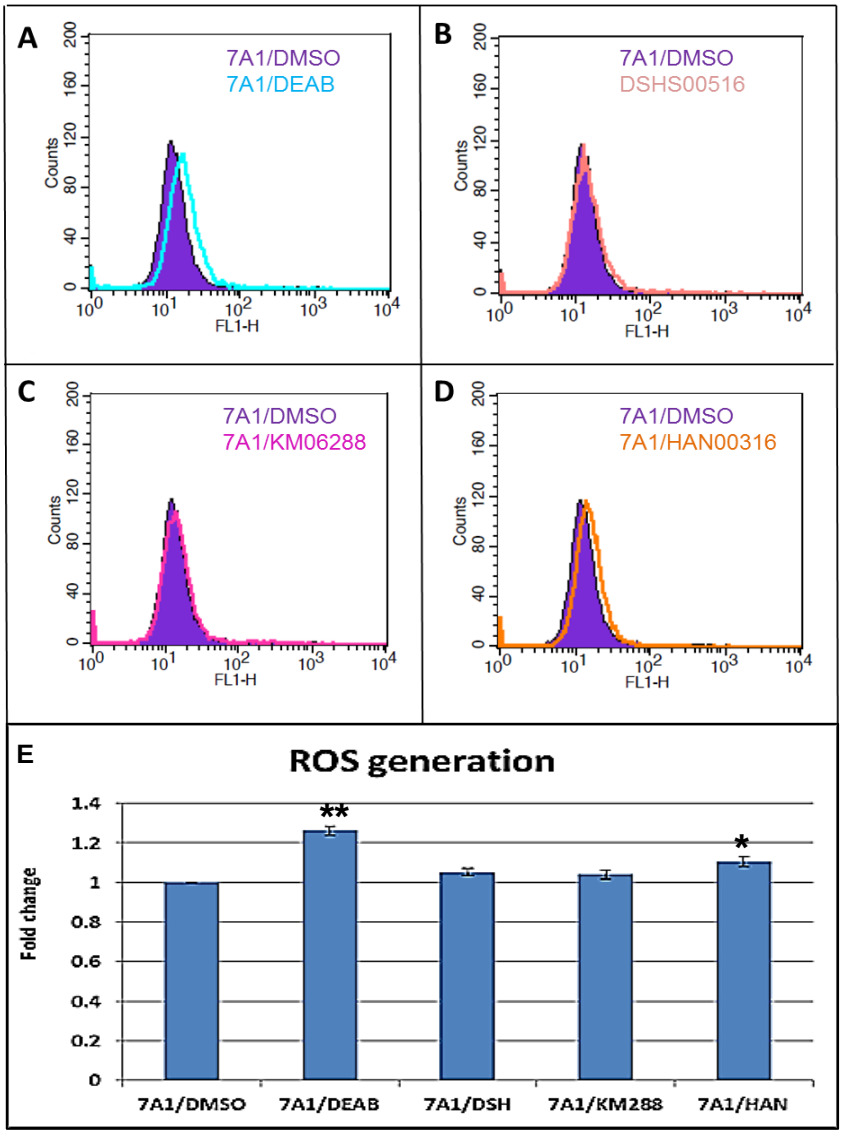

Figure 82 The effect of Maybridge compounds on ROS generation in H1299/ALDH7A1 cells. ROS generation curves of DEAB (A), DSHS00561 (B). KM06288 (C) and HAN00316 (D), and fold change of ROS generation (E). P values: * $p<0.05$, ** $p<0.01$.

4.3.10.3 The effect of Maybridge compounds on cell migration

H1299/ALDH7A1 cells showed more ability to migrate compared with H1299/RFP cells (Figure 69, section 4.3.4). Accordingly the effect of 24h treatment of HAN00316 (10 µM), KM06288 (10 µM), DSHS00561 (20 µM) or DEAB (100 µM) on cell migration was evaluated. These concentrations were chosen as they showed no toxic effect upon 24h treatment (Figure 80). Figure 83 shows the analysis of scratch assay results of H1299 cells. None of these compounds or DEAB inhibited the migration ability of H1299/RFP cells (Figure 84). HAN00316 appeared to suppress the migration of H1299/ALDH7A1 cells (Figure 85).

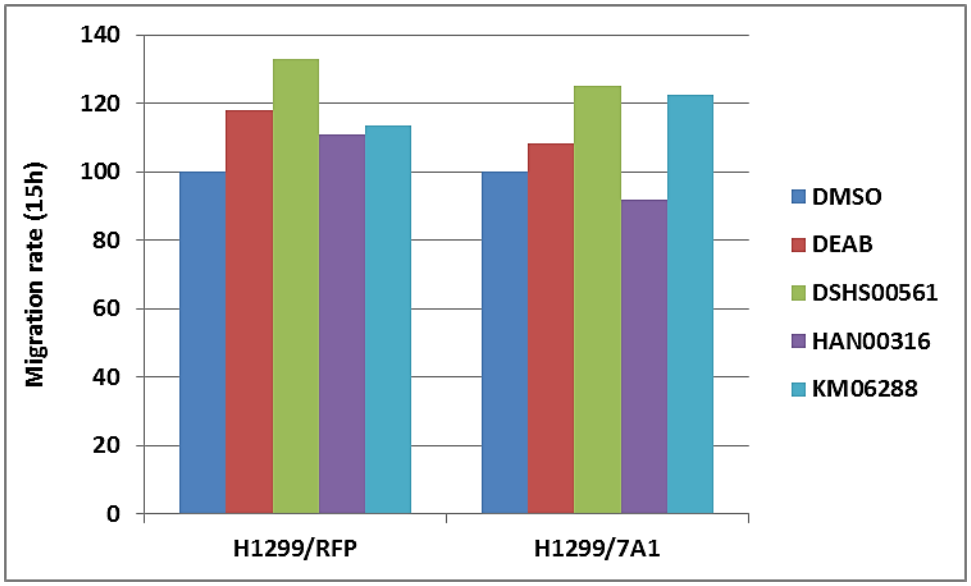

Figure 83 The migration rate of H1299/RFP and H1299/ALDH7A1 cells after treatment with DMSO, DEAB, DSHS00561, HAN00316 and KM06288 using the scratch assay. Values are the mean of 2 independent experiments.

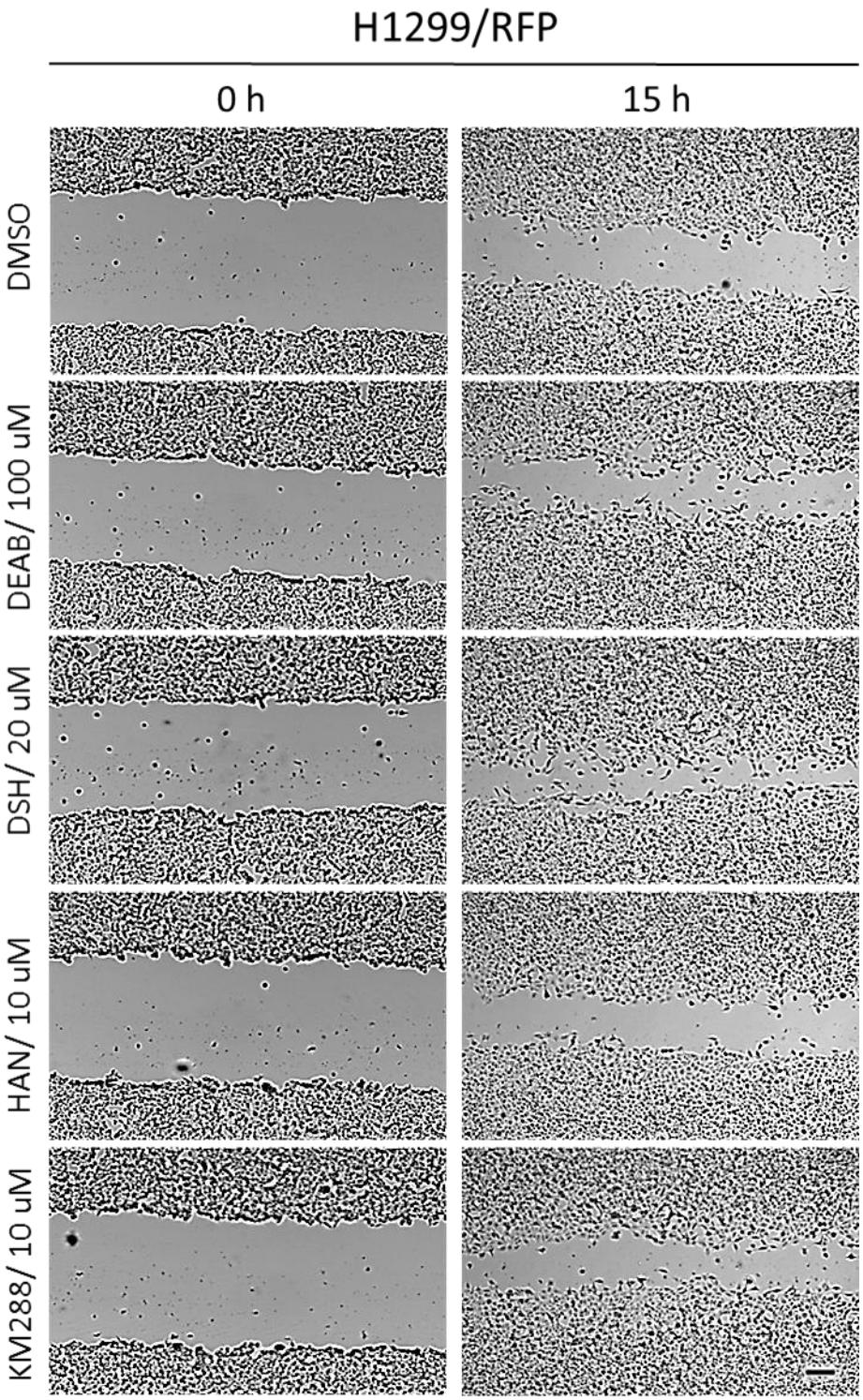

Figure 84 The cell migration of H1299/RFP cells using the scratch assay. The cells were treated with DMSO, DEAB, DSHS00561, HAN00316 and KM06288. Images are at 10x objective lens and scale bar = 100 µm.

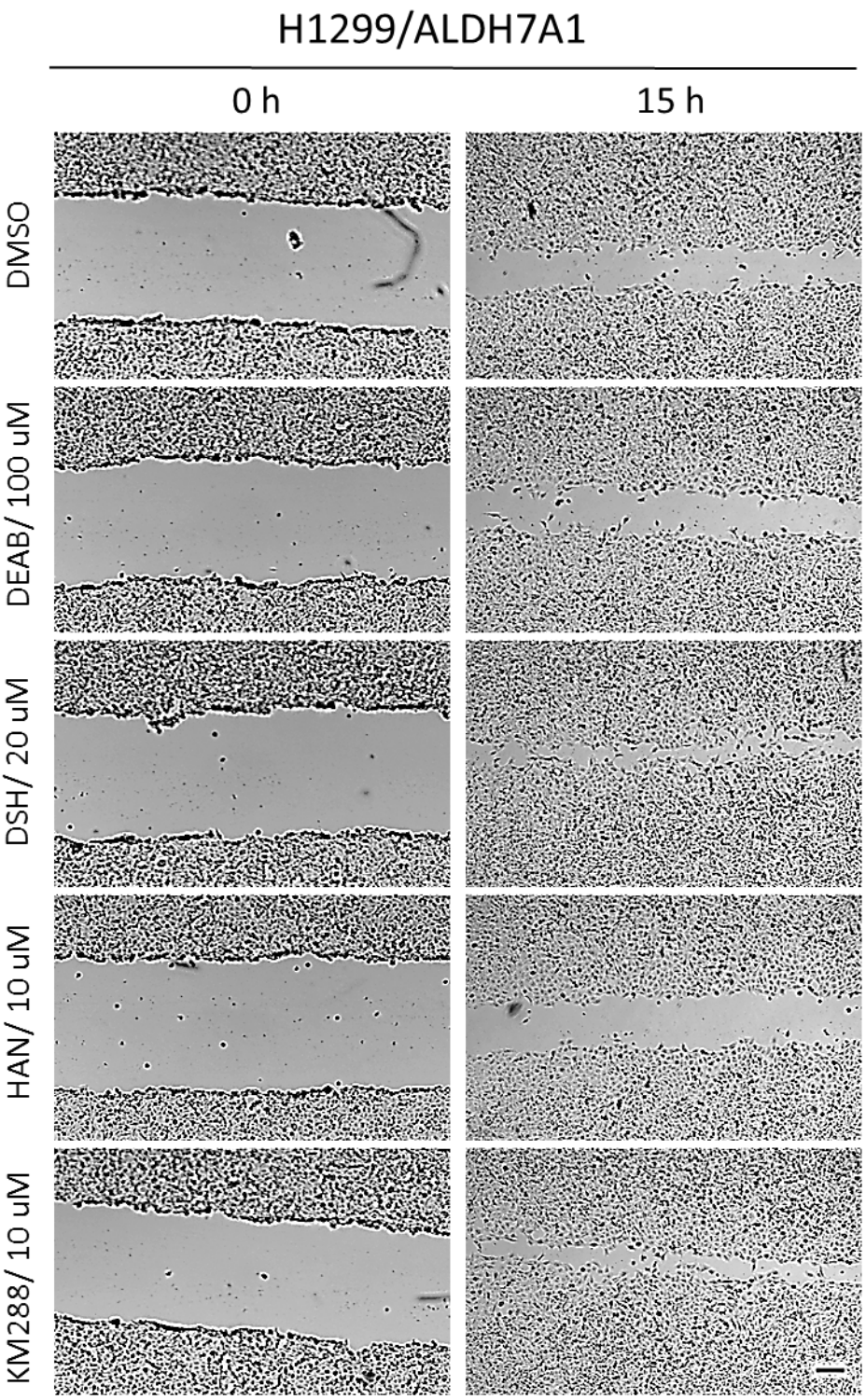

Figure 85 The cell migration of H1299/ALDH7A1 cells using the scratch assay. The cells were treated with DMSO, DEAB, DSHS00561, HAN00316 and KM06288. Images are at 10x objective lens and scale bar = 100 µm.

4.4 Discussion

The main focus of this Chapter was on the effects of ALDH7A1 overexpression. The role of ALDH7A1 enzyme was investigated using an isogenic system of the H1299 lung cancer cell line. H1299 is a NSCLC cell line that was considered as a negative model for ALDH expression (Moreb et al., 2012). Subsequent to this study, Moreb and co-workers transfected the H1299 cell line with lentiviral vectors containing the full cDNA for ALDH7A1 or red fluorescent protein (RFP). The isogenic cell line pair was made available for this study, enabling a more in-depth investigation to be carried out with focus on ALDH7A1.

First, the expression of ALDHs in the H1299 cell lines was evaluated and this showed very low level of expression in H1299/RFP cells, confirming that they are low in ALDH expression (Moreb et al., 2012). In contrast, significant upregulation of ALDH7A1 was found in H1299/ALDH7A1 cells at both the gene (85-fold) and protein (9-fold) levels in comparison to H1299/RFP cells. Gene analysis also showed upregulation of ALDH1A3 (4-fold) and ALDH2 (1.5-fold) in H1299/ALDH7A1 cells. However, these isoform were not detected at the protein level. Accordingly, a reasonable assumption to make is that any difference between these cell lines is due to direct or indirect effect of differential expression of ALDH7A1 enzyme.

The activity of ALDH in H1299 cells was measured using the ALDEFLUOR assay (Chapter 1, Introduction, section 1.4.5.1.1). This assay has been reported to be specific to ALDH1A1 (Marcato et al., 2011a), however, recent information suggests this assay can detect other ALDH isoforms, which have

implication for SC isolation (Levi et al., 2009, Marcato et al., 2011b). Accordingly, the ALDEFLUOR assay was employed to evaluate whether it can be used to measure the activity of ALDH7A1 in this study. It was found that H1299/ALDH7A1 cells had 17-fold increase in ALDH activity compared to H1299/RFP cells. This suggests that ALDEFLUOR assay is not solely specific for ALDH1A1 and supports the findings of other studies (Levi et al., 2009, Marcato et al., 2011b, Moreb et al., 2012). Levi *et al.* showed that ALDH1A1 deficiency did not reduce ALDEFLUOR activity of HSC and other ALDH isoforms (ALDH2, ALDH3A1 and ALDH9A1) have been detected and suggested to contribute to ALDEFLUOR activity (Levi et al., 2009). Knockdown studies in breast cancer showed that only suppression of ALDH1A3 expression resulted in the reduction of ALDH activity in ALDEFLUOR positive cells (Marcato et al., 2011b). Moreb *et al.* also showed that the enzymatic activity of ALDH1A2 and ALDH2 was detected by ALDEFLUOR assay (Moreb et al., 2012). The detection of higher ALDEFLUOR activity in H1299/ALDH7A1 cells combined with 9-fold higher ALDH7A1 protein levels suggests that ALDH7A1 might contribute to the ALDEFLUOR activity, and thus any difference between the responses of H1299 cells pair toward the functional assays explored in this study can be attributed to ALDH7A1.

The role of ALDH7A1 in mediating cell proliferation was investigated. It was found that H1299/ALDH7A1 cells proliferate at higher rate compared to H1299/RFP cells. This supports the findings of Chapter 3 where knockdown studies showed reduction in DLD-1 live cell number and is in agreement with

the role of ALDH7A1 in prostate cancer where ALDH7A1 knockdown led to significantly decreased cell clonogenicity and proliferation (van den Hoogen et al., 2011). The results from microarray analysis performed by Moreb's group on the cells with knockdown of ALDH1A1 and ALDH3A1 showed significant modulation in the expression of genes that are related to cell proliferation and cell cycle pathways (e.g. PPARG, CCNG1, BCAT1) (Moreb et al., 2008). In this regard, it is possible that the overexpression of ALDH7A1 affect similar genes that result in increased proliferation. Our results are in contrast to Moreb's group findings (Moreb et al, 2013), however this might be caused by difference in the cell density used in this study or difference in the day of evaluation (Time dependent).

The role of ALDH7A1 in mediating cell migration was evaluated and it was found that H1299/ALDH7A1 cells migrate at significantly higher rate compared to H1299/RFP cells (P value < 0.05). This supports the reported role of ALDH7A1 in mediating prostate cancer metastasis (van den Hoogen et al., 2011). However, further studies are needed to fully understand the mechanism(s) by which ALDH7A1 might promote cell migration. This might include evaluation of a number of genes/factors involved in migration, invasion and metastasis such transcription factors (snail, snail2, and twist) and osteopontin, an ECM molecule involved in metastasis which were found to be affected upon ALDH7A1 knockdown in PC-3M-Pro4lucA6, a prostate cancer cell line (van den Hoogen et al., 2011).

The potential role of ALDH7A1 in reducing ROS was evaluated and it was found that H1299/ALDH7A1 cells had significantly less ROS production

compared with H1299/RFP cells (> 90% reduction), which supports the antioxidant role previously described for this enzyme (Brocker et al., 2011). Further evidence for the potential involvement of ALDH7A1 in reducing ROS levels was described in Chapter 3 where knockdown of ALDH7A1 expression in DLD-1 cells resulted in more ROS generation. Direct effects of ROS include dsDNA breaks which if left unrepaired can lead to cell death (Li et al., 1994). Accordingly, the expression of phosphorylated H2AX histone protein as a marker of dsDNA damage (KUO and YANG, 2008) was measured and it was found that H1299/ALDH7A1 cells had significantly less phosphorylated H2AX expression, indicating less DNA damage, which is likely to be due to the protective properties of ALDH7A1.

Previous studies showed that ALDH7A1 also has a protective role against osmotic stress caused by sodium chloride (NaCl) or sucrose (Brocker et al., 2010). However, this role has not been investigated in cancer. In this study it was found that upon NaCl or sucrose treatment no differential in cell survival was observed between H1299/ALDH7A1 and H1299/RFP cell lines. However, this might be caused by the presence of other defence mechanisms in cancer cells that protect them against osmotic stress. This might include the activation of MAPKs, ERK1/2 and JNK in response to hyperosmolarity which for example has been shown to be mediated by HB-EGFdependent EGFR activation (Fischer et al., 2004).

Cancer cells possess varying capacities for spheroid formation and this correlates positively with tumourigenicity, invasive ability and drug resistance (Kelm et al., 2003, Ahmed et al., 2007). Thus, deciphering the mechanisms

that enable spheroid formation, with the goal of inhibiting this process, may improve therapeutic efficacy (Sodek et al., 2009). Accordingly, the ability of the H1299 cell line pair to form spheroids was evaluated in an attempt to understand whether ALDH7A1 is involved in spheroid formation. However, both cell types were able to generate similar sized compact spheroids after 48h of seeding using the hanging drop technique (Del Duca et al., 2004). The ability of spheroids generated from both cell lines to invade in 3D through ECM- like environment such as collagen matrix was explored and both spheroids were able to invade through the matrix with similar efficiency. This suggests that ALDH7A1 is not a critical protein for spheroids formation or invasion, at least for H1299 lung cancer cells.

The role of ALDH in mediating drug resistance for cytotoxic and targeted therapeutics has been described (Chapter 1, Introduction, section 1.4.4). However, only one recent study has revealed high expression of ALDH7A1 in a zoledronic acid-resistant prostate cancer cell line (DU145) via proteomics analysis (Milone et al., 2015). To further evaluate if ALDH7A1 has implications on drug sensitivity, a wide panel of conventional cytotoxic drugs and tyrosine kinase inhibitors was evaluated using the MTT assay (Results, section 4.3.8). However, both H1299 cell lines showed similar sensitivity upon drug exposure, suggesting that ALDH7A1 is not involved in mediating resistance to these drugs.

Because of the functional involvement of ALDH in CSCs and their correlation with poor clinical outcomes as well as drug resistance, the development of selective ALDH inhibitors is highly needed (Honoki et al., 2010). These

inhibitors can act as tools to probe the various roles of ALDHs in cancer and/or as leads in drug development (Pors and Moreb, 2014). However, selective targeting seems to be difficult for two main reasons. First, ALDH enzymes are characterised by being widely distributed in normal tissue, with the highest concentrations most often occurring in the liver and/or kidney. In addition, ALDHs have been shown to have broad substrate specificity although some more selective small molecules have been identified, which suggests that selectivity can be achieved (Pors and Moreb, 2014). Currently, the pharmacological inhibitors have been developed for only four ALDH isozymes: ALDH1A1, ALDH1A2, ALDH2 and ALDH3A1 that have been studied for their potential as pharmacologically relevant therapeutic targets (Koppaka et al., 2012).

DEAB is a well-known, but poorly characterized, ALDH inhibitor that has been described as a reversible competitive inhibitor of ALDH1 (competitive with the aldehyde substrate) (Russo et al., 1995) and it is employed as an allegedly ALDH1A1-specific inhibitor in the widely used ALDEFLUOR assay (Balber, 2011). However, more recent studies suggest that DEAB may be a broad inhibitor of ALDHs including 1A2 and 2 isoforms (Moreb et al., 2012). The first crystal structure of ALDH complexed with DEAB has only been described recently (Luo et al., 2015). Interestingly, Luo *et al.* showed that DEAB irreversibly inactivated ALDH7A1 via formation of a stable, covalent acyl-enzyme species (Luo et al., 2015). The evaluation of cell survival of H1299 cell lines upon treatment with DEAB showed that 24h exposure

resulted in more cell kill in H1299/ALDH7A1 cells than in H1299/RFP cells, suggesting that ALDH7A1 might be inhibited by DEAB.

The cell survival upon treatment by other non-specific inhibitors was also investigated The monoamine oxidase inhibitor pargyline is activated by CYP2E1 to yield a highly reactive propiolaldehyde that irreversibly inactivates ALDH2 (DeMaster and Nagasawa, 1978). Both cell lines were not sensitive to pargyline treatment. The anti-proliferative effect of salinomycin was also evaluated. Salinomycin has been shown to kill breast cancer stem cells in mice at least 100 times more effectively than the anti-cancer drug paclitaxel (Gupta et al., 2009). In addition, studies have shown that salinomycin is able to effectively eliminate CSCs and to induce partial clinical regression of heavily pretreated and therapy-resistant cancers (Naujokat and Steinhart, 2012). However, both H1299 cell lines showed similar sensitivity toward salinomycin treatment, indicating that high ALDH7A1 expression is not involved in mediating sensitivity to this compound.

Recent focused studies on the discovery of chemical modulators of ALDH resulted in broad-spectrum and specific inhibitors with *in vitro* activity (Khanna et al., 2011). The encouraging results were made feasible using computational modelling and *in vitro* screening assays as recently reviewed (Pors and Moreb, 2014). In this study, nine compounds identified from computational modelling to have high affinity for ALDH7A1 binding (Table 13, Materials and Methods, section 4.2.12) were purchased from Maybridge/UK and evaluated. First, the cell survival upon 96h treatment was evaluated using the MTT assay. H1299/ALDH7A1 cells were more sensitive toward

treatment with three compounds, HAN00316, KM06288 and DSHS00561 and thus these were considered for further evaluation. As a recent study showed DEAB to act as irreversible inhibitor of ALDH7A1 (Luo et al., 2015), it was also included in these assays. Cells were treated with HAN00316, KM06288, DSHS00561 and DEAB for 24h to choose non-toxic concentrations for the experiments to be carried out. Subsequently, the effect of these compounds on ROS generation was explored. It was found that both DEAB and HAN00316 resulted in significant more ROS generation in H1299/ALDH7A1 treated cells, suggesting that both compounds may have inhibited ALDH7A1 functional activity and hence accumulation of ROS.

Next the effect of HAN00316, KM06288, DSHS00561 and DEAB on cell migration was evaluated and it was found that only HAN00316 resulted in slight suppression of H1299/ALDH7A1 cell migration suggesting that its effect on ALDH7A1 activity might have contributed to this observation.

In summary, an isogenic system of ALDH7A1 expression was used to explore the biological roles of ALDH7A1 and study the possibility of targeting its activity. ALDH7A1 overexpression was found to enhance cell proliferation and migration. In addition, ALDH7A1 was found to reduce ROS levels and phosphorylated H2AX levels, suggesting a potential role in protecting cells from oxidative stress and DNA damage. The results with ALDH7A1 inhibitors suggest that DEAB and HAN00316 could be good starting points for medicinal chemistry to be performed, leading to more potent and selective ALDH7A1 inhibitors to be developed and used as tool compounds to explore

the importance of ALDH7A1 in cancer and other pathological diseases where this enzyme may be playing a key role.

The main findings of this Chapter were:

- ALDH7A1 overexpression increased H1299 cell proliferation.
- ALDH7A1 overexpression increased H1299 cell migration.
- ALDH7A1 overexpression significantly reduced the level of ROS and dsDNA damage.
- HAN00316 compound inhibited the activity of ALDH7A1 in reducing ROS level.

Chapter 5: General discussion, conclusion and future work

Colorectal cancer (CRC) is the third most common form of cancer in the UK and is one of the leading causes of cancer related deaths worldwide (Jemal et al., 2011). The overall survival rate of CRC patients has not improved dramatically over the last decade despite substantial progress in our understanding of the molecular mechanisms of CRC pathogenesis as well as the improvement in the current systemic chemotherapy and novel targeted drugs for CRC treatment (American Cancer Society, 2014).

One of the major challenges facing the clinicians is the lack of diagnostic kit to predict patients at risk of CRC relapsing and recurrence. Current screening tests including high-sensitivity faecal occult blood tests (FOBT), sigmoidoscopy or colonoscopy are not useful for predicting recurrence of aggressive CRC (Lieberman, 2010, Jorgensen and Knudtson, 2015). Additionally, characterisation of CRC based on molecular classification including microsatellite instability (MSI), CpG island methylator phenotype (CIMP), chromosomal instability (CIN), BRAF and KRAS mutations is at present not considered sufficiently accurate for prediction of CRC recurrence due to the complex heterogeneous nature of CRC (Winder and Lenz, 2010).

It is well established that solid tumours contain hypoxic regions that have been correlated with an aggressive cancer cell phenotype, and resistance to radiotherapy and chemotherapy (Semenza, 2012). Accumulative evidence supports important roles of selected ALDH isoforms in contributing to the aggressiveness of colorectal cancer (Chapter 2, Introduction, section 2.1). Given the importance of hypoxia on tumourigenesis and resistance, information about how selective ALDHs adapt to hypoxia in the tumour

microenvironment could have a profound impact on the understanding of drug resistance and CRC aggressiveness, which might help to predict cancer recurrence. Accordingly, the aim of this project was to explore if ALDH expression was affected by the presence of hypoxia in the tumour microenvironment.

To address this question, four CRC cell lines (HT29, DLD-1, HCT116 and SW480) were exposed to hypoxia (0.1% O_2) and its effect on 7 ALDH isoforms (1A1, 1A2, 1A3, 1B1, 2, 3A1 and 7A1) was evaluated. Notably, increased expression of ALDH7A1 was observed in HT29 and DLD-1 cells exposed to hypoxia. Spheroids generated from HT29 and DLD-1 cell lines showed high ALDH7A1 expression in the peripheral region that also increased toward the hypoxic region at both the mRNA and protein levels. Immunohistochemistry experiments of paraffin-embedded spheroids showed clear staining of ALDH7A1 in hypoxic regions, which was confirmed using intrinsic and extrinsic hypoxic markers, CAIX and pimonidazole, respectively (Results discussed in Chapter 2). Although ALDH7A1 was not induced in HCT116 and SW480 under the hypoxic conditions, it is possible that longer exposure to hypoxia such as 72h or 96h may show elevation in ALDH7A1 expression. It may also be possible that modulation of ALDH7A1 expression is cell-specific and hence further analysis of CRC molecular phenotype is required. Further supporting ALDH7A1 as an important enzyme in CRC was the observation of its abundant expression in 5 CRC xenografts. Unfortunately, due to technical issues using CAIX, the assessment of ALDH7A1 correlation and distribution with hypoxic regions was not possible.

As a consequence, future studies need to determine the inclusion of other intrinsic hypoxic markers such GLUT-1 (Airley et al., 2003) for co-localisation of ALDH7A1 with hypoxic regions of xenograft tumours.

In collaboration with Prof Federica Di Nicoleantonio (Candiolo Cancer Institute, Turin, Italy), investigation of ALDH expression in a panel of 150 CRC cell lines was carried out using Affymetrix Microarray (Medico et al., 2015) (Figure 86A). Log2 expression <10 is likely not to be translated into protein expression (personal communication, Prof Di Nicoleantonio). This revealed a wide range of expression of ALDH1 isoforms apart from 1A2, which is considered not expressed. This is in agreement with the cell lines used in this thesis and the study by Kim *et al.,* which suggested ALDH1A2 to act as TSG that is epigenetically silenced in prostate cancer (Kim et al., 2005). The results obtained from Prof Di Nicoleantonio's microarray data (Medico et al., 2015) (Figure 86B) is consistent with the ALDH gene expression profile discussed in Chapter 2, section 2.3.1.1.1. High expression of both ALDH1B1 and ALDH7A1 in most of the 150 cell lines was observed (Figure 86A and C). Very little is known regarding the regulation of ALDH1B1, but its high and reliable expression in clinical samples could be used as a potential biomarker for diagnosing the presence of CRC (Chen et al., 2011), while hypoxia-induced ALDH7A1 might be used to diagnose aggressive forms of CRC.

A

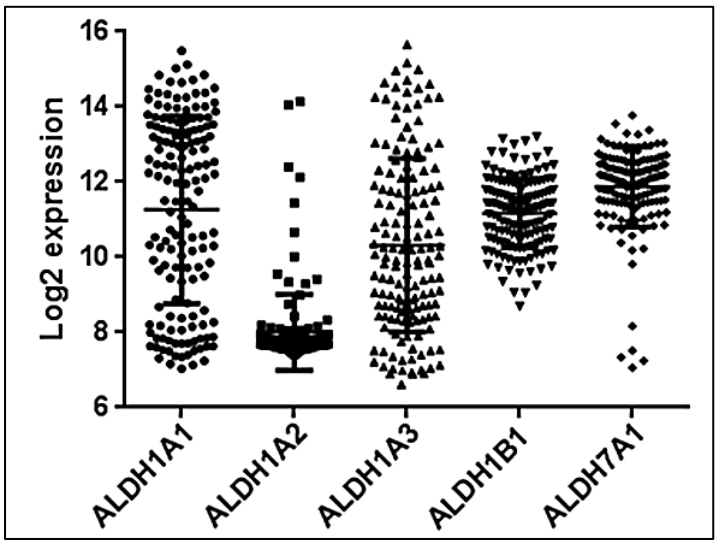

B

Cell line	1A1	1A2	1A3	1B1	7A1
DLD-1	7.57	7.66	9.91	11.43	12.33
HCT116	8.16	7.67	13.05	11.21	12.96
HT29	13.42	7.57	10.63	10.18	11.29
SW480	7.04	7.58	13.98	9.58	12.62

C

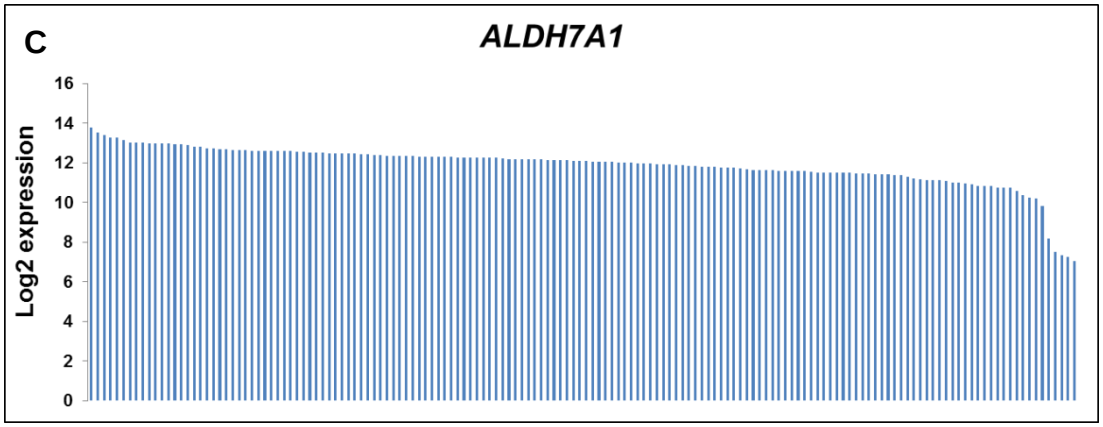

Figure 86 ALDH expression in a panel of 150 CRC cell lines. Data mining of ALDH1A1, 1A2, 1A3, 1B1 and 7A1 gene expression using Log 2 expression (A). Log2 expression of ALDH1A1, 1A2, 1A3, 1B1 and 7A1 gene in DLD-1, HCT116, HT29 and SW480 cell lines (B). Log2 expression of ALDH7A1 gene in 150 CRC cell lines (C). Adopted from Medico *et al*. 2015.

Human ALDH7A1 plays an important role in the protection of cells against hyperosmotic stress (Brocker et al., 2010). In addition, it was found to possess antioxidant activity preserving cells from oxidative stress induced cytotoxicity (Brocker et al., 2011). Mounting evidence indicates that hypoxic cancer cells undergoing exposure to oxidative stress develop adaptive strategies to survive hostile milieu (Fiaschi and Chiarugi, 2012), such as increasing antioxidant functionalities that may result in increased aggressiveness. Given the results observed with ALDH7A1 (Chapter 2), it is suggested that one of these adaptive responses is the upregulation of the antioxidant enzyme, ALDH7A1.

It is well known that major adaptive responses in hypoxic cells are mediated by HIFs (Semenza, 2012). To gain a better understanding of whether the regulation of ALDH7A1 is regulated by HIFs, cobalt chloride ($CoCl_2$) treatment was used to induce HIF-1α. Whilst $CoCl_2$ treatment induced HIF-1α, ALDH7A1 expression in both HT29 and DLD-1 cell lines was not affected, which point towards ALDH7A1 regulation being independent of the HIF-1α master regulator. Knockdown studies of HIF-1α and HIF-2α also indicated that ALDH7A1 is HIF-1α/HIF-2α independent and might be controlled by another cellular mechanism (Chapter 2). The role of other hypoxia-inducible transcriptional factors such as nuclear factor κB (NF-κB), activator protein I (AP-I) and p53 (Carroll and Ashcroft, 2005) need to be considered and future studies will be directed to understand whether they are involved in the regulation of ALDH7A1 expression.

To further evaluate the antioxidant properties of ALDH7A1, knockdown studies were carried out (discussed in Chapter 3) and their effect on the generation of DNA damaging reactive oxygen species (ROS) showed that ALDH7A1 presence is important in decreasing ROS generation. The use of isogenic cell line pair (H1299/RFP and H1299/ALDH7A1) further substantiated these findings (discussed in Chapter 4). These observations are in good accordance with ALDH7A1 as a key enzyme in combating oxidative stress signals and further emphasises a potential role of this enzyme in the hypoxic regions of solid tumours. To further unravel the antioxidant role of ALDH7A1, future studies may involve exploring oxidative stress biomarkers such as measuring superoxide dismutase (SOD), glutathione reductase/peroxidase, or benzo(a)pyrene diolepoxide (BPDE) (Ziech et al., 2010, Fan et al., 2008) in attempt to understand mechanistically if ALDH7A1 operates independently as an antioxidant enzyme or in conjunction with other enzymes or pathways in the CRC microenvironment. In addition, given the role of hypoxia and mitochondrial dysfunction in the generation of reactive nitrogen species (RNS) (Reuter et al., 2010), the role of ALDH7A1 in the protection of CRC cells against different types of radicals ought to be considered for evaluation (Haklar et al., 2001). Collectively, this might broaden the understanding of ALDH7A1 and enhance the knowledge of how CRC cells adapt to acute or chronic exposure to hypoxia.

Previously, the role of ALDH7A1 has been described in enhancing cell proliferation and colony formation in prostate cancer (van den Hoogen et al., 2011). Here, results using knockdown experiments in DLD-1 CRC cell line

and the isogenic H1299 cell line pair (Chapter 3 and 4, respectively) are suggestive of ALDH7A1 role in mediating cancer cell proliferation. Although the exact mechanism has not been investigated in this thesis, future work will be conducted to study possible downstream signalling pathways that mediate cell proliferation and survival. This might include oncogenic pathways such as ERK and MAPK pathways that are predominant in CRC (Fang and Richardson, 2005, Urosevic et al., 2014).

One of the main challenges in achieving successful CRC treatment outcome is the presence of intrinsic or acquired drug resistance (Holohan et al., 2013). It is well known that hypoxia mediates resistance and supresses the pharmacological activities of both chemotherapy and radiotherapy treatment modalities that ultimately will affect treatment outcome (Wouters et al., 2007). In this context, it was interesting to assess whether ALDH7A1 expression might also contribute to drug resistance. Using knockdown studies and the isogenic H1299 lung cancer cell line pair, the anti-proliferative activities of a wide panel of anticancer drugs including conventional cytotoxic and molecular-targeted drugs were evaluated. On the basis of these results (Chapters 3 and 4), the activity of ALDH7A1 has been shown not to be involved in causing drug resistance.

The possibility of inhibiting ALDH7A1 functional activity was also evaluated in order to study its potential as a pharmacological target. In collaboration with Dr Zoe Cournia (Athens Academy Biomedical Research Foundation), a Maybridge database consisting of 24,000 compounds were included in a virtual screen using the ALDH7A1 crystal protein structure. Nine compounds

with the highest binding affinity for ALDH7A1 were purchased from Maybridge and were used to probe ALDH7A1 activity using the isogenic H1299 lung cancer cell line pair. Results from cell survival assay and ROS generation assay showed that the compound HAN00316 could be a good starting point for medicinal chemistry to be performed. This can lead to more potent and selective ALDH7A1-affinic compounds which could be used as tool compounds to explore the importance of ALDH7A1 in cancer and other diseases. In addition to using the isogenic H1299 lung cancer cell line pair, HT29 and DLD-1 CRC cell lines, future studies will require a cell-free based assay using recombinant ALDH7A1 which is only recently has become commercially available. Although ALDH7A1 recombinant plasmid can be constructed as previously described (Brocker et al., 2010), it was not attempted in this PhD due to time limitation. However, for effective drug discovery to be carried out, the lack of recombinant ALDH7A1 protein is clearly a limitation in chemical probes discovery and will be required in future studies aimed at optimising compounds such as HAN00316.

Another challenge in CRC is the presence of CSCs which are characterised by being resistant to current cancer therapeutics and possessing the ability to cause cancer recurrence (Maugeri-Saccà et al., 2011). Hypoxia has been described to enhance the survival of CSC by acting as a niche and the dynamic interactions between CSCs and the microenvironment has been found to promote metastasis and development of drug resistance (Heddleston et al., 2010). ALDH1 has been shown to act as CSC marker in CRC, however the role of specific ALDH isoforms is not well understood. In

this study, the expression of ALDH in CSCs has not been explored due to time limitation. It is possible that CSCs will express elevated levels of ALDHs due their chemo-protecting properties and involvement in cell differentiation via the retinoic acid pathways (Chapter 1, Introduction, section 1.4.5). In this regard, it is proposed that future studies will interrogate the expression of ALDHs in CSCs derived from CRC cell lines and primary tissues to understand their potential as biomarkers for CSC identification and isolation. This information will be important to collate as well as how CSCs adapt to hypoxic environment. In this regard, it will be key issue to understand which ALDH1 isoforms are expressed and whether ALDH7A1 is present and induced under hypoxia, thereby potentially providing protection to the stem cell component of colon tumours.

All the work presented in this thesis was conducted using CRC cell lines, however to evaluate the significance of ALDH7A1 in a clinical context, future work should include the investigation of ALDH in clinical samples derived from patients at different stages of CRC. Specifically, it would be important to understand the context of ALDH expression with a specific focus on ALDH1A1 and 1A3 in the stem cell component, 1B1 in the different CRC molecular subtypes and 7A1 in the hypoxic fractions of clinical specimens. To compare, ALDH expression should also be analysed in normal colon tissue distant to the tumour tissue to assess if ALDH expression is significantly different, thereby providing a signature of CRC and perhaps stage of malignancy.

One of the important roles of ALDH7A1 that was not explored in this study is its role in lysine metabolism. ALDH7A1 plays a major role in lysine catabolism in the pipecolic acid pathway where it catalyses the oxidation of alpha-aminoadipic semialdehyde (α-AASA) to alpha-aminoadipate. Mutation in ALDH7A1 has been linked to pyridoxine-dependent epilepsy (PDE) as a result of defective lysine catabolism (Mills et al., 2010), which causes accumulating piperidine-6-carboxylate (PC6) to condense with pyridoxal 5'-phosphate (PLP) to inactivate this enzyme cofactor that is essential for normal metabolism of neurotransmitters (Mills et al., 2010) (Figure 87). As the investigations carried out in this thesis suggest ALDH7A1 as an indicator of aggressive forms of CRC due to hypoxia-related induction, development of a diagnostic assay to predict which patients are at risk of progressing to more advanced disease might be feasible. In PDE patients, this diagnostic kit relies on measuring α-AASA and PC6 compounds that are excreted from intracellular pools into urine and plasma, provides a simple way of confirming the diagnosis of PDE, while ALDH7A1 gene analysis provides a means for prenatal diagnosis as confirmed in clinical trials (Mills et al., 2010). Similarly, such a technology would allow CRC patients after stage I-III surgery to be routinely monitored for signs of tumour recurrence based on hypoxia/ALDH7A1 presence in tissue biopsies and measuring lysine metabolites as surrogate markers in urine and blood samples before and after surgical resection. Ultimately, earlier detection of aggressive forms of CRC could lead to better treatment options and thereby improve quality of life and survival rate. Another option for future research work could be

focussed around addressing the role of ALDH7A1 in lysine metabolism and how it might be linked to aggressive forms of CRC.

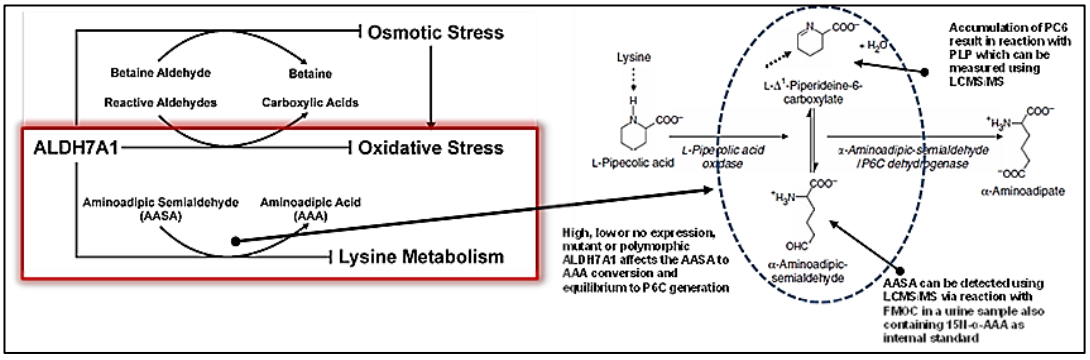

Figure 87 Catabolism of L-pipecolic acid. P6C is the cyclic Schiff base of a-AASA; in solution they are in equilibrium). The dotted arrow indicates the activated methylene that has been proposed to react with the carbonyl group of pyridoxal 5'-phosphate (PLP) by forming a Knoevenagel condensation product. Adopted from Brocker *et al*. 2010 (permission is not required for reuse in thesis) and Mills *et al*. 2006 with License Number: 3858771236223.

In conclusion, the data presented in this thesis points to ALDH7A1 isoform as being modulated by tumour hypoxia, however the regulation of its expression was shown to be independent of HIF1-α and HIF2-α. Results from knockdown studies and isogenic cell pair revealed that ALDH7A1 expression is associated with less ROS generation which points to its role as an antioxidant enzyme. This suggests that it is one of the adaptive responses by which hypoxia enhances cancer cell survival and progression. ALDH7A1 has also been suggested to be associated with cell proliferation as knockdown studies showed reduction in DLD-1 live cell number upon ALDH7A1 siRNA transfection, while ALDH7A1 overexpression in H1299 cells increased proliferation rate. Further work is needed to assess whether it is also involved in evading apoptosis. To further support the findings presented in this thesis, conducting knockdown studies using another CRC cell lines such as HT29 should be considered. Future work will be directed

toward studying ALDH7A1 expression in primary colon cancer tissues and normal tissues. This will provide better understanding to whether a possible link between ALDH7A1 and CRC aggressive phenotypes exists as recent studies have shown ALDH7A1 to be highly expressed in ovarian cancer compared to normal tissue and to be associated with recurrence in patients with surgically resected NSCLC. Further exploration of the antioxidant properties of ALDH7A1 against e.g. ROS and RNS may provide a better understanding of the mechanisms of CSC survival, which are associated with resistance and cancer recurrence. This will be made feasible through the discovery of ALDH7A1-affinic compounds, e.g. by structural optimisation of HAN00316 compound, which was found to inhibit the antioxidant activity of ALDH7A1 and hence, can be used as tool compounds to probe ALDH7A1 functional activities in cancer and other diseases. Considering the association between ALDH7A1 expression and the aggressive nature of hypoxic cells, developing screening assays to detect biomarkers associated with ALDH7A1 might provide a diagnostic tool for the earlier detection of recurrent disease, which is currently an unmet clinical need.

The novel findings of this work include:

- This is the first time to show that ALDH7A1 expression is increased by tumour hypoxia using both 2D and 3D CRC culture models (Chapter 2).
- This is the first time to show that ALDH7A1 is involved in the reduction of ROS in cancer setting using CRC DLD-1 cells under normoxic and

hypoxic conditions and H1299 isogenic cell lines system (Chapter 3 and 4).

- ALDH7A1 knockdown resulted in the upregulation of ALDH3A1, suggesting a cross talk between both enzymes that might be caused by compensatory mechanisms (Chapter 3).

The limitations of this work include:

- The expression of ALDH in 2D and 3D culture models was only explored using cell lines, however, to evaluate the significance of ALDH7A1 in a clinical context, investigation of ALDH should be carried out using clinical samples derived from patients at different stages of CRC (Chapter 2).
- The study of the functional roles of ALDH7A1 in CRC using knockdown experiments was only investigated in DLD-1 cells, however, the inclusion of another cell line such as HT29 will provide better understanding of the role of ALDH7A1 in CRC (Chapter 3).
- Knockdown experiments were conducted using single siRNA sequence, however, to confirm the specificity of the consequences of ALDH7A1 knockdown two siRNAs sequences targeting ALDH7A1 should be used (Chapter 3).
- The evaluation of ALDH7A1-affinic compounds was carried out using isogenic cell line system, however, for better understanding of the binding affinity of these compounds and ALDH7A1, the use of cell free based assays including ALDH7A1 recombinant enzyme should be considered (Chapter 4).

The hypothesis for future work is ALDH7A1 plays an important role in tumour hypoxia including the reduction of ROS level and protection of CSCs component from oxidative stress and helps in the diagnosis of aggressive CRC phenotypes. Future work will include:

- Investigation of ALDH7A1 expression in clinical samples derived from patients at different stages of CRC and normal colon tissues.
- Investigation of ALDH7A1 expression in CSCs component of CRC under normoxic and hypoxic conditions.
- Exploring the role of ALDH7A1 in protecting CRC cells against oxidative stress. This include knockdown studies of ALDH7A1 and evaluation of the effect of different oxidant sources such as hydrogen peroxide and superoxide on cell survival
- The development of a diagnostic assay to predict which patients with CRC are at risk of progressing to more advanced disease based on hypoxia/ALDH7A1 presence in tissue biopsies and measuring lysine metabolites as surrogate markers in urine and blood samples before and after surgical resection.
- Further structural optimisation of HAN00316 compound, which was found to inhibit the role of ALDH7A1 in reducing ROS levels and hence, can be used as tool compounds to probe ALDH7A1 functional activities in cancer and other diseases.

Chapter 6: References

AHMADI, M., AHMADIHOSSEINI, Z., ALLISON, S. J., BEGUM, S., ROCKLEY, K., SADIQ, M., CHINTAMANENI, S., LOKWANI, R., HUGHES, N. & PHILLIPS, R. M. 2014. Hypoxia modulates the activity of a series of clinically approved tyrosine kinase inhibitors. *British Journal of Pharmacology,* 171**,** 224-236.

AHMED, N., THOMPSON, E. W. & QUINN, M. A. 2007. Epithelial–mesenchymal interconversions in normal ovarian surface epithelium and ovarian carcinomas: An exception to the norm. *Journal of Cellular Physiology,* 213**,** 581-588.

AIRLEY, R. E., LONCASTER, J., RALEIGH, J. A., HARRIS, A. L., DAVIDSON, S. E., HUNTER, R. D., WEST, C. M. L. & STRATFORD, I. J. 2003. GLUT-1 and CAIX as intrinsic markers of hypoxia in carcinoma of the cervix: Relationship to pimonidazole binding. *International Journal of Cancer,* 104**,** 85-91.

AL-HAJJ, M., WICHA, M. S., BENITO-HERNANDEZ, A., MORRISON, S. J. & CLARKE, M. F. 2003. Prospective identification of tumorigenic breast cancer cells. *Proceedings of the National Academy of Sciences,* 100**,** 3983-3988.

ALISON, M. R., GUPPY, N. J., LIM, S. M. L. & NICHOLSON, L. J. 2010. Finding cancer stem cells: are aldehyde dehydrogenases fit for purpose? *The Journal of Pathology,* 222**,** 335-344.

ALLISON, S. J. & MILNER, J. 2014. RNA Interference by Single- and Double-stranded siRNA With a DNA Extension Containing a 3′ Nuclease-resistant Mini-hairpin Structure.*Molecular Therapy. Nucleic Acids,* 3**,** e141.

ÅMELLEM, Ø. & PETTERSEN, E. O. 1991. Cell inactivation and cell cycle inhibition as induced by extreme hypoxia: the possible role of cell cycle arrest as a protection against hypoxia-induced lethal damage. *Cell Proliferation,* 24**,** 127-141.

AMERICAN CANCER SOCIETY 2014. Colorectal Cancer Facts & Figures 2014-2016. *American Cancer Society*.

ASBY, D. J., CUDA, F., HOAKWIE, F., MIRANDA, E. & TAVASSOLI, A. 2014. HIF-1 promotes the expression of its [small alpha]-subunit via an epigenetically regulated transactivation loop. *Molecular BioSystems,* 10**,** 2505-2508.

BALAMURUGAN, K. 2016. HIF-1 at the crossroads of hypoxia, inflammation, and cancer. *International Journal of Cancer,* 138**,** 1058-1066.

BALBER, A. E. 2011. Concise Review: Aldehyde Dehydrogenase Bright Stem and Progenitor Cell Populations from Normal Tissues:

Characteristics, Activities, and Emerging Uses in Regenerative Medicine. *STEM CELLS,* 29**,** 570-575.

BALENDIRAN, G. K., DABUR, R. & FRASER, D. 2004. The role of glutathione in cancer. *Cell Biochemistry and Function,* 22**,** 343-352.

BÁRDOS, J. I. & ASHCROFT, M. 2004. Hypoxia-inducible factor-1 and oncogenic signalling. *BioEssays,* 26**,** 262-269.

BÁRDOS, J. I. & ASHCROFT, M. 2005. Negative and positive regulation of HIF-1: A complex network. *Biochimica et Biophysica Acta (BBA) - Reviews on Cancer,* 1755**,** 107-120.

BARR, M. P., BOUCHIER-HAYES, D. J. & HARMEY, J. J. 2008. Vascular endothelial growth factor is an autocrine survival factor for breast tumour cells under hypoxia. *International journal of oncology,* 32**,** 41-48.

BARR, M. P., GRAY, S. G., HOFFMANN, A. C., HILGER, R. A., THOMALE, J., O'FLAHERTY, J. D., FENNELL, D. A., RICHARD, D., O'LEARY, J. J. & O'BYRNE, K. J. 2013. Generation and Characterisation of Cisplatin-Resistant Non-Small Cell Lung Cancer Cell Lines Displaying a Stem-Like Signature. *PLoS ONE,* 8**,** e54193.

BARTSCH, H. & NAIR, J. 2004. Oxidative stress and lipid peroxidation-derived DNA-lesions in inflammation driven carcinogenesis. *Cancer Detection and Prevention,* 28**,** 385-391.

BARTSCH, H. & NAIR, J. 2006. Chronic inflammation and oxidative stress in the genesis and perpetuation of cancer: role of lipid peroxidation, DNA damage, and repair. *Langenbeck's Archives of Surgery,* 391**,** 499-510.

BELLOT, G., GARCIA-MEDINA, R., GOUNON, P., CHICHE, J., ROUX, D., POUYSSÉGUR, J. & MAZURE, N. M. 2009. Hypoxia-Induced Autophagy Is Mediated through Hypoxia-Inducible Factor Induction of BNIP3 and BNIP3L via Their BH3 Domains. *Molecular and Cellular Biology,* 29**,** 2570-2581.

BERGERS, G. & BENJAMIN, L. E. 2003. Tumorigenesis and the angiogenic switch. *Nature reviews. Cancer,* 3**,** 401-410.

BLACK, W. J., STAGOS, D., MARCHITTI, S. A., NEBERT, D. W., TIPTON, K. F., BAIROCH, A. & VASILIOU, V. 2009. Human aldehyde dehydrogenase genes: alternatively spliced transcriptional variants and their suggested nomenclature. *Pharmacogenetics and Genomics,* 19**,** 893-902 10.1097/FPC.0b013e3283329023.

BOONYARATANAKORNKIT, J. B., YUE, L., STRACHAN, L. R., SCALAPINO, K. J., LEBOIT, P. E., LU, Y., LEONG, S. P., SMITH, J. E. & GHADIALLY, R. 2010. Selection of Tumorigenic Melanoma Cells Using ALDH. *Journal of Investigative Dermatology,* 130**,** 2799–2808.

BOTCHKINA, G. 2013. Colon cancer stem cells – From basic to clinical application. *Cancer Letters,* 338**,** 127-140.

BRAUN, T., BOBER, E., SINGH, S., AGARWAL, D. P. & GOEDDE, H. W. 1987. Evidence for a signal peptide at the amino-terminal end of human mitochondrial aldehyde dehydrogenase. *FEBS Letters,* 215**,** 233-236.

BROCKER, C., CANTORE, M., FAILLI, P. & VASILIOU, V. 2011. Aldehyde dehydrogenase 7A1 (ALDH7A1) attenuates reactive aldehyde and oxidative stress induced cytotoxicity. *Chemico-Biological Interactions,* 191**,** 269-277.

BROCKER, C., LASSEN, N., ESTEY, T., PAPPA, A., CANTORE, M., ORLOVA, V. V., CHAVAKIS, T., KAVANAGH, K. L., OPPERMANN, U. & VASILIOU, V. 2010. Aldehyde Dehydrogenase 7A1 (ALDH7A1) Is a Novel Enzyme Involved in Cellular Defense against Hyperosmotic Stress. *Journal of Biological Chemistry,* 285**,** 18452-18463.

BROWN, J. M. 2002. Tumor Microenvironment and the Response to Anticancer Therapy. *Cancer Biology & Therapy,* 1**,** 453-458.

BROWN, J. M. & GIACCIA, A. J. 1998. The Unique Physiology of Solid Tumors: Opportunities (and Problems) for Cancer Therapy. *Cancer Research,* 58**,** 1408-1416.

CANCER RESEARCH UK,. 2016. TNM and number stages of bowel cancer [Online]. Available: http://www.cancerresearchuk.org/about-cancer/type/bowel-cancer/treatment/tnm-and-number-stages-of-bowel-cancer [Accessed 12 Jan 2016].

CARPENTINO, J. E., HYNES, M. J., APPELMAN, H. D., ZHENG, T., STEINDLER, D. A., SCOTT, E. W. & HUANG, E. H. 2009. Aldehyde Dehydrogenase-Expressing Colon Stem Cells Contribute to Tumorigenesis in the Transition from Colitis to Cancer. *Cancer Research,* 69**,** 8208-8215.

CARROLL, V. A. & ASHCROFT, M. 2005. Targeting the molecular basis for tumour hypoxia. *Expert Reviews in Molecular Medicine,* 7**,** 1-16.

CHAN, C.-L., WONG, J. W. Y., WONG, C.-P., CHAN, M. K. L. & FONG, W.-P. 2011. Human antiquitin: Structural and functional studies. *Chemico-Biological Interactions,* 191**,** 165-170.

CHANG, C., HSU, L. C., DAVÉ, V. & YOSHIDA, A. 1998. Expression of human aldehyde dehydrogenase-3 associated with hepatocellular carcinoma: promoter regions and nuclear protein factors related to the expression. *International Journal of Molecular Medicine,* 2**,** 333-341.

CHEN, J., IMANAKA, N., CHEN, J. & GRIFFIN, J. D. 2009. Hypoxia potentiates Notch signaling in breast cancer leading to decreased E-

cadherin expression and increased cell migration and invasion. *British Journal of Cancer,* 102**,** 351-360.

CHEN, Y., ORLICKY, D. J., MATSUMOTO, A., SINGH, S., THOMPSON, D. C. & VASILIOU, V. 2011. Aldehyde dehydrogenase 1B1 (ALDH1B1) is a potential biomarker for human colon cancer. *Biochemical and Biophysical Research Communications,* 405**,** 173-179.

CHEUNG, A. M. S., WAN, T. S. K., LEUNG, J. C. K., CHAN, L. Y. Y., HUANG, H., KWONG, Y. L., LIANG, R. & LEUNG, A. Y. H. 2007. Aldehyde dehydrogenase activity in leukemic blasts defines a subgroup of acute myeloid leukemia with adverse prognosis and superior NOD//SCID engrafting potential. *Leukemia,* 21**,** 1423-1430.

CHINTALA, S., TÓTH, K., CAO, S., DURRANI, F. A., VAUGHAN, M. M., JENSEN, R. L. & RUSTUM, Y. M. 2010. Se-methylselenocysteine sensitizes hypoxic tumor cells to irinotecan by targeting hypoxia-inducible factor 1α. *Cancer chemotherapy and pharmacology,* 66**,** 899-911.

CLEVERS, H. 2005. Stem cells, asymmetric division and cancer. *Nature Genetics* 37**,** 1027-1028.

CLEVERS, H. 2011. The cancer stem cell: premises, promises and challenges. *Nature Medicine,* 17**,** 313-319.

COMPORTI, M. 1998. Lipid peroxidation and biogenic aldehydes: from the identification of 4-hydroxynonenal to further achievements in biopathology. *Free radical research,* 28**,** 623-635.

CONDELLO, S., MORGAN, C. A., NAGDAS, S., CAO, L., TUREK, J., HURLEY, T. D. & MATEI, D. 2015. [beta]-Catenin-regulated ALDH1A1 is a target in ovarian cancer spheroids. *Oncogene,* 34**,** 2297-2308.

CORTI, S., LOCATELLI, F., PAPADIMITRIOU, D., DONADONI, C., SALANI, S., DEL BO, R., STRAZZER, S., BRESOLIN, N. & COMI, G. P. 2006. Identification of a Primitive Brain–Derived Neural Stem Cell Population Based on Aldehyde Dehydrogenase Activity. *STEM CELLS,* 24**,** 975-985.

CROKER, A. & ALLAN, A. 2012. Inhibition of aldehyde dehydrogenase (ALDH) activity reduces chemotherapy and radiation resistance of stem-like ALDHhiCD44+ human breast cancer cells. *Breast Cancer Research and Treatment,* 133**,** 75-87.

CROUCH, S. P. M., KOZLOWSKI, R., SLATER, K. J. & FLETCHER, J. 1993. The use of ATP bioluminescence as a measure of cell proliferation and cytotoxicity. *Journal of Immunological Methods,* 160**,** 81-88.

CUFFY, M., ABIR, F. & LONGO, W. E. 2006. Management of Less Common Tumors of the Colon, Rectum, and Anus. *Clinical Colorectal Cancer,* 5**,** 327-337.

DACHS, G. U. & TOZER, G. M. 2000. Hypoxia modulated gene expression: angiogenesis, metastasis and therapeutic exploitation. *European Journal of Cancer,* 36**,** 1649-1660.

DALERBA, P., DYLLA, S. J., PARK, I.-K., LIU, R., WANG, X., CHO, R. W., HOEY, T., GURNEY, A., HUANG, E. H., SIMEONE, D. M., SHELTON, A. A., PARMIANI, G., CASTELLI, C. & CLARKE, M. F. 2007. Phenotypic characterization of human colorectal cancer stem cells. *Proceedings of the National Academy of Sciences,* 104**,** 10158-10163.

DANDO, I., CORDANI, M., DALLA POZZA, E., BIONDANI, G., DONADELLI, M. & PALMIERI, M. 2015. Antioxidant Mechanisms and ROS-Related MicroRNAs in Cancer Stem Cells. *Oxidative Medicine and Cellular Longevity,* 2015.

DAS, A. B., LOYING, P. & BOSE, B. 2012. Human recombinant Cripto-1 increases doubling time and reduces proliferation of HeLa cells independent of pro-proliferation pathways. *Cancer Letters,* 318**,** 189-198.

DAVIDSON, B. L. & MCCRAY, P. B. 2011. Current prospects for RNA interference-based therapies. *Nature Reviews Genetics,* 12**,** 329-340.

DE GRAMONT, A., FIGER, A., SEYMOUR, M., HOMERIN, M., HMISSI, A., CASSIDY, J., BONI, C., CORTES-FUNES, H., CERVANTES, A., FREYER, G., PAPAMICHAEL, D., LE BAIL, N., LOUVET, C., HENDLER, D., DE BRAUD, F., WILSON, C., MORVAN, F. & BONETTI, A. 2000. Leucovorin and Fluorouracil With or Without Oxaliplatin as First-Line Treatment in Advanced Colorectal Cancer. *Journal of Clinical Oncology,* 18**,** 2938-2947.

DE LUCA, L. M. 1991. Retinoids and their receptors in differentiation, embryogenesis, and neoplasia. *The FASEB Journal,* 5**,** 2924-33.

DEL DUCA, D., WERBOWETSKI, T. & DEL MAESTRO, R. 2004. Spheroid Preparation from Hanging Drops: Characterization of a Model of Brain Tumor Invasion. *Journal of Neuro-Oncology,* 67**,** 295-303.

DEMASTER, E. G. & NAGASAWA, H. T. 1978. Inhibition of aldehyde dehydrogenase by propiolaldehyde, a possible metabolite of pargyline. *Research communications in chemical pathology and pharmacology,* 21**,** 497-505.

DENG, Y., ZHOU, J., FANG, L., CAI, Y., KE, J., XIE, X., HUANG, Y., HUANG, M. & WANG, J. 2014. ALDH1 is an independent prognostic

factor for patients with stages II-III rectal cancer after receiving radiochemotherapy. *British Journal of Cancer,* 110**,** 430-434.

DOEDENS, A. L., STOCKMANN, C., RUBINSTEIN, M. P., LIAO, D., ZHANG, N., DENARDO, D. G., COUSSENS, L. M., KARIN, M., GOLDRATH, A. W. & JOHNSON, R. S. 2010. Macrophage Expression of Hypoxia-Inducible Factor-1α Suppresses T-Cell Function and Promotes Tumor Progression. *Cancer Research,* 70**,** 7465-7475.

DOLLÉ, L., BOULTER, L., LECLERCQ, I. A. & VAN GRUNSVEN, L. A. 2015. Next generation of ALDH substrates and their potential to study maturational lineage biology in stem and progenitor cells. *American Journal of Physiology - Gastrointestinal and Liver Physiology,* 308**,** G573-G578.

DOUILLARD, J. Y., CUNNINGHAM, D., ROTH, A. D., NAVARRO, M., JAMES, R. D., KARASEK, P., JANDIK, P., IVESON, T., CARMICHAEL, J., ALAKL, M., GRUIA, G., AWAD, L. & ROUGIER, P. 2000. Irinotecan combined with fluorouracil compared with fluorouracil alone as first-line treatment for metastatic colorectal cancer: a multicentre randomised trial. *The Lancet,* 355**,** 1041-1047.

DYLLA, S. J., BEVIGLIA, L., PARK, I. K., CHARTIER, C., RAVAL, J., NGAN, L., PICKELL, K., AGUILAR, J., LAZETIC, S., SMITH-BERDAN, S., CLARKE, M. F., HOEY, T., LEWICKI, J. & GURNEY, A. L. 2008. Colorectal cancer stem cells are enriched in xenogeneic tumors following chemotherapy. *PloS one,* 3**,** e2428.

EBBEN, J. D., TREISMAN, D. M., ZORNIAK, M., KUTTY, R. G., CLARK, P. A. & KUO, J. S. 2010. The cancer stem cell paradigm: a new understanding of tumor development and treatment. *Expert opinion on therapeutic targets,* 14**,** 621-632.

EDDERKAOUI, M., HONG, P., VAQUERO, E. C., LEE, J. K., FISCHER, L., FRIESS, H., BUCHLER, M. W., LERCH, M. M., PANDOL, S. J. & GUKOVSKAYA, A. S. 2005. Extracellular matrix stimulates reactive oxygen species production and increases pancreatic cancer cell survival through 5-lipoxygenase and NADPH oxidase. *American Journal of Physiology - Gastrointestinal and Liver Physiology,* 289**,** G1137-G1147.

ELIZONDO, G., CORCHERO, J., STERNECK, E. & GONZALEZ, F. J. 2000. Feedback Inhibition of the Retinaldehyde Dehydrogenase GeneALDH1 by Retinoic Acid through Retinoic Acid Receptor Î± and CCAAT/Enhancer-binding Protein Î². *Journal of Biological Chemistry,* 275**,** 39747-39753.

EMADI, A., JONES, R. J. & BRODSKY, R. A. 2009. Cyclophosphamide and cancer: golden anniversary. *Nature Reviews Clinical Oncology,* 6**,** 638-647.

EMMINK, B. L., VERHEEM, A., VAN HOUDT, W. J., STELLER, E. J. A., GOVAERT, K. M., PHAM, T. V., PIERSMA, S. R., BOREL RINKES, I. H. M., JIMENEZ, C. R. & KRANENBURG, O. 2013. The secretome of colon cancer stem cells contains drug-metabolizing enzymes. *Journal of Proteomics,* 91**,** 84-96.

ERAMO, A., LOTTI, F., SETTE, G., PILOZZI, E., BIFFONI, M., DI VIRGILIO, A., CONTICELLO, C., RUCO, L., PESCHLE, C. & DE MARIA, R. 2007. Identification and expansion of the tumorigenic lung cancer stem cell population. *Cell Death and Differentiation,* 15**,** 504-514.

ERUSLANOV, E. & KUSMARTSEV, S. 2010. Identification of ROS using oxidized DCFDA and flow-cytometry. *Methods in molecular biology (Clifton, N.J.),* 594**,** 57-72.

FAN, J., CAI, H. & TAN, W.-S. 2007. Role of the plasma membrane ROS-generating NADPH oxidase in CD34+ progenitor cells preservation by hypoxia. *Journal of Biotechnology,* 130**,** 455-462.

FAN, J., CAI, H., YANG, S., YAN, L. & TAN, W. 2008. Comparison between the effects of normoxia and hypoxia on antioxidant enzymes and glutathione redox state in ex vivo culture of CD34(+) cells. *Comparative biochemistry and physiology. Part B, Biochemistry & molecular biology,* 151**,** 153-158.

FAN, X., OUYANG, N., TENG, H. & YAO, H. 2011. Isolation and characterization of spheroid cells from the HT29 colon cancer cell line. *International Journal of Colorectal Disease,* 26**,** 1279-1285.

FANG, D., NGUYEN, T. K., LEISHEAR, K., FINKO, R., KULP, A. N., HOTZ, S., VAN BELLE, P. A., XU, X., ELDER, D. E. & HERLYN, M. 2005. A Tumorigenic Subpopulation with Stem Cell Properties in Melanomas. *Cancer Research,* 65**,** 9328-9337.

FANG, J. Y. & RICHARDSON, B. C. 2005. The MAPK signalling pathways and colorectal cancer. *The Lancet Oncology,* 6**,** 322-327.

FARRES, J., GUAN, K.-L. & WEINER, H. 1989. Primary structures of rat and bovine liver mitochondrial aldehyde dehydrogenases deduced from cDNA sequences. *European Journal of Biochemistry,* 180**,** 67-74.

FIASCHI, T. & CHIARUGI, P. 2012. Oxidative stress, tumor microenvironment, and metabolic reprogramming: a diabolic liaison. *International journal of cell biology,* 2012**,** 762825.

FIDLER, I. J. 2003. The pathogenesis of cancer metastasis: the 'seed and soil' hypothesis revisited. *Nature Reviews Cancer* 3**,** 453-458.

FIRTH, J. D., EBERT, B. L. & RATCLIFFE, P. J. 1995. Hypoxic regulation of lactate dehydrogenase A Interaction between hypoxia-inducible factor 1

and cAMP response elements. *Journal of Biological Chemistry,* 270**,** 21021-21027.

FISCHER, O. M., HART, S., GSCHWIND, A., PRENZEL, N. & ULLRICH, A. 2004. Oxidative and Osmotic Stress Signaling in Tumor Cells Is Mediated by ADAM Proteases and Heparin-Binding Epidermal Growth Factor. *Molecular and Cellular Biology,* 24**,** 5172-5183.

FUJIWARA, S., NAKAGAWA, K., HARADA, H., NAGATO, S., FURUKAWA, K., TERAOKA, M., SENO, T., OKA, K., IWATA, S. & OHNISHI, T. 2007. Silencing hypoxia-inducible factor-1alpha inhibits cell migration and invasion under hypoxic environment in malignant gliomas. *International journal of oncology,* 30**,** 793-802.

GIACALONE, N. J., DEN, R. B., EISENBERG, R., CHEN, H., OLSON, S. J., MASSION, P. P., CARBONE, D. P. & LU, B. 2013. ALDH7A1 expression is associated with recurrence in patients with surgically resected non-small-cell lung carcinoma. *Future Oncology,* 9**,** 737-745.

GIANTONIO, B. J., CATALANO, P. J., MEROPOL, N. J., O'DWYER, P. J., MITCHELL, E. P., ALBERTS, S. R., SCHWARTZ, M. A. & BENSON, A. B. 2007. Bevacizumab in Combination With Oxaliplatin, Fluorouracil, and Leucovorin (FOLFOX4) for Previously Treated Metastatic Colorectal Cancer: Results From the Eastern Cooperative Oncology Group Study E3200. *Journal of Clinical Oncology,* 25**,** 1539-1544.

GINESTIER, C., HUR, M. H., CHARAFE-JAUFFRET, E., MONVILLE, F., DUTCHER, J., BROWN, M., JACQUEMIER, J., VIENS, P., KLEER, C. G., LIU, S., SCHOTT, A., HAYES, D., BIRNBAUM, D., WICHA, M. S. & DONTU, G. 2007. ALDH1 Is a Marker of Normal and Malignant Human Mammary Stem Cells and a Predictor of Poor Clinical Outcome. *Cell stem cell,* 1**,** 555-567.

GINZINGER, D. G. 2002. Gene quantification using real-time quantitative PCR: An emerging technology hits the mainstream. *Experimental Hematology,* 30**,** 503-512.

GIORGIANNI, F., BRIDSON, P. K., SORRENTINO, B. P., POHL, J. & BLAKLEY, R. L. 2000 Inactivation of aldophosphamide by human aldehyde dehydrogenase isozyme 3. *Biochemical Pharmacology,* 60**,** 325-338.

GODA, N., RYAN, H. E., KHADIVI, B., MCNULTY, W., RICKERT, R. C. & JOHNSON, R. S. 2003. Hypoxia-Inducible Factor 1α Is Essential for Cell Cycle Arrest during Hypoxia. *Molecular and Cellular Biology,* 23**,** 359-369.

GRUBER, G., GREINER, R. H., HLUSHCHUK, R., AEBERSOLD, D. M., ALTERMATT, H. J., BERCLAZ, G. & DJONOV, V. 2004. Hypoxia-

inducible factor 1 alpha in high-risk breast cancer: an independent prognostic parameter? *Breast cancer research : BCR,* 6**,** R191-8.

GUO, H., NAGY, T. & PIERCE, M. 2014. Post-translational Glycoprotein Modifications Regulate Colon Cancer Stem Cells and Colon Adenoma Progression in Apcmin/+ Mice through Altered Wnt Receptor Signaling. *Journal of Biological Chemistry,* 289**,** 31534-31549.

GUPTA, P. B., ONDER, T. T., JIANG, G., TAO, K., KUPERWASSER, C., WEINBERG, R. A. & LANDER, E. S. 2009. Identification of Selective Inhibitors of Cancer Stem Cells by High-Throughput Screening. *Cell,* 138**,** 645-659.

HAKLAR, G., SAYIN-ÖZVERI, E., YÜKSEL, M., AKTAN, A. Ö. & YALÇIN, A. S. 2001. Different kinds of reactive oxygen and nitrogen species were detected in colon and breast tumors. *Cancer Letters,* 165**,** 219-224.

HANAHAN, D. & WEINBERG, R. A. 2000. The Hallmarks of Cancer. *Cell,* 100**,** 57-70.

HANAHAN, D. & WEINBERG, ROBERT A. 2011. Hallmarks of Cancer: The Next Generation. *Cell,* 144**,** 646-674.

HASMIM, M., NOMAN, M. Z., LAURIOL, J., BENLALAM, H., MALLAVIALLE, A., ROSSELLI, F., MAMI-CHOUAIB, F., ALCAIDE-LORIDAN, C. & CHOUAIB, S. 2011. Hypoxia-Dependent Inhibition of Tumor Cell Susceptibility to CTL-Mediated Lysis Involves NANOG Induction in Target Cells. *The Journal of Immunology,* 187**,** 4031-4039.

HEDDLESTON, J. M., LI, Z., LATHIA, J. D., BAO, S., HJELMELAND, A. B. & RICH, J. N. 2010. Hypoxia inducible factors in cancer stem cells. *British journal of cancer,* 102**,** 789-795.

HEMMATI, H. D., NAKANO, I., LAZAREFF, J. A., MASTERMAN-SMITH, M., GESCHWIND, D. H., BRONNER-FRASER, M. & KORNBLUM, H. I. 2003. Cancerous stem cells can arise from pediatric brain tumors. *Proceedings of the National Academy of Sciences,* 100**,** 15178-15183.

HERMANN, P. C., HUBER, S. L., HERRLER, T., AICHER, A., ELLWART, J. W., GUBA, M., BRUNS, C. J. & HEESCHEN, C. 2007. Distinct Populations of Cancer Stem Cells Determine Tumor Growth and Metastatic Activity in Human Pancreatic Cancer. *Cell stem cell,* 1**,** 313-323.

HESS, D. A., MEYERROSE, T. E., WIRTHLIN, L., CRAFT, T. P., HERRBRICH, P. E., CREER, M. H. & NOLTA, J. A. 2004. Functional characterization of highly purified human hematopoietic repopulating cells isolated according to aldehyde dehydrogenase activity. *Blood,* 104**,** 1648-1655.

HILEMAN, E., LIU, J., ALBITAR, M., KEATING, M. & HUANG, P. 2004. Intrinsic oxidative stress in cancer cells: a biochemical basis for therapeutic selectivity. *Cancer Chemotherapy and Pharmacology,* 53**,** 209-219.

HIRSCHHAEUSER, F., MENNE, H., DITTFELD, C., WEST, J., MUELLER-KLIESER, W. & KUNZ-SCHUGHART, L. A. 2010. Multicellular tumor spheroids: An underestimated tool is catching up again. *Journal of Biotechnology,* 148**,** 3-15.

HIRSCHMANN-JAX, C., FOSTER, A. E., WULF, G. G., NUCHTERN, J. G., JAX, T. W., GOBEL, U., GOODELL, M. A. & BRENNER, M. K. 2004. A distinct "side population" of cells with high drug efflux capacity in human tumor cells. *Proceedings of the National Academy of Sciences of the United States of America,* 101**,** 14228-14233.

HO, M. M., NG, A. V., LAM, S. & HUNG, J. Y. 2007. Side Population in Human Lung Cancer Cell Lines and Tumors Is Enriched with Stem-like Cancer Cells. *Cancer Research,* 67**,** 4827-4833.

HOCKEL, M. & VAUPEL, P. 2001. Tumor Hypoxia: Definitions and Current Clinical, Biologic, and Molecular Aspects. *Journal of the National Cancer Institute,* 93**,** 266-276.

HOLOHAN, C., VAN SCHAEYBROECK, S., LONGLEY, D. B. & JOHNSTON, P. G. 2013. Cancer drug resistance: an evolving paradigm. *Nat Rev Cancer,* 13**,** 714-726.

HONOKI, K., FUJII, H., KUBO, A., KIDO, A., MORI, T., TANAKA, Y. & TSUJIUCHI, T. 2010. Possible involvement of stem-like populations with elevated ALDH1 in sarcomas for chemotherapeutic drug resistance. *Oncology Reports,* 24**,** 501-505.

HORST, D., KRIEGL, L., ENGEL, J., KIRCHNER, T. & JUNG, A. 2009. Prognostic Significance of the Cancer Stem Cell Markers CD133, CD44, and CD166 in Colorectal Cancer. *Cancer Investigation,* 27**,** 844-850.

HUANG, E. H., HYNES, M. J., ZHANG, T., GINESTIER, C., DONTU, G., APPELMAN, H., FIELDS, J. Z., WICHA, M. S. & BOMAN, B. M. 2009. Aldehyde Dehydrogenase 1 Is a Marker for Normal and Malignant Human Colonic Stem Cells (SC) and Tracks SC Overpopulation during Colon Tumorigenesis. *Cancer Research,* 69**,** 3382-3389.

HUANG, J., HU, N., GOLDSTEIN, A. M., EMMERT-BUCK, M. R., TANG, Z.-Z., ROTH, M. J., WANG, Q.-H., DAWSEY, S. M., HAN, X.-Y., DING, T., LI, G., GIFFEN, C. & TAYLOR, P. R. 2000. High frequency allelic loss on chromosome 17p13.3–p11.1 in esophageal squamous cell carcinomas from a high incidence area in northern China. *Carcinogenesis,* 21**,** 2019-2026.

JACKSON, B., BROCKER, C., THOMPSON, D., BLACK, W., VASILIOU, K., NEBERT, D. & VASILIOU, V. 2011. Update on the aldehyde dehydrogenase gene (ALDH) superfamily. *Human Genomics,* 5**,** 283 - 303.

JANUCHOWSKI, R., WOJTOWICZ, K. & ZABEL, M. 2013. The role of aldehyde dehydrogenase (ALDH) in cancer drug resistance. *Biomedicine & Pharmacotherapy,* 67**,** 669-680.

JEMAL, A., BRAY, F., CENTER, M. M., FERLAY, J., WARD, E. & FORMAN, D. 2011. Global cancer statistics. *CA: A Cancer Journal for Clinicians,* 61**,** 69-90.

JIANG, J., TANG, Y.-L. & LIANG, X.-H. 2011. EMT: a new vision of hypoxia promoting cancer progression. *Cancer biology & therapy,* 11**,** 714-723.

JORGENSEN, B. & KNUDTSON, J. 2015. Stop cancer colon. Colorectal cancer screening--updated guidelines. *South Dakota medicine : the journal of the South Dakota State Medical Association,* Spec No**,** 82-87.

KAHLERT, C., GAITZSCH, E., STEINERT, G., MOGLER, C., HERPEL, E., HOFFMEISTER, M., JANSEN, L., BENNER, A., BRENNER, H., CHANG-CLAUDE, J., RAHBARI, N., SCHMIDT, T., KLUPP, F., GRABE, N., LAHRMANN, B., KOCH, M., HALAMA, N., B¼CHLER, M. & WEITZ, J. 2012. Expression Analysis of Aldehyde Dehydrogenase 1A1 (ALDH1A1) in Colon and Rectal Cancer in Association with Prognosis and Response to Chemotherapy. *Annals of Surgical Oncology,* 19**,** 4193-4201.

KAUR, H., MAO, S., LI, Q., SAMENI, M., KRAWETZ, S. A., SLOANE, B. F. & MATTINGLY, R. R. 2012. RNA-Seq of Human Breast Ductal Carcinoma In Situ Models Reveals Aldehyde Dehydrogenase Isoform 5A1 as a Novel Potential Target. *PLoS ONE,* 7**,** e50249.

KAWASOE, M., YAMAMOTO, Y., OKAWA, K., FUNATO, T., TAKEDA, M., HARA, T., TSURUMI, H., MORIWAKI, H., ARIOKA, Y., TAKEMURA, M., MATSUNAMI, H., MARKEY, S. P. & SAITO, K. 2013. Acquired resistance of leukemic cells to AraC is associated with the upregulation of aldehyde dehydrogenase 1 family member A2. *Experimental Hematology,* 41**,** 597-603.e2.

KELM, J. M., TIMMINS, N. E., BROWN, C. J., FUSSENEGGER, M. & NIELSEN, L. K. 2003. Method for generation of homogeneous multicellular tumor spheroids applicable to a wide variety of cell types. *Biotechnology and Bioengineering,* 83**,** 173-180.

KHANNA, M., CHEN, C.-H., KIMBLE-HILL, A., PARAJULI, B., PEREZ-MILLER, S., BASKARAN, S., KIM, J., DRIA, K., VASILIOU, V., MOCHLY-ROSEN, D. & HURLEY, T. D. 2011. Discovery of a Novel

Class of Covalent Inhibitor for Aldehyde Dehydrogenases. *The Journal of Biological Chemistry,* 286**,** 43486-43494.

KIM, B., LEE, H. J., CHOI, H. Y., SHIN, Y., NAM, S., SEO, G., SON, D.-S., JO, J., KIM, J., LEE, J., KIM, J., KIM, K. & LEE, S. 2007. Clinical Validity of the Lung Cancer Biomarkers Identified by Bioinformatics Analysis of Public Expression Data. *Cancer Research,* 67**,** 7431-7438.

KIM, H., LAPOINTE, J., KAYGUSUZ, G., ONG, D. E., LI, C., VAN DE RIJN, M., BROOKS, J. D. & POLLACK, J. R. 2005. The Retinoic Acid Synthesis Gene ALDH1a2 Is a Candidate Tumor Suppressor in Prostate Cancer. *Cancer Research,* 65**,** 8118-8124.

KIM, R.-J., PARK, J.-R., ROH, K.-J., CHOI, A. R., KIM, S.-R., KIM, P.-H., YU, J. H., LEE, J. W., AHN, S.-H., GONG, G., HWANG, J.-W., KANG, K.-S., KONG, G., SHEEN, Y. Y. & NAM, J.-S. 2013. High aldehyde dehydrogenase activity enhances stem cell features in breast cancer cells by activating hypoxia-inducible factor-2α. *Cancer Letters,* 333**,** 18-31.

KLAUNIG, J. E., KAMENDULIS, L. M. & HOCEVAR, B. A. 2010. Oxidative Stress and Oxidative Damage in Carcinogenesis. *Toxicologic Pathology,* 38**,** 96-109.

KONDOH, M., OHGA, N., AKIYAMA, K., HIDA, Y., MAISHI, N., TOWFIK, A. M., INOUE, N., SHINDOH, M. & HIDA, K. 2013. Hypoxia-Induced Reactive Oxygen Species Cause Chromosomal Abnormalities in Endothelial Cells in the Tumor Microenvironment. *PLoS ONE,* 8**,** e80349.

KONG, Y., YOSHIDA, S., SAITO, Y., DOI, T., NAGATOSHI, Y., FUKATA, M., SAITO, N., YANG, S. M., IWAMOTO, C., OKAMURA, J., LIU, K. Y., HUANG, X. J., LU, D. P., SHULTZ, L. D., HARADA, M. & ISHIKAWA, F. 2008. CD34+CD38+CD19+ as well as CD34+CD38-CD19+ cells are leukemia-initiating cells with self-renewal capacity in human B-precursor ALL. *Leukemia,* 22**,** 1207-1213.

KOPPAKA, V., THOMPSON, D. C., CHEN, Y., ELLERMANN, M., NICOLAOU, K. C., JUVONEN, R. O., PETERSEN, D., DEITRICH, R. A., HURLEY, T. D. & VASILIOU, V. 2012. Aldehyde Dehydrogenase Inhibitors: a Comprehensive Review of the Pharmacology, Mechanism of Action, Substrate Specificity, and Clinical Application. *Pharmacological Reviews,* 64**,** 520-539.

KOUKOURAKIS, M. I., GIATROMANOLAKI, A., SIVRIDIS, E., SIMOPOULOS, C., TURLEY, H., TALKS, K., GATTER, K. C. & HARRIS, A. L. 2002. Hypoxia-inducible factor (HIF1A and HIF2A), angiogenesis, and chemoradiotherapy outcome of squamous cell head-and-neck cancer. *International Journal of Radiation Oncology • Biology • Physics,* 53**,** 1192-1202.

KOZOVSKA, Z., GABRISOVA, V. & KUCEROVA, L. 2014. Colon cancer: Cancer stem cells markers, drug resistance and treatment. *Biomedicine & Pharmacotherapy,* 68**,** 911-916.

KRISHAN, A. 1975. Rapid flow cytofluorometric analysis of mammalian cell cycle by propidium iodide staining. *The Journal of cell biology,* 66**,** 188-193.

KRUPENKO, S. A. & OLEINIK, N. V. 2002. 10-Formyltetrahydrofolate Dehydrogenase, One of the Major Folate Enzymes, Is Down-Regulated in Tumor Tissues and Possesses Suppressor Effects on Cancer Cells. *Cell Growth and Differentiation* 13**,** 227-236.

KUMAR, S., RAINA, K., AGARWAL, C. & AGARWAL, R. 2014. Silibinin strongly inhibits the growth kinetics of colon cancer stem cell-enriched spheroids by modulating interleukin 4/6-mediated survival signals. *Oncotarget,* 5**,** 4972-4989.

KUO, L. J. & YANG, L.-X. 2008. γ-H2AX - A Novel Biomarker for DNA Double-strand Breaks. *In Vivo,* 22**,** 305-309.

KUPERWASSER, C., HURLBUT, G. D., KITTRELL, F. S., DICKINSON, E. S., LAUCIRICA, R., MEDINA, D., NABER, S. P. & JERRY, D. J. 2000. Development of Spontaneous Mammary Tumors in BALB/c p53 Heterozygous Mice: A Model for Li-Fraumeni Syndrome. *The American Journal of Pathology,* 157**,** 2151-2159.

LACY, A. M., GARCÍA-VALDECASAS, J. C., DELGADO, S., CASTELLS, A., TAURÁ, P., PIQUÉ, J. M. & VISA, J. 2002. Laparoscopy-assisted colectomy versus open colectomy for treatment of non-metastatic colon cancer: a randomised trial. *The Lancet,* 359**,** 2224-2229.

LANGAN, R. C., MULLINAX, J. E., RAIJI, M. T., UPHAM, T., SUMMERS, T., STOJADINOVIC, A. & AVITAL, I. 2013. Colorectal Cancer Biomarkers and the Potential Role of Cancer Stem Cells. *Journal of Cancer,* 4**,** 241-250.

LAPIDOT, T., SIRARD, C., VORMOOR, J., MURDOCH, B., HOANG, T., CACERES-CORTES, J., MINDEN, M., PATERSON, B., CALIGIURI, M. A. & DICK, J. E. 1994. A cell initiating human acute myeloid leukaemia after transplantation into SCID mice. *Nature,* 367**,** 645-648.

LASSEN, N., BATEMAN, J. B., ESTEY, T., KUSZAK, J. R., NEES, D. W., PIATIGORSKY, J., DUESTER, G., DAY, B. J., HUANG, J., HINES, L. M. & VASILIOU, V. 2007. Multiple and additive functions of ALDH3A1 and ALDH1A1: cataract phenotype and ocular oxidative damage in Aldh3a1(-/-)/Aldh1a1(-/-) knock-out mice. *Journal of Biological Chemistry,* 282**,** 25668-25676.

LAURENT, J., FRONGIA, C., CAZALES, M., MONDESERT, O., DUCOMMUN, B. & LOBJOIS, V. 2013. Multicellular tumor spheroid models to explore cell cycle checkpoints in 3D. *BMC Cancer,* 13**,** 73.

LAW, P.-C., AUYEUNG, K., CHAN, L.-Y. & KO, J. 2012. Astragalus saponins downregulate vascular endothelial growth factor under cobalt chloride-stimulated hypoxia in colon cancer cells. *BMC Complementary and Alternative Medicine,* 12**,** 160.

LE MOGUEN, K., LINCET, H., MARCELO, P., LEMOISSON, E., HEUTTE, N., DUVAL, M., POULAIN, L., VINH, J., GAUDUCHON, P. & BAUDIN, B. 2007. A proteomic kinetic analysis of IGROV1 ovarian carcinoma cell line response to cisplatin treatment. *PROTEOMICS,* 7**,** 4090-4101.

LEE, S., BANG, S., SONG, K. & LEE, I. 2006. Differential expression in normal-adenoma-carcinoma sequence suggests complex molecular carcinogenesis in colon. *Oncology reports,* 16**,** 747-754.

LEVI, B. P., YILMAZ, Ã. M. H., DUESTER, G. & MORRISON, S. J. 2009. Aldehyde dehydrogenase 1a1 is dispensable for stem cell function in the mouse hematopoietic and nervous systems. *Blood,* 113**,** 1670-1680.

LI, C., HEIDT, D. G., DALERBA, P., BURANT, C. F., ZHANG, L., ADSAY, V., WICHA, M., CLARKE, M. F. & SIMEONE, D. M. 2007. Identification of Pancreatic Cancer Stem Cells. *Cancer Research,* 67**,** 1030-1037.

LI, P., ZHOU, C., XU, L. & XIAO, H. 2013. Hypoxia Enhances Stemness of Cancer Stem Cells in Glioblastoma: An In Vitro Study. *International Journal of Medical Sciences,* 10**,** 399-407.

LI, Y., TRUSH, M. A. & YAGER, J. D. 1994. DNA damage caused by reactive oxygen species originating from a copper-dependent oxidation of the 2-hydroxy catechol of estradiol. *Carcinogenesis,* 15**,** 1421-1427.

LIANG, C.-C., PARK, A. Y. & GUAN, J.-L. 2007. In vitro scratch assay: a convenient and inexpensive method for analysis of cell migration in vitro. *Nature Protocols* 2**,** 329-333.

LIAO, D. & JOHNSON, R. 2007. Hypoxia: A key regulator of angiogenesis in cancer. *Cancer and Metastasis Reviews,* 26**,** 281-290.

LIEBERMAN, D. 2010. Progress and Challenges in Colorectal Cancer Screening and Surveillance. *Gastroenterology,* 138**,** 2115-2126.

LIÈVRE, A., BACHET, J.-B., LE CORRE, D., BOIGE, V., LANDI, B., EMILE, J.-F., CÔTÉ, J.-F., TOMASIC, G., PENNA, C., DUCREUX, M., ROUGIER, P., PENAULT-LLORCA, F. & LAURENT-PUIG, P. 2006. KRAS Mutation Status Is Predictive of Response to Cetuximab Therapy in Colorectal Cancer. *Cancer Research,* 66**,** 3992-3995.

LIPINSKI, C. A. 2004. Lead- and drug-like compounds: the rule-of-five revolution. *Drug Discovery Today: Technologies,* 1**,** 337-341.

LIU, Q., BERCHNER-PFANNSCHMIDT, U., MÖLLER, U., BRECHT, M., WOTZLAW, C., ACKER, H., JUNGERMANN, K. & KIETZMANN, T. 2004. A Fenton reaction at the endoplasmic reticulum is involved in the redox control of hypoxia-inducible gene expression. *Proceedings of the National Academy of Sciences,* 101**,** 4302-4307.

LOPEZ-BARNEO, J. 2001. Cellular mechanisms of oxygen sensing. *Annual Review of Physiology,* 63**,** 259-287.

LUO, H.-Y., WEI, W., SHI, Y.-X., CHEN, X.-Q., LI, Y.-H., WANG, F., QIU, M.-Z., LI, F.-H., YAN, S.-L., ZENG, M.-S., HUANG, P. & XU, R.-H. 2010. Cetuximab enhances the effect of oxaliplatin on hypoxic gastric cancer cell lines. *Oncology reports,* 23**,** 1735-1745.

LUO, M., GATES, K. S., HENZL, M. T. & TANNER, J. J. 2015. Diethylaminobenzaldehyde Is a Covalent, Irreversible Inactivator of ALDH7A1. *ACS Chemical Biology,* 10**,** 693-697.

LUOTO, K. R., KUMARESWARAN, R. & BRISTOW, R. G. 2013. Tumor hypoxia as a driving force in genetic instability. *Genome Integrity,* 4**,** 5-5.

MA, I. & ALLAN, A. 2011. The Role of Human Aldehyde Dehydrogenase in Normal and Cancer Stem Cells. *Stem Cell Reviews and Reports,* 7**,** 292-306.

MA, S., CHAN, K. W., HU, L., LEE, T. K. W., WO, J. Y. H., NG, I. O. L., ZHENG, B. J. & GUAN, X. Y. 2007. Identification and Characterization of Tumorigenic Liver Cancer Stem/Progenitor Cells. *Gastroenterology,* 132**,** 2542-2556.

MAHMOOD, T. & YANG, P.-C. 2012. Western Blot: Technique, Theory, and Trouble Shooting. *North American Journal of Medical Sciences,* 4**,** 429-434.

MAO, P., JOSHI, K., LI, J., KIM, S.-H., LI, P., SANTANA-SANTOS, L., LUTHRA, S., CHANDRAN, U. R., BENOS, P. V., SMITH, L., WANG, M., HU, B., CHENG, S.-Y., SOBOL, R. W. & NAKANO, I. 2013. Mesenchymal glioma stem cells are maintained by activated glycolytic metabolism involving aldehyde dehydrogenase 1A3. *Proceedings of the National Academy of Sciences,* 110**,** 8644-8649.

MARCATO, P., DEAN, C. A., GIACOMANTONIO, C. A. & LEE, P. W. 2011a. Aldehyde dehydrogenase: its role as a cancer stem cell marker comes down to the specific isoform. *Cell cycle (Georgetown, Tex.),* 10**,** 1378-1384.

MARCATO, P., DEAN, C. A., PAN, D., ARASLANOVA, R., GILLIS, M., JOSHI, M., HELYER, L., PAN, L., LEIDAL, A., GUJAR, S.,

GIACOMANTONIO, C. A. & LEE, P. W. K. 2011b. Aldehyde Dehydrogenase Activity of Breast Cancer Stem Cells Is Primarily Due To Isoform ALDH1A3 and Its Expression Is Predictive of Metastasis. *STEM CELLS,* 29**,** 32-45.

MARCHITTI, S. A., BROCKER, C., STAGOS, D. & VASILIOU, V. 2008. Non-P450 aldehyde oxidizing enzymes: the aldehyde dehydrogenase superfamily. *Expert Opinion on Drug Metabolism & Toxicology,* 4**,** 697-720.

MARCHITTI, S. A., CHEN, Y., THOMPSON, D. C. & VASILIOU, V. 2011. Ultraviolet Radiation: Cellular Antioxidant Response and the Role of Ocular Aldehyde Dehydrogenase Enzymes. *Eye & contact lens,* 37**,** 206-213.

MARCHITTI, S. A., ORLICKY, D. J., BROCKER, C. & VASILIOU, V. 2010. Aldehyde Dehydrogenase 3B1 (ALDH3B1): Immunohistochemical Tissue Distribution and Cellular-specific Localization in Normal and Cancerous Human Tissues. *Journal of Histochemistry & Cytochemistry,* 58**,** 765-783.

MATHONNET, M., PERRAUD, A., CHRISTOU, N., AKIL, H., MELIN, C., BATTU, S., JAUBERTEAU, M.-O. & DENIZOT, Y. 2014. Hallmarks in colorectal cancer: Angiogenesis and cancer stem-like cells. *World Journal of Gastroenterology : WJG,* 20**,** 4189-4196.

MAUGERI-SACCÀ, M., VIGNERI, P. & DE MARIA, R. 2011. Cancer Stem Cells and Chemosensitivity. *Clinical Cancer Research,* 17**,** 4942-4947.

MAYBRIDGE, UK. 2015. *Screening libraries* [Online]. Available: http://www.maybridge.com/portal/alias__Rainbow/lang__en/tabID__191/DesktopDefault.aspx [Accessed 08/02/2016 2016].

MEDICO, E., RUSSO, M., PICCO, G., CANCELLIERE, C., VALTORTA, E., CORTI, G., BUSCARINO, M., ISELLA, C., LAMBA, S., MARTINOGLIO, B., VERONESE, S., SIENA, S., SARTORE-BIANCHI, A., BECCUTI, M., MOTTOLESE, M., LINNEBACHER, M., CORDERO, F., DI NICOLANTONIO, F. & BARDELLI, A. 2015. The molecular landscape of colorectal cancer cell lines unveils clinically actionable kinase targets. *Nature Communications,* 6.

MILLS, P. B., FOOTITT, E. J., MILLS, K. A., TUSCHL, K., AYLETT, S., VARADKAR, S., HEMINGWAY, C., MARLOW, N., RENNIE, J., BAXTER, P., DULAC, O., NABBOUT, R., CRAIGEN, W. J., SCHMITT, B., FEILLET, F., CHRISTENSEN, E., DE LONLAY, P., PIKE, M. G., HUGHES, M. I., STRUYS, E. A., JAKOBS, C., ZUBERI, S. M. & CLAYTON, P. T. 2010. Genotypic and phenotypic spectrum of pyridoxine-dependent epilepsy (ALDH7A1 deficiency). *Brain,* 133**,** 2148-2159.

MILONE, M. R., PUCCI, B., BIFULCO, K., IANNELLI, F., LOMBARDI, R., CIARDIELLO, C., BRUZZESE, F., CARRIERO, M. V. & BUDILLON, A. 2015. Proteomic analysis of zoledronic-acid resistant prostate cancer cells unveils novel pathways characterizing an invasive phenotype. *Oncotarget,* 6**,** 5324-5341.

MINN, I., WANG, H., MEASE, R. C., BYUN, Y., YANG, X., WANG, J., LEACH, S. D. & POMPER, M. G. 2014. A red-shifted fluorescent substrate for aldehyde dehydrogenase. *Nature Communications,* 5.

MOREB, J., BAKER, H., CHANG, L.-J., AMAYA, M., LOPEZ, M. C., OSTMARK, B. & CHOU, W. 2008. ALDH isozymes downregulation affects cell growth, cell motility and gene expression in lung cancer cells. *Molecular Cancer,* 7**,** 87.

MOREB, J. S., MONA, M., CHANG, L.-J., YEH, Y.-L., AMORY, J. & GOLDSTEIN, A. 2013. Abstract 3762: The role of aldehyde dehydrogenase isoenzymes in cancer cell proliferation, migration and drug resistance. Cancer Research, 73, 3762.

MOREB, J., MUHOCZY, D., OSTMARK, B. & ZUCALI, J. 2007. RNAi-mediated knockdown of aldehyde dehydrogenase class-1A1 and class-3A1 is specific and reveals that each contributes equally to the resistance against 4-hydroperoxycyclophosphamide. *Cancer Chemotherapy and Pharmacology,* 59**,** 127-136.

MOREB, J. S., SCHWEDER, M., GRAY, B., ZUCALI, J. & ZORI, R. 1998. In vitro selection for K562 cells with higher retrovirally mediated copy number of aldehyde dehydrogenase class-1 and higher resistance to 4-hydroperoxycyclophosphamide. *Human Gene Therapy,* 9**,** 611-619.

MOREB, J. S., UCAR, D., HAN, S., AMORY, J. K., GOLDSTEIN, A. S., OSTMARK, B. & CHANG, L.-J. 2012. The enzymatic activity of human aldehyde dehydrogenases 1A2 and 2 (ALDH1A2 and ALDH2) is detected by Aldefluor, inhibited by diethylaminobenzaldehyde and has significant effects on cell proliferation and drug resistance. *Chemico-Biological Interactions,* 195**,** 52-60.

MUZIO, G., MAGGIORA, M., PAIUZZI, E., ORALDI, M. & CANUTO, R. A. 2012. Aldehyde dehydrogenases and cell proliferation. *Free Radical Biology and Medicine,* 52**,** 735-746.

MUZIO, G., TROMBETTA, A., MARTINASSO, G., CANUTO, R. A. & MAGGIORA, M. 2003. Antisense oligonucleotides against aldehyde dehydrogenase 3 inhibit hepatoma cell proliferation by affecting MAP kinases. *Chemico-Biological Interactions,* 143–144**,** 37-43.

NAGANO, M., KIMURA, K., T, Y., K, O., D, N., H, H., H, Y., N, O. & O, O. 2010. Hypoxia responsive mesenchymal stem cells derived from human

umbilical cord blood are effective for bone repair. *Stem Cells and Development,* 19**,** 1195-210.

NAKAMURA, M., BODILY, J. M., BEGLIN, M., KYO, S., INOUE, M. & LAIMINS, L. A. 2009. Hypoxia-specific stabilization of HIF-1alpha by human papillomaviruses. *Virology,* 387**,** 442-448.

NAUJOKAT, C. & STEINHART, R. 2012. Salinomycin as a drug for targeting human cancer stem cells. *Journal of biomedicine & biotechnology,* 2012**,** 950658.

O'CONNOR, K. C. 1999. Three-Dimensional Cultures of Prostatic Cells: Tissue Models for the Development of Novel Anti-Cancer Therapies. *Pharmaceutical Research,* 16**,** 486-493.

O/'BRIEN, C. A., POLLETT, A., GALLINGER, S. & DICK, J. E. 2007. A human colon cancer cell capable of initiating tumour growth in immunodeficient mice. *Nature,* 445**,** 106-110.

OKAMURA, S., NG, C. C., KOYAMA, K., TAKEI, Y., ARAKAWA, H., MONDEN, M. & NAKAMURA, Y. 1999. Identification of seven genes regulated by wild-type p53 in a colon cancer cell line carrying a well-controlled wild-type p53 expression system. *Oncology research,* 11**,** 281-285.

OLEINIK, N. V. & KRUPENKO, S. A. 2003. Ectopic Expression of 10-Formyltetrahydrofolate Dehydrogenase in A549 Cells Induces G1 Cell Cycle Arrest and Apoptosis1 1 NIH grant DK54388. *Molecular Cancer Research,* 1**,** 577-588.

PAPPA, A., CHEN, C., KOUTALOS, Y., TOWNSEND, A. J. & VASILIOU, V. 2003a. Aldh3a1 protects human corneal epithelial cells from ultraviolet- and 4-hydroxy-2-nonenal-induced oxidative damage. *Free Radical Biology and Medicine,* 34**,** 1178-1189.

PAPPA, A., ESTEY, T., MANZER, R., BROWN, D. & VASILIOU, V. 2003b. Human aldehyde dehydrogenase 3A1 (ALDH3A1): biochemical characterization and immunohistochemical localization in the cornea. *Biochemical journal,* 376**,** 615–623.

PARAJULI, B., FISHEL, M. L. & HURLEY, T. D. 2014. Selective ALDH3A1 Inhibition by Benzimidazole Analogues Increase Mafosfamide Sensitivity in Cancer Cells. *Journal of Medicinal Chemistry,* 57**,** 449-461.

PARKER GIBBS, V. G. K., JOHN D REITH, OLGA N TCHIGRINOVA, OLEG N SUSLOV, EDWARD W SCOTT, STEVEN C. GHIVIZANNI, TATYANA N IGNATOVA AND DENNIS A. STEINDLER 2005. Stem-like cells in bone sarcomas: implications for tumorigenesis. *Neoplasia,* 7**,** 967–976.

PATEL, M., LU, L., ZANDER, D. S., SREERAMA, L., COCO, D. & MOREB, J. S. 2008. ALDH1A1 and ALDH3A1 expression in lung cancers:

Correlation with histologic type and potential precursors. *Lung Cancer,* 59**,** 340-349.

PHILLIPS, R. M., DE LA CRUZ, A., TRAVER, R. D. & GIBSON, N. W. 1994. Increased Activity and Expression of NAD(P)H:Quinone Acceptor Oxidoreductase in Confluent Cell Cultures and within Multicellular Spheroids. *Cancer Research,* 54**,** 3766-3771.

PIRET, J.-P., MOTTET, D., RAES, M. & MICHIELS, C. 2002. CoCl2, a Chemical Inducer of Hypoxia-Inducible Factor-1, and Hypoxia Reduce Apoptotic Cell Death in Hepatoma Cell Line HepG2. *Annals of the New York Academy of Sciences,* 973**,** 443-447.

POON, E., HARRIS, A. L. & ASHCROFT, M. 2009. Targeting the hypoxia-inducible factor (HIF) pathway in cancer. *Expert Reviews in Molecular Medicine,* 11**,** e26.

PORS, K. & MOREB, J. S. 2014. Aldehyde dehydrogenases in cancer: an opportunity for biomarker and drug development? *Drug Discovery Today,* 19**,** 1953-1963.

PRINCE, M. E., SIVANANDAN, R., KACZOROWSKI, A., WOLF, G. T., KAPLAN, M. J., DALERBA, P., WEISSMAN, I. L., CLARKE, M. F. & AILLES, L. E. 2007. Identification of a subpopulation of cells with cancer stem cell properties in head and neck squamous cell carcinoma. *Proceedings of the National Academy of Sciences,* 104**,** 973-978.

PROKOPCZYK, B., SINHA, I., TRUSHIN, N., FREEMAN, W. M. & EL-BAYOUMY, K. 2009. Gene expression profiles in HPV-immortalized human cervical cells treated with the nicotine-derived carcinogen 4-(methylnitrosamino)-1-(3-pyridyl)-1-butanone. *Chemico-biological interactions,* 177**,** 173-180.

PUPPA, G., SONZOGNI, A., COLOMBARI, R. & PELOSI, G. 2010. TNM Staging System of Colorectal Carcinoma: A Critical Appraisal of Challenging Issues. *Archives of Pathology & Laboratory Medicine,* 134**,** 837-852.

QU, X., YANG, M.-X., KONG, B.-H., QI, L., LAM, Q. L. K., YAN, S., LI, P., ZHANG, M. & LU, L. 2005. Hypoxia inhibits the migratory capacity of human monocyte-derived dendritic cells. *Immunology and Cell Biology,* 83**,** 668-673.

QUIRKE, P., WILLIAMS, G. T., ECTORS, N., ENSARI, A., PIARD, F. & NAGTEGAAL, I. 2007. The future of the TNM staging system in colorectal cancer: time for a debate? *The Lancet Oncology,* 8**,** 651-657.

RAHA, D., WILSON, T. R., PENG, J., PETERSON, D., YUE, P., EVANGELISTA, M., WILSON, C., MERCHANT, M. & SETTLEMAN, J. 2014. The Cancer Stem Cell Marker Aldehyde Dehydrogenase Is

Required to Maintain a Drug-Tolerant Tumor Cell Subpopulation. *Cancer Research,* 74**,** 3579-3590.

RAO, D. D., VORHIES, J. S., SENZER, N. & NEMUNAITIS, J. 2009. siRNA vs. shRNA: Similarities and differences. *Advanced Drug Delivery Reviews,* 61**,** 746-759.

REISDORPH, R. & LINDAHL, R. 1998. Hypoxia Exerts Cell-Type-Specific Effects on Expression of the Class 3 Aldehyde Dehydrogenase Gene. *Biochemical and Biophysical Research Communications,* 249**,** 709-712.

REISDORPH, R. & LINDAHL, R. 2001. Aldehyde dehydrogenase 3 gene regulation: studies on constitutive and hypoxia-modulated expression. *Chemico-Biological Interactions,* 130–132**,** 227-233.

REUTER, S., GUPTA, S. C., CHATURVEDI, M. M. & AGGARWAL, B. B. 2010. Oxidative stress, inflammation, and cancer: How are they linked? *Free Radical Biology and Medicine,* 49**,** 1603-1616.

REXER, B. N., LI ZHENG, W. & ONG, D. E. 2001. Retinoic Acid Biosynthesis by Normal Human Breast Epithelium Is via Aldehyde Dehydrogenase 6, Absent in MCF-7 Cells. *Cancer Research,* 61**,** 7065-7070.

RICCI-VITIANI, L., LOMBARDI, D. G., PILOZZI, E., BIFFONI, M., TODARO, M., PESCHLE, C. & DE MARIA, R. 2007. Identification and expansion of human colon-cancer-initiating cells. *Nature,* 445**,** 111-115.

RIEGER, A. M., NELSON, K. L., KONOWALCHUK, J. D. & BARREDA, D. R. 2011. Modified Annexin V/Propidium Iodide Apoptosis Assay For Accurate Assessment of Cell Death. *Journal of Visualized Experiments : JoVE***,** 2597.

ROHWER, N., ZASADA, C., KEMPA, S. & CRAMER, T. 2013. The growing complexity of HIF-1[alpha]/'s role in tumorigenesis: DNA repair and beyond. *Oncogene,* 32**,** 3569-3576.

ROSE, A. E., POLISENO, L., WANG, J., CLARK, M., PEARLMAN, A., WANG, G., VEGA Y SAENZ DE MIERA, E. C., MEDICHERLA, R., CHRISTOS, P. J., SHAPIRO, R., PAVLICK, A., DARVISHIAN, F., ZAVADIL, J., POLSKY, D., HERNANDO, E., OSTRER, H. & OSMAN, I. 2011. Integrative Genomics Identifies Molecular Alterations that Challenge the Linear Model of Melanoma Progression. *Cancer Research,* 71**,** 2561-2571.

ROSS, S. W., DALTON, D. A., KRAMER, S. & CHRISTENSEN, B. L. 2001. Physiological (antioxidant) responses of estuarine fishes to variability in dissolved oxygen. *Comparative biochemistry and physiology. Toxicology & pharmacology : CBP,* 130**,** 289-303.

RUAN, K., SONG, G. & OUYANG, G. 2009. Role of hypoxia in the hallmarks of human cancer. *Journal of Cellular Biochemistry,* 107**,** 1053-1062.

RUSSO, J., CHUNG, S., CONTRERAS, K., LIAN, B., LORENZ, J., STEVENS, D. & TROUSDELL, W. 1995. Identification of 4-(N,N-dipropylamino)benzaldehyde as a potent, reversible inhibitor of mouse and human class I aldehyde dehydrogenase. *Biochemical Pharmacology,* 50**,** 399-406.

SAIGUSA, S., TANAKA, K., TOIYAMA, Y., YOKOE, T., OKUGAWA, Y., IOUE, Y., MIKI, C. & KUSUNOKI, M. 2009. Correlation of CD133, OCT4, and SOX2 in Rectal Cancer and Their Association with Distant Recurrence After Chemoradiotherapy. *Annals of Surgical Oncology,* 16**,** 3488-3498.

SAW, Y.-T., YANG, J., NG, S.-K., LIU, S., SINGH, S., SINGH, M., WELCH, W., TSUDA, H., FONG, W.-P., THOMPSON, D., VASILIOU, V., BERKOWITZ, R. & NG, S.-W. 2012. Characterization of aldehyde dehydrogenase isozymes in ovarian cancer tissues and sphere cultures. *BMC Cancer,* 12**,** 329.

SCHACHT, V. & KERN, J. S. 2015. Basics of Immunohistochemistry. *J Invest Dermatol,* 135**,** e30.

SCHATTON, T., MURPHY, G. F., FRANK, N. Y., YAMAURA, K., WAAGA-GASSER, A. M., GASSER, M., ZHAN, Q., JORDAN, S., DUNCAN, L. M., WEISHAUPT, C., FUHLBRIGGE, R. C., KUPPER, T. S., SAYEGH, M. H. & FRANK, M. H. 2008. Identification of cells initiating human melanomas. *Nature,* 451**,** 345-349.

SEMENZA, G. L. 2010. Defining the role of hypoxia-inducible factor 1 in cancer biology and therapeutics. *Oncogene,* 29**,** 625-634.

SEMENZA, G. L. 2012. Hypoxia-inducible factors: mediators of cancer progression and targets for cancer therapy. *Trends in Pharmacological Sciences,* 33**,** 207-214.

SEMENZA, G. L. 2016. The hypoxic tumor microenvironment: A driving force for breast cancer progression. *Biochimica et Biophysica Acta (BBA) - Molecular Cell Research,* 1863**,** 382-391.

SHMELKOV, S. V., BUTLER, J. M., HOOPER, A. T., HORMIGO, A., KUSHNER, J., MILDE, T., ST. CLAIR, R., BALJEVIC, M., WHITE, I., JIN, D. K., CHADBURN, A., MURPHY, A. J., VALENZUELA, D. M., GALE, N. W., THURSTON, G., YANCOPOULOS, G. D., D'ANGELICA, M., KEMENY, N., LYDEN, D. & RAFII, S. 2008. CD133 expression is not restricted to stem cells, and both CD133(+) and CD133(–) metastatic colon cancer cells initiate tumors. *The Journal of Clinical Investigation,* 118**,** 2111-2120.

SIEUWERTS, A., KLIJN, J., PETERS, H. & FOEKENS, J. A. 1995. The MTT tetrazolium salt assay scrutinized: how to use this assay reliably to measure metabolic activity of cell cultures in vitro for the assessment of growth characteristics, IC50-values and cell survival. *European journal of clinical chemistry and clinical biochemistry,* 33**,** 813-23.

SILVA, I. A., BAI, S., MCLEAN, K., YANG, K., GRIFFITH, K., THOMAS, D., GINESTIER, C., JOHNSTON, C., KUECK, A., REYNOLDS, R. K., WICHA, M. S. & BUCKANOVICH, R. J. 2011. Aldehyde Dehydrogenase in Combination with CD133 Defines Angiogenic Ovarian Cancer Stem Cells That Portend Poor Patient Survival. *Cancer Research,* 71**,** 3991-4001.

SLADEK, N., KOLLANDER, R., SREERAMA, L. & KIANG, D. 2002. Cellular levels of aldehyde dehydrogenases (ALDH1A1 and ALDH3A1) as predictors of therapeutic responses to cyclophosphamide-based chemotherapy of breast cancer: a retrospective study. *Cancer Chemotherapy and Pharmacology,* 49**,** 309-321.

SLÁDEK, N. E. 2003. Human aldehyde dehydrogenases: Potential pathological, pharmacological, and toxicological impact. *Journal of Biochemical and Molecular Toxicology,* 17**,** 7-23.

SODEK, K. L., RINGUETTE, M. J. & BROWN, T. J. 2009. Compact spheroid formation by ovarian cancer cells is associated with contractile behavior and an invasive phenotype. *International Journal of Cancer,* 124**,** 2060-2070.

SONG, I.-S., WANG, A.-G., YOON, S. Y., KIM, J.-M., KIM, J. H., LEE, D.-S. & KIM, N.-S. 2009. Regulation of glucose metabolism-related genes and VEGF by HIF-1[alpha] and HIF-1[beta], but not HIF-2[alpha], in gastric cancer. *Experimental and Molecular Medicine* 41**,** 51-58.

SOREIDE, K., BERG, M., SKUDAL, B. S. & NEDREBOE, B. S. 2011. Advances in the understanding and treatment of colorectal cancer. *Discovery medicine,* 12**,** 393-404.

SREERAMA, L. & SLADEK, N. E. 1993. Identification and characterization of a novel class 3 aldehyde dehydrogenase overexpressed in a human breast adenocarcinoma cell line exhibiting oxazaphosphorine-specific acquired resistance. *Biochemical Pharmacology,* 45**,** 2487-2505.

SREERAMA, L. & SLADEK, N. E. 1997. Cellular levels of class 1 and class 3 aldehyde dehydrogenases and certain other drug-metabolizing enzymes in human breast malignancies. *Clinical Cancer Research,* 3**,** 1901-1914.

STEWART, M. J., MALEK, K., XIAO, Q., DIPPLE, K. M. & CRABB, D. W. 1995. The Novel Aldehyde Dehydrogenase Gene, ALDH5, Encodes an Active Aldehyde Dehydrogenase Enzyme. *Biochemical and Biophysical Research Communications,* 211**,** 144-151.

STORMS, R. W., TRUJILLO, A. P., SPRINGER, J. B., SHAH, L., COLVIN, O. M., LUDEMAN, S. M. & SMITH, C. 1999. Isolation of primitive human hematopoietic progenitors on the basis of aldehyde dehydrogenase activity. *Proceedings of the National Academy of Sciences,* 96**,** 9118-9123.

STORZ, P. 2005. Reactive oxygen species in tumor progression. *Frontiers in bioscience*, 10,1881-1896.

STROBER, W. 2001. Trypan Blue Exclusion Test of Cell Viability. *Current Protocols in Immunology.* John Wiley & Sons, Inc.

SU, Y., QIU, Q., ZHANG, X., JIANG, Z., LENG, Q., LIU, Z., STASS, S. A. & JIANG, F. 2010. Aldehyde Dehydrogenase 1 A1-Positive Cell Population Is Enriched in Tumor-Initiating Cells and Associated with Progression of Bladder Cancer. *Cancer Epidemiology Biomarkers & Prevention,* 19**,** 327-337.

SUN, Q.-L., SHA, H.-F., YANG, X.-H., BAO, G.-L., LU, J. & XIE, Y.-Y. 2011. Comparative proteomic analysis of paclitaxel sensitive A549 lung adenocarcinoma cell line and its resistant counterpart A549-Taxol. *Journal of Cancer Research and Clinical Oncology,* 137**,** 521-532.

SUTHERLAND, R. M. 1998. Tumor Hypoxia and Gene Expression: Implications for Malignant Progression and Therapy. *Acta Oncologica,* 37**,** 567-574.

TANEI, T., MORIMOTO, K., SHIMAZU, K., KIM, S. J., TANJI, Y., TAGUCHI, T., TAMAKI, Y. & NOGUCHI, S. 2009. Association of Breast Cancer Stem Cells Identified by Aldehyde Dehydrogenase 1 Expression with Resistance to Sequential Paclitaxel and Epirubicin-Based Chemotherapy for Breast Cancers. *Clinical Cancer Research,* 15**,** 4234-4241.

TANG, X., KUHLENSCHMIDT, T. B., LI, Q., ALI, S., LEZMI, S., CHEN, H., PIRES-ALVES, M., LAEGREID, W. W., SAIF, T. A. & KUHLENSCHMIDT, M. S. 2014. A mechanically-induced colon cancer cell population shows increased metastatic potential. *Molecular cancer* [Online], 13. [Accessed 2014].

TODARO, M., IOVINO, F., ETERNO, V., CAMMARERI, P., GAMBARA, G., ESPINA, V., GULOTTA, G., DIELI, F., GIORDANO, S., DE MARIA, R. & STASSI, G. 2010. Tumorigenic and Metastatic Activity of Human Thyroid Cancer Stem Cells. *Cancer Research,* 70**,** 8874-8885.

TORRECILLA, J., RODRÍGUEZ-GASCÓN, A., SOLINÍS, M. Á. & DEL POZO-RODRÍGUEZ, A. 2014. Lipid nanoparticles as carriers for RNAi against viral infections: current status and future perspectives. *BioMed research international,* 2014**,** 161794.

TOUIL, Y., IGOUDJIL, W., CORVAISIER, M., DESSEIN, A.-F., VANDOMME, J., MONTÉ, D., STECHLY, L., SKRYPEK, N., LANGLOIS, C., GRARD, G., MILLET, G., LETEURTRE, E., DUMONT, P., TRUANT, S., PRUVOT, F.-R., HEBBAR, M., FAN, F., ELLIS, L. M., FORMSTECHER, P., VAN SEUNINGEN, I., GESPACH, C., POLAKOWSKA, R. & HUET, G. 2014. Colon Cancer Cells Escape 5FU Chemotherapy-Induced Cell Death by Entering Stemness and Quiescence Associated with the c-Yes/YAP Axis. *Clinical Cancer Research,* 20**,** 837-846.

TURNER, L., SCOTTON, C., NEGUS, R. & BALKWILL, F. 1999. Hypoxia inhibits macrophage migration. *European Journal of Immunology,* 29**,** 2280-2287.

UCAR, D., COGLE, C. R., ZUCALI, J. R., OSTMARK, B., SCOTT, E. W., ZORI, R., GRAY, B. A. & MOREB, J. S. 2009. Aldehyde dehydrogenase activity as a functional marker for lung cancer. *Chemico-Biological Interactions,* 178**,** 48-55.

UROSEVIC, J., NEBREDA, A. R. & GOMIS, R. R. 2014. MAPK signaling control of colon cancer metastasis. *Cell Cycle,* 13**,** 2641-2642.

USHIO-FUKAI, M. & NAKAMURA, Y. 2008. Reactive oxygen species and angiogenesis: NADPH oxidase as target for cancer therapy. *Cancer Letters,* 266**,** 37-52.

VAN DEN HOOGEN, C., VAN DER HORST, G., CHEUNG, H., BUIJS, J., PELGER, R. M. & VAN DER PLUIJM, G. 2011. The aldehyde dehydrogenase enzyme 7A1 is functionally involved in prostate cancer bone metastasis. *Clinical & Experimental Metastasis,* 28**,** 615-625.

VAN DEN HOOGEN, C., VAN DER HORST, G., CHEUNG, H., BUIJS, J. T., LIPPITT, J. M., GUZMÁN-RAMÍREZ, N., HAMDY, F. C., EATON, C. L., THALMANN, G. N., CECCHINI, M. G., PELGER, R. C. M. & VAN DER PLUIJM, G. 2010. High Aldehyde Dehydrogenase Activity Identifies Tumor-Initiating and Metastasis-Initiating Cells in Human Prostate Cancer. *Cancer Research,* 70**,** 5163-5173.

VARIA, M. A., CALKINS-ADAMS, D. P., RINKER, L. H., KENNEDY, A. S., NOVOTNY, D. B., FOWLER, W. C., JR. & RALEIGH, J. A. 1998. Pimonidazole: A Novel Hypoxia Marker for Complementary Study of Tumor Hypoxia and Cell Proliferation in Cervical Carcinoma. *Gynecologic Oncology,* 71**,** 270-277.

VASILIOU, V. & NEBERT, D. 2005. Analysis and update of the human aldehyde dehydrogenase (ALDH) gene family. *Human Genomics,* 2**,** 138 - 143.

VASILIOU, V., PAPPA, A. & ESTEY, T. 2004. Role of Human Aldehyde Dehydrogenases in Endobiotic and Xenobiotic Metabolism. *Drug Metabolism Reviews,* 36**,** 279-299.

VERDUZCO, D., LLOYD, M., XU, L., IBRAHIM-HASHIM, A., BALAGURUNATHAN, Y., GATENBY, R. A. & GILLIES, R. J. 2015. Intermittent Hypoxia Selects for Genotypes and Phenotypes That Increase Survival, Invasion, and Therapy Resistance. *PLoS ONE,* 10**,** e0120958.

VIALE, A., DE FRANCO, F., ORLETH, A., CAMBIAGHI, V., GIULIANI, V., BOSSI, D., RONCHINI, C., RONZONI, S., MURADORE, I., MONESTIROLI, S., GOBBI, A., ALCALAY, M., MINUCCI, S. & PELICCI, P. G. 2009. Cell-cycle restriction limits DNA damage and maintains self-renewal of leukaemia stem cells. *Nature,* 457**,** 51-56.

WALEH, N. S., BRODY, M. D., KNAPP, M. A., MENDONCA, H. L., LORD, E. M., KOCH, C. J., LADEROUTE, K. R. & SUTHERLAND, R. M. 1995. Mapping of the Vascular Endothelial Growth Factor-producing Hypoxic Cells in Multicellular Tumor Spheroids Using a Hypoxia-specific Marker. *Cancer Research,* 55**,** 6222-6226.

WANG, L., PARK, P., LA MARCA, F., THAN, K. D. & LIN, C.-Y. 2015. BMP-2 inhibits tumor-initiating ability in human renal cancer stem cells and induces bone formation. *Journal of cancer research and clinical oncology,* 141**,** 1013-1024.

WARFEL, N. A. & EL-DEIRY, W. S. 2014. HIF-1 Signaling in Drug Resistance to Chemotherapy. *Current Medicinal Chemistry,* 21**,** 3021-3028.

WEBER, T. S., JAEHNERT, I., SCHICHOR, C., OR-GUIL, M. & CARNEIRO, J. 2014. Quantifying the Length and Variance of the Eukaryotic Cell Cycle Phases by a Stochastic Model and Dual Nucleoside Pulse Labelling. *PLoS Computational Biology,* 10**,** e1003616.

WELJIE, A. M. & JIRIK, F. R. 2011. Hypoxia-induced metabolic shifts in cancer cells: Moving beyond the Warburg effect. *The International Journal of Biochemistry & Cell Biology,* 43**,** 981-989.

WILSON, W. R. & HAY, M. P. 2011. Targeting hypoxia in cancer therapy. *Nature Reviews Cancer* 11**,** 393-410.

WINDER, T. & LENZ, H.-J. 2010. Molecular Prognostic Markers in Colon Cancer. *In:* BEAUCHEMIN, N. & HUOT, J. (eds.) *Metastasis of Colorectal Cancer.* Springer Netherlands.

WOUTERS, A., PAUWELS, B., LARDON, F. & VERMORKEN, J. B. 2007. Review: Implications of In Vitro Research on the Effect of Radiotherapy

and Chemotherapy Under Hypoxic Conditions. *The Oncologist,* 12**,** 690-712.

YAMASHITA, S., TSUJINO, Y., MORIGUCHI, K., TATEMATSU, M. & USHIJIMA, T. 2006. Chemical genomic screening for methylation-silenced genes in gastric cancer cell lines using 5-aza-2′-deoxycytidine treatment and oligonucleotide microarray. *Cancer Science,* 97**,** 64-71.

YANAGAWA, Y., CHEN, J. C., HSU, L. C. & YOSHIDA, A. 1995. The transcriptional regulation of human aldehyde dehydrogenase I gene. The structural and functional analysis of the promoter. *Journal of Biological Chemistry,* 270**,** 17521-17527.

YANG, J., STAPLES, O., THOMAS, L. W., BRISTON, T., ROBSON, M., POON, E., SIM, XF, ES, M. L., EL-EMIR, E., BUFFA, F. M., AHMED, A., ANNEAR, N. P., SHUKLA, D., PEDLEY, B. R., MAXWELL, P. H., HARRIS, A. L. & ASHCROFT, M. 2012. Human CHCHD4 mitochondrial proteins regulate cellular oxygen consumption rate and metabolism and provide a critical role in hypoxia signaling and tumor progression. *The Journal of Clinical Investigation,* 122**,** 600-611.

YANG, Z.-L., YANG, L., ZOU, Q., YUAN, Y., LI, J., LIANG, L., ZENG, G. & CHEN, S. 2013. Positive ALDH1A3 and negative GPX3 expressions are biomarkers for poor prognosis of gallbladder cancer. *Disease markers,* 35**,** 163-172.

YANG, Z. F., HO, D. W., NG, M. N., LAU, C. K., YU, W. C., NGAI, P., CHU, P. W. K., LAM, C. T., POON, R. T. P. & FAN, S. T. 2008. Significance of CD90+ Cancer Stem Cells in Human Liver Cancer. *Cancer cell,* 13**,** 153-166.

YOKOYAMA, A., MURAMATSU, T., OHMORI, T., YOKOYAMA, T., OKUYAMA, K., TAKAHASHI, H., HASEGAWA, Y., HIGUCHI, S., MARUYAMA, K., SHIRAKURA, K. & ISHII, H. 1998. Alcohol-related cancers and aldehyde dehydrogenase-2 in Japanese alcoholics. *Carcinogenesis,* 19**,** 1383-1387.

YOON, K.-A., NAKAMURA, Y. & ARAKAWA, H. 2004. Identification of ALDH4 as a p53-inducible gene and its protective role in cellular stresses. *Journal of Human Genetics,* 49**,** 134-140.

YOSHIDA, A., RZHETSKY, A., HSU, L. C. & CHANG, C. 1998. Human aldehyde dehydrogenase gene family. *European Journal of Biochemistry,* 251**,** 549-557.

ZENG, W., LIU, P., PAN, W., SINGH, S. R. & WEI, Y. 2015. Hypoxia and hypoxia inducible factors in tumor metabolism. *Cancer Letters,* 356**,** 263-267.

ZHOU, B.-B. S., ZHANG, H., DAMELIN, M., GELES, K. G., GRINDLEY, J. C. & DIRKS, P. B. 2009. Tumour-initiating cells: challenges and opportunities for anticancer drug discovery. *Nature Reviews Drug Discovery* 8**,** 806-823.

ZIECH, D., FRANCO, R., GEORGAKILAS, A. G., GEORGAKILA, S., MALAMOU-MITSI, V., SCHONEVELD, O., PAPPA, A. & PANAYIOTIDIS, M. I. 2010. The role of reactive oxygen species and oxidative stress in environmental carcinogenesis and biomarker development. *Chemico-Biological Interactions,* 188**,** 334-339.

Appendix

Appendix I: Composition and storage of cell culture media (Storage in brackets).

Phosphate buffer saline (PBS, pH 7.4)

PBS was obtained from sigma and stored at room temperature.

1x RPMI culture media

Complete RPMI 1640 (4ºC) was prepared from incomplete RPMI 1640 (Sigma) (4ºC), foetal bovine serum (Sigma) (-20ºC) 10% (v/v), L-glutamine (Sigma) (-20ºC) 1% (v/v) and sodium pyruvate (Sigma) (4ºC) 1% (v/v).

2x RPMI culture media

Complete RPMI 1640 (4ºC) was prepared from incomplete RPMI 1640 (Sigma) (4ºC), foetal bovine serum (Sigma) (-20ºC) 20% (v/v), L-glutamine (Sigma) (-20ºC) 2% (v/v) and sodium pyruvate (Sigma) (4ºC) 2% (v/v).

1x RPMI phenol red free culture media

Complete RPMI (4ºC) was prepared from incomplete phenol red free RPMI (Gibco) (4ºC), foetal bovine serum (Sigma) (-20ºC) 10% (v/v), L-glutamine (Sigma) (-20ºC) 1% (v/v) and sodium pyruvate (Sigma) (4ºC) 1% (v/v).

2x RPMI phenol red free culture media

Complete RPMI (4ºC) was prepared from incomplete phenol red free RPMI (Gibco) (4ºC), foetal bovine serum (Sigma) (-20ºC) 20% (v/v), L-glutamine (Sigma) (-20ºC) 2% (v/v) and sodium pyruvate (Sigma) (4ºC) 2% (v/v).

Trypsin/ EDTA solution

Trypsin/ EDTA solution 0.25% was obtained from sigma (-20ºC).

Appendix II: Composition and storage of MTT assay solutions.

3-(4,5-dimethylthiazol-2-yl)-2,5-diphenyltetrazolium bromide (MTT) stock solution

The MTT stock solution (5 mg/ml) was prepared by dissolving MTT powder (sigma) in ultrapure water, which was then passed through a 0.2 µM sterile syringe filter (corning incorporated). The resulting solution was stored at 4ºC for a maximum 4-6 weeks.

The MTT working solution (0.5 mg/ml) was prepared immediately before use by diluting 2 ml of MTT stock solution in 18 ml of complete RPMI medium.

Dimethyl sulfoxide (DMSO) solution

DMSO was obtained from sigma and stored at room temperature.

Appendix III: qRT-PCR primers

All primers were purchased from PrimerDesign^{TM}.

Target gene	Sense Primer	Anti-sense Primer	Amplicon length (bp)	Tm (C˚)
ALDH 1A1	CCAAGTGCTCTATCAGAACCAAAT	TCGGTGAGTAGGACAGGTAAGT	108	74.9
ALDH1A2	AATAACTCAGACTTTGGACTCGTA	TGGGCATTTAAGGCATTGTAAC	125	72.2
ALDH1A3	CAGCAGCCGTGTTCACAAA	ATAGAGGGCGTTGTAGCAGTT	98	73.5
ALDH1B1	CAGTCACAGTCCAGCAATTCC	GCTTTATTTGTGGGGTTTCTTCTAA	119	71.5
ALDH 2	GTGGGTCAACTGCTATGATGTG	TATGAGTTCTTCTGAGGCACTTTG	150	77.3
ALDH 3A1	GATGAGCCCGTGGAGAAGA	GCTGGATGGTGAGGTTGAAG	121	79.4
ALDH7A1	TGTCACAAAGATAATAGCCAAGGTT	CAGCAGGTTCACTCGTTCATC	124	74
VEGFA	CCAGGAAAGACTGATACAGAACG	GGTTTCTGGATTAAGGACTGTTC	93	85.3
HIF1α	TGCCACATCATCACCATATAGAG	TGACTCAAAGCGACAGATAACA	132	72.8
HIF2α (EPAS1)	CCTCCCCACCTTCAATGACT	CTCCCTACAGAAGAACAGACATG	121	71.9

Table 14 qRT-PCR primers.

Appendix IV: Solutions for molecular biology (Western blot)

All reagents were purchased from Sigma unless otherwise specified.

RIPA lysis buffer stock solution

150 mM NaCl, 1.0% IGEPAL® CA-630, 0.5% sodium deoxycholate, 0.1% SDS (GE Healthcare), 50 mM Tris, pH 8.0.

RIPA lysis buffer working solution

940 µl RIPA buffer, 50 µl protease inhibitor (1x cOmplete mini EDTA free, S8830) , 10 µl 1x phosphatase inhibitor (P5726)

4x sample loading buffer (Lammeli buffer)

300 mM Tris-HCl pH 6.8, 35% glycerol (GE Healthcare), 12% SDS, 0.02% bromophenol blue, 6% mercaptoethanol, made up to 20 ml with deionised water.

12% Resolving gel

H_2O	6.6 ml
30% acrylamide mix	8.0 ml
1.5 M Tris-HCl (pH 8.8)	5.0 ml
10% SDS (GE Healthcare)	0.2 ml
10% ammonium persulfate	0.2 ml
TEMED	0.01 ml

15% Resolving gel

H_2O	4.6 ml
30% acrylamide mix	10.0 ml
1.5 M Tris-HCl (pH 8.8)	5.0 ml
10% SDS (GE Healthcare)	0.2 ml
10% ammonium persulfate	0.2 ml
TEMED	0.01 ml

5% Stacking gel

H_2O	6.8 ml
30% acrylamide mix	1.7 ml
1 M Tris-HCl (pH 8.8)	1.25 ml
10% SDS (GE Healthcare)	0.1 ml
10% ammonium persulfate	0.1 ml
TEMED	0.01 ml

10x Running buffer

15 g Tris base, 72 g Glycine, 5 g SDS (GE Healthcare) in 500 ml deionised water.

10x Transfer buffer

30 g Tris base, 144 g Glycine in 1 L deionised water.

1x Transfer buffer

100 ml 10x Transfer buffer, 200 ml methanol, 10 ml 10% SDS (GE Healthcare) and 690 ml deionised water.

PBS Tween 20 (PBST)

1 ml of Tween 20 in 1 L PBS (pH 7.4)

5% blocking solution

5 g milk (less than 0.1% fat) in 100 ml of 0.1% PBST.

Developing solution

50 ml multigrade developer (ILFORD) in 500 ml d.H_2O.

Fixation solution

50 ml rapid fixer (ILFORD) in 500 ml d.H_2O

Appendix V: Primary and secondary antibodies for western blot

Primary antibody	Host species	Molecular weight (kDa)	Dilution	Manufacturer of primary antibody	Secondary antibody	Manufacturer of secondary antibody
ALDH1A1	Polyclonal goat	56.2	1:400	Santa Cruz Biotechnology	1:5,000	Dako
ALDH1A2	Monoclonal rabbit	57	1:2000	Abcam	1:2500	Dako
ALDH1A3	Polyclonal goat	64	1:400	Santa Cruz Biotechnology	1:5,000	Dako
ALDH2	Monoclonal rabbit	56	1:500	Abcam	1:5,000	Dako
ALDH3A1	Monoclonal mouse	50	1:500	Santa Cruz Biotechnology	1:5,000	Dako
ALDH7A1	Monoclonal rabbit	55	1:20,000	Abcam	1:5,000	Dako
Actin	Monoclonal mouse	43	1:80,000	Millipore	1:10,000	Dako
HIF-1α	Monoclonal mouse	120	1:1000	BD Transduction Laboratories	1:5,000	Dako
HIF-2α	Polyclonal rabbit	118	1:500	Novus biologicals	1:2500	Dako
LDH-A	Monoclonal rabbit	28-36	1:5,000	Abcam	1:5,000	Dako
Phosphorylated H2AX	Monoclonal rabbit	15	1:1000	Cell Signalling Technologies	1:2500	Dako

Table 15 Primary and secondary antibodies for western blot.

Appendix VI: Buffers and antibodies for histology (IHC)

1x Citrate buffer

2.1 g citric acid monohydrate in 1000 ml dH_2O. PH was adjusted to 6.0 with 2M NaOH.

Primary and secondary antibodies for IHC

Primary antibody	Antigen retrieval	Blocking reagents	Dilution of primary antibody	Primary antibody incubation condition	Secondary antibody
ALDH1A1 (Polyclonal goat, Santa Cruz)	2 x 15 min Citrate Buffer	• 3% H_20_2 block • Normal Rabbit Serum (1.5:100 in PBS for 30 min, Vector Laboratories)	1:10	1h at 37˚C	biotinylated rabbit anti goat antibody (1:200) Vector Laboratories
ALDH1A3 (Polyclonal goat, Santa Cruz)	2 x 15 min Citrate Buffer	• 3% H_20_2 block • Normal Rabbit Serum (1.5:100 in PBS for 30 min, Vector Laboratories)	1:10	1h at 37˚C	biotinylated rabbit anti goat antibody (1:200) Vector Laboratories
ALDH3A1 (Monoclonal mouse, Santa Cruz)	2 x 15 min Citrate Buffer	• 3% H_20_2 block • Normal Horse Serum (5:100 in PBS for 30 min, Vector Laboratories)	1:10	1h at 37˚C	biotinylated horse anti mouse antibody (1:200) Vector Laboratories
ALDH7A1 (Monoclonal rabbit, Abcam)	1 x 20 min Citrate Buffer	• 3% H_20_2 block • Normal Goat Serum (1.5:100 in PBS for 30 min, Vector Laboratories)	1:100	1h at room temperature	biotinylated goat anti rabbit antibody (1:200) Vector Laboratories
CAIX (Monoclonal rabbit, Abcam)	1 x 20 min Citrate Buffer	• 3% H_20_2 block • Normal Goat Serum (1.5:100 in PBS for 30 min, Vector Laboratories)	1:100	1h at room temperature	biotinylated goat anti rabbit antibody (1:200) Vector Laboratories

Table 16 Primary and secondary antibodies for IHC.

Appendix VII: siRNAs information

siRNAs for target genes were purchased from Ambion/Life Technologies.

ALDH1A3 siRNA	Sense	Antisense
Sequence (5'->3')	GUAUCGAAGAAGUGAUAAAtt	UUUAUCACUUCUUCGAUACtt
Length	21	21
Percent G/C	29%	29%
Molecular Weight	6800	6500
Molar Extinction Coefficient	231700	200600
Annealed Molecular Weight	13300	13300

ALDH3A1 siRNA	Sense	Antisense
Sequence (5'->3')	GGAACUCAGUGGUCCUCAAtt	UUGAGGACCACUGAGUUCCct
Length	21	21
Percent G/C	48%	52%
Molecular Weight	6700	6600
Molar Extinction Coefficient	205100	199900
Annealed Molecular Weight	13400	13400

ALDH7A1 siRNA	Sense	Antisense
Sequence (5'->3')	GGAAAUUAUGUAGAACCGAtt	UCGGUUCUACAUAAUUUCCag
Length	21	21
Percent G/C	33%	38%
Molecular Weight	6800	6600
Molar Extinction Coefficient	223100	208700
Annealed Molecular Weight	13400	13400

HIF1α siRNA	Sense	Antisense
Sequence (5'->3')	CCUCAGUGUGGGUAUAAGAtt	UCUUAUACCCACACUGAGGtt
Length	21	21
Percent G/C	43%	43%
Molecular Weight	6800	6600
Molar Extinction Coefficient	213200	201400
Annealed Molecular Weight	13400	13400

HIF2α siRNA	Sense	Antisense
Sequence (5'->3')	CAAUAGCCCUGAAGACUAUtt	AUAGUCUUCAGGGCUAUUGgg
Length	21	21
Percent G/C	38%	48%
Molecular Weight	6700	6700
Molar Extinction Coefficient	208800	213100
Annealed Molecular Weight	13400	13400

Appendix VIII: Solutions for spheroids formation and invasion

Methylcellulose for spheroids formation

6 g methylcellulose (Sigma) was autoclaved in a 500ml flask containing a magnetic stirrer. 250 ml of RPMI medium (preheated at 60°C) was added and mixed for 30 min. Another 250 ml medium was added and stirred for further 30 min at room temperature. The methylcellulose solution was left for 1-2 h at 4°C to ensure that it was completely dissolved. The 500 ml of methylcellulose solution was then centrifuged (5,000 rcf, 2h, room temperature). The clear highly viscous supernatant was kept at 4°C until required.

Collagen matrix for invasion assay

To prepare collagen matrix on ice:

- Volume of collagen stock (4.88 mg/ml, collagen type 1 rat tail, Corning) to achieve final concentration of 1.5 mg/ml
- Volume of NaOH (1M) = volume of collagen stock/40
- Volume of PBS (5x) to achieve 1x final concentration
- Volume of distilled water= Volume of collagen matrix – (Volume of collagen stock+ Volume of NaOH+ Volume of PBS)

Appendix IX: Raw data for ΔCt values from qRT-PCR of ALDH1A1, 1A2, 1A3, 1B1, 2, 3A1 and 7A1 in DLD-1 cells.

		Experiment 1	Experiment 2	Experiment 3	Average	SD	T.Test
ALDH1A1	Control	14.23	13.05	13.34	13.54	0.50	
	6h	15.96	13.85	13.83	14.55	1.00	0.16
	24h	15.09	13.35	13.33	13.92	0.82	0.61
	48h	13.38	12.65	13.23	13.09	0.31	0.35

		Experiment 1	Experiment 2	Experiment 3	Average	SD	T.Test
ALDH1A2	Control	13.83	14.52	14.31	14.22	0.29	
	6h	14.09	15.24	14.57	14.63	0.47	0.36
	24h	14.42	14.43	14.69	14.51	0.12	0.29
	48h	12.27	12.72	12.71	12.57	0.21	0.00

		Experiment 1	Experiment 2	Experiment 3	Average	SD	T.Test
ALDH1A3	Control	9.16	8.94	9.23	9.11	0.12	
	6h	9.08	8.68	8.57	8.78	0.22	0.15
	24h	9.6	8.52	9.07	9.06	0.44	0.90
	48h	8.38	8.41	8.69	8.49	0.14	0.01

		Experiment 1	Experiment 2	Experiment 3	Average	SD	T.Test
ALDH1B1	Control	4.93	4.75	5.14	4.94	0.16	
	6h	4.28	3.62	4.89	4.26	0.52	0.20
	24h	5.17	4.65	5.93	5.25	0.53	0.50
	48h	4.52	5.01	5.35	4.96	0.34	0.95

		Experiment 1	Experiment 2	Experiment 3	Average	SD	T.Test
ALDH2	Control	5.76	5.65	5.53	5.65	0.09	
	6h	6.55	6.35	6.36	6.42	0.09	0.001
	24h	5.64	5.56	5.34	5.51	0.13	0.30
	48h	6.05	5.34	5.38	5.59	0.33	0.83

		Experiment 1	Experiment 2	Experiment 3	Average	SD	T.Test
ALDH3A1	Control	5.77	6.7	6.49	6.32	0.40	
	6h	5.97	6.76	6.4	6.38	0.32	0.88
	24h	5.36	6.05	5.70	5.70	0.28	0.16
	48h	5.64	6.38	5.96	6.00	0.30	0.42

		Experiment 1	Experiment 2	Experiment 3	Average	SD	T.Test
ALDH7A1	Control	6.96	7.07	7.05	7.03	0.05	
	6h	7.23	7.15	7.21	7.20	0.03	0.02
	24h	5.64	4.94	5.44	5.34	0.30	0.01
	48h	5.68	4.70	5.95	5.44	0.54	0.05

Appendix X: Raw data for geometric mean values of area under the curve from ROS detection in DLD-1 cells after knockdown under normoxic and hypoxic conditions

I. ROS in normoxia:

	Experiment 1	Experiment 2	Experiment 3	Average	SD	T.Test
Lipo	21.77	21.55	19.82	21.047	0.872	
Lipo/H_2O_2	27.51	25.28	23.32	25.37	1.7117	0.050629
3A1 siRNA	22.48	20.67	19.6	20.917	1.1886	0.907282
7A1 siRNA	24.87	24.22	22.62	23.903	0.9455	0.035127
3A1 & 7A1 siRNAs	24.78	23.63	22.18	23.53	1.0638	0.065446
1A3 siRNA	17.87	17.28	16.49	17.213	0.5654	0.009739

II. ROS in hypoxia:

	Experiment 1	Experiment 2	Experiment 3	Average	SD	T.Test
H Mock	11.86	11.96	11.85	11.89	0.0497	
H H_2O_2	23.36	23.42	23.36	23.38	0.0283	4.22E-08
N Lipo	21.2	21.28	20.91	21.13	0.159	
H Lipo	12.66	12.42	12.43	12.503	0.1109	1.43E-06
H Lipo	12.66	12.42	12.43	12.503	0.1109	
H 1A3 siRNA	12.74	12.67	12.6	12.67	0.0572	0.155393
H 3A1 siRNA	13.96	14.36	14.46	14.26	0.216	0.002034
H 7A1 siRNA	15.31	15.04	14.91	15.087	0.1666	0.00014
H 3A1 & 7A1 siRNAs	16.54	16.57	16.53	16.547	0.017	0.000283

Appendix XI: Raw data for geometric mean values of area under the curve from ROS detection in H1299 cells

I. H1299/RFP and H1299/7A1

	Experiment 1	Experiment 2	Experiment 3	Average	SD	T.Test
H1299/RFP	58.47	56.74	60.67	58.627	1.6082	
H1299/7A1	4.01	3.9	3.96	3.9567	0.045	0.0004

II. H1299/RFP treated with ALDH7A1 inhibitors

	Experiment 1	Experiment 2	Experiment 3	Average	SD	T.Test
RFP/DMSO	178.39	164.02	171.205	171.205	5.8665	
RFP/DEAB	171.25	158.11	164.68	164.68	5.3644	0.3108
RFP/DSHS00561	135.99	132.77	134.38	134.38	1.3146	0.0097
RFP/KM06288	143.77	135.12	139.445	139.445	3.5313	0.0054
RFP/HAN00316	163.54	151.09	157.315	157.315	5.0827	0.0659

III. H1299/7A1 treated with ALDH7A1 inhibitors

	Experiment 1	Experiment 2	Experiment 3	Average	SD	T.Test
7A1/DMSO	12.78	13.32	13.57	13.223	0.3297	
7A1/DEAB	16.27	17.06	16.68	16.67	0.3226	0.0005
7A1/DSHS00561	13.59	14.23	13.93	13.917	0.2614	0.0836
7A1/KM06288	13.54	13.98	13.72	13.747	0.1806	0.1406
7A1/HAN00316	14.54	14.62	14.62	14.593	0.0377	0.0265

Appendix XII: Abstracts presented to attended conferences

Poster: School of Life Sciences, Research and Development Open Day, March 2013, University of Bradford

Modulation of drug metabolising enzymes and ABC drug transporters with decitabine has no bearing on the chemosensitivity of paclitaxel

L. Cosentino1, L. Elsalem1, N. Masrour2, J. Burns3, R.M. Phillips1, R. Brown2, P. Burns3 and K. Pors1

1Institute of Cancer Therapeutics, University of Bradford, BD7 1DP, U.K.; 2Imperial College London, Hammersmith Hospital Campus, London W12 0NN,U.K.; 3Leeds Institute of Molecular Medicine, St James's Hospital, Leeds LS9 7TF, U.K.

The literature describes the role of DNA methylation in regulation of tumour suppressor genes, DNA repair genes, but not much attention has been paid to drug metabolising enzymes (DMEs). Some evidence has been reported and includes methylation in the promoter regions of CYP450 and ABC transporters. Cotreatment of decitabine (DAC) and paclitaxel (PAC) has been reported in several studies, but few of these have in a focused manner reported on the effect on DMEs. As a consequence, the major DMEs involved in the detoxification of PAC (namely ABCB1, CYP2C8 and CYP3A4) were investigated. Also the aldehyde dehydrogenase enzymes (ALDH1A1, ALDH2 and ALDH3A1) were explored, as they recently have been shown to play a chemo-protective role against taxanes. A549, HT29, HeLa and MCF7 cells were treated with DAC (0.1 or 1uM for 24 h). DNA methylation was analysed using pyrosequencing. Gene expression was determined by quantitative RT-PCR (qRT-PCR). Western blotting analysis was used for protein expression analysis. The chemosensitivity of cotreatment of DAC (0.1 uM 24 h) and paclitaxel (0.0001 to 10 uM) on day 6 or 8 was evaluated by the MTT assay. Analysis of the CpG island methylation level indicated that all the above-mentioned DMEs were densely methylated and that treatment of MCF-7 cells with DAC resulted in a decrease in methylation within the gene promoter region. Furthermore, correlation of decrease in DNA methylation with increase in gene expression of ABCB1, CYP3A4, ALDH2 and ALDH3A1 was observed, but not in CYP2C8 and ALDH1A1. However, only the ABCB1 protein level was shown to noticeably increase. Evaluation of the cotreatment of DAC and PAC on cell survival demonstrated that the cytotoxic potential of PAC was not significantly affected by the exposure to DAC suggesting that modification of ABCB1 at the protein level was not sufficient to alter the activity of PAC. The

same experiments were also conducted in HeLa, HT29 and A549 cells and similar results were observed: no significant modification at the protein level despite changes to the DNA methylation and gene levels and hence no alteration in the chemosensitivity of PAC after pretreatment of these cancer cells with DAC.

Our data demonstrates that pretreatment of four different cancer cell lines with DAC has no significant affect on the chemosensitivity of PAC, indicating that modulation of drug metabolising enzymes and drug transporters at the DNA methylation and gene level is not translated into modified protein levels. Our observations provide vital information for further clinical evaluation of combination strategies that involves the use of DAC.

Poster: YCR Annual Scientific Meeting, June 2013, Pavilions of Harrogate, Great Yorkshire Showground

Re-engineering of the Duocarmycin Structural Architecture Enables Tumour-Selective CYP2W1-mediated Drug Activation in Human Colon Cancer Xenografts.

Klaus Pors, Sandra Travica**, Paul M. Loadman, Steven D. Shnyder, Lina Elsalem, Mark Sutherland, Helen M. Sheldrake, Mark Searcey*, Inger Johansson**, Souren Mkrtchian**, Magnus Ingelman-Sundberg** and Laurence H. Patterson.

University of Bradford, BD7 1DP, *University of East Anglia, NR4 7TJ;** Karolinska Institute, SE-17177, Sweden.

CYP2W1 is detected in 30% of colon cancers while its protein expression in non-transformed adult tissues is absent or insignificant CYP2W1. Here we present data on furanoindole-based duocarmycins that have the potential to be used as a chemical probe (e.g. ICT2726) to show CYP2W1 functional activity. Significantly, we also demonstrate indoline-based bioprecursors ICT2705 and ICT2706 to elicit potent antiproliferative activity in CYP2W1-transfected human HEK293 and SW480 cells but not in mock-transfected cells. Moreover, ICT2706 was shown to prevent tumour growth when administered to SCID mice bearing SW480-2W1 xenografts (dosed daily with 100 mg/kg for 8 days). Using H2A.X phosphorylation as a marker for DNA damage, our data revealed a time-dependent increase in expression supporting CYP2W1-mediated activation of ICT2706 in vivo. Our findings reveal the opportunities in targeting CYP2W1 as a novel therapeutic approach in colon cancer chemotherapy.

Poster: School of Life Sciences, Research and Development Open Day, March 2014, University of Bradford, UK

The impact of hypoxia on the expression of aldehyde dehydrogenases in colon cancer.

Lina Elsalem[1], Mark Sutherland[1], Roger Phillips[1], Klaus Pors[1]

1Institute of Cancer Therapeutics/ School of Life Sciences, Bradford, West Yorkshire, UK

Introduction: Cancer cells become resistant to chemotherapy by a variety of different mechanisms. One of the main components is due to increased expression of drug metabolising enzymes (DMEs) including, aldehyde dehydrogenases (ALDHs). Currently, it is well known that tumour hypoxia is associated with invasive and metastatic properties of cancer tissues as well as resistance to chemotherapy and radiation therapy, which together constitute the lethal cancer phenotype and ultimately lead to patient mortality. The contribution of hypoxia to anticancer drugs resistance through different mechanisms is well established, however, its role in the regulation of drug metabolising enzyme expression, particularly ALDHs, is still to be elucidated. This research project is focussed on investigating the expression of ALDH in colon cancer cells and aims to understand the impact of hypoxia might have on the expression of specific ALDHs.

Methods: Monolayer cells (HT29, DLD-1, SW480 and HCT116) were either incubated at normoxic conditions or exposed to very low oxygen level (0.1 %) for 6, 24 and 48 h. Multicellular spheroids (MCS) were grown from HT29 using spinner flasks culture technique. Paraffin embedded spheroids were sectioned and stained with haematoxylin and eosin. Hypoxia was detected in spheroid frozen sections using immunofluorescence staining for the hypoxia marker, pimonidazole. Cells residing in the hypoxic regions or in the surface layers were isolated using sequential trypsinisation. The gene expression analysis of ALDH isoforms (1A1, 1A2, 1A3, 1B1, 2, 3A1 and 7A1) in monolayer cells and MCS was evaluated using quantitative RT-PCR.

Results: The gene analysis data of monolayer cells revealed that hypoxia exerts cell type specific effects on ALDHs expression, whether this effect was manifested as an up-regulation or down-regulation of the specific genes. The ALDH gene expression profile of cells residing in the surface layer of HT29 spheroids was variable, with up-regulation of ALDH (1A1, 1A2, 1B1, and 7A1), down-regulation of ALDH (1A3 and 3A1) and no change in the expression of ALDH2 compared to monolayer cells. Interestingly, cells

residing in the hypoxic region showed further up-regulation of ALDH (2 and 7A1), no change in the expression of ALDH (1A3 and 3A1) and down-regulation of ALDH(1A and 1B1) compared to surface layer cells.

Conclusion: Our data reveals that the expression of ALDHs in colon cancer cells can be modulated as a result of tumour hypoxia exposure, at least at the gene level. Knowledge about the location of ALDHs within the tumour microenvironment and how these enzymes are affected by hypoxic conditions will contribute to a better understanding of cancer drug resistance mechanisms, and ultimately will enhance the development of ALDH-targeted cancer therapeutics in hypoxic cells and potentially also cancer stem cells. Therefore, in order to fully establish the role of hypoxia, future work will include investigation of a wide panel of ALDH isoforms in monolayer cell lines, MCS tumour models and primary colon cancer cells.

Oral presentation: Postgraduate Research Mini conference 2014, Faculty of life Sciences, University of Bradford, UK

The impact of hypoxia on the expression of aldehyde dehydrogenases in colon cancer.

Lina Elsalem[1], Mark Sutherland[1], Roger Phillips[1], Klaus Pors[1]

1Institute of Cancer Therapeutics/ School of Life Sciences, Bradford, West Yorkshire, UK

Cancer cells become resistant to chemotherapy by a variety of different mechanisms. One of the main components is due to increased expression of drug metabolising enzymes (DMEs) including, aldehyde dehydrogenases (ALDHs). Currently, it is well known that tumour hypoxia contributes to anticancer drugs resistance through different mechanisms; however, its role in the regulation of ALDHs is still to be elucidated. This research project is focussed on investigating the expression of ALDH in colon cancer cells and aims to understand the impact of hypoxia might have on the expression of specific ALDHs. Monolayer cells were exposed to 0.1% O2 and gene analysis data of revealed that hypoxia exerts cell type specific effects on ALDHs expression, whether this effect was manifested as an up-regulation or down-regulation of the specific genes. The ALDH gene expression profile was also investigated in multicellular spheroids (MCS) and showed that the expression of certain isoforms was enhanced in cells residing in the hypoxic region compared to cells in the surface layer. Our data reveals that the expression of ALDHs in colon cancer cells can be modulated as a result of tumour hypoxia, at least at the gene level. This knowledge will contribute to a better understanding of cancer drug resistance mechanisms, and ultimately will enhance the development of ALDH-targeted cancer therapeutics in hypoxic cells and potentially in cancer stem cells. Therefore, in order to fully establish the role of hypoxia, future work will include investigation of a wide panel of ALDH isoforms in monolayer cell lines, MCS tumour models and primary colon cancer cells.

Poster: The 10th National Cancer Research Institute Conference November 2014, Liverpool, UK

The impact of hypoxia on the expression of aldehyde dehydrogenases in colon cancer.

Lina Elsalem1, Mark Sutherland1, Roger Phillips1, Klaus Pors1,

1Institute of Cancer Therapeutics/ School of Life Sciences, Bradford, West Yorkshire, UK,

Background: Cancer cells become resistant to chemotherapy by different mechanisms. One of the main components is due to increased expression of drug metabolising enzymes (DMEs) including, aldehyde dehydrogenases (ALDHs). It is well known that tumour hypoxia contributes to anticancer drugs resistance, however, its effect on the regulation of ALDHs is still to be elucidated. Accordingly, the focus of our research was to investigate the expression of ALDH in colon cancer cells under normoxic and hypoxic conditions in attempt to gain information of these isoforms as potential biomarkers.

Method: Monolayer cells (HT29, DLD-1, SW480 and HCT116) were incubated at normoxic conditions or exposed to (0.1 %) oxygen level for 6, 24 and 48h. Multicellular spheroids (MCS) were grown from HT29 and DLD-1 cells using spinner flasks culture technique. Paraffin embedded spheroids were stained with haematoxylin and eosin. Hypoxia was detected using immunofluorescence staining for the hypoxia marker, pimonidazole. Cells residing in the hypoxic regions or in the surface layers were isolated using sequential trypsinisation. The gene expression of ALDH isoforms (1A1, 1A2, 1A3, 1B1, 2, 3A1 and 7A1) was evaluated using quantitative RT-PCR.

Results: Gene analysis data of monolayer cells revealed that hypoxia exerts cell type specific effects on ALDHs expression, whether this effect was manifested as an up-regulation or down-regulation of the specific genes. The ALDH gene profile of MCS showed that ALDH2 and 7A1 were up-regulated in the hypoxic region compared to the surface layer in both HT29 and DLD-1 MCS.

Conclusion: Our data reveals that the gene expression of ALDHs in colon cancer cells can be modulated upon exposure to hypoxic conditions. This knowledge will contribute to a better understanding of cancer drug resistance mechanisms present in colon cancer, but further studies are required to correlate the increased expression of specific ALDHs in hypoxic fractions of colon tumours.

Oral presentation: Postgraduate Research Mini conference 2015, Faculty of life Sciences, University of Bradford, UK

Exploration of the role of ALDH in colon cancer progression and influence on chemotherapy

L. Elsalem[1], S. Allison[1], R.M. Phillips[2] and K. Pors[1]

1: Institute of Cancer Therapeutics, Faculty of Life Sciences, University of Bradford, UK
2: Department of Pharmacy, University of Huddersfield, UK

Introduction: Colorectal cancer is the third most common cancer in the world. For patients with advanced colon cancer, the 5 year survival rate is less than 10%. Recently, ALDHs were used as markers to isolate, propagate and track colon cancer stem cells. In addition, the expression of certain ALDH isoforms in primary colon cancer samples was found to be significantly associated with shorter overall survival, suggesting its clinical relevance as prognostic or predictive marker in colorectal cancer. The aim of this study is to investigate the expression of ALDH isoforms in colorectal cancer cell lines and study their functional role in colorectal cancer progression and chemotherapy.

Methods: in this study we used siRNA duplexes to knockdown one (1A3, 3A1 or 7A1) or two isoforms together (3A1 and 7A1) in the DLD-1 colorectal cancer cell line in order to investigate the role of each one in mediating cells proliferation, migration, drug resistance and inhibition of reactive oxygen species (ROS) generation.

Result: The results show that significant and specific knockdown of each isoform can be achieved at both the gene and protein levels with a role of ALDH7A1 in regulating the expression of ALDH3A1. Only ALDH7A1 was found to be associated with enhanced cell proliferation and inhibition of ROS generation. In addition ALDH3A1 and 7A1 were found to promote cell migration. However, no significant role of the three isoforms was observed in mediating drug resistance.

Conclusion: Our data suggests that ALDH7A1 has an important role in colon cancer progression through mediating cell proliferation and migration. In addition, it might be involved in protection against cell death caused by (ROS) through antioxidant regulatory pathways.

Poster: EACR-AACR-SIC Special Conference June 2015, Florence, Italy

Hypoxia modulates the expression of aldehyde dehydrogenases in colon cancer cells with ALDH7A1 emerging as a key enzyme whose functional involvement is dependent on the tumour microenvironment

L. Elsalem[1], S. Allison[1], R.M. Phillips[2] and K. Pors[1]

1: Institute of Cancer Therapeutics, Faculty of Life Sciences, University of Bradford, UK
2: Department of Pharmacy, University of Huddersfield, UK

Introduction: Most solid tumours generate hypoxic regions as a consequence of poorly developed and incomplete neovasculature. It is well known that hypoxia is associated with an aggressive cancer phenotype, causing resistance to both radiotherapy and chemotherapy.The aldehyde dehydrogenase (ALDH) superfamily, which belongs to the class of phase 1 drug metabolising enzymes, is thought to be involved in drug resistance. However, their regulation and expression within the tumour microenvironment is poorly understood. Accordingly, we have initiated an investigation to understand the role of ALDHs in tumour tissues and explored the impact hypoxia might have on the expression of these enzymes in colon cancer.

Methods: Colon cancer cell lines (HT29, DLD-1, SW480 and HCT116) were grown under normoxic or hypoxic conditions (0.1% O_2) for 6, 24 and 48h. HT29 and DLD-1 cells were also grown in spinner flasks until multicellular spheroids (MCS) were obtained (diameter ≈600μm). The hypoxic regions of the MCS were detected using the hypoxia marker, pimonidazole, and isolated using sequential trypsinisation. Gene expression analysis of ALDH isoforms (1A1, 1A2, 1A3, 1B1, 2, 3A1 and 7A1) in monolayer cells and MCS was carried out using quantitative RT-PCR. The protein expression was evaluated using Western blot and immunohistochemistry.

Results: The gene analysis data of monolayer cells showed that hypoxia exerts upregulation of ALDH(1A1, 1A2 and 7A1) in DLD-1 and HT29, ALDH1A3 in SW480 and all investigated ALDH in HCT116 with the exception to ALDH(2 and 7A1). However, on the protein level, only ALDH7A1 was upregulated in HT29 and DLD-1 and ALDH1A3 in HCT116 and SW480. Cells residing in the hypoxic region of HT29 and DLD-1 MCS showed upregulation of ALDH7A1 compared to surface layer cells and monolayer cells at both gene and protein levels.

Conclusion: Our results reveal that tumour hypoxia has impact on the expression of ALDHs in colon cancer cells at both gene and protein levels. An understanding of how these enzymes are affected by hypoxic conditions and their location within the tumour microenvironment will elucidate the role of these enzymes in colon cancer progression and drug resistance. Our data suggests that ALDH7A1 is increased by exposure to hypoxia and current studies are focussed on understanding how this enzyme may be linked to HIF-1 and/or metabolic signalling pathways. The data from these studies will also be presented at the meeting.